An Analysis of Polycomb Repressive Complex 2 Function Through Imprinted Mouse X-chromosome Inactivation

by

Michael R. Hinten

A dissertation submitted in partial fulfillment
of the requirements for the degree of
Doctor of Philosophy
(Human Genetics)
in the University of Michigan
2016

Doctoral Committee:

Professor Sundeep Kalantry, Chair
Professor David Burke
Professor Yali Dou
Professor John Kim, Johns Hopkins University

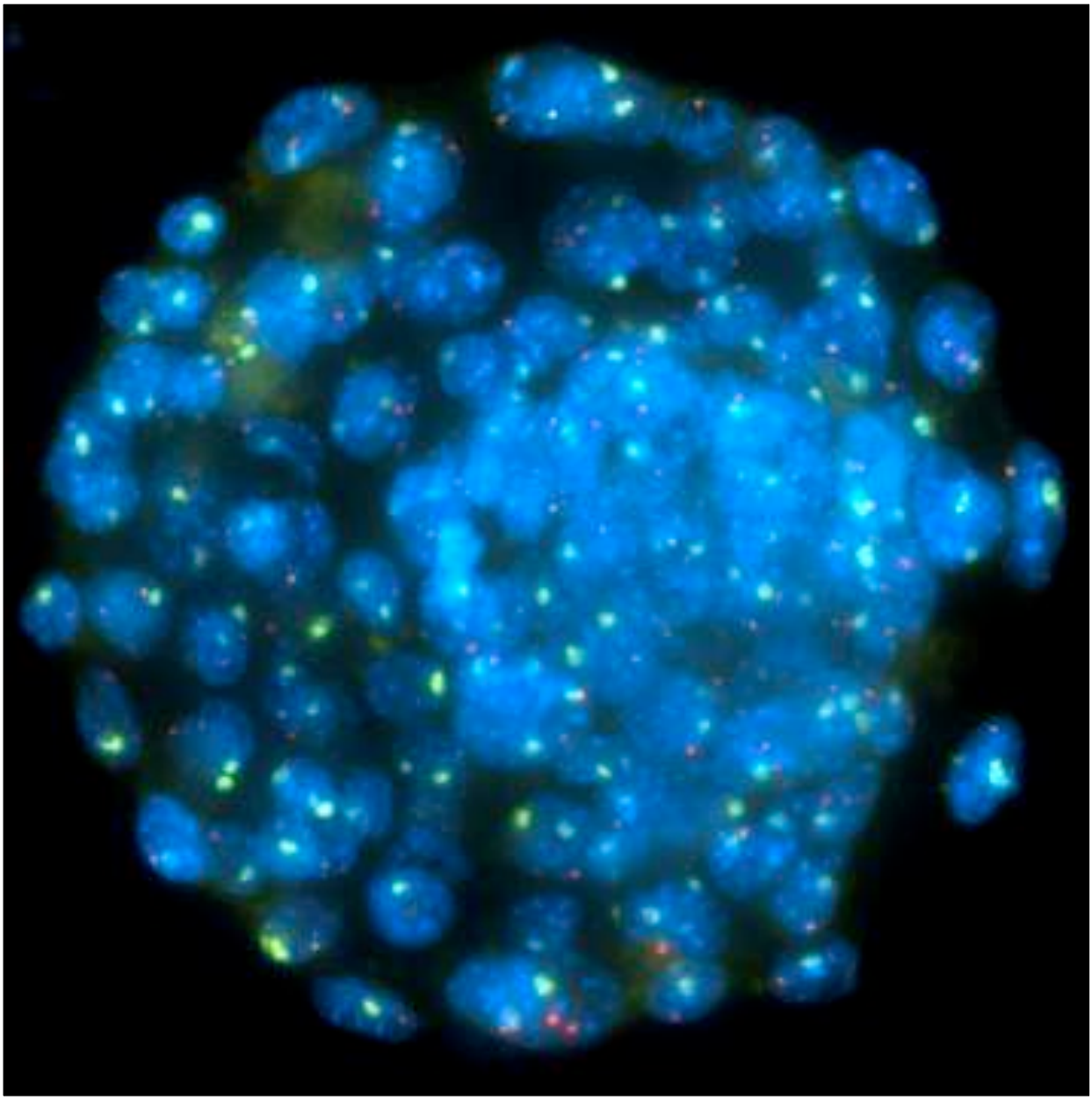

Dedication

To my wife, Stephanie, my life-long partner and friend, with you by my side, completion of my graduate degree was always a reality.

Acknowledgements

I would first like to acknowledge my graduate mentor and dissertation advisor, Sundeep Kalantry. It has been my sincere privilege to train under Sundeep. He is without a doubt one of the smartest scientists I have had the fortune of knowing. I have learned a vast amount from him, and I feel that my skills as both a critical thinker and analytical experimenter have been honed by working in his lab. I truly feel that his mentorship has bestowed upon my training an immense degree of preparedness to go out in to the research world as an independent scientist.

I would also like to acknowledge my thesis committee members, David Burke, Yali Dou, and John Kim. They are also among the smartest people with whom I have worked. With their knowledge and expertise regarding genetics, Polycomb group proteins, and epigenetic mechanisms, they have been invaluable assets over the years towards my development as a graduate student and independent researcher. Dave, John, and Yali contributed to important discussions during my thesis committee meetings, many of which shaped the way Sundeep and I designed our future experiments. I wish to also thank Sue Hammoud for graciously stepping in on such short notice to serve as John's proxy during my defense and committee meeting. John was unable to attend my thesis defense, and Sue kindly agreed to discuss with him and communicate his evaluations on his behalf to the rest of the committee.

I wish to next acknowledge all of the input, both conceptual and technical, by others who have assisted me throughout my graduate work. Emily Maclary, a recent fellow graduate student in the Kalantry lab, contributed towards data collection and bioinformatic data analysis. Prior rotation students and fellow graduate students, Peter Larson and Arushi Varshney, also contributed to data collection and analysis. Clair Harris and Emily Buttigieg, our lab manager and previous undergraduate student, respectively, trained me on essentially all of the technical aspects of my work to include tissue culture and all the molecular biology protocols I used in my tenure as a graduate student. Our recent undergraduate students, Miguel Pedraza, Hassan Bazzi,

and Brandon Lee deserve much credit for ear tagging our mice and running all of the genotyping assays. Lastly, I would like to thank everyone in the Kalantry lab that provided support in other ways. I always appreciated advice from Surinder Batra, Srimonta Gayen, and Mrinal Sarkar and their helpful discussions throughout my time at Michigan. I owe all of these individuals a great deal of gratitude.

The researchers at the University of Michigan Animal Transgenic Core and DNA Sequencing Core facilities also deserve acknowledgment. I want to thank Tom Saunders and his group for injecting our targeted ESCs into pseudopregnant females for germline transmission and generation of our floxed *Eed* conditionally mutant mice. I also wish to thank Bob Lyons and his research staff for all of the work they performed to generate important sequencing data for my projects. In particular, I want to acknowledge Ellen Pedersen for working with us to implement my pyrosequencing assays and Jeanne Geskes for consulting with us on developing and optimizing my RNA sequencing experiments on single whole mouse embryos.

Last, but not least, I want to thank my family to include my wife, parents, in-laws, siblings, extended family, and my friends. They all provided much support and encouragement over the years as I worked to finish my Ph.D. I could not have completed this journey without them.

Table of Contents

Dedication	ii
Acknowledgements	iii
List of Figures	vi
List of Tables	viii
List of Appendices	ix
Abstract	x
Chapter 1: Introduction	1
Chapter 2: A Comparative Analysis of Polycomb Repressive Complex 2 Proteins in Imprinted X-chromosome Inactivation: Mouse Trophoblast Stem Cells	58
Chapter 3: A Comparative Analysis of Polycomb Repressive Complex 2 Proteins in Imprinted X-chromosome Inactivation: Mouse Embryos	117
Chapter 4: Unveiling a Differential Requirement for the Xist RNA and the *Xist* DNA In Imprinted Mouse X-chromosome Inactivation	181
Chapter 5: Discussion, Reflections, Future Directions, and Concluding Remarks	207
Appendix A: Towards Understanding a Role for Novel Antisense lncRNAs within the Xist Locus in X-chromosome Inactivation	237
Appendix B: Understanding the Contribution of the Polycomb Protein EZH2 to the Pluripotency Network During Mouse Embryogenesis	248

List of Figures

Figure 1.1 Key long non-coding RNAs in the X-inactivation center 39

Figure 1.2 Enrichment of Xist RNA, Polycomb group protein EED, and H3-K27me3 on the inactive X-chromosome during mitosis DAPI stains the nuclei blue 41

Figure 1.3 Mouse blastocyst embryo stained to detect Xist RNA coating (in green), Tsix RNA (green pinpoint), and histone H3 lysine 27 tri-methylation (H3-K27me3; in purple). DAPI stains the nuclei blue 43

Figure 2.1 EZH2 is dispensable for propagating the inactive-X state in mouse trophoblast stem cells 94

Figure 2.2 EZH1 does not contribute to imprinted X-chromosome inactivation in mouse trophoblast stem cells 96

Figure 2.3 EZH1 does not contribute to imprinted X-chromosome inactivation in mouse trophoblast stem cells 98

Figure 2.4 *Ezh2*$^{-/-}$;*Ezh1*$^{-/-}$ trophoblast stem cells do not proliferate and are devoid of other Polycomb factors/histone marks on the inactive-X 100

Figure 2.5 Xist coats have a reduced volume in *Ezh2*$^{-/-}$;*Ezh1*$^{-/-}$ TSCs 102

Figure 2.6 EED is only partially required for stable silencing of the inactive-X in mouse trophoblast stem cells 104

Figure 2.7 *Eed*$^{-/-}$ trophoblast stem cells are devoid of other Polycomb proteins/histone marks on the inactive-X 106

Figure 2.8 Transiently transduced *Eed*$^{fl/fl}$ TS cells show a similar pattern of derepressed genes compared to constitutively *Eed*$^{-/-}$ TSCs 108

Figure 3.1 EZH2 is dispensable during the initiation phase of imprinted X-chromosome inactivation 153

Figure 3.2 Maternal EZH2 does not enrich on the inactive-X in blastocysts 155

Figure 3.3 EZH2 is dispensable during the initiation phase of imprinted X-chromosome inactivation 157

Figure 3.4 EZH2 is not required to maintain imprinted X-chromosome inactivation 159

Figure 3.5 EZH2 is not required to maintain imprinted X-chromosome inactivation 161

Figure 3.6 EZH1 does not contribute to the initiation of imprinted X-chromosome inactivation 163

Figure 3.7 EZH1 does not contribute to the initiation of imprinted X-chromosome inactivation 165

Figure 3.8 EED is critical for the proper initiation of imprinted X-chromosome inactivation 167

Figure 3.9 EED is critical for the proper initiation of imprinted X-chromosome inactivation 169

Figure 3.10 Xist RNA enriches on the inactive-X in *Eed*$^{m-/-;z-/-}$ blastocysts 171

Figure 4.1 Outline of rational for studying *Xist*$^{+/-}$ TSCs vis-à-vis *Eed*$^{-/-}$ TSCs 198

Figure 4.2 Transient transduction of *Xist*$^{+/fl}$ with Cre reveals derepression of *Atrx* and two classes of nuclei with respect to Xist RNA enrichment 200

Figure 4.3 Deletion of *Xist* exons 1-3 in *Xist*$^{+/fl}$ TSCs leads to derepression of genes that are not derepresssed in *Eed*$^{-/-}$ TSCs 202

Figure A.1 Novel-II, an RNA transcript expressed antisense to Xist, is expressed from the inactive X-chromosome in *Eed*$^{-/-}$ TSCs 245

Figure B.1 Assessing the pluripotency network in *Ezh2*$^{m-/-;z-/-}$ blastocysts 253

List of Tables

Table of Primers I 90

Table of Primers II 148

Table 3.1 173

Table 3.2 174

Table of Primers III 196

List of Appendices

Appendix A: Towards Understanding a Role for Novel Antisense lncRNAs within the Xist Locus in X-chromosome Inactivation 237

Appendix B: Understanding the Contribution of the Polycomb Protein EZH2 to the Pluripotency Network During Mouse Embryogenesis 248

Abstract

Polycomb group proteins comprise two major classes of evolutionarily conserved epigenetic transcription repressors, Polycomb repressive complex 2 and 1 (PRC2 and PRC1). PRCs are thought to catalyze epigenetic silencing via histone modifications and/or physical compaction of the surrounding chromatin. The inactive X-chromosome is a common target of PRCs. X-chromosome inactivation is a paradigmatic epigenetic phenomenon resulting in the equal expression of genes from the X-chromosome between XY male and XX female mammals. The initial form of X-inactivation during murine embryogenesis is imprinted X-inactivation, during which the paternally inherited X-chromosome is preferentially silenced. The core PRC proteins are physically enriched on the inactive-X at the onset of X-inactivation. However, the extent to which each subunit of PRC2 is genetically required for X-linked gene silencing is not definitively known. In my thesis work, I tested the hypothesis that PRC2 proteins orchestrate gene silencing on the paternal X-chromosome during imprinted X-inactivation.

To test if PRC2 subunits are required to propagate the X-inactive state, I derived and investigated X-linked gene silencing in mouse trophoblast stem cells (TSCs), an *ex vivo* model of imprinted X-inactivation. In TSCs lacking the core PRC2 proteins EZH2 and its homologue EZH1, which catalyze trimethylation of histone H3 at lysine 27 (H3-K27me3), I found that X-inactivation was unperturbed. In TSCs lacking EED, which is required for the assembly of PRC2, I found that imprinted X-inactivation was defective. In *Eed*$^{-/-}$ TSCs, enrichment of H3-K27me3 and the Xist long non-coding RNA, which is required for stable X-inactivation, are lost from the inactive-X. Despite the absence of H3-K27me3 and Xist RNA, only a subset of the genes on the inactive X-chromosome is reactivated in *Eed*$^{-/-}$ TSCs. Lack of a silencing defect for a majority of X-linked genes in *Eed*$^{-/-}$ TSCs suggests that factors other than EED, H3-K27me3, and Xist RNA are essential for propagating X-chromosome inactivation. To assess if my findings from TSCs applied *in vivo*, I generated embryos lacking maternal and zygotic EZH2, or EZH2 and 1, or EED. I discovered that EED, but not EZH2/1, is necessary to trigger imprinted X-inactivation in the embryo. This comparative analysis of PRC2 components suggests a PRC2 independent role

for EED in imprinted X-inactivation. Moreover, these results are the initial demonstration that a maternal factor controls the silencing of the X-chromosome in the embryo, an example of a transgenerational epigenetic regulation.

Xist RNA has long been believed to be necessary and sufficient for X-inactivation. For my final study, I tested the hypothesis that the *Xist* locus executes X-inactivation independently of producing the Xist RNA. I found that a deletion of Xist exons 1-3 leads to a more pronounced defect in X-linked gene silencing than loss of just the Xist RNA that characterizes *Eed*$^{-/-}$ TSCs. My results point to a feature of the *Xist* locus that is independent of Xist RNA transcription in the execution of X-inactivation.

Chapter 1

Introduction

Note: A portion of this introduction was adopted from a review on long non-coding RNAs implicated in X-chromosome inactivation:

Maclary, E.*, Hinten, M.*, Harris, C.*, Kalantry, S. (2013). Long non-coding RNAs in the X-inactivation center. Chromosome Res. *21*, 601–614.

*denotes equally contributing authors

Maclary, E contributed the *Xist* and *Tsix* portion of the review

Hinten, M. contributed the *Ftx* and *RepA* portion of the review

Harris, C. contributed the *Jpx*/*Enox* and *Tsx* portion of the review

Evolutionary Origins of X-chromosome Inactivation

X-chromosome inactivation (X-inactivation) evolved as a dosage compensation mechanism to equalize the X-linked gene expression levels between XX female and XY male mammals. X-inactivation occurs by inactivating one of the two X-chromosomes in females early during embryogenesis. Typically investigated in placental-bearing mammals (*eutheria*), conservation of X-inactivation as a sex chromosome method of dosage compensation dates back phylogenetically to the eutherian relatives of the class *Mammalia*, including marsupials (*metatheria*), and egg-laying monotremes (*prototheria*). Together with eutherians, marsupials and monotremes constitute a phylogenetic crown-group (Whitworth and Pask, 2016). Eutherians and marsupials are thought to have broad similarities in their mechanisms for inactivating one of the two X-chromosomes. Although, X-inactivation appears to be more simple and unstable in marsupials compared to eutherians. One fundamental difference between these groups of therians

is that eutherians have the *Xist* locus, which generates a long non-coding RNA that is instrumental in X-inactivation (Duret et al., 2006). However, marsupials lack *Xist,* suggesting that *Xist* evolved in eutherians sometime after the marsupial and eutherian split (Duret et al., 2006; Hore et al., 2007). Recent evolutionary work on monotremes however has provided new insight into the evolution of the XY sex chromosome system as well as X-inactivation as a dosage compensation mechanism (Wallis et al., 2008). Such work offered a fresh perspective on the ancestral phylogenies of early mammals, which indicate monotremes may have shared similarities in their sex chromosome system with the ZW bird sex chromosome system (Wallis et al., 2008). The XY sex chromosome system may have thus evolved from an ancient set of sex chromosomes that preceded the split between mammals and reptiles. The XY sex chromosome system is also found in some insects. This is most evident in the species *Drosophila melanogaster*, where females are XX and males are XY. Dosage compensation of the heterogametic sex in *Drosophila* functions to maintain equal expression levels of X-linked genes by upregulating the male X two-fold (Conrad et al., 2012; Birchler et al., 2003; Straub et al., 2005). Classically, most if not all, XX/XY bearing mammals contrastingly inactivate one of the two X-chromosomes in female cells during embryogenesis to achieve dosage compensation of the sex chromosomes (Lyon, 1962; Beutler et al., 1962). However, functional monosomy of the mammalian X-chromosome resulted from divergence of the mammalian sex chromosomes into the X and Y. Effectively expression from just one X-chromosome leaves an imbalance of the X-chromosome to autosome expression ratio due to diploid somatic cells in male animals possessing one X-chromosome for every pair of autosomes. To equalize potential dosage haploinsufficiency in males, genes along the X-chromosome have been proposed to essentially double in their expression outputs (Ohno, 1967). *Drosophila* is a clear example of this type of

dosage compensation, where only the males upregulate their X-chromosome expression levels (Conrad et al., 2012; Birchler et al., 2003; Straub et al., 2005). Furthermore, upregulation of the X-chromosomes in mammals is observed to occur early in embryonic development, but this is thought to occur in both males and females (Nguyen and Disteche, 2003). Ultimately mammals would still possess an imbalance of X-linked dosage between females and males (i.e. twice as much in females compared to males). To protect the female embryo from such functional tetrasomy of the X-chromosome resulting from upregulation of the X, one X-chromosome in females must concomitantly become silenced early on during embryogenesis.

The evolution of X-chromosome inactivation as a method of dosage compensation likely was a consequence of the divergence and evolution of the sex chromosomes, which left unequal X-linked gene expression levels. The X- and Y-chromosomes are believed to have evolved from a pair of autosomes (Graves and Schmidt, 1992; Ohno, 1967). Ancestrally there existed a set of autosomes, largely homologous in sequence (Graves and Schmidt, 1992). Once able to pair up and undergo recombination events during meiosis, one of these autosomes acquired an inversion that led to site-specific suppression of recombination during meiosis (Graves and Schmidt, 1992). Through a successive combination of additional inversion events on this autosome, the two chromosomes were largely unable to pair at all, leading to the divergence of the two autosomes, the so-called proto-sex chromosomes. As the proto-X and proto-Y diverged, the proto Y-chromosome became more susceptible to deletions and mutations. The proto-Y was thus prone to losing many of its genes. The sex chromosome differentiation is also thought to have occurred as result of the proto-Y acquiring mutations. It is posited that one mutagenic event on one of the ancestral autosomes (the proto-Y) was a truncation mutation of *Sox3*, which led to the development of the sex determination gene *Sry* (Wallis et al., 2008). The other ancestral

autosome (the proto-X) did not acquire a *Sox3* mutation. A *Sox3* mutation event combined with inversions/lack of recombination between the ancestral autosomes likely played defining roles in the establishment of the proto-Y and proto-X. In the sex chromosome research field, we now call these divergent sex chromosomes the Y-chromosome (which bears the *Sry* gene responsible for sex determination) and the X-chromosome. Further evidence that mammalian sex chromosomes evolved from a pair of autosomes comes from the homologous pseudo autosomal regions (PARs) of the X and the Y. PARs are regions that are similar in structure to autosomes, and they are sufficient in allowing pairing and subsequent recombinatory events during male meiosis (Graves and Schmidt, 1992). Such differentiation of the two sex chromosomes eventually led to an imbalance of X-chromosomal dosage to autosomal dosage ratios in XX/XY bearing animals. Since females have two X-chromosomes, and males only one, there needed to be a way to balance this level of X-linked gene expression compared to autosomes. Hence, biologists believe the X-chromosome underwent upregulation to equilibrate its dosage levels to autosome levels (Nguyen and Disteche, 2003). In *Drosophila* this makes sense, as the upregulation of X-linked gene expression levels only occurs in males, which only bear one X-chromosome. Male and female flies therefore have an equal balance of sex to autosome expression levels and an equal level of X-chromosome expression output between XY males and XX females. But since this X-chromosome dosage increase occurs in both males and female mammals (Nguyen and Disteceh, 2003), there is still an unequal balance of X-linked-specific gene dosage, twice as much in females compared to males. The idea of X-chromosome inactivation thus logically equalizes X-linked gene expression levels between males and females, a process that likely evolved gradually (Bellott et al., 2014; Jegalian and Page, 1998; Lahn and Page, 1999). For example, the X-inactive specific transcript (*Xist*) appears to reside within the group of genes that underwent dosage

compensation early, if not first, during the evolution of the sex chromosomes (Bellott et al., 2014; Cortez et al., 2014). As mentioned above, comparison of X-inactivation between marsupials and eutherian mammals suggests that X-inactivation evolved in the absence of Xist RNA, but the *Xist* sequence subsequently arose and became essential for stable X-linked gene silencing in eutherian mammals (Chaumeil et al., 2011; Grant et al., 2012; Kalantry et al., 2009; Nadaf et al., 2012). Thus to establish equal X-linked gene expression levels between female and male mammals, one of the two X-chromosomes ultimately becomes transcriptionally silenced in female cells early on during embryogenesis.

Genes on the mammalian X-chromosome are thought to have undergone dosage compensation in distinct waves over evolutionary time. Genes are therefore grouped into evolutionary strata on the mammalian X-chromosome. On the human X-chromosomes, for example, the groups of genes that underwent dosage compensation at similar times during evolution are collinear with map position, allowing for extrapolation of strata of X-linked genes. On the other hand, in the mouse the X-chromosome underwent copious rearrangements. An analysis of nucleotide divergence, however, has demonstrated that mouse X-chromosome genes correspond to human evolutionary strata, despite the observed rearrangements (Sandstedt and Tucker, 2004).

How X-chromosome Inactivation Operates

Evidence of X-chromosome inactivation abounds. Take, for instance, calico cats, which are almost exclusively female. The coat color of the calico cat comprises two colored patches of fur on white background. The colored patches, one orange and the other brown, arise due to two different alleles of the same X-linked gene. One of the alleles is actively expressed in cells, while

the other remains transcriptionally inert. By extension, it is not just the coat color allele that is subjected to a divergent transcriptional fate; it is essentially the entire X-chromosome that is affected. Mary Lyon formulated the idea that one X-chromosome in female cells is active and the other is inactive into a formal hypothesis in 1961 (Lyon 1961). X-inactivation also represents a clonal expansion of migrating melanocytes; the white color, resulting from an autosomal gene effect, dictates the size of the colored patches as the patches of colored cells migrate.

X-chromosome inactivation is a model of epigenetic inheritance. In a single nucleoplasm in undifferentiated female mammalian cells (pluripotent cells), there are two X-chromosomes, largely identical in sequence. Upon differentiation, one X-chromosome is chosen for inactivation. Going back to the calico cat example, nuclei contain the X-chromosome bearing the black coat color allele as well as the X-chromosome bearing the orange coat color allele. When differentiation occurs during embryogenesis, in one cell the X-chromosome harboring the black coat color allele is chosen for inactivation, while in another cell the X-chromosome possessing the orange coat color allele is chosen for inactivation. Importantly, once one X-chromosome is inactivated that same X-chromosome is then maintained as the inactive X-chromosome over multiple rounds of mitotic division essentially for the lifetime of the organism. The fact that two X-chromosomes of largely identical genetic sequence succumb to divergent transcriptional fates and that the same X-chromosome, once chosen, is maintained as the inactive X-chromosome in a stable, heritable manner over cellular division cycles highlight X-chromosome inactivation as an archetype of epigenetic transmission of transcriptional information.

The mouse is the preferred model organismal system for X-chromosome inactivation. Owing to the relatively slow nature of mouse embryonic progression and the ease with which we can dissect essentially every individual stage of the early mouse embryo allows X-inactivation

researchers to effectively and systematically investigate the mechanism of X-inactivation in the mouse. Two types of X-chromosome inactivation exist in the mouse, imprinted and random. Imprinted X-inactivation is the first type of X-chromosome inactivation to occur in the mouse embryos. During early mouse development, exclusive silencing (imprinting) of the paternally inherited X-chromosome occurs initially in all cells in the developing mouse embryo (Mak et al., 2004; Takagi et al., 1978; Kay 1994). Silencing of only the paternal-X implies that the two X-chromosomes are differentially marked in the germ cell to undergo divergent transcriptional fates in the zygote. Imprinted X-inactivation is subsequently maintained in the extra-embryonic tissues of the embryo, the trophectoderm and the primitive endoderm lineages (Takagi and Sasaki, 1975; West et al., 1977; West et al., 1978). At peri-implantation, and post-implantation, however, the cells in the epiblast will display a different pattern of X-chromosome inactivation (Mak et al., 2004). This type of X-inactivation in called random X-inactivation, and it is unique to the epiblast precursors that will ultimately develop in to the embryo proper. At E4.5 the cells of the inner cell mass will reactivate the paternal X-chromosome (Mak et al., 2004; Williams et al., 2011). These cells will then randomly choose to inactivate either the maternal-X or the paternal-X (Mak et al., 2004). Importantly, once one X-chromosome in a given epiblast precursor cell is chosen for inactivation, descendant cells will maintain that same X-chromosome as inactive through multiple mitotic divisions essentially for the lifetime of the organism.

In the developing mouse embryo, a set of temporal events occurs as imprinted X-inactivation is initiated and established. At the two-cell stage Xist RNA is transcribed. It will then physically coat in *cis* the paternally inherited X-chromosome (the future inactive-X) at the four-cell stage; Xist RNA marks the inactive-X (Brown et al., 1992; Clemson et al., 1996; Jonkers et al., 2008). By the eight-cell stage, members of the Polycomb group (PcG), proteins

involved in histone modifications and heterochromatin formation, are found enriched coincident with Xist RNA on the inactive-X (Mak, 2002; Erhardt et al., 2003; Okamoto et al., 2004; Plath et al., 2003; Silva et al., 2003). As embryogenesis proceeds, these factors associate on the inactive-X while genes are being silenced along the inactive (paternal) X-chromosome. Tsix expression from the active (maternal) X-chromosome occurs concomitant with Polycomb protein enrichment and silencing of genes on the future inactive X-chromosome (Lee 2000; Sado et al., 2001) (Figure 1.3). Imprinted X-inactivation, as well as the associated enrichment of the same epigenetic factors (Xist RNA, Polycomb proteins, etc.) along the inactive-X, will then be maintained in the extra-embryonic tissue of the developing embryo. The early embryonic events that typify X-linked gene silencing are widely believed to be tightly associated with the initiation and maintenance of the appropriate pattern of X-inactivation in the developing mouse embryo.

Considering that the two X-chromosomes in a shared nuclear space are fundamentally identical in sequence, what is it about the X-chromosome that leads to differential transcriptional fates between the paternal-X and maternal-X? This precise question was investigated initially through a series of molecular biology experiments (in both mouse and human samples), which identified a section of the inactive X-chromosome that is both necessary and sufficient for proper X-chromosome inactivation (Rastan et al., 1983; Rastan et al., 1985; Rastan et al., 1990; Takagi et al., 1980). This region, now known as the X-inactivation center (XIC), was identified through translocation studies (Rastan et al., 1983; Rastan et al., 1985; Rastan et al., 1990; Takagi et al., 1980). The X-inactivation center is replete with functional long non-coding RNAs (lncRNAs) in eutherian mammals (Figure 1.1). Much work has been done to elucidate the role of a multitude of long non-coding RNAs housed within the mouse X-inactivation center (see below). These RNAs are widely believed to orchestrate the epigenetic transcriptional states of the two X-

chromosomes in females and the single X-chromosome in males. Important insights came from the chromosomal translocations and truncations involving the X-chromosome in mouse embryos, mouse embryonic stem cells (mESCs), and human disorders (Rastan et al., 1983; Rastan et al., 1985; Rastan et al., 1990; Takagi et al., 1980). Thus, the XIC is strongly believed to be an integral portion of the mouse and human X-chromosome, due in part to the multitude of non-coding RNAs housed with in the XIC, some of which are considered to be necessary and sufficient for X-inactivation.

The XIC was originally defined via cytological studies of mouse and human cells harboring chromosomal translocations involving the X-chromosome. A comparative analysis of these translocations defined the XIC as a region on the X-chromosome required for heterochromatinization of the X-chromosome or X-autosome translocation products in female cells, as evidenced by the characteristic features of the inactive X-chromosome such as late replication timing or differential staining. One of the most well studied translocations is the mouse T16H Searle's translocation, a reciprocal translocation between the X-chromosome and chromosome 16. Assessments by replication timing and Kanda staining of the inactive-X suggested that only one of the translocation products, 16^{X}, but not the other, X^{16}, is able to undergo inactivation (Rastan, 1983; Takagi, 1980). These observations supported the idea that a region required for X-inactivation (i.e. the XIC) resides distal to the T16H breakpoint. A second mutation, termed HD3 in mouse ESCs, truncated the X-chromosome, but it did not impede X-inactivation (Rastan and Robertson, 1985). Thus, the X-inactivation center was delimited to the interval between the T16H and HD3 breakpoints. Initial banding studies of these chromosomes followed by genetic studies of rearranged X-chromosomes in mice, including the T16H translocation, narrowed the X-inactivation center to roughly eight centimorgans (CM) (Augui et

al., 2011; Brown S.D., 1991). Physical mapping experiments further pinpointed the mouse T16H breakpoint just proximal to the *Zfx* locus (Brown, 1991; Keer et al., 1990). The human X-inactivation center was additionally defined by X-chromosomal abnormalities. The XIC was therefore mapped distal to the *AR*, *CCG-1*, *RPS4X*, and *PHKA* loci and proximal to *Pgk1* (Brown C.J. et al., 1991; Brown S.D., 1991). A comparison of the X-inactivation center regions of mice and humans demonstrated that they both belonged to a conserved linkage group (Brown, 1991). Molecular studies subsequently showed that the X-inactivation center housed a number of long non-coding RNAs that play essential roles in the execution of X-inactivation. Of these, Xist, Tsix, Jpx/Enox, Tsx, Ftx, and RepA will be discussed.

Long Non-coding RNAs in the X-inactivation Center

Xist (Figure 1.1)

XIST was first identified based on hybridization of a human cDNA probe to female samples exclusively. This cDNA clone happened to map to the human X-inactivation center (Brown et al., 1991). The sex-specific expression and the location of the transcript within the XIC made XIST an intriguing candidate regulator of X-inactivation. The mouse orthologue, Xist, was identified shortly thereafter, and similarly found to show inactive X-specific expression (Borsani et al., 1991; Brockdorff et al., 1991). Xist RNA was subsequently found to physically coat the inactive-X chromosome in *cis*, and studies in mice demonstrated that Xist might remain associated with the inactive-X during mitosis (Brown et al., 1992; Clemson et al., 2006; Jonkers et al., 2008). The presence of Xist on the mitotic inactive-X supports its role as the transmitter of the epigenetic state of the inactive-X from one cell division cycle to the next. In human cells,

however, Xist RNA appears to dissociate from the X-chromosome during mitosis (Clemson et al., 2006; Hall and Lawrence, 2003; Hall et al., 2009).

Xist has been shown to be instrumental in both forms of inactivation found in mice, the primary experimental model system for X-inactivation: imprinted and random X-inactivation. During imprinted X-inactivation, the paternally inherited X-chromosome is preferentially inactivated. Imprinted X-inactivation initiates at the 4-8 cell-stage of zygotic development, and is accompanied by Xist induction only from the paternal-X and coating by the RNA in *cis* (Kalantry et al., 2009; Okamoto et al., 2004; Patrat et al., 2009). Following the blastocyst stage, at the peri-implantation stage of development, the paternal-X is reactivated in the epiblast lineage (Mak et al., 2004). These cells, which will give rise to all embryonic tissues, subsequently undergo random X-inactivation (Rastan et al., 1982). In random X-inactivation, either the maternally inherited or paternally inherited X-chromosome is stochastically selected for inactivation. The extra-embryonic lineages, on the other hand, maintain imprinted inactivation of the paternal-X throughout gestation.

Xist RNA is induced from the X-chromosome that will become inactivated at the onset of both imprinted and random X-inactivation. Following its transcriptional induction, Xist RNA also coats the inactive-X in both forms of inactivation. Moreover, mutational studies have shown that Xist is essential for both imprinted and random X-inactivation. Embryos that inherit a paternally transmitted Xist mutation die due to compromised extra-embryonic development, consistent with a defect in imprinted X-inactivation (Kalantry et al., 2009; Marahrens et al., 1997). Analysis of lineages subject to random X-inactivation in early embryos indicates that all cells of the epiblast lineage harboring a heterozygous Xist mutation will preferentially inactivate the wild-type X-chromosome (Marahrens et al., 1998). In differentiating female embryonic stem

cells (ESCs), which are derived from the epiblast lineage and are the favored *in vitro* model system for random X-inactivation, X-inactivation is also biased in cells heterozygous for a null Xist mutation (Penny et al., 1996). These biases in random X-inactivation suggest that Xist may be required in *cis* to bring about silencing of the chromosome from which it is expressed. However, Xist heterozygosity biases the choice of which X-chromosome becomes inactivated, such that the wild-type X is preferentially selected to become inactivated; the mutant-X therefore never has the option of being inactivated. Thus, strictly speaking, the biased choice step (see the Tsix section below for a discussion of X-chromosome choice) precludes knowing if Xist is required for inactivation itself.

The most convincing evidence supporting a role for Xist in triggering silencing is via transgenes ectopically expressing Xist (Plath et al., 2002; Wutz and Jaenisch, 2000; Wutz, Rasmussen, and Jaenisch, 2002). In cultured ESCs, Xist transgenes can variably induce silencing of reporter constructs or endogenous genes surrounding the insertion site. Silencing is dependent on the site of insertion, the expression level, copy number of the transgene, as well as the inclusion of Xist regulatory regions present in the transgene. For example, a multi-copy 450 kb mouse transgene, has been shown to induce Xist RNA expression and coating, as well as silencing of a LacZ reporter within the transgene in male ESCs and of four endogenous autosomal genes spread across the length of the transgene-bearing chromosome in fibroblast cells that were derived from adult chimeric mice generated by injecting the transgenic ESCs into wild-type embryos (Lee et al., 1996; Lee and Jaenisch, 1997). The conclusion of these studies was that the entire X-inactivation center function could be recapitulated by the 450 kb transgene sequence. Haploinsufficiency for large regions of autosomes, which would occur in these cells if the Xist transgene resulted in extensive silencing of endogenous autosomal genes, typically

results in early embryonic lethality, as indicated by studies of monosomic embryos and embryos bearing large chromosomal deletions (Baranov, 1983; Magnuson et al., 1985). The extensive contribution of transgenic ESCs to adult chimeric mice, which were estimated to show up to 90% chimerism, suggests that silencing of endogenous genes by this transgene may be weak (Lee et al., 1996).

While multi-copy transgenes can bring about Xist induction and potentially gene silencing, single copies of similarly large transgenes are unable to induce silencing in ESCs (Heard et al., 1999). A single-copy 460 kb X-inactivation center transgene including Xist showed negligible Xist induction in a number of adult cell types and was insufficient to silence a linked LacZ reporter cassette in mice, leading to the conclusion that the transgene does not contain sequences within it to induce Xist expression (Heard et al., 1996). The same animals, however, display imprinted Xist expression in early mouse embryos when the transgene is paternally inherited (Okamoto et al., 2005). Ectopic Xist RNA expression and coating correlates with transcriptional silencing of a gene within the transgene construct; whether endogenous genes near the insertion site are also silenced, though, is not known. The fact that the development of these animals is not defective argues against large-scale inactivation of endogenous loci that reside at or near the site of insertion. Moreover, given the failure of transgenic Xist expression in cells that undergo random X-inactivation, the ability of the same transgene to express Xist and silence during imprinted X-inactivation is paradoxical. This differential silencing ability may suggest divergent mechanisms that influence both the expression and function of Xist RNA during imprinted vs. random X-inactivation.

While large transgenes that harbor the Xist locus as well as other elements of the X-inactivation center are not always sufficient to induce silencing, single-copy inducible Xist

transgenes often are. For example, inducible Xist cDNA transgenes targeted to the *Hprt* locus on the X-chromosome or on autosomes are able to trigger silencing of endogenous genes (Wutz, Rasmussen, and Jaenisch, 2002; Jiang et al., 2013; Wutz and Jaenisch, 2000). This silencing function may, however, be due to the artificially high levels of Xist expression from these inducible transgenes. Some evidence also suggests that ectopic Xist induction is able to silence genes in some cell types *in vivo*, not just in *in vitro* cultured cells. In transgenic mice harboring an inducible Xist transgene, Xist expression is able to lead to ectopic X-inactivation in immature hematopoietic precursor cells, but not hematopoietic stem cells or mature cells (Savarese et al., 2006). Similar to studies of Xist transgenes in ESCs, this work suggests that there is a window of opportunity during development when Xist RNA is able to silence. Furthermore, this implies that this silencing function is closely linked to the differentiation state of cells and to the level of Xist expression (Savarese et al., 2006; Wutz and Jaenisch 2000).

Xist is thought to function by recruiting proteins to the prospective inactive-X to modify its chromatin structure and alter gene expression. Xist RNA expression is followed by the formation of a repressive chromatin (heterochromatin) state that excludes transcriptional machinery from the inactive-X, potentially by recruiting chromatin-modifying proteins (Chaumeil et al., 2006). These proteins are thought to help establish the heterochromatic and transcriptionally inert chromatin state characteristic of the inactive X-chromosome. Xist RNA is known to recruit Polycomb group proteins (PcGs, see below), a process in which the RepA non-coding RNA that is encoded within Xist may play a role (Kalantry et al., 2006; Kohlmaier et al., 2004; Schoeftner et al., 2006). The Polycomb group proteins form two complexes, Polycomb repressive complex 2 (PRC2) and Polycomb repressive complex 1 (PRC1). These complexes catalyze repressive histone modifications that are enriched on the inactive-X, such as

trimethylation of histone H3 lysine 27 (H3K27me3, PRC2) and ubiquitylation of lysine 119 in histone H2A (H2AK119ub, PRC1) (Plath et al., 2003; Simon and Kingston, 2009). While Polycomb group proteins are perhaps the best known of the Xist recruits, a number of other proteins are also localized to the inactive-X, potentially via Xist RNA. Ash2l, a member of the Trithorax group of chromatin modifying proteins, is recruited to the inactive-X following the onset of X-inactivation (Pullirsch et al., 2010). Paradoxically, the trithorax group proteins catalyze H3K4 trimethylation, a chromatin modification typically associated with active transcription (Steward et al., 2006). The recruitment of Ash2l coincides with the recruitment of SAF-A, a nuclear scaffolding factor (Pullirsch et al., 2010). The histone variant macroH2A, a variant associated with transcriptional repression, is enriched on the inactive-X as well (Constanzi and Pehrson, 1998; Perche et al., 2000; Rasmussen et al., 2000).

While important advances have been made in mechanisms underlying Xist function in X-inactivation, numerous crucial gaps remain. First, the temporal and lineage-specific function of Xist in X-linked gene silencing remains unclear; the Xist RNA appears to be required during precise developmental windows in both imprinted and random X-inactivation. Evidence shows that Xist is dispensable during the early initiation phase of imprinted X-inactivation for many X-linked genes assayed (Kalantry et al., 2009). Conversely, Xist is also not required to maintain random X-inactivation in differentiated cells, despite the persistence of Xist RNA coating in somatic cells (Brown and Willard, 1994; Csankovski et al., 1999; Wutz and Jaenisch, 2000). The data therefore suggest that Xist plays a tightly regulated, temporally specific role in controlling X-inactivation. Additionally, in both imprinted and random X-inactivation, changes in gene expression in the absence of Xist vary from gene to gene. Some genes are dependent more on Xist for silencing, while others are less so (Kalantry et al., 2009; Csankovski et al., 1999).

In addition to questions regarding the context-dependent requirement for Xist RNA in transcriptional silencing, how precisely Xist RNA acts as a catalyst for inactivation—i.e., through which of its recruited proteins—remains largely unknown. Both PRC2 and PRC1 that are recruited to the inactive-X by Xist are dispensable for random X-inactivation (Kalantry et al., 2006; Leeb et al., 2007; Schoeftner et al., 2006). Mutations in SAF-A, another recruit of Xist, disrupt both Xist localization and X-linked gene silencing in ES cells, though not absolutely (Hasegawa et al., 2010). Both SAF-A and Ash2l, which are recruited to the inactive-X after the onset of X-inactivation, are able to be recruited to the X-chromosome by mutant Xist transcripts that are unable to induce X-linked gene silencing (Pullirsch et al., 2010). Furthermore, a null mutation in macroH2A1 does not result in defective X-inactivation (Changolkar et al., 2007). MacroH2A1 has a paralogue, macroH2A2, which can potentially substitute for macroH2A1. In studies in which both macroH2A genes are knocked-down, X-inactivation is again normal (Tanasijevic and Rasmussen, 2001). These data suggest that additional *trans*-acting factors contribute to X-linked gene silencing. These may include additional proteins recruited by Xist RNA or proteins shuttled to the inactive-X through Xist-independent mechanisms.

Tsix (Figure 1.1)

The anti-sense transcript to Xist, Tsix, was identified following the observation that the region 3' to Xist influences X-chromosome counting, a process during which the cell senses the number of X-chromosomes present and determines how many, if any, to inactivate (Clerc and Avner, 1998). In the seminal study by Clerc and Avner, XX female cells inactivate a single X-chromosome, as expected. However, XO female cells that have lost the wild-type X-chromosome and which also harbor a 65 kb deletion 3' of Xist on their intact X-chromosome induce Xist RNA and initiate silencing of their single X-chromosome. The expectation is that

cells with a single X-chromosome should not activate Xist expression and undergo X-inactivation. Thus, in the absence of the Xist 3' region, the cells failed to correctly identify the number of X-chromosomes present (Clerc and Avner, 1998). The 65 kb deleted segment, therefore, normally controls X-chromosome counting by suppressing Xist.

Shortly after the study by Clerc and Avner, assessment of the Xist 3' region using RNA fluorescence *in situ* hybridization (RNA-FISH) detected an RNA anti-sense to Xist in both male and female ESCs (Lee et al., 1999). The transcript, termed Tsix (Xist spelled backwards) is expressed from both X-chromosomes prior to X-inactivation; however, upon differentiation of female ESCs that triggers X-inactivation, Tsix is downregulated from the Xist-expressing inactive-X and is expressed only from the active X-chromosome. Following the onset of X-inactivation, Xist and Tsix thus show mutually exclusive expression from the inactive and active X-chromosomes, respectively. Unlike Xist, however, Tsix RNA is expressed at relatively low levels and does not coat the X-chromosome.

Tsix transcription has been proposed to repress Xist at multiple key developmental time points. First, due to the early expression of Tsix, the Tsix RNA has been nominated as the instrument of the oocyte-derived imprint that inhibits Xist expression from the maternally inherited X-chromosome during the onset of imprinted X-inactivation (Lee, 2000; Sado et al., 2001). Continued expression of Tsix is then posited to maintain imprinted X-inactivation in the extra-embryonic tissues of the developing embryo. This function of Tsix is clearly illustrated by the death of embryos harboring maternally inherited Tsix mutations due to failed development of the extra-embryonic tissues (Lee, 2000; Sado et al., 2001).

Tsix also plays a prominent role in random X-inactivation. As part of its role as a repressor of Xist, Tsix has been proposed to function in the counting and choice processes of random X-inactivation. Random X-inactivation is though to be a linear three-step process, with counting, choice, and initiation as the three steps. In the first step, counting, the cell senses how many X-chromosomes it has (Lyon, 1962; Grumbach, 1963). If and only if there are two or more X-chromosomes does the choice step proceed. During the choice step, the cell selects which X-chromosome will remain active, and which will be inactivated. Following the choice step, X-inactivation initiates (Rastan, 1983).

Evidence for a counting step in X-inactivation is supported by observations of cells harboring abnormal complements of sex chromosomes. While normal XY male cells do not undergo X-inactivation, XXY nuclei initiate inactivation of one of their two X-chromosomes. Furthermore, in females, diploid cells with more than two X-chromosomes will inactivate all but one X, while XO cells do not undergo X-inactivation. This suggests that inactivation occurs, in part, as a function of the number of X-chromosomes in the cell. The autosomal complement also plays a critical role in X-chromosome counting. While diploid XX cells always have a single active and single inactive X-chromosome, tetraploid cells maintain two active- and two inactive-X chromosomes (Monkhorst et al., 2008; Webb et al., 1992). Tetraploid cells can therefore tolerate two active X-chromosomes. This suggests that both X-linked and autosomal factors contribute to X-chromosome counting, thereby mediating the decision as to whether to undergo X-inactivation.

Tsix was initially implicated as a counting factor based on a series of deletions adjacent to and upstream of the Tsix locus. These mutations can lead to aberrant Xist induction in differentiating XO female and XY male ESCs, a phenotype that is considered indicative of a

counting defect (Clerc and Avner, 1998; Cohen et al., 2007; Vigneau et al., 2006). The DXPas34 repetitive sequence, located adjacent to Tsix exon 3, has been identified as a regulator of counting based on these genetic studies. DXPas34 functions to enhance Tsix expression, thereby influencing X-chromosome counting (Cohen et al., 2007; Navarro et al., 2010).

Tsix is also suggested to control the choice of which X-chromosome will be inactivated. In Tsix-heterozygous female embryos and ESCs, the Tsix-mutant X-chromosome is observed to always be the inactive-X (Lee and Lu, 1999; Sado et al., 2001). There are two models that could explain this bias. The first and most popular model is a primary non-random X-chromosome choice model, where the Tsix-mutant X is always chosen for inactivation, due to ectopic Xist induction from the mutant-X at the onset of inactivation (Lee, 2000; Sado et al., 2001). A second possibility that could give rise to the observed bias is that random X-inactivation occurs normally, with both the wild type and the mutant X-chromosome are equally likely to undergo inactivation. Subsequently, Xist is ectopically expressed from the Tsix mutant X-chromosome if the WT X is initially chosen for inactivation. These cells would then rapidly be selected away due to two inactive X-chromosomes. Since inactivation of the wild-type X-chromosome is not observed at significant rates in differentiating Tsix-mutant ESCs and embryos, the model of primary non-random choice is favored. Incidentally, a secondary cell-selection effect has been invoked to explain X-inactivation patterns in Xist-heterozygous ESCs (Penny et al., 1996).

Numerous questions remain regarding the precise role of Tsix in X-inactivation. First, the role of Tsix in counting is highly contested. Mutations that abrogate Tsix RNA expression sometimes, but not always, lead to aberrant Xist induction (Lee, 2000; Luikenhuis et al., 2001; Morey et al., 2001; Sado et. al., 2002; Ohhata et al., 2006; Vigneau et al., 2006). Since Xist is not always induced in cells lacking Tsix, Tsix RNA itself may not be directly involved in counting.

The DXPas34 enhancer of Tsix has also been implicated in counting, and was initially presumed to act through Tsix RNA (Cohen et al., 2007; Navarro et al., 2010). While deletion of DXPas34 results in ectopic Xist induction that is consistent with a counting defect, an overdose of the DXPas34 genomic segment unexpectedly leads to failure of Xist induction (Lee, 2005). This genomic segment is therefore also proposed to function in counting by sequestering proteins that would normally activate Xist, i.e., by repressing Tsix.

Questions also remain about the mechanisms underlying Tsix-mediated regulation of Xist. DNA methylation and chromatin modifications of the Xist promoter region have been proposed as mechanisms through which Tsix may influence Xist expression. Tsix transcription across the Xist promoter indeed leads to DNA methylation and accumulation of repressive histone modifications at the promoter of Xist of the active X-chromosome (Navarro et al., 2006). Moreover, mutations that ablate Tsix RNA transcription lead to hypomethylation and altered histone modifications at the Xist promoter (Navarro et al., 2005; Navarro et al., 2006; Sado et al., 2009). DNA methylation changes induced by Tsix, however, may not be a primary mechanism for regulation of Xist, as loss of both Dnmt3a and Dnmt3b, the *de novo* methyltransferases shown to associate with Tsix, does not lead to defects in X-inactivation (Sado et al., 2004).

Understanding the regulation of Tsix expression itself is also a work in progress. Induction of Tsix is dependent on the recruitment of REX1, a pluripotency factor, to the Tsix locus (Navarro et al., 2010). Interestingly, *Rex1*$^{-/-}$ female and male mice are born at the same rate and show no defects in survival. This suggests that, while REX1 may contribute to Tsix regulation, it is not required for the establishment or maintenance of X-inactivation (Masui et al., 2008). Tsix regulation is also mediated by Xite, a non-coding RNA lying upstream of Tsix, that promotes Tsix expression (Ogawa and Lee, 2003). The DXPas34 repetitive element additionally

serves a dual role as both an enhancer and repressor of Tsix (Cohen et al., 2007). While these regulators of Tsix have been identified, the temporal requirement of these elements in regulating Tsix, Xist, and X-inactivation *in vivo* at the onset of both imprinted and random X-inactivation needs more scrutiny.

The Tsix RNA is also thought to be involved in the reactivation of the inactive paternal X-chromosome prior to random X-inactivation. The reactivation of the paternal-X is characterized by loss of Xist RNA coating in epiblast precursor cells, a process posited to be mediated by Tsix. However, no direct genetic evidence supports this assertion (Sheardown et al., 1997; Mak et al., 2004; Navarro et al., 2009; Nesterova et al., 2011). In contrast, reactivation is not disrupted in the epiblast lineage of embryos harboring paternally inherited Tsix mutations, suggesting that Tsix may in fact be dispensable during reactivation of the inactive-X (Kalantry and Manguson, 2006). Moreover, surprisingly, X-linked gene reactivation appears to occur prior to the loss of Xist coating during reactivation (Williams et al., 2011). If Tsix is involved in Xist repression and X-reactivation, how Tsix is induced from the inactive paternal-X is also unclear. Careful analysis of the expression and function of Tsix in these early embryonic stages in future studies may help elucidate the precise role of the Tsix lncRNA in these processes.

Jpx/Enox (Figure 1.1)

Jpx, also known as Enox (*E*xpressed *n*eighbor *o*f *X*ist), is a non-coding RNA whose transcription starts around 10kb upstream of Xist and in the antisense orientation to Xist (Johnston et al., 2002). The study of Jpx/Enox was inspired by the observation that a transgene containing an 80kb region of the X-inactivation center, including Xist, Tsix, and Xite, is not capable of inducing Xist and potentially causing inactivation, suggesting that additional factors

surrounding the Xist locus are required to recapitulate X-inactivation center function (Lee et al., 1999b). Jpx/Enox has been proposed to serve as an Xist activator and is required for inactivation to occur (Tian et al., 2010; Sun et al., 2013).

Jpx is expressed both in male and female ESCs, and becomes upregulated over the course of differentiation. This upregulation mimics Xist induction during differentiation of female ESCs and was used to suggest the involvement of Jpx RNA in Xist regulation. Jpx was subsequently shown to escape inactivation, consistent with its increased expression in females (Tian et al., 2010). However, Jpx is upregulated in both differentiating male and female ESCs, which may suggest an X-inactivation independent role.

To functionally address the role of Jpx, Tian et al. deleted Jpx in male and female ESCs. In males, Jpx loss did not display a marked effect on expression of X-linked genes. Female ESCs heterozygous for Jpx, however, showed a severe phenotype upon differentiation. The cells have growth defects, high levels of cell death, as well as a significant decrease in nuclei with Xist RNA coating (Tian et al., 2010). The conclusion drawn from these data is that female cells expressing only half their normal levels of Jpx (equal to that in males) are deficient in Xist induction. Of note, the mutant female cells do display some low-level Xist expression, suggesting Jpx-independent activation of Xist in female cells.

In over-expression studies, a Jpx transgene rescued defective Xist induction and cell death in heterozygous Jpx mutant female cells (Tian et al., 2010). Both the growth phenotype, as well as levels of Xist expression, were brought back to normal with exogenous Jpx. These data therefore suggest that Jpx can quite unusually act in *trans* to activate Xist.

In wild-type ES cells, the same transgene leads to very low levels of ectopic Xist induction in both males and females (Sun et al., 2014). Tested with two different promoters, increased Jpx expression concorded with higher Xist expression, suggesting that Jpx activation of Xist works in a dose-dependent manner. It should be noted, though, that the Jpx transgene-mediated ectopic induction of Xist in male ESCs observed by Sun et al., was not recapitulated in an independent study (Jonkers et al., 2009).

If Jpx activates Xist, then it should antagonize Tsix function, which normally represses Xist. In agreement, cells heterozygous for both a Jpx and a Tsix mutation on the same X-chromosome do not appear to suffer the same degree of cellular lethality that Jpx heterozygosity alone causes. Moreover, Xist expression in these cells is restored (Sun et al., 2013). Thus, if the Xist repressor Tsix is absent then Jpx is not needed to activate Xist.

Further experiments in which Tsix and Jpx levels are modulated support the opposing activities of the two lncRNAs in Xist regulation. Male Tsix-mutant ESCs displayed low levels of ectopic Xist expression. The addition of a genomic Jpx transgene increased the level of Xist expression in Tsix-mutant cells (Sun et al., 2013). The level of Xist induction by Jpx in a Tsix-mutant male background is also greater than that seen by Sun et al. in wild-type male cells. Nevertheless, the increase in Xist coating is relatively small, even though Jpx levels are doubled and equal to that of females. This finding therefore reinforces the idea that activators in addition to Jpx RNA function to upregulate Xist during X-inactivation. It appears that the effect Jpx has on Xist expression is most obvious in a Tsix-mutant background. The Xist inhibitory effects of Tsix seem to overpower potential Xist activating function of Jpx.

The mechanism by which Jpx is proposed to activate Xist is through the zinc finger protein CTCF (Sun et al., 2013). CTCF has binding sites upstream of the Xist promoter, and CTCF binding is thought to normally inhibit Xist expression. In male ESCs CTCF binding remains constant upon differentiation. However, in female cells CTCF binding is reduced on the inactive-X early during differentiation, which corresponds to the period when inactivation is commencing. Increasing levels of CTCF reduced Xist expression, but a Jpx transgene restored normal levels of Xist RNA. Sun et al., therefore conclude that Jpx RNA and the Xist promoter DNA may compete for binding of CTCF, and Jpx is required to remove CTCF in order for Xist expression to occur. Consistently, Sun et al. (2013) also show that CTCF binds Jpx RNA in a dose-dependent manner. A conclusive role for Jpx in Xist activation, though, awaits genetic loss- and gain-of-function studies in mice.

Tsx (Figure 1.1)

The Tsx non-coding RNA is transcribed approximately 40kb from the 3' end of Xist in the antisense orientation to Xist (Simmler et al., 1996). Tsx is expressed at high levels in the testes and to a much lesser extent in the adult male and female brain (Anguera et al., 2011).

Once thought to be protein coding, the Tsx (Testes-specific X-linked) gene was postulated to produce a 144 amino acid protein of almost 16 kDa (Simmler et al., 1996). However, immunostaining with anti-Tsx antiserum later showed premeiotic, testes specific staining that is inconsistent with Tsx mRNA expression (Cunningham et al., 1998). Based on this fact, a recent study has looked more closely at the coding potential of the Tsx locus (Anguera et al., 2011). Anguera et al. tested whether putative Tsx open reading frames can express proteins. No protein was detected from multiple constructs containing Tsx ORFs, leading to the

conclusion that Tsx may actually be non-coding. A major caveat of this interpretation, though, is that absence of evidence does not equal evidence of absence.

In order to study the affects of Tsx *in vivo*, Anguera et al. also generated Tsx-mutant mice. Homozygous deletion of Tsx led to a small decrease in fertility of females that resulted in a sex-ratio distortion favoring, paradoxically, female offspring. Hemizygous males, on the other hand, did not display decreased fertility. However, during pachytene-stage of spermatogenesis, when Tsx expression is normally at its highest, mutant male testes did show unusually high levels of apoptosis.

Mice exhibit a significant increase in Tsx expression during meiosis I of spermatogenesis (Anguera et al., 2011). This is the stage of male meiosis during which meiotic sex chromosome inactivation (MSCI) occurs. In MSCI, the X and Y-chromosomes are made transcriptionally inert, due to the lack of synapsis along most of the X and Y-chromosomes (Turner et al., 2005).

Despite the stringent silencing of X-linked genes during MSCI, Tsx is one of the few X-chromosomal loci that escape MSCI (Namekawa et al., 2006). It could be postulated from this observation that Tsx may play a role in MSCI; however, the apoptotic spermatocytes of Tsx-mutant males do not show a defect in MSCI (Anguera et al., 2011). The cause of apoptosis in these mutant cells is unidentified, although it doesn't seem to be MSCI related, and the observed cell death does not cause male fertility defects.

The close proximity of Tsx to the Xist locus suggested involvement of Tsx in X-inactivation. Loss-of-function studies in ES cells in fact support a role for Tsx in Xist regulation (Anguera et al., 2011). Both female and male ESCs express Tsx in the undifferentiated state, but female expression is significantly higher than in males. This is consistent with two Tsx alleles in

females vs. the one in males. Upon ESC differentiation, Tsx is downregulated in females and this coincides with Xist upregulation and initiation of X-inactivation. Both female and male Tsx-mutant ESCs show an increase in Xist coating on the active-X in small numbers of nuclei (Anguera et al., 2011). This finding suggests that Tsx may play a role in repressing Xist expression. Tsix, which represses Xist expression, is also greatly reduced in Tsx-mutant cells. The downregulation of Tsx, along with the position of Tsx just upstream of Tsix, suggests that Tsx may serve to activate Tsix RNA expression. Thus, Tsx mutations may only indirectly lead to Xist upregulation, by causing a decrease in Tsix expression.

X-inactivation studies have yet to be done in Tsx-mutant mice. However, the female fertility defect seen in Tsx-homozygous mutants leads to a relative increase in female offspring, making it unlikely that the problem is caused by an X-chromosome inactivation defect.

Ftx (Figure 1.1)

The Ftx transcript, transcribed in the sense orientation to Xist, is posited to activate *Xist*. Ftx is localized about 150 kb upstream of *Xist*, is roughly 63 kb in length, and is composed of 15 exons, (Chureau et al., 2011). The Ftx genomic region generates various isoforms through a combination of different promoters, alternative splicing, and transcriptional termination. Recent experimental data also indicate the presence of two micro RNA (miRNA) clusters, miR-374 and miR-471, embedded within intron 12 of Ftx (Miska et al., 2004 and Suh et al., 2004). Ftx is expressed ubiquitously in adult tissues and the transcript is restricted to the nucleus (Chureau et al., 2011).

Ftx lncRNA is upregulated during the onset of X-inactivation in differentiating female ESCs. Moreover, Ftx partially escapes X-inactivation, but is expressed at lower levels from the

inactive X-chromosome compared to the active X-chromosome (Chureau et al., 2011). Ftx is also found to escape imprinted X-inactivation in female extra-embryonic endoderm (XEN) stem cells (Kunath et al., 2005 and Mak et al., 2002).

Through a genetic deletion, Chureau et al. functionally characterized Ftx in male ESCs. An interesting pattern was noted upon *Ftx* deletion in that transcription of genes in the vicinity of *Ftx* whose orientation was in the same direction as *Ftx* (and *Xist*), but not ones transcribed in the opposite orientation, were affected. *Ftx* deletion led to a significant reduction in expression of surrounding genes, with a greater effect seen for genes closer to *Ftx*. This suggests a preferential role for Ftx in regulating genes that lie near it and which are transcribed in the same 5' to 3' orientation as *Ftx*. Of note, absence of Ftx lncRNA led to a significant decrease in Xist RNA levels and a change in the DNA methylation profile at the 5' end of *Xist* (Chureau et al., 2011). It should be pointed out that *Xist* expression is normally quite low in male ESCs and is not upregulated upon differentiation. Therefore, a decrease in Xist lncRNA levels upon *Ftx* ablation is challenging to interpret. *Ftx* deletion in female ESCs would be more informative, since Xist expression is normally induced upon differentiation in female ESCs.

In *Ftx* mutant ESCs, DNA methylation is increased at a CpG island in exon 1 of *Xist*; this increase in DNA methylation coincided with reduced histone H3 lysine 4 dimethylation (H3K4me2) levels, a mark of transcriptional activation, at the *Xist* promoter. These findings suggested that Ftx lncRNA plays a part in configuring the chromatin architecture in and around the *Xist* locus. The *Ftx* genomic region also harbors histone H3 lysine 9 (H3K9me2) and lysine 27 (H3K27me3) methylation marks that are associated with transcriptional silencing (Heard et al., 2001; Rougeulle et al., 2004). Both of these marks, however, were found to be largely

unaltered in the absence of Ftx in ESCs. Ftx lncRNA therefore appears to regulate transcription by modulating the surrounding chromatin environment, including *Xist*.

While much is known about *Ftx* expression and function, several crucial gaps remain. For example, if *Ftx* in fact normally activates *Xist* expression in females, then its over-expression should be expected to induce *Xist* in males. It is also unclear to what extent *Ftx* functions in a direct vs. an indirect manner. Genomic deletions themselves are acute chromatin modifying events; it is difficult to rule out that the histone modification changes observed upon *Ftx* deletion may in fact be due the acute removal of a segment of the *Ftx* genomic locus, rather than via loss of the Ftx lncRNA per se. The structural alterations in chromatin may then cause transcriptional changes nearby. More subtle mutations that abrogate expression but leave the locus relatively unchanged may address this conundrum. Finally, it will be important to validate any implied function via cell culture studies through loss- and gain-of-function experiments in animals.

RepA (Figure 1.1)

An obvious extension to the discovery of lncRNAs in the X-inactivation center is that proteins must be recruited by these lncRNAs to bring about epigenetic gene regulation. Xist lncRNA has been long postulated to interact with chromatin modifiers to exert its function (Brown et al., 1992; Penny et al., 1996; Plath et al., 2008); however, the physical interaction of proteins with Xist has only recently been described. In 2008, Zhao et al. identified direct interactions between Xist RNA and Polycomb group proteins EZH2, SUZ12, and EED, members of the Polycomb Repressive Complex 2 (PRC2) (Zhao et al., 2008). These RNA-protein complexes are not static; rather they seem to follow a time-dependent spread along Xist RNA over the course of X-inactivation during ESC differentiation. PRC2 proteins initially bind the 5’

end of Xist RNA and are then encompassed to the more 3' regions of Xist RNA (Zhao and Science, 2008). They also assessed loading of PRC2 onto chromatin/*Xist* genomic region via DNA ChIP, which displayed a time dependent enrichment on DNA over the course of 6 days of differentiation (Zhao et al., 2008). The 5' region of *Xist* Zhao et al. examined contained within it a novel promoter activity. This segment of *Xist*, which harbors a repeat sequence termed 'A' repeat, was found to encode a distinct transcriptional unit, termed *RepA*, in the same transcriptional orientation as *Xist*. RepA RNA spans bp 300-1948 in exon 1 of *Xist* and is expressed prior to *Xist* upregulation (Zhao et al., 2008). RepA RNA interacts with PRC2 proteins prior to PRC2 binding to Xist. The deposition of PRC2-catalyzed H3-K27me3, a mark of transcriptional silencing, at the 5'end of Xist paradoxically led to Xist upregulation. In agreement with a role for the Polycomb group in inducing *Xist* expression, shRNA knockdown of EZH2 or EED led to a reduction in Xist levels and decreased H3-K27me3 enrichment in differentiating female ESCs (Zhao et al., 2008). *Xist* RNA then itself is posited to bind PRC2 and thereby promulgate the spread of H3-K27me3 across the X-chromosome, leading to chromosome-wide inactivation. Of note, however, absence of PRC2 function in the epiblast lineage, the source of ESCs, in developing female embryos does not diminish *Xist* expression.

To functionally investigate the RepA element, Zhao et al. set out to disrupt RepA via shRNA-mediated knockdown. Depletion of the RepA RNA led to reduced Xist RNA levels and attenuated enrichment of H3-K27me3 on the inactive-X. A caveat in these experiments is that an shRNA targeting RepA is expected to also impact Xist RNA, since the *RepA* element is wholly contained within the *Xist* locus, and, importantly, is transcribed in the same orientation to Xist. Thus, it is difficult to rule out that a shRNA against RepA is not also knocking-down Xist. A central role for RepA RNA in the recruitment of PRC2 to Xist is also questioned by the

observation that PRC2 can be recruited to Xist in the absence of RepA (Plath et al., 2003). Thus, it is possible that other sequences within *Xist* can recruit PRC2, in tandem with or independent of *RepA*.

The discovery and characterization of non-coding RNAs within the X-inactivation center has engendered much enthusiasm. Starting with the discovery of Xist in 1991, these non-coding RNAs have shed much light on our understanding of both long non-coding RNA function and X-inactivation. There is still much to learn. How do these lncRNAs mechanistically recruit proteins to the inactive-X? How do chromatin modifying complexes actually configure the chromatin environment of the inactive-X to a heterochromatic state. Are there unidentified lncRNAs that play an integral role in the X-chromosome inactivation process? Future experimental investigation will answer such questions and elucidate the true functions of lncRNAs in X-chromosome inactivation.

The Relationship Between X-chromosome Inactivation and Polycomb Group Proteins

Not only are lncRNAs thought to be vital to the X-chromosome process, a plethora of proteins and chromatin modifying complexes are also known to interact with the inactive X-chromosome (Nakajima and Sado, 2014; Plath et al., 2003; Silva et al., 2003). One of the key events during X-inactivation initiation (both imprinted and random) is the recruitment and physical enrichment of chromatin modifying protein complexes on the future inactive X-chromosome (Figure 1.2 and 1.3). It is largely believed that one function of lncRNAs expressed from the XIC is to bind to and recruit chromatin modifying complexes to the inactive-X. The Polycomb group proteins (PcGs) comprise one prominent class of chromatin modifying complexes (Jurgens, 1985). These protein complexes consist of a set of evolutionary conserved

epigenetic developmental regulators first identified in *Drosophila melanogaster* (Pirrotta, 1997; Ng et al., 2000; Lewis, 1978; Jurgens, 1985). They were found to be necessary in maintaining transcriptional repression of *Hox* loci once silencing of *Hox* loci was triggered by other repressive factors (i.e. Hunchback and Krupple) during *Drosophila* embryogenesis (Ng et al., 2000; Simon, 1995; Pirrotta, 1997; Pirrotta et al., 1998; Shao et al., 1999; van der Vlag et al., 1999; Tie et al., 1998). For example, Hunchback was shown to directly repress *Ubx* (a homeotic gene housed within the bithorax complex (BX-C) *Hox* locus) in early stages of *Drosophila* embryogenesis to ensure *Ubx* silencing in regions outside the normal *Ubx* expression domain (Zhang and Bienz, 1992). During later stages of embryogenesis, the Polycomb proteins maintained *Hox* loci (to include *Ubx*) silencing. This combined activity of early repressors and subsequent maintenance of silencing through Polycomb activity allowed for proper segmental specification during *Drosophila* anterior-posterior (A-P) axial patterning (Ng et al., 2000; Simon, 1995; Pirrotta, 1997; Pirrotta et al., 1998; Shao et al., 1999; van der Vlag, et al., 1999; Tie et al., 1998; Jurgens, 1985; Lewis, 1978).

Roughly 15 Polycomb genes have been identified (Simon et al., 2002). Through cloning and characterization experiments, much evidence suggests that Polycomb proteins (PcGs) function in large multimeric protein complexes (Bornemann et al., 1996; Brunk et al., 1991; DeCamillis et al., 1992; Gutjahr et al., 1995; Jones et al., 1993). Moreover, prior work indicates some of these complexes can be quite heterogeneous. Different complexes appear to house specific proteins (Ng et al., 2000; Decamillis et al., 1992; Franke et al., 1992; Lonie et al., 1994; Martin et al., 1993; Strutt et al., 1997). In turn these distinct protein complexes likely exert differential activities at their respective target loci to ensure maintenance of gene repression in a developmental and tissue specific manner. Such observations further suggested that separate

Polycomb group protein complexes may silence genes through independent mechanisms. Evidence for these ideas stem from the differential localization of PcGs at polytene chromosomes in *Drosophila* (Decamillis et al., 1992; Franke et al., 1992; Lonie et al., 1994; Martin et al., 1993; Strutt et al., 1997). Historically, many Polycomb proteins are widely held to serve an essential function by guaranteeing gene repression in a temporal and spatial specific manner during *Drosophila* embryogenesis (Pirrotta, 1997; Ng et al., 2000; Lewis, 1978). Thus PcGs and the higher-order heterogenic multimeric complexes they assume represent a core constituent of the cellular epigenetic machinery.

In Polycomb mutants, flies were observed to have misexpression of *Hox* genes outside of the normal A-P domains (McKeon and Brock, 1991; Simon et al., 1992; Struhl and Akam, 1985). Such *Hox* gene misexpression is referred to as a homeotic transformation. Normally segment specific expression of genes within the *Antennapedia* complex (ANT-C) and *Bithorax* complex (BX-C) is required for proper segmental specification (Lewis, 1978; Kaufman et al., 1990; Lewis et al., 1980a; Lewis et al., 1980b; Waikimoto and Kaufman, 1981; Karch et al., 1985; Sanchez-Herrero et al., 1985). Many mutations affected genes within the ANT-C and BX-C complexes of *Hox* loci; however, the phenotypic outcomes of some PcG mutants were found to be genetically distinct. For example, mutation in *ph* (polyhomeotic) led to an epidermal phenotype, which was not the case for many other PcG mutants (Dura et al., 1987). Furthermore, mutation of the H3-K27me3 histone methyltransferase *E(z)* (enhancer of zeste) led to de-repression and spatial misexpression of *Ubx*, a gene within the BX-C, as well as other *Hox* loci inside the BX-C cluster (Pengelly et al., 2013). These results were recapitulated using histone and histone variant mutations (H3K27R and H3.3K27M), which suggests that the histone residues themselves (modified by specific Polycomb proteins) are important for proper silencing of Polycomb target

loci (Pengelly et al., 2013; Herz et al., 2014). The histone modifications catalyzed by specific PcGs thus potentially represent a major conduit through which epigenetic transcriptional memories are passed on to daughter cells over multiple mitotic divisions. *Pc* genes, their protein products, and the post-translational histone modifications they exert function as negative regulators of target gene expression, including genes within *Hox* clusters.

The above data suggest that although there are many PcG loci, they likely possess a multitude of different functions. Support from this stems from heterogeneous nuclear distribution of PcG protein products as well as the complexes they form. Such complexes were observed to have different functions, as mutations of various PcGs did not yield identical homeotic transformations (Dura et al., 1987; Decamillis et al., 1992; Franke et al., 1992; Lonie et al., 1994; Martin et al., 1993; Strutt et al., 1997; Pengelly et al., 2013; Herz et al., 2014). We cannot however exclude the possibility that some Polycomb proteins have redundant function. For instance, in mammals, we know that EZH1 and RING1A are homologues of EZH2 and RING1B, respectively, which serve to carry out similar functions (i.e. EZH2/1 are both H3-K27me3 histone methyltransferases and RING1A/B are both H2A-K119ub1 histone ubiquityltransferases) (Kerppola, 2009). Therefore care needs to be given when considering unique and redundant activities of all Polycomb proteins.

We now know that Polycomb proteins are catalogued into two major complexes, Polycomb repressive complex 2 (PRC2), also known as an EED-EZH2 complex, and Polycomb repressive complex 1 (PRC1). Mammalian PRC2 comprises the core subunits Enhancer of Zeste Homologue 2 or Enhancer of Zeste Homologue 1(EZH2/EZH1), Suppressor of Zeste 12 (SUZ12) and Extra-embryonic Ectoderm Development (EED), derived from their *Drosophila* homologues Enhancer of Zeste (E(z)), Suppressor of Zeste 12 (Su(z)12), and Extra Sex Combs

(Esc), respectively (Cao et al., 2002; Czermin et al., 2002; Kuzmichev et al., 2002; Müller et al., 2002; Tie et al., 2001). PRC1 is a more heterogeneous complex, one containing a variety of different protein components highly based on tissue and cellular contexts. It contains the proteins Polycomb (Pc), Polyhomeotic (Ph), Posterior Sex Combs (Psc), and dRing as well as additional polypeptides (Saurin et al., 2001; Shao et al., 1999). EZH2, the catalytic subunit of PRC2, serves to tri-methylate Histone H3 at lysine residue 27 (H3-K27me3) (Margueron and Reinberg, 2001; Di Croce and Helin, 2013; Zhang et al., 2015). CBX family members are then believed to read H3-K27me3 residues via their chromodomains and recruit PRC1, the mammalian version of which houses BMI1, MEL18, RING1A or RING1B, and one of a variety of the CBX family members (Bernstein et al., 2006). PRC1 will monoubiquitinate Histone H2A at lysine residue 119 (H2A-K119Ub1) (Wang et al., 2004). It is generally thought this then will lead to facultative heterochromatin formation and hence transcriptional inactivation (Bernstein et al., 2006).

One of the remaining areas of much debate in Polycomb research is the conserved mechanism(s) by which PcGs are recruited to target loci to exert their repressive functions. Polycomb proteins are historically recruited to their target loci by conserved recognition sequences in DNA. This is readily evident in *Drosophila*, where a great deal of investigation identified DNA elements, known as Polycomb response elements (PREs), to which PcGs bind (Mueller and Kassis, 2006). PREs are widely held to be cis-regulatory elements (CREs) of PcG target genes that serve as part of a recruiting mechanism for Polycomb repressive complexes (Mueller and Kassis, 2006). Despite much work, the extent to which PREs are conserved or not through mammals and the function of putative mammalian PREs remains poorly understood (Bauer et al., 2015). It is possible that mammalian PcGs are targeted to genomic loci by other means. One hypothesis is that PRC2 is a genome surveyor. It actively and transiently interacts

with nascent transcripts all throughout the genome, only to take up residence at genes it needs to silence in a developmental and tissue specific manner. The "decision" to remain at some loci or to pursue other loci is potentially based on the surrounding chromatin environment, which warrants silencing of some genes, but obviates that need at other genes. This posits a promiscuous behavior for PRC2, one in which PRC2 can transiently bind to many nascent mRNA species (Cifuentes-Rojas et al., 2014; Davidovich et al., 2015).

An integral function of Polycomb repressive complexes (PRCs) is to post-translationally modify the N-terminus of histone tails. Modified histones within chromatin are thought to propagate epigenetic transcriptional states across cell division (Margueron and Reinberg, 2011; Zhang et al., 2015). The histone H3-K27me3 modification constitutes one key chromatin modification. To reiterate, H3-K27me3 is deposited at target loci by the Polycomb repressive complex 2 (PRC2) (Cao et al., 2002; Czermin et al., 2002; Kuzmichev et al., 2002; Müller et al., 2002; Tie et al., 2001). In mammals, PRC2 and H3-K27me3 are implicated in many physiological processes, including pluripotency, differentiation, tumorigenesis, and X-chromosome inactivation (Brockdorff, 2013; Laugesen and Helin, 2014; Margueron and Reinberg, 2011).

The focus of my thesis work is Polycomb repressive complex 2. Mammalian PRC2, as discussed above, consists of the core components EZH2 or EZH1, EED, and SUZ12 (Cao et al., 2002; Kuzmichev et al., 2002). EZH2 is the major enzymatic subunit of PRC2 that ultimately catalyzes H3-K27me3 (Margueron and Reinberg, 2011; Di Croce and Helin, 2013; Zhang et al., 2015). The PRC2 protein EED then acts to propagate H3-K27me3 at target loci (Margueron et al., 2009). PRC2 (through EED) binds to pre-deposited H3-K27me3 in S-phase and in turn stimulates EZH2 to further catalyze H3-K27me3 on newly deposited histones (Hansen et al.,

2008; Margueron et al., 2009). EED is also believed to be necessary for H3-K27me3 catalysis; without EED, H3-K27me3 catalysis is drastically impaired and the protein levels of the other core PRC2 proteins are reduced, indicating that PRC2 does not assemble (Montgomery et al., 2005). Thus, EED is required for PRC2 stability and robust enzymatic catalysis of H3-K27me3.

X-chromosome inactivation has provided essential insights into PRC2 function (Brockdorff, 2013; Froberg et al., 2013; Pontier and Gribnau, 2011). The co-localized enrichment of Polycomb proteins with the Xist RNA (Figure 1.2 and 1.3) at the interface of X-chromosome inactivation initiation has led to the idea that lncRNAs participate by recruiting proteins to the inactive X-chromosome. Indeed, experimental evidence suggests that Xist RNA recruits PRC2 to the inactive-X chromosome (Zhao et al., 2008). Xist RNA is only transcribed from the inactive X-chromosome and is necessary for stable X-inactivation (Marahrens et al., 1997; Penny et al., 1996, Kalantry et al., 2009). However, the true requirement of PcGs, through functional genetic studies, in X-chromosome inactivation remains unknown. At the onset of both random and imprinted X-inactivation, PRC2 proteins and H3-K27me3 are enriched on the inactive X-chromosome (Mak, 2002; Erhardt et al., 2003; Okamoto et al., 2004; Plath et al., 2003; Silva et al., 2003). By virtue of its early enrichment on the inactive-X and its gene silencing function, PRC2 is thought to be critical for the stable silencing of X-linked genes (Plath et al., 2003; Silva et al., 2003). In agreement with this idea, loss-of-function studies suggest that PRC2 is required in imprinted mouse X-inactivation (Wang et al., 2001). The extra-embryonic tissues in differentiating *Eed*$^{-/-}$ mouse embryos and *Eed*$^{-/-}$ trophoblast stem cells (TSCs) are defective in maintaining silencing of paternal X-linked genes (Kalantry et al., 2006a; Wang et al., 2001). Although EED loss appears to compromise X-inactivation, whether each subunit of PRC2

is required for triggering silencing and propagating an inactive-X *in vivo* and *in vitro* is not fully known.

Considerable work has already been accomplished to elucidate the requirement of PcGs in random X-inactivation and epigenetic transcriptional regulation *in vitro* with mouse embryonic stem cells (mESCs). For instance evidence of an interaction between EZH2 and a short repeat of Xist (RepA) has been established (Zhao et al., 2008). Moreover, *Ezh2* knockdown led to reduced Xist RNA levels, thereby suggesting a positive role for PRC2 in X-inactivation in ESCs (Zhao et al., 2008). EED mutation, however, did not appear to overtly confer a defect in random X-inactivation *in vivo*; mouse embryos devoid of functional EED are able to initiate random X-inactivation normally (Kalantry et al., 2006b). These data conversely exclude a role for PRC2 and H3-K27me3 in random X-inactivation. To gauge activity of other PcGs in random X-inactivation, different research groups looked at the involvement of core PRC1 components. In mESCs, EED absence led to loss of MPH1 and MPH2, but continued RING1B (H2A-K119ub1 histone ubiquityltransferase) enrichment on the inactive-X (Shoeftner et al., 2006). They also found that PRC2 (i.e. EED) deficient ESCs were still able to robustly catalyze H2A-K119ub1 on the inactive-X, thus indicating that random X-inactivation may be sufficiently executed through PRC2 independent means (Shoeftner et al., 2006). Although the core catalytic PRC1 subunit (RING1B) and its catalytic readout (H2A-K119ub1) are enriched on the inactive-X as random X-inactivation ensues in differentiating mouse ESCs (Fang et al., 2004), it remains to be fully known if RING1B, H2A-K119ub1, or other PRC1 components are genetically required for random X-inactivation. Future work will reveal more about the roles for PRC1 and PRC2 in random X-inactivation.

The preceding data only go as far to potentially explain the role, or lack thereof, of Polycomb proteins in random X-chromosome inactivation. The precise contribution of Polycomb group proteins to imprinted X-chromosome inactivation, the other key form of X-inactivation, remains very poorly understood. Although the molecular and cytological events that characterize random X-inactivation are also found to typify imprinted X-inactivation, it is not definitively known if the both types of X-inactivation require the same epigenetic factors. The extent to which PRC2 components are suggested to be involved in initiating mouse imprinted X-chromosome inactivation comes from a series of observations that these Polycomb genes are expressed and that their protein products are physically enriched on the future inactive X-chromosome during the early phases of X-chromosome inactivation in mouse embryogenesis. Such an early accumulation of Polycomb proteins on the inactive-X led me to hypothesize that PRC2 components execute epigenetic gene silencing during imprinted X-inactivation initiation. Here, I further defined the function of key components of PRC2 as well as one of its closely associated factors, Xist RNA, in epigenetic transcriptional repression through investigations of imprinted mouse X-chromosome inactivation. In the following chapters, I describe below work on three projects to address the role of Polycomb proteins and the *Xist* locus in imprinted X-inactivation. By critically examining the intricate role of PRC2 and Xist RNA in imprinted X-inactivation, I gained insight into how these epigenetic factors function broadly, including roles in initiating epigenetic transcriptional states both in normal embryonic development and potentially in human disease.

Figure 1.1

Figure 1.1. Adopted from: Maclary, E.*, Hinten, M.*, Harris, C.*, Kalantry, S. (2013). Long non-coding RNAs in the X-inactivation center. Chromosome Res. *21*, 601–614.

*equal author

Figure 1.1. Key long non-coding RNAs in the X-inactivation center.

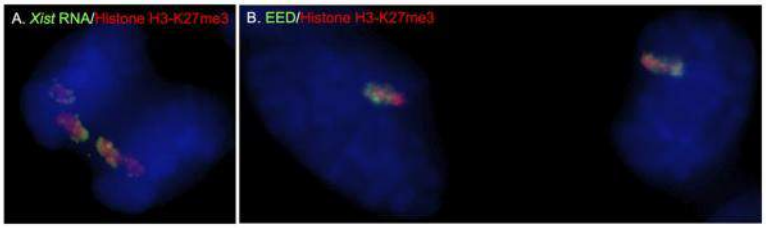

Figure 1.2

Figure 1.2. Adopted from: Maclary, E.*, Hinten, M.*, Harris, C.*, Kalantry, S. (2013). Long non-coding RNAs in the X-inactivation center. Chromosome Res. *21*, 601–614.

*equal author

Figure 1.2. Enrichment of Xist RNA, Polycomb group protein EED, and H3-K27me3 on the inactive X-chromosome during mitosis. DAPI stains the chromosomes blue.

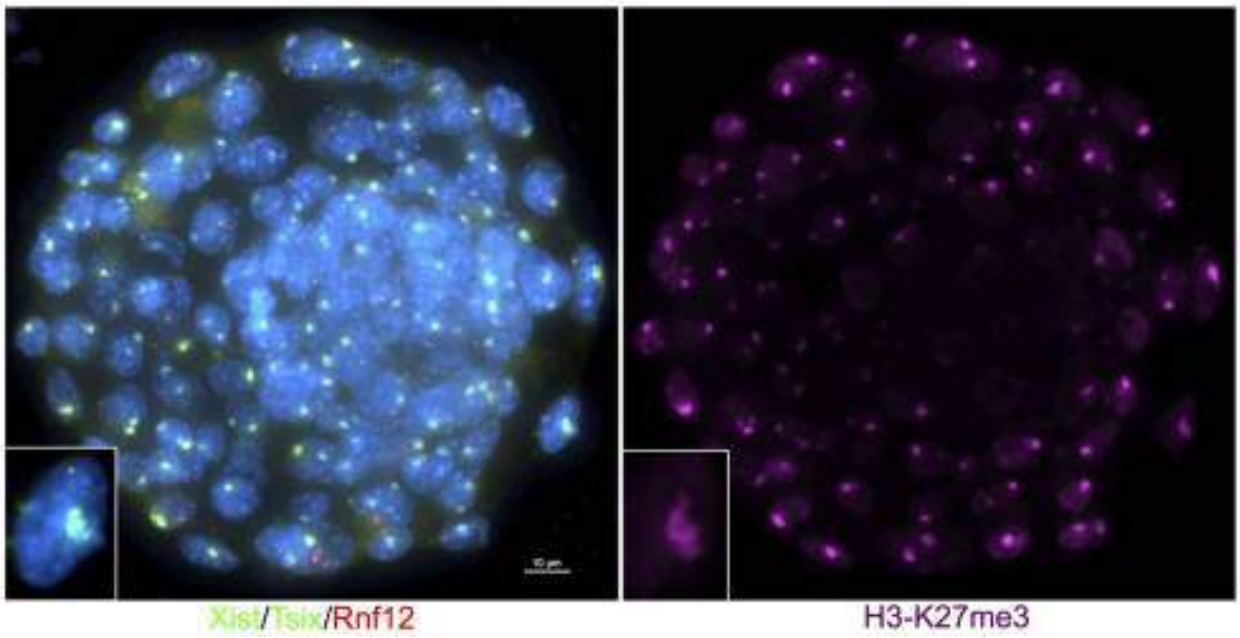

Figure 1.3

Figure 1.3. Adopted from: Maclary, E.*, Hinten, M.*, Harris, C.*, Kalantry, S. (2013). Long non-coding RNAs in the X-inactivation center. Chromosome Res. *21*, 601–614.

*equal author

Figure 1.3. Mouse blastocyst embryo stained to detect Xist RNA coating (in green), Tsix RNA (green pinpoint), and histone H3 lysine 27 tri-methylation (H3-K27me3; in purple). DAPI stains the nuclei blue.

Anguera, M.C., Ma, W., Clift, D., Namekawa, S., Kelleher, R.J., 3rd, Lee, J.T. (2011). Tsx produces a long noncoding RNA and has general functions in the germline, stem cells, and brain. PLoS Genet. *7*, e1002248.

Baranov, V.S. (1983). Chromosomal control of early embryonic development in mice. II. Experiments on embryos with structural aberrations of autosomes 7, 9, 14 and 17. Genet Res. *41*, 227–39.

Bauer, M., Trupke, J., and Ringrose, L. (2015). The quest for mammalian Polycomb response elements: are we there yet? Chromosoma.

Bellott, D.W., Hughes, J.F., Skaletsky, H., Brown, L.G., Pyntikova, T., Cho, T.-J., Koutseva, N., Zaghlul, S., Graves, T., Rock, S., et al. (2014). Mammalian Y chromosomes retain widely expressed dosage-sensitive regulators. Nature *508*, 494–499.

Bernstein, E., Duncan, E.M., Masui, O., Gil, J., Heard, E., and Allis, C.D. (2006). Mouse polycomb proteins bind differentially to methylated histone H3 and RNA and are enriched in facultative heterochromatin. Mol. Cell. Biol. *26*, 2560–2569.

Beutler, E., YEH, M., and FAIRBANKS, V.F. (1962). The normal human female as a mosaic of X-chromosome activity: studies using the gene for C-6-PD-deficiency as a marker. Proc. Natl. Acad. Sci. U.S.A. *48*, 9–16.

Birchler, J.A., Pal-Bhadra, M., and Bhadra, U. (2003). Dosage dependent gene regulation and the compensation of the X chromosome in Drosophila males. Genetic *117(2-3)*, 179-90.

Brockdorff, N., Ashworth, A., Kay, G.F., Cooper, P., Smith, S., McCabe, V.M., Norris, D.P., Penny, G.D., Patel, D., and Rastan, S. (1991). Conservation of position and exclusive expression of mouse Xist from the inactive X chromosome. Nature *351*, 329–31.

Brockdorff, N. (2013). Noncoding RNA and Polycomb recruitment. Rna *19*, 429–442.

Bornemann, D., Miller, E., and Simon, J. (1996). The Drosophila Polycomb group gene Sex comb on midleg (Scm) encodes a zinc finger protein with similarity to polyhomeotic protein. Development *122*, 1621–1630.

Borsangi, G., Tonlorenzi, R., Simmler, C., Dandolo, L., Aranud, D., Capra, V., Grompe, M., Pizzuti, A., Muzny, D., Lawrence, C., et al. (1991). Characterization of a murine gene expressed from the inactive X chromosome. Nature *351*, 325–9.

Brown, C.J., Ballabio, A., Rupert, J.L, Lafreniere, R.G., Grompe, M., Tonlorenzi, R., and Willard, H.F. (1991a). A gene from the region of the human X inactivation centre is expressed exclusively from the inactive X chromosome. Nature *349*, 38–44.

Brown, C.J., Hendrich, B.D., Rupert, J.L., Lafreniere, R.G., Xing, Y., Lawrence, J., and Willard, H.F. The human XIST gene: analysis of a 17 kb inactive X-specific RNA that contains conserved repeats and is highly localized within the nucleus. Cell *71*, 527–42.

Brown, C.J., Lafreniere, R.G., Powers, V.E., Sebastio, G., Ballabio, A., Pettigrew, A.L., Ledbetter, D.H., Levy, E., Craig, I.W., and Willard, H.F. (1991b). Localization of the X inactivation centre on the human X chromosome in Xq13. Nature *349*, 82–4.

Brown, C.J. and Willard, H.F. (1994). The human X-inactivation centre is not required for maintenance of X-chromosome inactivation. Nature. *368*, 154–6.

Brown, S.D. (1991). XIST and the mapping of the X chromosome inactivation centre. Bioessays. *13*, 607–12.

Brunk, B.P., Martin, E.C., and Adler, A.N. (1991). Drosophila genes Posterior sex combs and suppressor two of zeste encode proteins with homology to the murine bmi-1 oncogene. Nature *353*, 351–353.

Cao, R., Wang, L., Wang, H., Xia, L., Erdjument-Bromage, H., Tempst, P., Jones, R.S., and Zhang, Y. (2002). Role of histone H3 lysine 27 methylation in Polycomb-group silencing. Science *298*, 1039–1043.

Changolkar, L.N., Costanzi, C., Leu, N.A., Chen, D., McLaughlin, K.J., and Perhson, J.R. (2007). Developmental changes in histone macroH2A1-mediated gene regulation. Mol. Cell Biol. *27*, 2758–64.

Chaumeil, J., Le Baccon, P., Wutz, A., Heard, E. (2006). A novel role for Xist RNA in the formation of a repressive nuclear compartment into which genes are recruited when silenced. Genes Dev. *20*, 2223–37.

Chureau, C., Chantalat, S., Romito, A., Galvani, A., Duret, L., Avner, P., and Rougeulle, C. (2011). Ftx is a non-coding RNA which affects Xist expression and chromatin structure within the X-inactivation center region. Hum Mol Genet. *20*, 705–18.

Cifuentes-Rojas, C., Hernandez, A.J., Sarma, K., and Lee, J.T. (2014). Regulatory interactions between RNA and polycomb repressive complex 2. Mol. Cell. *55(2)*, 171-85.

Clemson, C.M., Mcneil, J.A., Willard, H.F., and Lawrence, J.B. (1996). XIST RNA paints the inactive X chromosome at interphase: evidence for a novel RNA involved in nuclear/chromosome structure. J. Cell Biol. *132*, 259–75.

Clerc, P., Avner, P. (1998). Role of the region 3' to Xist exon 6 in the counting process of X-chromosome inactivation [see comments] Nat Genet. *19*, 249–53.

Cohen, D.E., Davidow, L.S., Erwin, J.A., Xu, N., Warshawsky, D., Lee, J.T. The DXPas34 repeat regulates random and imprinted X inactivation. Dev. Cell *12*, 57–71.

Conrad, T., Akhar, A. (2012). Dosage compensation in drosophila melanogaster: epigenetic fine-tuning of chromosome-wide transcription. Nat. Rev. Genet. *13(2)*, 123-34.

Cortez, D., Marin, R., Toledo-Flores, D., Froidevaux, L., Liechti, A., Waters, P.D., Grützner, F., and Kaessmann, H. (2014). Origins and functional evolution of Y chromosomes across mammals. Nature *508*, 488–493.

Costanzi C, Pehrson JR. Histone macroH2A1 is concentrated in the inactive X chromosome of female mammals. Nature. 1998;393:599–601.

Csankovszki, G., Panning, B., Bares, B., Peherson, J.R., and Jaenisch, R. (1999). Conditional deletion of Xist disrupts histone macroH2A localization but not maintenance of X inactivation. Nat. Genet. *22*, 323–4.

Cunningham, D.B., Segretain, D., Arnaud, D., Rogner, U.C., and Avner, P. (1998). The mouse Tsx gene is expressed in Sertoli cells of the adult testis and transiently in premeiotic germ cells during puberty. Dev. Biol. *204*, 345–60.

Czermin, B., Melfi, R., McCabe, D., Seitz, V., Imhof, A., and Pirrotta, V. (2002). Drosophila enhancer of Zeste/ESC complexes have a histone H3 methyltransferase activity that marks chromosomal Polycomb sites. Cell *111*, 185–196.

Davidovich, C., Wang, X., Cifuentes-Rojas, C., Goodrich, K.J., Gooding, A.R., Lee, J.T., and Cech, T.R. (2015). Toward a consensus on the binding specificity and promiscuity of PRC2 for RNA. Mol. Cell. *57(3)*, 552-8.

DeCamillis, M., Cheng, N., Pierre, D., and Brock, H.W. (1992). The polyhomeotic gene of Drosophila encodes a chromatin protein that shares polytene chromosome-binding sites with Polycomb. Genes Dev. *6*, 223–232.

Di Croce, L., and Helin, K. (2013). Transcriptional regulation by Polycomb group proteins. Nat. Struct. Mol. Biol. *20*, 1147–1155.

Dura, J.-M., Randsholt, N. B., Deatrick, J., Erk, I. Santamaria, P. Freeman, J.D., Freeman, S. J., Weddell, D., and Brock, H. W. (1987). A complex genetic locus, polyhomeotic, is required for segmental specification and epidermal development in D. melanogaster. Cell *51*, 829–839.

Duret, L., Chureau, C., Samain, S., Weissenbach, J. and Avner, P. (2006). The Xist RNA gene evolved in eutherians by pseudogenization of a protein-coding gene. Science *312*, 1653–1655.

Eicher, E.M., Nesbitt, M.N., and Francke, U. (1972). Cytological identification of the chromosomes involved in Searle's translocation and the location of the centromere in the X chromosome of the mouse. Genetics. *71*, 643–8.

Erhardt, S., Su, I.-H., Schneider, R., Barton, S., Bannister, A.J., Perez-Burgos, L., Jenuwein, T., Kouzarides, T., Tarakhovsky, A., and Surani, M.A. (2003). Consequences of the depletion of zygotic and embryonic enhancer of zeste 2 during preimplantation mouse development. Development *130*, 4235–4248.

Fang, J., Chen, T., Chadwick, B., Li, E., and Zhang, Y. (2004). Ring1b-mediated H2A ubiquitination associates with inactive X chromosomes and is involved in initiation of X inactivation. J. Biol. Chem. *279(51)*, 52812-5.

Franke, A., DeCamillis, M., Zink, D., Cheng, N., Brock, H. W., and Paro, R. (1992). Polycomb and polyhomeotic are constituents of a multimeric protein complex in chromatin of Drosophila melanogaster. EMBO J. *11*, 2941–2950.

Froberg, J.E., Yang, L., and Lee, J.T. (2013). Guided by RNAs: X-inactivation as a model for lncRNA function. J. Mol. Biol. *425*, 3698–3706.

Gieni, R.S. and Hendzel, M.J. (2009). Polycomb group protein gene silencing, non-coding RNA, stem cells, and cancer. Biochem Cell Biol. *87*, 711–46.

Graves, J.A. and Schmidt, MM. (1992). Mammalian sex chromosomes: design or accident? Curr Opin. Genet. Dev. *6*, 890-901.

Grumbach, M. M., Morishima, A., and Taylor, J.H. (1963). Human Sex Chromosome Abnormalities in Relation to DNA Replication and Heterochromatinization. Proc. Natl. Acad. Sci. U.S.A. *49*, 581–9.

Gutjahr, T., Frei, E. Spicer, C., Baumgartner, S., White, R. A., and Noll, M. (1995). The Polycomb-group gene, extra sex combs, encodes a nuclear member of the WD-40 repeat family. EMBO J. *14*, 4296–4306.

Hall, L.L. and Lawrence, J.B. (2003). The cell biology of a novel chromosomal RNA: chromosome painting by XIST/Xist RNA initiates a remodeling cascade. Semin Cell Dev. Biol. *14*, 369–78.

Hans-Martin Herz, Morgan, M., Gao, X., Jackson, J., Rickels, R., Selene, K. Swanson, L. F., Michael, P. Washburn, J, Eissenberg, C., and Shilatifard, A. (2014). Science. *345(6200)*, 1065-70.

Hansen, K.H., Bracken, A.P., Pasini, D., Dietrich, N., Gehani, S.S., Monrad, A., Rappsilber, J., Lerdrup, M., and Helin, K. (2008). A model for transmission of the H3K27me3 epigenetic mark. Nat. Cell Biol. *10*, 1291–1300.

Harper, M.I., Fosten, M., and Monk, M. (1982). Preferential paternal X inactivation in extraembryonic tissues of early mouse embryos. J. Embryol. Exp. Morphol. *67*, 127–35.

Hasegawa, Y., Brockdorff, N., Kawano, S., Tsutui, K., Tsutui, K., and Nakagawa, S. (2010). The matrix protein hnRNP U is required for chromosomal localization of Xist RNA. Dev. Cell *19*, 469–76.

Heard, E, Kress, C., Mongelard, F., Courtier, B., Rougeulle, C., Ashworth, A., Vourc'h, C., Babinet, C., and Avner, P. (1996). Transgenic mice carrying an Xist-containing YAC. Hum Mol Genet. *5*, 441–50.

Heard, E., Mongelard, F., Arnaud, D., and Avner, P. (1999). Xist yeast artificial chromosome transgenes function as X-inactivation centers only in multicopy arrays and not as single copies. Mol. Cell Biol. *19*, 3156–66.

Heard, E., Rougeuelle, C., Arnaud, D., Avner, P., Allis, C.D., and Spector, D.L. (2001). Methylation of histone H3 at Lys-9 is an early mark on the X chromosome during X inactivation. Cell *107*, 727–38.

Hore, T. A., Koina, E., Wakefield, M. J. and Graves, J. A. M. (2007). The region homologous to the X-chromosome inactivation centre has been disrupted in marsupial and monotreme mammals. Chromosomal Res. *15*, 147–161.

Jegalian, K., and Page, D.C. (1998). A proposed path by which genes common to mammalian X and Y chromosomes evolve to become X inactivated. Nature *394*, 776–780.

Jiang, J., Jing, Y., Cost, G.J., Chiang, J.C., Kolpa, H.J., Cotton, A.M., Carone, D.M., Carone, B.R., Shivak, D.A., Guschin, D.Y., Pearl, J.R., Rebar, E.J., Byron, M., Gregory, P.D., Brown, C.J., Urnov, F.D., Hall, L.L., Lawrence, J.B. (2013). Translating dosage compensation to trisomy 21.Nature *500*, 296–300.

Johsnton, C.M., Newall, A.E., Brockdorff, N., and Nesterova, T.B. (2002). Enox, a novel gene that maps 10 kb upstream of Xist and partially escapes X inactivation. Genomics 80, 236–44.

Jones, R. S., and W. M. Gelbart. 1993. The Drosophila Polycomb-group gene enhancer of zeste contains a region with sequence similarity to trithorax. Mol. Cell. Biol. *13*, 6357–6366.

Jonkers, I., Barakat, T.S., Achame, E.M., Monkhorst, K., Kenter, A., Rentmeester, E., Grosveld F., Grootegoed, J.A., and Gribnau, J. (2009). RNF12 is an X-Encoded dose-dependent activator of X chromosome inactivation. Cell *139*, 999–1011.

Jonkers, I., Monkhorst, K., Rentmeester, E., Grootegoed, J.A., Grosveld, F., and Gribnau, J. (2008). Xist RNA is confined to the nuclear territory of the silenced X chromosome throughout the cell cycle. Mol Cell Biol. *28*, 5583–94.

Jurgens, G. (1985). A group of genes controlling the spatial expression of the bithorax complex in *Drosophila*. Nature *315*, 153-155.

Kalantry, S., Mills, K.C., Yee, D., Otte, A.P., Panning, B., and Magnuson, T. (2006a). The Polycomb group protein Eed protects the inactive X-chromosome from differentiation-induced reactivation. Nat. Cell Biol. *8*, 195–202.

Kalantry, S. and Maguson, T. (2006b). The Polycomb protein EED is dispensable for the initation of random X-chromosome inactivation. PLoS Genet. *2(5)*, e66.

Kalantry, S., Purushothaman, S., Bowen, R.B., Starmer, J., and Magnuson, T. (2009). Evidence of Xist RNA-independent initiation of mouse imprinted X-chromosome inactivation. Nature *460*, 647–651.

Karch, F., Weiffenbach, B., Pfeifer, M., Bender, W., Duncan, I., Celniker, S., Crsoby, M., and Lewus, E.B. (1985). The abdominal region of the bithorax complex. Cell *43.* 81-95.

Kaufman, T.C., Lewis, R. and Wakimoto, B. (1980). Cytogenetic Analysis of Chromosome 3 in DROSOPHILA MELANOGASTER: The Homoeotic Gene Complex in Polytene Chromosome Interval 84a-B. Genetics. *94(1)*, 115-33.

Kay, G.F., Barton, S.C., Surani, M. A., and Rastan, S. (1994). Imprinting and X-chromosome counting mechanisms determine Xist expression in early mouse development. Cell. 77, 639-650.

Keer, J.T., Hamvas, R.M., Brockdorff, N., Page, D., Rastan, S., and Brown, S.D. (1990). Genetic mapping in the region of the mouse X-inactivation center. Genomics *7*, 566–72.

Kerppola, TK. (2009). Polycomb group complexes--many combinations, many functions. Trends Cell Biol. 19(12):692-704.

Kohlmajer, A., Savarese, F., Lachner, M., Martens, J., Jenuwein, T., and Wutz, A. (2004). A chromosomal memory triggered by xist regulates histone methylation in x inactivation. PLoS Biol. *2*, E171.

Kunath, T., Arnaud, D., Uy, G.D., Okamoto, I., Chureau, C., Yamanaka, Y., Heard, E., and Gardner, R.L., Avner, P., and Rossant, J. (2005). Imprinted X-inactivation in extra-embryonic endoderm cell lines from mouse blastocysts. Development *132*, 1649–61.

Kuzmichev, A., Nishioka, K., Erdjument-Bromage, H., Tempst, P., and Reinberg, D. (2002). Histone methyltransferase activity associated with a human multiprotein complex containing the Enhancer of Zeste protein. Genes Dev. *16*, 2893–2905.

Lahn, B.T., and Page, D.C. (1999). Four evolutionary strata on the human X chromosome. Science *286*, 964–967.

Laugesen, A., and Helin, K. (2014). Chromatin repressive complexes in stem cells, development, and cancer. Cell Stem Cell *14*, 735–751.

Lee, J.T. (2000). Disruption of imprinted X inactivation by parent-of-origin effects at Tsix. Cell *103*, 17–27.

Lee, J.T. (2005). Regulation of X-chromosome counting by Tsix and Xite sequences. Science *309*, 768–71.

Lee, J.T., Davidow, L.S., and Warshawsky, D. (1999a). Tsix, a gene antisense to Xist at the X-inactivation centre. Nat. Genet. *21*, 400–4.

Lee, J.T. and Jaenisch, R. (1997). Long-range cis effects of ectopic X-inactivation centres on a mouse autosome. Nature *386*, 275–9.

Lee, J.T. and Lu, N. (1999a). Targeted mutagenesis of Tsix leads to nonrandom X inactivation. Cell *99*, 47–57.

Lee, J.T., Lu, N., and Han, Y. (1999b). Genetic analysis of the mouse X inactivation center defines an 80-kb multifunction domain. Proc. Natl. Acad. Sci. U.S.A. *96*, 3836–41.

Lee, J.T., Strauss, W.M., Dausman, J.A., and Jaenisch, R. (1996). A 450 kb transgene displays properties of the mammalian X-inactivation center. Cell *86*, 83–94.

Leeb, M., and Wutz, A. (2007). Ring1B is crucial for the regulation of developmental control genes and PRC1 proteins but not X inactivation in embryonic cells. J. Cell. Biol. *178*, 219–29.

Lewis, E.B. (1978). A gene complex controlling segementation in*Drosophila*. Nature *276*, 565-570.

Lewis, R.A., Kaufman, T.C., Denell, R.E., and Tallerico, P. (1980a). Genetics analysis of the Antennapedia gene complex (ANT-C) and adjacent chromosomal regions of *Drosophila melanogaster* I. Polytene chromosome segments 84B-D. Genetics *95*, 367-381.

Lewis, R. A., Wakimoto, B., Denell, R.E., and Kaufman, T.C. (1980b). Genetics analysis of the Antennapedia gene complex (ANT-C) and adjacent chromosomal regions of *Drosophila melanogaster* I. Polytene chromosome segments 84A-B1,2. Genetics *95*, 383-397.

Lonie, A., R. D'Andrea, R. Paro, and Saint, R. (1994). Molecular characterization of the Polycomblike gene of Drosophila melanogaster, a trans-acting negative regulator of homeotic gene expression. Development *120*, 2629–2636.

Luikenhuis, S., Wutz, A., and Jaenisch, R. (2001). Antisense transcription through the Xist locus mediates Tsix function in embryonic stem cells. Mol Cell Biol. *21*, 8512–20.

Lyon, M.F. (1962). Sex chromatin and gene action in the mammalian X-chromosome. Am J Hum Genet. 14, 135–48.

Magnuson, T., Debrot. S., Dimpfl, J., Zweig, A., Zamora, T., and Epstein, C.J. (1985). The early lethality of autosomal monosomy in the mouse. J. Exp. Zool. *236*, 353–60.

Mak, W., Baxter, J., Silva, J., Newall, A.E., Otte, A.P., and Brockdorff, N. (2002). Mitotically stable association of polycomb group proteins eed and enx1 with the inactive x chromosome in trophoblast stem cells. Curr. Biol. *12*, 1016–20.

Mak, W., Nesterova, T.B., De Napoles, M., Appanah, R., Yamanaka, S., Otte, A.P., and Brockdorff, N. (2004). Reactivation of the paternal X chromosome in early mouse embryos. Science *303*, 666–9.

Marahrens, Y., Loring, J., and Jaenisch, R. (1998). Role of the Xist gene in X chromosome choosing.Cell *92*, 657–64.

Marahrens, Y., Panning, B., Dausman, J., Strauss, W., and Jaenisch, R. (1997). Xist-deficient mice are defective in dosage compensation but not spermatogenesis. Genes Dev. *11*, 156–66.

Margueron, R., Justin, N., Ohno, K., Sharpe, M.L., Son, J., Drury, W.J., Voigt, P., Martin, S.R., Taylor, W.R., De Marco, V., et al. (2009). Role of the polycomb protein EED in the propagation of repressive histone marks. Nature *461*, 762–767.

Margueron, R., Reinberg, D. (2011). The Polycomb complex PRC2 and its mark in life. Nature *469*, 343–9.

Martin, E. C., and Adler, P.N. (1993). The Polycomb group gene Posterior sex combs encodes a chromosomal protein. Development *117*, 641–655.

Masui, S., Ohtsuka, S., Yagi, R., Takahashi, K., Ko, M.S., and (2008). Niwa, H. Rex1/Zfp42 is dispensable for pluripotency in mouse ES cells. BMC Dev Biol. *8*, 45.

McMahon, A., Fosten, M. and Monk, M. (1983). X-chromosome inactivation mosaicism in the three germ layers and the germ line of the mouse embryo. J. Embryol. Exp. Morphol. *74*, 207–20.

Miska, E.A., Alvarez-Saavedra, E., Townsend, M., Yoshii, A., Sestan, N., Rakic, P., Cinstantine-Paton, M., and Horvitz, H.R. (2004). Microarray analysis of microRNA expression in the developing mammalian brain. Genome Biol. *5*, R68.

Monkhorst, K., Jonkers, I., Rentmeester, E., Grosveld, F., and Gribnau, J. (2008). X inactivation counting and choice is a stochastic process: evidence for involvement of an X-linked activator. Cell *132*, 410–21.

Montgomery, N.D., Yee, D., Chen, A., Kalantry, S., Chamberlain, S.J., Otte, A.P., and Magnuson, T. (2005). The murine polycomb group protein Eed is required for global histone H3 lysine-27 methylation. Curr. Biol. *15*, 942–947.

Morey, C., Arnaud, D., Avner, P., and Clerc, P. (2001). Tsix-mediated repression of Xist accumulation is not sufficient for normal random X inactivation. Hum. Mol. Genet. *10*, 1403–11.

Mueller, J. and Kassis, J.A. (2006). Polycomb response elements and targeting of Polycomb group proteins in Drosophila. Curr. Opin. Genet. Dev. *16(5)*, 476-84.

Müller, J., Hart, C.M., Francis, N.J., Vargas, M.L., Sengupta, A., Wild, B., Miller, E.L., O'Connor, M.B., Kingston, R.E., and Simon, J.A. (2002). Histone methyltransferase activity of a Drosophila Polycomb group repressor complex. Cell *111*, 197–208.

Nakajima, T. and Sado, T. (2014). Current view of the potential roles of proteins enriched on the inactive X chromosome. Genes Genet Syst. *89(4)*, 151-7.

Namekawa, S.H., Park, P.J., Zhang, L.F., Shima, J.E., McCarrey, J.R., Griswold, M.D., and Lee, J.T. (2006). Postmeiotic sex chromatin in the male germline of mice. Curr. Biol. *16*, 660–7.

Namekawa, S.H., Payer, B., Huynh, K.D., Jaenisch, R., and Lee, J.T. (2010). Two-step imprinted X inactivation: repeat versus genic silencing in the mouse. Mol. Cell Biol. *30*, 3187–205.

Navarro, P., Chambers, I., Karwacki-Neisius, V., Chureau, C., Morey, C., Rouegulle, C., and Avner, P. (2008). Molecular coupling of Xist regulation and pluripotency *321*, 1693–5.

Navarro, P., Chantalat, S., Foglio, M., Chureau, C., Vigneau, S., Clerc, P., Avner, P., and Rougeulle, C. (2009). A role for non-coding Tsix transcription in partitioning chromatin domains within the mouse X-inactivation centre. Epigenetics Chromatin *2*, 8.

Navarro, P., Oldfield, A., Legoupi, J., Festuccia, N., Dubois, A., Attia, M., Schoorlemmer, J., Rougeulle, C., Chambers, I., and Avner, P. (2010). Molecular coupling of Tsix regulation and pluripotency. Nature *468*, 457–60.

Navarro, P., Page, D.R., Avner, P., and Rougeulle, C (2006). Tsix-mediated epigenetic switch of a CTCF-flanked region of the Xist promoter determines the Xist transcription program. Genes Dev. *20*, 2787–92.

Nesterova, T.B., Senner, C.E., Schneider, J., Alcayna-Stevens, T., Tattermusch, A., Hemberger, M., and Brockdorff, N. (2011). Pluripotency factor binding and Tsix expression act synergistically to repress Xist in undifferentiated embryonic stem cells. Epigenetics Chromatin *4*, 17.

Nguyen, D.K. and Disteche, C.M. (2003). Dosage compensation of the active X chromosome in mammals. Nature Genetics *38,* 47 – 53.

Ogawa. Y., Lee, J.T. (2003). Xite, X-inactivation intergenic transcription elements that regulate the probability of choice. Mol. Cell *11*, 731–43.

Ohhata, T., Hoki, Y., Sasaki, H., and Sado, T. (2006). Tsix-deficient X chromosome does not undergo inactivation in the embryonic lineage in males: implications for Tsix-independent silencing of Xist. Cytogenet. Genome Res. *113*, 345–9.

Ohno, S. (1967). Sex chromosomes and sex linked (Springer, Berlin).

Okamoto, I., Arnaud, D., Le Baccon, P., Otte, A.P., Disteche, C.M., Avmer, P., and Heard, E. (2005). Evidence for de novo imprinted X-chromosome inactivation independent of meiotic inactivation in mice. Nature *438*, 369–73.

Okamoto, I., Otte, A.P., Allis, C.D., Reinberg, D., and Heard, E. (2004). Epigenetic dynamics of imprinted X inactivation during early mouse development. Science *303*, 644–9.

Patrat, C., Okamoto, I., Diabangouaya, P., Vialon, V., Le Baccon, P., Chow, J., and Heard, E. (2009). Dynamic changes in paternal X-chromosome activity during imprinted X-chromosome inactivation in mice. Proc. Natl. Acad. Sci. U.S.A. *106*, 5198–203.

Pengelly, A.R., Copur, Ö, Jäckle, H., Herzig, A., and Müller, J. (2013). A histone mutant reproduces the phenotype caused by loss of histone-modifying factor Polycomb. Science. *339(6120)*, 698-9.

Penny, G.D., Kay, G.F., Sheardown, S.A., Rastan, S., and Brockdorff, N. (1996). Requirement for Xist in X chromosome inactivation. Nature *379*, 131–7.

Perche, P.Y., Vourc'h, C., Konecny, L., Souchier, C., Robert-Nicoud, M., Dimitrov, S., and Kochbin, S. (2000). Higher concentrations of histone macroH2A in the Barr body are correlated with higher nucleosome density. Curr Biol. *10*, 1531–4.

Plath, K., Fang, J., Mlynarczyk-Evans, S.K., Cao, R., Worringer, K.A., Wang, H., De La Cruz, C.C., Otte, A.P., Panning, B., and Zhang, Y. (2003). Role of histone H3 lysine 27 methylation in X inactivation. Science *300*, 131–5.

Pontier, D.B., and Gribnau, J. (2011). Xist regulation and function explored. Hum. Genet. *130*, 223–236.

Pullirsch, D., Hartel, R., Kishimoto, H., Leeb, M., Steiner, G., and Wutz, A. (2010). The Trithorax group protein Ash2l and Saf-A are recruited to the inactive X chromosome at the onset of stable X inactivation. Development *137*, 935–43.

Rasmussen, T.P., Mastrangelo, M.A., Eden, A., Pehrson, J.R., and Jaenisch, R. (2000). Dynamic relocalization of histone MacroH2A1 from centrosomes to inactive X chromosomes during X inactivation [In Process Citation] J Cell Biol. *150*, 1189–98.

Rastan, S. (1982). Timing of X-chromosome inactivation in postimplantation mouse embryos. J. Embryol. Exp. Morphol. *71*, 11–24.

Rastan S. (1983). Non-random X-chromosome inactivation in mouse X-autosome translocation embryos—location of the inactivation centre. J. Embryol. Exp. Morphol. *78*, 1–22.

Rastan, S. and Brown, S.D. (1990). The search for the mouse X-chromosome inactivation centre. Genet. Res. *56*, 99–106.

Rastan, S. and Robertson, E.J. (1985). X-chromosome deletions in embryo-derived (EK) cell lines associated with lack of X-chromosome inactivation. J Embryol Exp Morphol. *90*, 379–88.

Rougeulle, C, Chaumeil, J., Sarma, K., Allis, C.D., Reinberg, D., Avner, P., and Heard, E. (2004). Differential histone H3 Lys-9 and Lys-27 methylation profiles on the X chromosome. Mol. Cell Biol *24*, 5475–84.

Sado, T., Hoki, Y, and Sasaki, H.. (2005). Tsix silences Xist through modification of chromatin structure. Dev. Cell *9*, 159–65.

Sado, T., Okano, M., Li, E., and Sasaki, H. (2004). De novo DNA methylation is dispensable for the initiation and propagation of X chromosome inactivation. Development *131*, 975–82.

Sado, T., Wang, Z., Sasaki, H., and Li, E. (2001). Regulation of imprinted X-chromosome inactivation in mice by Tsix. Development *128*, 1275–86.

Sánchez-Herrero, E., Vernós, I., Marco, R., Morata, G. (1985). Genetic analysis of a *Drosophila* bithorax complex. Nature *313(5998)*, 108-113.

Sandstedt, S.A., and Tucker, P.K. (2004). Evolutionary strata on the mouse X chromosome correspond to strata on the human X chromosome. Genome Res. *14*, 267–272.

Saurin, A.J., Shao, Z., Erdjument-Bromage, H., Tempst, P., and Kingston, R.E. (2001). A *Drosophila* polycomb group complex includes zeste and dTAFII proteins. Nature *412, 655-660*.

Sauvageau, M., and Sauvageau, G. (2010). Polycomb group proteins: multi-faceted regulators of somatic stem cells and cancer. Cell Stem Cell. *7*, 299–313.

Savarese, F., Flahndorfer, K., Jaenisch, R., Busslinger, M., and Wutz, A. (2006). Hematopoietic precursor cells transiently reestablish permissiveness for X inactivation. Mol. Cell Biol. *26*, 7167–77.

Schoeftner, S., Sengupta, A.K., Kubicek, S., Mechtler, K., Spahn, L., Koseki, H., Jenuwein, T., and Wutz, A. (2006). Recruitment of PRC1 function at the initiation of X inactivation independent of PRC2 and silencing. EMBO J. *25*, 3110–22.

Shao, Z., Raible, F., Mollaaghababa, R., Guyon, J.R., Wu, C.T., Bender, W., and Kingston, R.E. (1999). Stabilization of chromatin structure by PRC1, a polycomb complex. Cell *98*, 37–46.

Sheardown, S.A., Duthie, S.M., Johnston, C.M., Newall, A.E., Formstone, E.J., Arkell, R.M., Nesterova, T.B., Alghisi, G.C., Rastan, S., and Brockdorff, N. (1997). Stabilization of Xist RNA mediates initiation of X chromosome inactivation. Cell *91*, 99–107.

Silva, J., Mak, W., Zvetkova, I., Appanah, R., Nesterova, T.B., Webster, Z., Peters, A.H., Jenuwein, T., Otte, A.P., and Brockdorff, N. (2003). Establishment of histone h3 methylation on the inactive X chromosome requires transient recruitment of Eed-Enx1 polycomb group complexes. Dev. Cell. *4*, 481–95.

Simmler, M.C., Cunningham, D.B., Clerc, P., Vermat, T., Cauron, B., Cruad, C., Pawlak, A., Szpirer, C., Weissenbach, J., Claverie, J.M., and Avner, P. (1996). A 94 kb genomic sequence 3' to the murine Xist gene reveals an AT rich region containing a new testis specific gene Tsx. Hum. Mol. Genet. *5*, 1713–26.

Simon, J., A. Chiang, and Bender, W. (1992). Ten different Polycomb group genes are required for spatial control of the AbdA and AbdB homeotic products. Development *114*, 493–505.

Steward, M.M., Lee, J.S., O'Donovan, A., Wyatt, M., Bernstein, B.E., and Shilatifard, A. (2006). Molecular regulation of H3K4 trimethylation by ASH2L, a shared subunit of MLL complexes. Nat Struct. Mol. Biol. *13*, 852–4.

Straub, T., Dahlsveen, I.K., and Becker, P.B. (2005). Dosage compensation in flies: mechanism, models, mystery. FEBS Lett. *15*, 3258-63.

Strutt, H., and Paro, R. (1997). The Polycomb group protein complex of Drosophila melanogaster has different compositions at different target genes. Mol. Cell Biol. *17*, 6773–6783.

Suh, M.R., Lee, Y., Kim, J.Y., Kim, S.K., Moon, S.H., Lee, J.Y., Cha, K.Y., Chung, H.M., Yoon, H.S., Moon, S.Y., Kim, V.N., and Kim, K.S. (2004). Human embryonic stem cells express a unique set of microRNAs. Dev. Biol. *270*, 488–98.

Sun, S., Del Rosario, B.C., Szanto, A., Ogawa, Y., Jeon, Y., and Lee, J.T. (2013). Jpx RNA activates Xist by evicting CTCF. Cell *153*, 1537–51.

Surface, L.E., Thornton, S.R., and Boyer, L.A. (2010). Polycomb group proteins set the stage for early lineage commitment. Cell Stem Cell. *7*, 288–98.

Takagi, N. Primary and secondary nonrandom X chromosome inactivation in early female mouse embryos carrying Searle's translocation T(X; 16)16H. Chromosoma *81*, 439–59.

Takagi, N., and Sasaki, M. (1975). Preferential inactivation of the paternally derived X chromosome in the extraembryonic membranes of the mouse. Nature *256*, 640–2.

Takagi, N., Wake, N., and Sasaki, M. (1978). Cytologic evidence for preferential inactivation of the paternally derived X chromosome in XX mouse blastocysts. Cytogenet. Cell Genet. *20*, 240–8.

Tanasijevic, B., and Rasmussen, T.P. (2011). X chromosome inactivation and differentiation occur readily in ES cells doubly-deficient for macroH2A1 and macroH2A2. PLoS One *6*, e21512.

Tian, D., Sun, S., and Lee, J.T. (2010). The long noncoding RNA, Jpx, is a molecular switch for X chromosome inactivation. Cell *143*, 390–403.

Tie, F., Furuyama, T., Prasad-Sinha, J., Jane, E., and Harte, P.J. (2001). The Drosophila Polycomb Group proteins ESC and E(Z) are present in a complex containing the histone-binding protein p55 and the histone deacetylase RPD3. Development *128*, 275–286.

Turner, J.M., Mahadevaiah, S.K., Fernandez-Cappetillo, O., Nussenzweig, A., Xu, X., Deng, C.X., and Burgoyne, P.S. (2005). Silencing of unsynapsed meiotic chromosomes in the mouse. Nat. Genet. *37*, 41–7.

Vigneau, S., Augui, S., Navarro, P., Avner, P., and Clerc, P. (2006). An essential role for the DXPas34 tandem repeat and Tsix transcription in the counting process of X chromosome inactivation. Proc. Natl. Acad. Sci. U.S.A. *103*, 7390–5.

Wakimoto, B. and Kaufman, T.C. (1981). Analysis of larval segmentation in lethal genotypes with the Antennapedia gene complex in *Drosophila melanogaster*. Dev. Biol. *81*, 51-64.

Wallis, M.C., Waters, P.D., and Graves, J.A.M. (2008). Sex determination in mammals – Before and after the evolution of SRY. Cell Mol. Life Sci. *65*, 3182 – 3195.

Wang, H, Wang, L, Erdjument-Bromage, H, Vidal, M, Tempst, P, Jones, RS, Zhang, Y. (2004) Role of histone H2A ubiquitination in polycomb silencing. Nature *431*, 873–878.

Webb, S., De Vries, T.J., and Kaufman, M.H. (1992). The differential staining pattern of the X chromosome in the embryonic and extraembryonic tissues of postimplantation homozygous tetraploid mouse embryos. Genet. Res. *59*, 205–14.

West, J.D., Frels, W.I., Chapman, V.M., and Papaiaonnou, V.E. (1977). Preferential expression of the maternally derived X chromosome in the mouse yolk sac. Cell *12*, 873–82.

Whitworth, D.J. and Pask, A.J. (2016). The X factor: X chromosome dosage compensation in the evolutionarily divergent monotremes and marsupials. Semin Cell Dev Biol.

Williams, L.H., Kalanry, S., Starmer, J., and Magnuson, T. (2011). Transcription precedes loss of Xist coating and depletion of H3K27me3 during X-chromosome reprogramming in the mouse inner cell mass. Development *138*, 2049–57.

Wutz, A. and Jaenisch, R. (2000). A shift from reversible to irreversible X inactivation is triggered during ES cell differentiation. Mol Cell. *5*, 695–705.

Wutz, A., Rasmussen, T.P., and Jaenisch, R. (2002). Chromosomal silencing and localization are mediated by different domains of Xist RNA. Nat. Genet. *30*, 167–74.

Zhang, C.C. and Bienz, M. (1992). Segmental determination in Drosophila conferred by hunchback (hb), a repressor of the homeotic gene Ultrabithorax (Ubx). Proc. Natl. Acad. Sci. U.S.A. *89(16)*, 7511–7515.

Zhang, T., Cooper, S., and Brockdorff, N. (2015). The interplay of histone modifications - writers that read. EMBO Rep.

Zhao, J., Sun, B.K., Erwin, J.A., Song, J.J., and Lee, J.T. (2008). Polycomb proteins targeted by a short repeat RNA to the mouse X chromosome. Science *322*, 750–6.

Chapter 2

A Comparative Analysis of Polycomb Repressive Complex 2 Proteins in Imprinted X-chromosome Inactivation: Mouse Trophoblast Stem Cells

Abstract

Proper embryonic development requires the intricate modulation of gene expression states, controlled in part by the cellular epigenetic machinery. The Polycomb group proteins (PcGs) constitute an evolutionarily conserved set of key epigenetic developmental regulators. The Polycomb repressive complex 2 (PRC2) acts to methylate lysine at amino acid position 27 on histone H3 (H3-K27me3), via its catalytic subunit Enhancer of Zeste Homologue 2 or 1 (EZH2 or EZH1). PRC2 is posited to maintain imprinted X-chromosome inactivation in mouse trophoblast stem cells (TSCs), an *ex vivo* model of imprinted X-inactivation. However, the precise role of individual PRC2 components in propagating imprinted X-inactivation remains unknown. PRC2 components along with H3-K27me3 are enriched on the inactive-X in mouse TSCs. This accumulation on the inactive-X suggests a role for PRC2 in maintaining X-linked gene silencing. Here, I genetically evaluated PRC2 by interrogating if its individual subunits are necessary for X-inactivation. In TSCs devoid of EZH2 and/or EZH1, I unexpectedly found that X-inactivation could function properly. On the contrary, I observed an inability to maintain repression of a subset of X-linked genes when the PRC2 subunit EED is missing. The divergent requirements for EZH2/EZH1 and EED in maintaining X-inactivation highlight alternatives to

H3-K27 methyltransferases and their associated repressive histone mark H3-K27me3 in X-inactivation. Furthermore, these observations suggest a more complex interplay between the Polycomb group in epigenetic transcriptional repression.

Introduction

X-chromosome inactivation (X-inactivation) is a paradigmatic epigenetic phenomenon that occurs in order to equalize the X-linked gene dosage between XX female and XY male mammals (Lyon, 1961; Beutler et al., 1962). Through classical genetic experiments in both mouse and human, a segment of the X-chromosome, denoted the X-inactivation center (XIC), was found to be necessary and sufficient for X-inactivation (Eicher et al., 1972; Rastan et al., 1980 and 1983; Takagi, 1980). Within the XIC lie two critical long non-coding (lnc)RNAs, Xist (X-inactive specific transcript), expressed from the inactive X-chromosome, and Tsix (Xist spelled backwards), expressed from the active X-chromosome. Xist RNA physically coats in *cis* the future inactive-X (Brown et al., 1992; Clemson et al., 1996; Jonkers et al., 2008). Tsix, however, is expressed in the antisense orientation to Xist and is thought to repress Xist induction from the active X-chromosome. Both of these lncRNAs are widely believed to be necessary and sufficient for X-inactivation (Marahrens et al., 1997; Penny et al., 1996; Kalantry et al., 2009; Stavropoulos et al., 2001). The mutual exclusivity with which these two transcripts are expressed also suggests that they are important players in establishing and maintaining the transcriptional fates of the X-chromosome from which they are transcribed (Marahrens et al., 1997; Penny et al., 1996, Kalantry et al., 2009; Stavropoulos et al., 2001; Avner and Heard, 2001). Thus, X-inactivation serves as a model system for understanding how epigenetic mechanisms occur broadly.

Two types of X-chromosome inactivation exist in the mouse, imprinted and random. Imprinted X-inactivation, exclusive silencing of the paternally inherited X-chromosome, occurs initially in all cells in the developing mouse embryo (Mak et al., 2004; Takagi et al., 1978; Kay, 1994). This form of X-inactivation is subsequently maintained in the extra-embryonic tissues of the embryo, the trophectoderm and the primitive endoderm lineages (Takagi and Sasaki, 1975; West et al., 1977 and 1978). At peri-implantation, and post-implantation, however, the cells in the epiblast will display a random pattern of X- chromosome inactivation (Mak et al., 2004). Random X-inactivation is unique to the epiblast precursors that will ultimately develop in to the embryo proper. To achieve this, at E4.5 the cells of the inner cell mass will reactivate the paternal X-chromosome (Mak et al., 2004; Williams et al., 2011). These cells will then randomly choose to inactivate either the maternal-X or the paternal-X (Mak et al., 2004). Importantly, once one X-chromosome in a given nucleoplasm is chosen for inactivation, it will remain as the inactive-X in descendant cells over multiple mitotic divisions essentially for the lifetime of the organism. This stable and heritable transcriptional memory is a key facet that highlights X-chromosome inactivation as an epigenetic phenomenon.

In the developing mouse embryo, a set of temporal events occurs as imprinted X-inactivation is initiated and established. At the two-cell stage Xist RNA is transcribed. It will then physically coat in *cis* the paternally inherited X-chromosome (the future inactive-X) at the four-cell stage; Xist RNA marks the inactive-X (Brown, et al. 1992; Clemson et al., 1996; Jonkers et al., 2008). By the eight-cell stage, members of the Polycomb group (PcG) are found enriched coincident with Xist RNA on the inactive-X (Mak, 2002; Erhardt et al., 2003; Okamoto et al., 2004; Plath et al., 2003; Silva et al., 2003). As embryogenesis proceeds, these factors associate on the inactive-X while genes are being silenced along the inactive (paternal) X-

chromosome. Tsix expression from the active (maternal) X-chromosome occurs concomitant with Polycomb protein enrichment and silencing of genes on the future inactive X-chromosome (Lee, 2000; Sado et al., 2001). These events are widely believed to be tightly associated as the appropriate pattern of X-inactivation is initiated and established in the developing embryo.

Polycomb proteins (PcGs) comprise a set of evolutionary conserved epigenetic factors first identified in *Drosophila melanogaster* (Pirrotta, 1997; Ng et al., 2000, Lewis, 1978). They were found to be necessary in maintaining the transcriptional repression of *Hox* loci once silencing of *Hox* loci was triggered by other epigenetic repressive factors during *Drosophila* embryogenesis (Ng et al., 2000; Simon, 1995; Pirrotta, 1997; Pirrotta et al., 1998; Shao et al., 1999; van der Vlag et al., 1999; Tie et al., 1998; Lewis, 1978). This allowed for proper anterior-posterior (A-P) axial patterning (Lewis, 1978). In Polycomb mutants, flies exhibited misexpression of *Hox* genes outside of the normal A-P domains (McKeon and Brock, 1991; Simon et al., 1992; Struhl and Akam, 1985). Polycomb proteins are catalogued into two major complexes, Polycomb repressive complex 2 (PRC2), and Polycomb repressive complex 1 (PRC1). Mammalian PRC2 comprises the core subunits Enhancer of Zeste Homologue 2 (EZH2), Suppressor of Zeste 12 (SU(Z)12) and Extra-embryonic Ectoderm Development (EED), derived from their *Drosophila* homologues Enhancer of Zeste (E(z)), Suppressor of Zeste (Su(z)), and Extra Sex Combs (Esc), respectively (Cao et al., 2002; Czermin et al., 2002; Kuzmichev et al., 2002; Müller et al., 2002; Tie et al., 2001). EZH2, the catalytic subunit of PRC2, serves to post-translationally modify Histone H3 by trimethylating lysine residue 27 (H3-K27me3) (Margueron and Reinberg, 2011; Di Croce and Helin, 2013; Zhang et al., 2015). CBX family members are then believed to read H3-K27me3 via their chromodomains and recruit PRC1 (Bernstein et al., 2006). PRC1 will monoubiquitinate Histone H2A at lysine residue 119 (H2A-K119Ub1) (Wang

et al., 2004). It is generally thought that Polycomb protein recruitment and histone modifications will then lead to facultative heterochromatin formation and transcriptional inactivation (Bernstein et al., 2006).

I, and others, have shown that Polycomb group proteins are physically enriched on the inactive-X *in vitro* (Plath et al., 2003; Silva et al., 2003, Kalantry et al., 2006). Given that these proteins coat the inactive-X supports my hypothesis that they are critical for proper X-linked gene silencing. Previous loss-of-function studies suggest that PRC2 is required in maintaining imprinted X-inactivation (Wang et al., 2001). Furthermore, *Eed*$^{-/-}$ trophoblast stem cells (TSCs) are defective in maintaining silencing of paternal X-linked genes upon differentiation of TSCs (Kalantry et al., 2006). However, it is unknown whether there is a problem in maintaining the X-inactive state in undifferentiated TSCs. Therefore, the explicit roles and the functional interdependence of Polycomb proteins in stably propagating imprinted X-inactivation still remain elusive. Here, I have undertaken a systematic genetic approach to ascertain roles for PRC2 components in imprinted X-chromosome inactivation. Looking at undifferentiated TSCs gives insight into what may be happening in the embryo as X-inactivation is initiated. I therefore hypothesized that PRC2 proteins are crucially required for stable inheritance of X-linked gene silencing through development, once it is initiated in the early embryo. This is in agreement with the classical function for PcGs, that is, maintaining transcriptional repression once the genes are effectively silenced by some other epigenetic repressive factor (Ng et al., 2000; Simon, 1995; Pirrotta, 1997; Pirrotta et al., 1998; Shao et al., 1999; van der Vlag et al., 1999; Tie et al., 1998; Lewis, 1978). Through a conditional mutagenesis approach I show evidence of EZH2-independent stabile inheritance of the X-inactive state. Furthermore, I found that EZH1, the only other known mammalian specific H3-K27me3 histone methyltransferase, is neither necessary for

maintaining X-linked gene silencing nor does it compensate for EZH2 loss in X-inactivation. I indented, however, a requirement for EED in keeping a fraction of X-linked genes repressed. My findings suggest alternatives to canonical PRC2 and H3-K27me3 mediated mechanisms of gene silencing in X-chromosome inactivation.

Results

EZH2 is dispensable for H3-K27me3 and Xist RNA enrichment on the inactive-X

To understand the role of individual PRC2 proteins in X-inactivation, I first wanted to interrogate EZH2. EZH2 is the major histone methyltransferase of PRC2 (Schuettengruber et al., 2007; Di Croce and Helin, 2013; Margueron and Reinberg, 2011; Zhang et al., 2015). EZH2 catalyzes H3-K27me3 enrichment along the inactive-X (Schuettengruber et al., 2007; Margueron et al, 2008; Di Croce and Helin, 2013; Margueron and Reinberg, 2011; Zhang et al., 2015). To ascertain a role for EZH2 in X-inactivation *in vitro*, I derived *Ezh2*$^{-/-}$ TSCs from a parental *Ezh2*$^{fl/fl}$ TSC line. TSCs are stem cells of the trophectodermal lineage of the early mouse embryo and an *ex vivo* model of imprinted X-chromosome inactivation, thus giving rise to a cell type that propagates exclusive silencing of the paternal X-chromosome (Oda et al., 2006). The conditional mutation for the *Ezh2* alleles harbors a SET domain flanked by loxP sites (Su et al., 2003) (Figure 2.1). The mutation removes the SET domain, which spans exons 16-20 of *Ezh2*. loxP sites (red triangles), were integrated after exon 15 and before exon 20. The WD-binding domain is also indicated at exons 2 and 3 (Figure 2.1). This is the site of interaction between EZH2 and EED (Denisenko et al., 1998). The SET domain is the conserved domain of many chromatin modifying enzymes (Kerppola 2009). Historically it refers to **S**u(var)3-9, **E**nhancer of Zeste, and **T**rithorax enzymes discovered in *Drosophila* that contain this conserved enzymatic region

(Kerppola, 2009). To generate our mutant *Ezh2* cell line, I transiently transfected *Ezh2*$^{fl/fl}$ TSCs with a dual Cre-recombinase and Puro-resistance expressing plasmid. Puromycin selection was carried out to remove cells that were not effectively excised for their *Ezh2* floxed alleles, and hence were not successfully transfected with the plasmid (sensitive to Puromycin treatment). Following multiple rounds of subcloning, I obtained a pure population of *Ezh2*$^{-/-}$ TSCs. Having a stable line thus permitted me to investigate unequivocally the requirement for EZH2 in X-inactivation.

To gauge the effect of EZH2 loss, I first assayed for H3-K27me3 enrichment on the inactive-X. *Ezh2*$^{-/-}$ TSCs were visualized on a single nucleus level by immunofluorescence (IF) due to lack of detection of EZH2 enrichment, compared to robust EZH2 enrichment in *Ezh2*$^{fl/fl}$ cells. It is also known that deletion of the EZH2 SET domain with this very conditional approach leads to no protein product (Su et al., 2003). Surprisingly, I found that *Ezh2*$^{-/-}$ TSCs still had H3-K27me3 enrichment vis-à-vis *Ezh2*$^{fl/fl}$ TSCs (Figure 2.1). Furthermore, through RNA-FISH, I found that Xist strongly coated the inactive-X in *Ezh2*$^{-/-}$ TSCs (Figure 2.1). Continued Xist RNA enrichment is contrary to previous reports indicating that *Ezh2* downregulation leads to reduced Xist RNA levels (Zhao et al., 2008). My observation that EZH2 absence does not affect Xist coating of the inactive-X suggests that EZH2 does not act directly upstream of Xist. To assess the potential activity of PRC2 at the inactive-X in the absence of EZH2, I profiled other PcG enrichment in *Ezh2*$^{-/-}$ TSCs. Because H3-K27me3 still coats the inactive-X in *Ezh2* null TS cells, I assayed for EED enrichment on the inactive-X. EED has been shown to be a reader of H3-K27me3 (Margueron et al., 2009). The conventional model is that EED binds to H3-K27me3 and stimulates further H3-K27me3 catalysis via activity of EZH2 (Margueron et al., 2009). Indeed, I observed that EED still coated the inactive-X in *Ezh2*$^{-/-}$ TSCs vis-à-vis *Ezh2*$^{fl/fl}$ TSCs (Figure 2.1).

EED accumulation and continued H3-K27me3 catalysis at the inactive-X, despite loss of EZH2, suggests that EZH2 absence does not affect the heterochromatinization of the inactive-X chromosome. Furthermore, this implies that other histone methyltransferases, possibly through a non-canonical PRC2, are responsible for interacting with EED and catalyzing H3-K27me3 to propagate Xist RNA enrichment along the inactive-X.

EZH2 loss does not confer a defect in X-inactivation

Because there is not an apparent loss of the heterochromatic state associated with the inactive X-chromosome in *Ezh2*$^{-/-}$ TSCs, I waned to next ask how EZH2 absence affected X-linked gene silencing. To assess X-linked gene silencing in *Ezh2*$^{-/-}$ TSCs vis-à-vis *WT* cells, I subjected my cells to RNA-FISH for Xist to mark the inactive X-chromosome and 4 different X-linked genes to ascertain any defects in stable silencing of the inactive-X. I found that X-linked gene silencing is unperturbed in *Ezh2*$^{-/-}$ TS cells (Figure 2.1). All together, I conclude that EZH2 is not required for imprinted X-inactivation *in vitro*. These data suggest that other factors must operate to propagate the X-inactive state in mouse TSCs.

EZH1 does not contribute to X-inactivation

EZH1, a mammalian specific homologue of EZH2, can catalyze low-level H3-K27me3 in *Ezh2*$^{-/-}$ mouse embryonic stem cells (ESCs) (Shen et al., 2008). Continued H3-K27me3 catalysis suggests that EZH1 can compensate for loss of EZH2 function. Given my finding that EZH2 is dispensable for imprinted X-inactivation (Figure 2.1), I next hypothesized that EZH1 may have a substantial contribution to X-inactivation in mouse TSCs. To assess a role for EZH1 in stably propagating the inactive-X state, I generated polymorphic *Ezh2*$^{-/-}$;*Ezh1*$^{-/-}$;X^{Lab}/X^{JF1} TSCs (heretofore referred to as *Ezh2*$^{-/-}$;*Ezh1*$^{-/-}$ TSCs) from a polymorphic *Ezh2*$^{fl/fl}$;*Ezh1*$^{-/-}$;X^{Lab}/X^{JF1}

(heretofore referred to as *Ezh2*$^{fl/fl}$;*Ezh1*$^{-/-}$ TSCs) parental cell line. Having a polymorphic cell line is quite advantageous; I can profile, in an allele-specific manner, the expression of X-linked genes by utilizing single nucleotide polymorphisms for any given gene. In our cross, the maternal-X is derived from the *Mus musculus* 129/S1 mouse strain and the paternal-X is derived from the *Mus molossinus* JF1/Ms strain. The genomes of the 129/S1 and JF1/Ms strains are highly divergent and contain many defined single nucleotide polymorphisms (SNPs) (Keane et al., 2011; Takada et al., 2013; Yalcin et al., 2011). The *Ezh2* mutation is the same as described above, and the *Ezh1* mutation contains a LacZ/Neo cassette inserted into exon 7. This cassette renders the gene unable to be fully transcribed; the transcript does not contain the SET domain. The SET domain for *Ezh1* is encoded by exons 17-21 (Figure 2.2). The WD-binding domain is also indicated at exons 3 and 4. These WD domains are the site of interaction between EZH1 and EED (Figure 2.2). EED has been shown to interact with EZH1 (Margueron et al., 2008). We first wanted to assess the H3-K27me3 enrichment on the inactive-X in *Ezh2*$^{-/-}$;*Ezh1*$^{-/-}$ double mutant cells. Compared to *Ezh2*$^{-/-}$ TSCs, which still have H3-K27me3 enrichment on the inactive-X, *Ezh2*$^{-/-}$;*Ezh1*$^{-/-}$ TSCs lose H3-K27me3 enrichment vis-à-vis *Ezh2*$^{fl/fl}$;*Ezh1*$^{-/-}$ TSCs (Figure 2.2). Because I now observed loss of this histone mark, I hypothesized that there would be a defect in stable X-linked gene silencing. To gauge the effect on X-linked gene silencing in *Ezh2*$^{-/-}$*;Ezh1*$^{-/-}$ TSCs, I carried out RNA-FISH for Xist and 4 different X-linked genes. I surprisingly found that all cells whether mutant for *Ezh1* or double mutant for *Ezh2* and *Ezh1* were monoallelic (expressed only from the active X-chromosome) for all genes analyzed (Figure 2.2). Although absent for H3-K27me3 enrichment, *Ezh2*$^{-/-}$;*Ezh1*$^{-/-}$ TSCs still harbor inactive-X enrichment of Xist RNA (Figure 2.2). Absence of defect in gene silencing in *Ezh2*$^{-/-}$;*Ezh1*$^{-/-}$ TSCs could be due to preservation of the heterochromatic state, as indicated in part by Xist RNA enrichment.

Furthermore, I validated our RNA-FISH data by assaying gene expression via allele-specific RT-PCR coupled with Sanger sequencing for the same 4 X-linked genes. All genes assayed were monoallelically expressed in both *Ezh2*$^{fl/fl}$;*Ezh1*$^{-/-}$ and *Ezh2*$^{-/-}$;*Ezh1*$^{-/-}$ TSCs (Figure 2.3). I note that in both *Ezh2*$^{fl/fl}$;*Ezh1*$^{-/-}$ and *Ezh2*$^{-/-}$;*Ezh1*$^{-/-}$ TSCs, *Atrx* is slightly derepressed from the inactive-X (both maternal and paternal alleles expressed). This has been reported before (Corbel et al., 2013). Putting all of these data together, loss of either EZH1 alone or together with EZH2 does not confer a defect in X-inactivation. This indicates that EZH1 is not required for X-inactivation (my *Ezh2*$^{fl/fl}$; *Ezh1*$^{-/-}$ data). Moreover, these data further suggest that EZH1 does not contribute to X-inactivation by compensating for loss of EZH2 (my *Ezh2*$^{-/-}$;*Ezh1*$^{-/-}$ data).

<u>*Ezh2*$^{-/-}$;*Ezh1*$^{-/-}$ TSCs are deficient in cell division</u>

Of note, I was unsuccessful in deriving a stable, pure population of *Ezh2*$^{-/-}$;*Ezh1*$^{-/-}$ TSCs. My *Ezh2*$^{-/-}$;*Ezh1*$^{-/-}$ TSCs for the above experiments were acquired and observed so in a transient manner. Upon transduction with an episomal adenoviral construct with a Cre-expressing component (Ad5-CMV-Cre) followed with subsequent subcloning, I noticed that the mutant allele for *Ezh2* slowly disappeared over time, suggesting that *Ezh2*$^{-/-}$;*Ezh1*$^{-/-}$ TSCs are lost. I therefore resorted to a transient transduction method to capture *Ezh2*$^{-/-}$;*Ezh1*$^{-/-}$ TSCs. I transduced cells and harvested them for EZH2 and H3-K27me3 immunofluorescent analysis at 48, 72, and 96 hours post-Adeno-Cre delivery. At 72 hours after transduction I was able to achieve the highest degree of Cre-mediated excision of the *Ezh2* floxed alleles (roughly 50%) (Figure 2.4). Cells without EZH2 and EZH1 were lost over time, as indicated by a lack of *Ezh2*$^{-/-}$;*Ezh1*$^{-/-}$ cells (without EZH2 and H3-K27me3 inactive-X enrichment) at 96 hours post transduction (Figure 2.4). I therefore hypothesized that cells losing both EZH2 and EZH1 are subjected to a proliferative defect, and are therefore drowned out by *Ezh2*$^{fl/fl}$;*Ezh1*$^{-/-}$ TSCs that continue to

divide. To assess the mitotic index of these cells, I stained *Ezh2*$^{fl/fl}$;*Ezh1*$^{-/-}$ and *Ezh2*$^{-/-}$;*Ezh1*$^{-/-}$ TSCs with a phospho-Histone H3 (H3-S10p) antibody, a marker of actively dividing cells (Hendzel et al., 1997). Specifically, H3-S10 becomes phosphorylated during G2 phase of the cell cycle (Hendzel et al., 1997). All double mutant cells (assessed as so due to lack of H3-K27me3 enrichment on the inactive-X) displayed absence of staining for phospho-Histone H3 (Figure 2.4). I found that on average roughly 40% of *Ezh2*$^{fl/fl}$;*Ezh1*$^{-/-}$ cells are positive for H3-S10p. This supports my hypothesis that TSCs that lose both known H3-K27me3 histone methyltransferases cannot divide due to a mitotic defect.

Ezh2$^{-/-}$;*Ezh1*$^{-/-}$ TSCs lose enrichment of other PRC factors and associated repressive histone marks on the inactive-X

Due to the inactive-X being devoid of H3-K27me3 foci in *Ezh2*$^{-/-}$;*Ezh1*$^{-/-}$ TSCs, I hypothesized that these cells are also lacking in EED enrichment. This makes sense, as previous studies indicate that EED interaction and enrichment at the inactive-X is important for propagating the H3-K27me3 mark (Margueron et al., 2009). Indeed, I found that *Ezh2*$^{-/-}$;*Ezh1*$^{-/-}$ TSCs lose EED enrichment on the inactive X-chromosome (Figure 2.4). Considering that I observed no defect in X-linked gene silencing in the absence of both EZH2 and EZH1, I next hypothesized that perhaps Polycomb repressive complex 1 (PRC1) is playing a role in executing stable inactivation of X-linked genes. PRC1 is known to bind to H3-K27me3 through CBX subunits (Bernstein et al., 2006). In turn, PRC1 is recruited to the inactive-X, where it catalyzes H2A-K119ub1, the functional readout of PRC1 (Wang et al., 2004). This is widely believed to contribute to gene silencing at target loci (Bernstein et al., 2006). It is still unclear whether PRC1 functions independently or dependently of PRC2 in X-chromosome inactivation. To gain insight into a role for PRC1 in X-inactivation, I subjected *Ezh2*$^{fl/fl}$;*Ezh1*$^{-/-}$ and *Ezh2*$^{-/-}$;*Ezh1*$^{-/-}$ TSCs to

immunofluorescence detection of H2A-K119ub1 while co-staining for H3-K27me3 to genotype the cells (cells that lose H3-K27me3 are *Ezh2*$^{-/-}$;*Ezh1*$^{-/-}$). I also performed RNA-FISH in the same experiments to mark the inactive-X with Xist RNA coating. I observed absence of H2A-K119ub1 enrichment along the inactive-X in *Ezh2*$^{-/-}$;*Ezh1*$^{-/-}$ cells compared to *Ezh2*$^{fl/fl}$;*Ezh1*$^{-/-}$ cells that do display co-enrichment of H3-K27me3 and H2A-K119ub1 (Figure 2.4). Taken together, my data imply that neither PRC2 (through H3-K27me3 catalysis) nor PRC1 (through H2A-K119ub1 catalysis) are important for stable X-inactivation. This suggests that there is perhaps another histone mark or other repressive proteins that function in X-inactivation. To address additional histone marks, I interrogated H4-K20me1, a mark that is posited to be associated with transcriptional repression (Kalakonda et al., 2008; Karachentsev et al., 2005; Kohlmaier et al., 2004). I observed that EZH2 and EZH1 loss, and hence H3-K27me3 loss, also resulted in a lack of H4-K20me1 foci on the inactive-X in *Ezh2*$^{-/-}$;*Ezh1*$^{-/-}$ TSCs vis-à-vis *Ezh2*$^{fl/fl}$;*Ezh1*$^{-/-}$ TSCs (Figure 2.4). Taking all of these data together, EZH2 and EZH1 mutation leads to loss of multiple known Polycomb factors and associated repressive histone marks on the inactive-X in mouse TSCs. However, absence of all of these marks does not appear to confer a defect in X-linked gene silencing (Figure 2.2 and Figure 2.3), suggesting that other factors are at play in stable X-inactivation.

<u>*Ezh2*$^{-/-}$;*Ezh1*$^{-/-}$ TSCs have reduced Xist coating of the inactive-X</u>

I also noticed that in a sub-population of *Ezh2*$^{-/-}$;*Ezh1*$^{-/-}$ TSCs, the volume of the Xist domain on the inactive-X is seemingly less so compared to just Ezh1$^{-/-}$ TSCs. An alternate interpretation of my preceding data is that Xist RNA is on its way to being lost from the inactive-X chromosome. Thus, it is possible that once Xist is lost, if perhaps *Ezh2*$^{-/-}$;*Ezh1*$^{-/-}$ TSCs were able to continually divide, that X-linked genes would then become derepressed. To address the

size of the Xist coat along the inactive-X in both *Ezh2*$^{-/-}$;*Ezh1*$^{-/-}$ and *Ezh2*$^{fl/fl}$;*Ezh1*$^{-/-}$, I subjected cells from my RNA-FISH experiments to volumetric analysis of the Xist domain. After comparing these two sets of cells, I found that there is a statistically significant drop in the volume of the Xist RNA coat between *Ezh2*$^{-/-}$; *Ezh1*$^{-/-}$ TSCs and *Ezh2*$^{fl/fl}$; *Ezh1*$^{-/-}$ TSCs (Figure 2.5).

It is therefore possible that in *Ezh2*$^{-/-}$;*Ezh1*$^{-/-}$ TSCs the inactive-X is still in a partial heterochromatic state; however, upon further division, Xist, along with this repressive state, will eventually be lost. Ultimately, I alternatively hypothesize that progressive loss of Xist RNA coating will lead to derepression of X-linked genes. Erosion of the heterochromatinization of the inactive-X chromosome, through loss of Xist RNA enrichment (Sun et al, 2006), is sufficient to confer a defect in X-linked gene silencing, as I report herein (see *Eed*$^{-/-}$ TSC results below) and previously (Kalantry, et al., 2006; Maclary et al, 2016, in preparation).

EED is only partially required for propagating the silencing of X-linked genes

EED is considered the glue of PRC2. When EED is missing, PRC2 as a complex fails to form appropriately, and the other core subunits degraded (Montgomery et al., 2005). Furthermore, when cells are lacking functional EED, it is known that H3-K27me3 deposition at PRC2 target genes is reduced (Montgomery et al., 2005). Considering that EED is enriched on the inactive-X in mouse TSCs (Plath et al., 2003, Silva et al., 2003), I hypothesized that EED is critical for imprinted X-inactivation.

Our lab has shown in previous studies that EED is crucial for the recruitment of PRC2 and PRC1 components as well their catalytic readouts on the inactive-X (Kalantry et al., 2006). In the 2006 study, a homozygous *Eed* point mutation conferred loss of PRC2 and PRC1 activity;

PRC2/PRC1 components are not enriched and H3-K27me3/H2A-K119ub1 catalysis is lost on the inactive-X in TS cells (Kalantry et al., 2006). In light of these prior data, I further hypothesized that EED is vital for proper X-inactivation. Utilizing a different mutation, one which removes of exon 7 (Figure 2.6), I generated a stable pure population of polymorphic $Eed^{-/-}$ TSCs from an $Eed^{fl/fl};X^{Lab}/X^{JF1}$ parental line (heretofore referred to as $Eed^{fl/fl}$) (Figure 2.6). Exon 7 encodes WD40 domain #3. This domain is necessary for interaction between EZH2 and EED (Denisenko et al., 1998; Han et al., 2007). loxP sites (red triangles) were integrated after exon 6 and before exon 8. The brackets also indicate other WD-binding domains (Figure 2.6). Deletion of WD40 domains of EED is known to adversely affect interaction between EZH2 and EED (Denisenko et al., 1998; Han et al., 2007). The same logic likely also applies to the interaction between EED and EZH1 (Margueron et al., 2008). Accordingly, I first characterized these cells for their H3-K27me3 inactive-X enrichment profile. Compared to $Eed^{fl/fl}$ TSCs, $EED^{-/-};X^{Lab}/X^{JF1}$ cells (heretofore referred to as $Eed^{-/-}$) lose all detectable enrichment of H3-K27me3 on the inactive-X (Figure 2.5). I also observed that loss of EED and H3-K27me3 ablated Xist RNA enrichment of Xist along the inactive-X (Figure 2.6), consistent with previous data (Kalantry et al., 2006). It is known that there is a transient heterochromatic state induced at the Xist locus (Sun et al., 2006). This heterochromatic state is characterized by H4 hypoacetylation, a reduction in H3-K4 dimethylation, and an increase in PRC2-catalyzed H3-K27me3 (Sun et al., 2006). Through a mechanism that the X-inactivation field does not yet fully understand, this transient heterochromatic state somehow paradoxically leads to Xist induction and Xist RNA enrichment on the inactive-X. The marking of the Xist chromatin in this manner may therefore be necessary for Xist RNA expression, potentially explaining why the EED and H3-K27me3 absence adversely affects Xist RNA expression and abrogates Xist RNA enrichment. Indeed, I

hypothesized that perturbation of PRC2 function through loss of EED negatively affects formation of this transient heterochromatinization. Xist RNA expression is, in turn, hindered (Kalantry et al., 2006; Maclary et al., 2016, in preparation). This is plausibly why in *Eed*$^{-/-}$ TSCs lose Xist RNA coating of the inactive-X.

I next wanted to assess how EED loss affected X-linked gene silencing. Previously, a defect in X-linked gene silencing was only observed when TSCs and embryonic trophoblast tissues differentiated (Kalantry et al., 2006). The Kalantry et al., 2006 point mutant may not have been as detrimental as my mutation, deletion of exon 7/WD40 domain repeat #3. I hypothesized that my *Eed*$^{-/-}$ TSCs would display a defect in stable X-linked gene silencing even in undifferentiated cells, which maybe analogous to what occurs in the early mouse embryo. When analyzing my cells via RNA-FISH, I interestingly found that upon EED deletion, not every gene is derepressed (Figure 2.6). Of the genes assayed, *Atrx, Rnf12,* and *Pdha1* are not derepressed, but *Pgk1* is derepressed in *Eed*$^{-/-}$ TSCs (Figure 2.6). I validated these results through allele-specific RT-PCR followed by Sanger sequencing (Figure 2.6). Because only a subset of genes appears to be affected, I further hypothesized that the chromatin architecture or configuration of epigenetic marks around those genes that are derepressed is likely different than those genes that remain silenced. As a lab, we found that genes that are upregulated in *Eed*$^{-/-}$ TSCs possess characteristics of open chromatin and are transcribed at low levels even in *WT* TSCs. Because a majority of genes are not affected in *Eed*$^{-/-}$ TSCs, our observations imply that there must be at least one additional mechanism (PRC2 independent) by which a majority of genes are silenced as the inactive state is stably inherited across cell divisions. This idea of open chromatin marking genes that are repressed through an EED and Xist RNA mediated mechanism is discussed in further detail in a manuscript in progress (Maclary et al., 2016, in preparation). Taking all these

data together my results indicate that EED is not strictly necessary for stable inheritance of the inactive-X state.

Conditionally mutant *EED*$^{-/-}$ TSCs lose inactive-X enrichment of other repressive associated histone marks

In the X-inactivation field, we already know that *Eed* point mutant TSCs lose enrichment of other PRC2 components (Kalantry et al., 2006). This study also showed evidence for loss of H2A-K119ub1 enrichment, suggesting that PRC1 is not recruited to the inactive-X in *Eed*$^{-/-}$ TS cells. To investigate this further, I profiled my undifferentiated *Eed*$^{-/-}$ TSCs (conditionally missing exon 7/WD40 domain #3 (Figure 2.6)) for enrichment of H2A-K119ub1. Indeed, I nicely replicated these results in my experiments; *Eed*$^{-/-}$ TSCs do not harbor inactive-X enrichment of H2A-K119ub1 (Figure 2.7). This suggests that PRC1 is not recruited to the inactive-X when EED is gone. Considering that we observed only a faction of genes derepressed in *Eed*$^{-/-}$ TSCs (Figure 2.6, Maclary et al., 2016, in preparation), H2A-K119ub1 loss further implies that PRC1 is not broadly responsible for executing silencing of X-linked genes. To interrogate other histone marks as potentially active players in X-inactivation I profiled my *Eed*$^{-/-}$TSCs for H4K20me1 enrichment. In accordance with previous data (Kalantry et al., 2006), my *Eed*$^{-/-}$ TSCs also lose all detectable enrichment of H4-K20me1 along the inactive-X (Figure 2.7), thereby discounting a potential mechanism for PRSET7 in X-inactivation. The fact that only a subset of genes (Figure 2.6; Maclary et al., 2016, in preparation) is derepressed in *Eed*$^{-/-}$ TSCs suggests there are alternatives to EED, H3-K27me3, and Xist in stable X-linked gene silencing. Furthermore, in light of such a small phenotypic outcome due to EED absence, I believe that there is at least more than one, likely multiple, mechanisms by which X-inactivation

is propagated. Further work will untangle the mechanism(s) by which the majority of X-linked genes are tightly silenced.

Transiently transduced *Eed*$^{fl/fl}$ TSCs are similar to constitutive *Eed*$^{-/-}$ TSCs in their X-inactivation phenotype

To formally elucidate the genetic equivalency, or lack thereof, between *Ezh2*$^{-/-}$;*Ezh1*$^{-/-}$ and *Eed*$^{-/-}$ TSCs with respect to an X-inactive derepression phenotype, I transiently transduced my *Eed*$^{fl/fl}$ TSCs in the same manner as my *Ezh2*$^{fl/fl}$;*Ezh1*$^{-/-}$ TSCs (see materials and methods below). After 72 hours of transduction, I harvested cells and performed RNA-FISH for Xist (to differentiate *Eed*$^{fl/fl}$ from *Eed*$^{-/-}$ cells, as *Eed*$^{-/-}$ cells lose Xist RNA enrichment) and 4 X-linked genes, *Atrx*, *Rnf12*, *Pdha1*, and *Pgk1*. I observed a similar result with respect to my constitutively null *Eed* TS cells shown in Figure 2.6. Compared to mock transduced *Eed*$^{fl/fl}$ TSCs, which display monoallelic nascent RNA detection of Atrx, Rnf12, Pdha1, and Pgk1, *Eed*$^{-/-}$ TSCs (Xist negative nuclei transiently transduced with our *Cre* construct for 72 hours) still display monoallelic expression for Atrx, Rnf12, and Pdha1 in a majority of Xist negative nuclei; but, these cells are biallelic for Pgk1 in roughly half of Xist negative nuclei (Figure 2.8). To assess the deletion efficiency in our *Eed*$^{fl/fl}$ TSCs, I scored a total of 100 nuclei from mock and transduced samples for Xist RNA enrichment. I found that transiently transduced *Eed*$^{fl/fl}$ TSCs display, on average, 36% of nuclei that are Xist negative compared to just 5% of mock transduced cells without Xist RNA enrichment. Differential Xist RNA coated inactive X-chromosomes indicate that the increase in Xist RNA negative nuclei in our transduced samples must be a direct result of the Cre construct acting upon *Eed*$^{fl/fl}$ cells to convert them to *Eed*$^{-/-}$. My data strongly suggests that even transiently transduced cells are defective for maintaining silencing of a fraction of X-linked genes just as constitutive *Eed*$^{-/-}$ TSCs exhibit faulty X-

inactivation for a subset of X-linked genes vis-à-vis *Eed*$^{fl/fl}$ TSCs (as we report herein and previously; Kalantry et al., 2006; Maclary et al., 2016, in preparation). Moreover, these data suggest that my *Eed* mutation is not genetically equivalent to my *Ezh2*/*Ezh1* mutations in terms of an X-inactivation defect. Whereas *Eed*$^{-/-}$ TSCs (constitutive or transiently transduced) show aberrant silencing for *Pgk1* (and a subset of other genes (Maclary et al., 2016, in preparation)) but faithful silencing of *Atrx*, *Rnf12*, and *Pdha1* (and the majority of X-liked genes, Maclary et al., 2016, in preparation) despite absence of Xist RNA enrichment, transiently transduced *Ezh2*$^{-/-}$;*Ezh1*$^{-/-}$ TSCs show maintained silencing for *Atrx*, *Rnf12*, *Pdha1*, and *even* Pgk1. Still it is possible that a defect might not be observed in my *Ezh2*$^{-/-}$;*Ezh1*$^{-/-}$ TSCs if and when Xist RNA is ultimately lost; our Xist RNA volumetric analyses suggest that Xist RNA might eventually be lost from the inactive-X compared to *Ezh2*$^{fl/fl}$;*Ezh1*$^{-/-}$ TSCs (Figure 2.5). If this is truly the case, I could then conclude that Xist RNA is what is responsible for holding a subset of genes in a silenced state, as the only fundamental difference between the two genotypes (*Eed*$^{-/-}$ versus *Ezh2*$^{-/-}$;*Ezh1*$^{-/-}$) is the inactive-X Xist RNA enrichment profile. However, only a defect in X-linked gene silencing is seen in our *Eed*$^{-/-}$ TSCs (both constitutive and transient). Based on my current data, these two cell lines are identical in every other respect; both *Eed*$^{-/-}$ TSCs and *Ezh2*$^{-/-}$;*Ezh1*$^{-/-}$ TSCs lack other Polycomb protein, H3-K27me3, H2A-K119ub1, and H4-K20me1 inactive-X enrichment. Altogether, my observations strongly suggest that EED is acting outside of its canonical PRC2 function to ensure damped silencing of a subset of paternal X-linked genes. That the majority of genes remained tightly silenced in *Eed*$^{-/-}$ TSCs is indicative of an alternate mechanism other than EED in X-inactivation.

Discussion

In this study, I evaluated the role of the Polycomb repressive complex 2 in mouse imprinted X-chromosome inactivation through exploitation of moue trophoblast stem cells. Furthermore, by dissecting apart PRC2 and separately investigating its individual core components, I systematically ascertained a more complete understanding of the differential requirement for PRC2 proteins in X-inactivation. Previously, work identified Polycomb protein enrichment on the inactive-X both *in vitro* (Plath et al., 2003, Silva et al., 2003; Kalantry et al., 2006). However, no one has genetically evaluated the complete role of PCR2 in stably propagating the X-inactive state in mouse trophoblast stem cells. Given that PcGs actively enrich on the inactive-X during imprinted X-inactivation, I hypothesized that PcGs are critically required for proper X-inactivation. Here I elucidated the true function of PRC2, and its subunits, in mouse trophoblast stem cells, an *ex vivo* model of imprinted X-inactivation.

First, I investigated the activity of EZH2, the major H3-K27me3 methyltransferase of PRC2 (Schuettengruber et al., 2007; Di Croce and Helin, 2013; Margueron and Reinberg, 2011; Zhang et al., 2015). In *Ezh2*$^{-/-}$ TSCs, I found that H3-K27me3 is still enriched on the inactive-X comparably to *Ezh2*$^{fl/fl}$ TSCs. Moreover, X-linked gene silencing patterns in *Ezh2*$^{-/-}$ TSCs remains identical to those in *Ezh2*$^{fl/fl}$ counterparts. In other words, *Ezh2*$^{-/-}$ TSCs do not display any observable defect in silencing of their X-linked genes. Such evidence of EZH2 independent stable inheritance of the inactive-X state suggests that other epigenetic factors are more important for X-inactivation. I hypothesized that sustained catalysis of H3-K27me3 is occurring by a non-canonical PRC2 complex. To support this idea, I observed continued EED enrichment, along with H3-K27me3, along the inactive-X in *Ezh2*$^{-/-}$ TSCs. By all accounts, I believe that EZH2 is dispensable for imprinted X-chromosome inactivation in TSCs.

I next hypothesized that because EZH2 is dispensable for X-linked gene silencing, there must be factors that supplant the activities of EZH2 to properly carry out X-inactivation. EZH1, the only other known H3-K27me3 mammalian homologue of EZH2, has previously been shown to compensate for loss of EZH2 in mouse embryonic stem cells to execute H3-K27me3 catalytic activity (Shen et al., 2008). Importantly I, and others, note that there is essentially no known phenotype for the loss of EZH1. I observed extensively the normal capability of *Ezh1*$^{-/-}$ mice (and *Ezh2*$^{fl/fl}$;*Ezh1*$^{-/-}$ mice) to interbreed and yield litters of equal sex ratios (see chapter 3). These mice furthermore can live a normal life span and are themselves fertile. These data would suggest that absence of EZH1 alone does not confer a defect in X-inactivation, further suggesting that EZH1 is not necessary for X-inactivation. The question then becomes, does EZH1 compensate for EZH2 loss? This is concluded to be the case in the work of Shen et al., 2008. To assess a role for EZH1 in compensating for EZH2 loss in X-inactivation, I generated transient *Ezh2*$^{-/-}$;*Ezh1*$^{-/-}$ TSCs and compared them to my parental *Ezh2*$^{fl/fl}$;*Ezh1*$^{-/-}$ cell line. I found that when both EZH2 and EZH1 are lost, but not EZH1 alone, H3-K27me3 is lost from the inactive-X. Surprisingly, in my *Ezh2*$^{-/-}$;*Ezh1*$^{-/-}$ TSCs, loss of H3-K27me3 did not confer a defect in X-inactivation, as my RNA-FISH and allele-specific RT-PCR results indicated no X-linked gene derepression from the inactive-X in *Ezh2*$^{-/-}$;*Ezh1*$^{-/-}$ TSCs vis-à-vis my parental *Ezh2*$^{fl/fl}$;*Ezh1*$^{-/-}$ TSCs. To rule out continued activity of PRC2 in X-inactivation, I further profiled my cells for EED enrichment. *Ezh2*$^{-/-}$;*Ezh1*$^{-/-}$ TSCs lose enrichment of EED at the inactive-X. These data argue that EED, and any conventional PRC2 complex, do not actively enrich on the inactive-X. This does not, however, preclude the possibility of EED participating with other repressive factors, which may transiently interact with the inactive-X to maintain X-linked gene silencing.

It remains to be formally known if EED is expressed in *Ezh2*$^{-/-}$;*Ezh1*$^{-/-}$ TSCs. Further biochemical experimentation will shed light on these hypotheses.

To gauge whether PRC1 may be participating to enact gene silencing, I profiled my *Ezh2*$^{fl/fl}$;*Ezh1*$^{-/-}$ and *Ezh2*$^{-/-}$;*Ezh1*$^{-/-}$ cells for inactive-X enrichment of H2A-K119ub1, the catalytic readout of PRC1 (Wang et al., 2004). *Ezh2*$^{-/-}$;*Ezh1*$^{-/-}$ TSCs do not display H2A-K119ub1 enrichment on the inactive-X, whereas *Ezh2*$^{fl/fl}$;*Ezh1*$^{-/-}$ TSCs do show H2A-K119ub1 enrichment. This suggests that PRC1 may not be an active player in X-inactivation, although such a hypothesis requires systematic genetic evaluation of actual PRC1 components. Lack of H2A-K119ub1 enrichment in the absence of H3-K27me3 does however suggest that PRC1 works in tandem with PRC2 to lay down their respective histone marks at target loci. The conventional model is that PRC2 deposits H3-K7me3 via EZH2, which is then read by CBX subunit of PRC1 (Margueron and Reinberg, 2011). In turn PRC1 catalyzes H2A-K119ub1 through Ring1B/A activity (Wang et al., 2004). It is therefore possible that by perturbing PRC2 through EZH2 and EZH1 loss, I am also negatively affecting the downstream incidental PRC1 activity at the inactive-X. Taking all of these data together, I conclude that gene silencing is occurring at the inactive-X in *Ezh2*$^{-/-}$;*Ezh1*$^{-/-}$ TSCs by a mechanism other than normal PRC2, and, potentially, PRC1 function. To shed light on this hypothesis, I profiled my *Ezh2*$^{-/-}$;*Ezh1*$^{-/-}$ TSCs for H4K20me1 enrichment, a mark that is observed to coat the inactive-X in normal TSCs and one that has been linked to gene silencing (Kalakonda et al., 2008; Karachentsev et al., 2005; Kohlmaier et al., 2004). *Ezh2*$^{-/-}$;*Ezh1*$^{-/-}$ TSCs do not harbor H4-K20me1 enrichment indicating that this mark is also likely not responsible for X-inactivation. More work will need to be performed, however, to address a true role for PRSET7, the enzyme that catalyzes H4-K20me1, in imprinted X-inactivation.

I also discovered that *Ezh2*$^{-/-}$;*Ezh1*$^{-/-}$ mutant TSCs appear to not proliferate. Upon assaying the mitotic activity of my cells with immunofluorescence detection of H3-S10p, I failed to observe any *Ezh2*$^{-/-}$;*Ezh1*$^{-/-}$ TSCs cells that were positive for phosphorylated H3-S10. This histone mark is well established as a marker of entry into G2 phase of the cell cycle (Hendzel et al., 1997). I conclude that *Ezh2*$^{-/-}$;*Ezh1*$^{-/-}$ TSCs cannot divide indefinitely compared to *Ezh2*$^{fl/fl}$;*Ezh1*$^{-/-}$ TSCs. Further investigation will uncover a potential combinatorial role for EZH2 and EZH1 in trophoblast stem cell proliferation and survival.

Ezh2$^{-/-}$;*Ezh1*$^{-/-}$ TSCs also appear to have a smaller volume for their Xist domain at the inactive-X compared to *Ezh2*$^{fl/fl}$;*Ezh1*$^{-/-}$ TSCs. This implies that Xist RNA is on its way to being fully lost in *Ezh2*$^{-/-}$;*Ezh1*$^{-/-}$ TSCs. I alternatively hypothesize that, although I do not observe a defect in X-linked gene silencing in our transient *Ezh2*$^{-/-}$;*Ezh1*$^{-/-}$ TSCs, eventual loss of Xist may inexorably confer a defect in X-inactivation. However, as described above, I know that *Ezh2*$^{-/-}$;*Ezh1*$^{-/-}$ TSCs do not divide indefinitely. Further experimentation will need to be carried out to derive a constitutive *Ezh2*$^{-/-}$;*Ezh1*$^{-/-}$ TS cell line to examine for defects in X-inactivation. I alternatively propose that if *Ezh2*$^{-/-}$;*Ezh1*$^{-/-}$ TSCs were able to proliferate, that a constitutive null cell line for *Ezh2* and *Ezh1* would display defects in X-inactivation. Such a defect would be in synchrony with what I observed with our *Eed*$^{-/-}$ TS cell line (discussed below and previously reported, Kalantry et al., 2006; Maclary et al., 2016, in preparation).

The third and final core PRC2 component I wished to investigate was EED. EED is the "glue" of PRC2. Without EED, PRC2 does not form properly, and other subunits (EZH2, SUZ12) are degraded (Montgomery et al., 2005). Defects in X-inactivation both *in vivo* and *in vitro* when EED is missing have been previously documented (Mak et al., 2004; Kalantry et al., 2006; Maclary et al., 2016, in preparation). To more thoroughly investigate the role of EED in

propagating the X-inactive state, I derived an *Eed*$^{-/-}$ line from an *Eed*$^{fl/fl}$ cell line. My line is conditionally deficient for exon 7, which encodes for a WD40 domain #3 necessary for interaction with EZH2 (Denisenko et al., 1998; Han et al., 2007). Whereas the Kalantry et al. 2006 study concluded that loss of EED (with a point mutant for *Eed*) was only detrimental to cells upon differentiation of trophoblast tissues, I observed in my study a defect in X-inactivation in undifferentiated cells. In my *Eed*$^{-/-}$ TSCs, I observed a derepressive phenotype, albeit for only 25% (RNA-FISH and allele-specific RT-PCR results reported herein) of the genes along the inactive-X (18% when considering RNA-seq analysis of the entire X-chromosome (Maclary et al., 2016, in preparation)). This is in comparison to a lack of an observed defect in X-linked gene silencing in my *Ezh2*$^{-/-}$ and *Ezh2*$^{-/-}$;*Ezh1*$^{-/-}$ TSCs. It is therefore possible that EED complexes with other proteins to form a yet unidentified version of Polycomb repressive complex 2. I also know that EED has been shown interact with members of PRC1 (Cao et al., 2014). My alternative hypothesis here is that PRC1 is involved in X-inactivation through interaction with EED. My data suggest that PRC1 may perhaps not be involved in X-inactivation, however, as loss of H2A-K119ub1 is observed in both *Ezh2*/*Ezh1* double mutant and *Eed* mutant TS cells. It remains to be fully known, though, if PRC1 components themselves are genetically required for proper X-inactivation. Further genetic experiments will elucidate a true role for PRC1 components in X-inactivation. To interrogate additional histone marks that enrich on the inactive-X, I profiled for H4K20me1 enrichment in my *Eed*$^{-/-}$ TSCs vis-à-vis my *Eed*$^{fl/fl}$ TSCs. I found that my *Eed*$^{-/-}$ TSCs also lack H4-K20me1 inactive-X enrichment. Loss of multiple PRC2/PRC1 associated components, PRC2 as well as PRC1 enzymatic readouts, and other inactive-X associated repressive histone marks do indeed imply that the majority of X-linked genes are silenced by some other mechanism(s). Future work will unravel the key critical players in X-inactivation.

Based on my current data, I propose that EZH2/EZH1 and EED may be genetically distinct in terms of their requirement for X-chromosome condensation and X-linked gene silencing in mouse TSCs. I believe that loss of EED leads to loss of the transiently induced heterochromatinization of the inactive-X, which is thought to be important in Xist transcriptional activation (Sun et al., 2006; Zhao et al., 2008). Indeed, I observe Xist RNA enrichment loss in *Eed*$^{-/-}$ TSCs. In turn, EED, H3-K27me3, and Xist RNA absence led to a derepression of a select set of genes along the inactive-X. This is in stark contrast to *Ezh2*$^{-/-}$ or *Ezh2*$^{-/-}$;*Ezh1*$^{-/-}$ TSCs, which both display continued Xist RNA coating and silencing of X-linked genes. To understand why there is a defect in X-inactivation when ultimately Xist RNA is absent, I speculate that loss of Xist RNA may perturb interaction among several key players implicated in X-inactivation. Thus, silencing may be maintained in part by the collection of factors recently shown to interact with Xist RNA (Chan et al., 2011; Chu et al., 2015; McHugh et al., 2015; Minajigi et al., 2015; Minkovsky et al., 2015; Moindrot et al., 2015; Monfort et al., 2015). Future studies will disentangle the extent to which other epigenetic factors are involved in stable silencing of X-linked genes in mouse trophoblast stem cells. Such further experimentation will in turn elucidate the potential supplementary mechanism(s) that must operate to silence the majority of X-linked genes.

Conclusion

In conclusion, I uncovered distinct roles for the members of the Polycomb group repressive complex 2 with respect to imprinted X-chromosome inactivation. Previously an open question in the field, here I revealed an answer with direct genetic evidence for a divergent role among PRC2 protein subunits in stably propagating the inactive-X state *in vitro*. Whereas EZH2 and/or EZH1 are not required in maintaining imprinted X-inactivation, EED is required partially

for propagating the silencing of some X-linked genes. A divergent requirement for EZH2/EZH1 and EED in silencing a subset of X-linked genes suggests that there is perhaps a histone H3-K27me3 specific independent function of PRC2 (through the activities of EED) in X-chromosome inactivation. Furthermore, H3-K27me3/PRC2 independent silencing of genes extends to a majority of X-linked genes, as most of the inactive-X is still silenced upon loss of EZH2/EZH1 and even EED (Maclary et al., 2016, in preparation). My results potentially open up new routes of investigation to identify the key factors at play in X-linked gene silencing. It is possible that there are a multitude of epigenetic factors, such as proteins, RNAs, or even other repressive complexes, that contribute to imprinted X-inactivation. My observations hint towards at least more than one mechanism, which must operate simultaneously to carry out X-linked gene silencing. My data also imply that EED, but not EZH2/1, is necessary to maintain silencing of a select set of genes in undifferentiated TSCs. Divergent requirements for PRC2 proteins in undifferentiated TSCs may predict what is happening *in vivo* as X-inactivation is established in the early mouse embryo. Further experiments will shed light on these hypotheses. In turn, better knowledge of the intricate molecular mechanism(s) underlying imprinted X-chromosome inactivation will hopefully expose the method by which epigenetic phenomena operate broadly both in normal development as well as in human disease.

Materials and Methods

Ethics Statement

My study was performed in strict accordance with the recommendations in the guide for the Care and Use of Laboratory Animals of the National Institutes of Health. All animals were handled according to protocols approved by the University Committee on Use and Care of Animals (UCUCA) at the University of Michigan (protocol #PRO00006455).

Mice

Mice harboring a conditional mutation in *Eed* were generated by the University of Michigan Transgenic Animal Model Core using $Eed^{tm1a(EUCOMM)Wtsi}$ targeted ES cells (EUCOMM). Briefly, ES cells were injected into blastocysts and implanted into pseudo-pregnant females. Mice with high percentages of chimerism were bred and assessed for germline transmission. To generate homozygous *Eed* mutant mice harboring polymorphic X-chromosomes, male and female mice on a B6 *Mus musculus* background carrying the conditional mutant allele for *Eed* were intercrossed ($Eed^{fl/+}$ x $Eed^{fl/+}$) to achieve homozygosity. To obtain mice conditionally mutant for *Eed* and on the JF1 *Mus molossinus* divergent background, $Eed^{fl/fl}$ males (B6 *Mus musculus* background) were bred to *WT* JF1 *Mus molossinus* females. This gave us F1 hybrid $Eed^{fl/+}$ males that possessed an X-chromosome from the JF1 *Mus molossinus* background (X^{JF1}/Y). Such males were backcrossed to *WT* JF1 *Mus molossinus* females to derive $Eed^{fl/+}$ females that were a mix of B6 *Mus musculus* and JF1 *Mus molossinus* and also harbored two X-chromosomes from the JF1 *Mus molossinus* background (X^{JF1}/X^{JF1}). $Eed^{fl/+};X^{JF1}/X^{JF1}$ females were bred against $Eed^{fl/+};X^{JF1}/Y$ males to derive $Eed^{fl/fl};X^{JF1}/Y$ males. To obtain our female embryos used for TS cell

derivation, *Eed*$^{fl/fl}$ females on the B6 *Mus musculus* background were bred with an *Eed*$^{fl/fl}$ male that was a mix of B6 *Mus musculus* and JF1 *Mus molossinus* but possessed an X-chromosome from the JF1 *Mus molossinus* background (X^{JF1}/Y). The JF1/Ms strain has been described previously.

Ezh2$^{fl/fl}$ mice were gifted from Alexander Tarakhovsky and maintained on a 129 background. Mice were crossed in homozygosity for deriving my *Ezh2*$^{fl/fl}$ TS cells.

Ezh1$^{-/-}$ mice were gifted from Alexander Tarakhovsky, originally bred by Dønal O'Carroll in Thomas Jenuwein's laboratory and were maintained on a BL/6 background.

Ezh2 and *Ezh1* mice were intercrossed and bred to generate my *Ezh2*/*Ezh1* mice in a similar manner as described for the generation of our *Eed* mice for deriving our *Ezh2*$^{fl/fl}$;*Ezh1*$^{-/-}$;X^{Lab}/X^{JF1} TS cells.

TS cell derivation and culture

Blastocysts were dissected out of pregnant mice 3.5 dpc and plated in four well dishes pre-seeded with mouse embryonic fibroblasts (MEFs). Hatched embryos were cultured in standard TS medium supplemented with 1.5x FGF4 and Heparin for 4-5 days until blastocyst outgrowths were of ideal size. Blastocysts were then trypsinized in 0.05% Trypsin-EDTA, neutralized with TS media supplemented with 1.5x FGF4 and Heparin, and cultured in 96 well dishes. Once lines were well established, XX/XY PCRs confirmed female lines and respective genotypes PCRs for *Ezh2*, *Ezh2*/*Ezh1*, and *Eed* confirmed *Ezh2*$^{fl/fl}$, *Ezh2*$^{fl/fl}$;*Ezh1*$^{-/-}$;X^{Lab}/X^{JF1}, and *Eed*$^{fl/fl}$;X^{Lab}/X^{JF1}lines. Cell lines were then cultured in standard TS media supplemented with FGF4 and Heparin. RNA was harvested from TS cells using TRIzol (Invitrogen, #15596-018) and RT-PCR was performed as described below. For IF or IF combined with RNA-FISH, TS cells were split onto gelatin-coated glass coverslips and allowed to grow for 2-3 days. The cells were then permeabilized

through sequential treatment with ice-cold cytoskeletal extraction buffer (CSK; 100 mM NaCl, 300 mM sucrose, 3 mM $MgCl_2$, and 10 mM PIPES buffer, pH 6.8) for 30 seconds, ice-cold CSK buffer containing 0.4% Triton X-100 (Fisher Scientific, #EP151) for 30 seconds, followed twice with ice-cold CSK for 30 seconds. After permeabilization, cells were fixed by incubation in 4% paraformaldehyde at room temperature for 10 minutes. Cells were then rinsed three times each in 70% ethanol and stored in 70% ethanol at -20°C prior to IF or IF combined with RNA-FISH.

Generating stable *Ezh2*$^{-/-}$ and *Eed*$^{-/-}$ TSCs

Ezh2$^{fl/fl}$ and *Eed*$^{fl/fl}$ TSCs were plated at a 1:24-1:48 dilution into six well dishes pre-seeded with MEFs and allowed to adhere until the next day. Cells were then transfected with Cre-Puro plasmids (*Ezh2*$^{fl/fl}$ TSCs) *or* transduced with Ad5-CMV-Cre (*Eed*$^{fl/fl}$ TSCs, Adenovirus type 5, University of Michigan Viral Vector Core adenoviral construct, 4 x 10^{12} particles/mL) at an MOI of 1000. For *Ezh2*$^{fl/fl}$ TS cells, subcloning and PCR screening was immediately carried out to isolate a pure population of *Ezh2*$^{-/-}$ cells. For *Eed*$^{fl/fl}$ TS cells, once cell colonies were large enough following the initial transduction, they were subcloned into 96 well dishes pre-seeded with MEFs and re-transduced 24 hours later with Adeno-Cre at a multiplicity of infection (MOI) of 1000. Following this expanded 96, well samples were split into six well dishes pre-seeded MEFs and again transduced 24 hours later. A portion of each 96 well samples was lysed for DNA genotyping to assess the efficiency of Cre-mediated deletion of the *Eed* floxed alleles. Subcloning, transduction, and genotyping procedures were repeated until a pure population of *Eed*$^{-/-}$ TSCs was achieved.

Ezh2$^{-/-}$ and *Eed*$^{-/-}$ TSCs were maintained in culture as described above.

Generating Transient *Ezh2*$^{-/-}$;*Ezh1*$^{-/-}$ TSCs

Ezh2$^{fl/fl}$;*Ezh1*$^{-/-}$ TS cells were plated at a 1:24 dilution on gelatinized coverslips in six well dishes. Cells were transduced with Ad5-CMV-Cre viral vector at an MOI of 1000 for 48, 72, and 96 hours. Cells adherent on the coverslips were then CSK-treated and fixed with 4% PFA and stored for immunofluorescence and/or RNA-FISH. The remaining adherent cells on the edges of each well of the six well dishes were washed once with 1 mL cold 1X PBS, followed by aspiration of PBS. Cells were then incubated in 1mL TRIzol at 4°C for five minutes. Lysates were stored in TRIzol at -80°C until RNA extraction.

Immunofluorescence

Sample coverslips containing CSK-treated and 4% PFA-fixed cells were placed in a six well dish that contained 2ml of 1X PBS in each well. Samples were then washed briefly with three changes of 1X PBS to remove ethanol followed by three successive washes with 1X PBS for three minutes each on a rocker. Samples were blocked for 30 minutes at 37°C in 50 μl pre-warmed blocking buffer in a humid chamber. Samples were then incubated for one hour at 37°C in 50 μL diluted primary antibody (dilution depends on primary antibody used, i.e. 1:500 EED primary Ab, previously used in (Kalantry et al., 2006; Plath et al., 2003; Silva et al., 2003); 1:5000 H3-K27me3 primary Ab, Millipore, #ABE44; 1:100 EZH2 primary Ab, Cell Signaling; 1:10 H2A-K119ub1 primary Ab, Cell Signaling; 1:150 H3-S10p primary Ab, Cell Signaling, 1:1000 H4-K20me1 primary Ab, Abcam) in a humid chamber. After incubation, samples were washed three times with 1X PBS/0.2% Tween-20 for three minutes each on a rocker. Coverslips were then placed back in 50 μL pre-warmed blocking buffer in a humid chamber for five minutes at 37°C followed by an additional incubation for 30 minutes at 37°C in 50 μL diluted secondary antibody. Alexa Fluor conjugated secondary antibodies were used at a 1:300 dilution.

Following secondary incubation, coverslips were washed three times with 1X PBS/0.2% Tween-20 for three minutes each on a rocker. Samples were incubated in 100 μl of 2% PFA on a glass plate wrapped in parafilm for ten minutes at room temperature. Following this, samples were dehydrated through room temperature ethanol series (five minutes each for 70%, 85%, 95%, and 100% ethanol). Coverslips were allowed to dry for 15 minutes after the 100% ethanol wash, followed by hybridizing the samples overnight with the appropriate RNA-FISH probe. After hybridization, samples were washed for seven minutes at 39°C, three times each in 2X SSC/50% formamide. This was followed by three-seven minute washes at 39°C, in 2X SSC (1:100,000-1:200,000 dilution of DAPI added at third wash of 2X SSC) and followed by two-seven minute washes at 39°C, in 1X SSC. Sample coverslips were then mounted onto glass microscope slides with Vectashield. Coverslips were sealed to the glass slides with clear nail polish.

RNA-FISH

Samples were dehydrated through room temperature ethanol series (five minutes each for 70%, 85%, 95%, and 100% ethanol). Coverslips were allowed to dry for 15 minutes at room temperature after the 100% ethanol wash, followed by hybridizing the samples overnight with the appropriate RNA-FISH probe. After the hybridization, samples were washed for seven minutes, at 39°C, three times each in 2X SSC/50% formamide. This was followed by three-seven minute washes at 39°C, in 2X SSC (1:100,000-1:200,000 dilution of DAPI added at third wash of 2X SSC) and followed by two-seven minute washes at 39°C, in 1X SSC. Sample coverslips were then mounted onto glass microscope slides with Vectashield. Coverslips were sealed to the glass slides with clear nail polish.

Isolation of Total RNA and mRNA

Total RNA was purified from cultured TS cell lines using TRIzol reagent (Life Technologies, #15596018). Total RNA was treated with DNase (Life Technologies, #AM1906) to remove any contaminant genomic DNA. mRNA was isolated from total RNA using Dynabeads mRNA DIRECT Micro Kit (Life Technologies, #61012).

Allele-Specific Reverse Transcriptase Polymerase Chain Reaction (RT-PCR)

Total RNA was isolated from TRIzol following manufacturers instructions. mRNA was then purified from Total RNA lysates according to manufacturers instructions (Life Technologies Dynabeads mRNA direct kit). SuperScript III One-Step RT-PCR Kit with Platinum *Taq* enzyme mixture (Invitrogen, #12574-035) was used to prepare and amplify the complimentary DNA (cDNA). Amplified cDNAs were run on agarose gels and purified using the Clontech NucleoSpin Kit (Clontech, #740609). The purified cDNAs were then sequenced and sequencing traces were examined for single nucleotide polymorphisms (SNPs) characteristic of the *M. molossinus*-derived X^{JF1} chromosome and the *M. musculus*-derived X^{Lab} chromosomes.

PCR

For DNA isolation, cell pellets from TSCs were lysed in buffer composed of 50mM KCl, 10mM Tris-Cl (pH 8.3), 2.5mM $MgCl_2$, 0.1mg/ml gelatin, 0.45%NP-40, and 0.45% Tween-20. Cells in lysis buffer were incubated at 50^0C overnight, and then stored at 4^0C until use. Genomic PCR reactions were carried out in ChromaTaq buffer (Denville Scientific) with 1.5mM Magnesium Chloride using RadiantTaq DNA polymerase (Alkali Scientific, #C109).

Microscopy

Images of all stained samples were captured using a Nikon Eclipse TiE inverted microscope build with a Photometrics CCD camera. The images were analyzed after deconvolution using

NIS-Elements software. All images were processed uniformly. The volume of Xist RNA signals were measured using the NIS elements "3D Measurement; 3D thresholding, 3D viewing and voxel based measurements" software package (Nikon Instruments, 77010582). Briefly, the fluorescence channel with the Xist RNA-FISH stain was extracted from each image, and uniform thresholds were set for signal size across all images to avoid inclusion of background signal. For all regions above threshold within an image, the volume of each discrete region was calculated.

Statistical Analysis

All analyses utilized Welch's two sample t-tests. Significance level was set at $\alpha=0.05$.

Table of Primers I
Primers for PCR/RT-PCR
Sanger sequencing (S)/Genotyping (G)

Primer	Sequence	Use
Atrx-F	GGGATTGCTGCTGTGAGTCT	PCR (S)
Atrx-R	CCACCATCTTCTTGCCATCT	RT, PCR (S)
Rnf12-F	GAGCCCCGATGAAAATAGAGC	PCR (S)
Rnf12-R	GGTCGGCACTTCTGTTACTGC	RT, PCR (S)
Pdha1-F	GGGACGTCTGTTGAGAGAGC	PCR (S)
Pdha1-R	GCACTTCAAAGGGAGGATCA	RT, PCR. (S)
Pgk1-F	GAAGGGAAGGGAAAAGATGC	PCR (S)
Pgk1-R	TGTGCCAATCTCCATGTTGT	RT, PCR (S)
Xist (XF)-9229	GACAACAATGGGAGCTGGTT	PCR (G)
Xist (XR)-9572	CCAGGCAATCCTTCTTCTTG	RT, PCR (G)
WUStL-Cre-F	GCATTACCGGTCGATGCAACGAGTGATGAG	G
WUStL-Cre-R	GAGTGAACGAACCTGGTCGAAATCAGTGCG	G
EED-F2	CCTGTCAGGCAGTCATTTCA	G
EED-R2	CCTACTGGTCGGTCTTGCAT	G
Eed-5'arm	GGACTCATCCTCTGGTAGAGCAGC	G

Eed-3'arm	TGCCTACTGCAAACTTTTAGTATGCC	G
WT-R2:	GCTCCTGTCCTCATAGCAAGA	G
SA-1:	GTACTCTTAACCACTGGACTG	G
LACZ-2:	AAGCGCCATTCGCCATTCAGG	G
Enx1-3-loxP:	CTGCTCTGAATGGCAACTCC	G
Ezh2-5-loxp-3	CTGGCTCTGTGGAACCAAAC	G
Ezh2-L5-loxp-1	ATGGGCCTCATAGTGACAGG	G
SK-Fabpi-S-F	TGGACAGAACTGGACCTCTGCTTTCCTA	G
SK-Fabpi-S-R	TAGAGCTTTGCCACATCACAGGTCATTC	G
Flp-F	GGT CCA ACT GCA GCC CAA GCT TCC	G
Flp-R	GTG GAT CGA TCC TAC CCC TTG CG	G
JR-eGFPf	CTG AAG TTC ATC TGC ACC ACC	G
JR-eGFPr	ATG CCG TTC TTC TGC TTG TCG	G
LacZ SK-WUStL-B-gal-F	GTTGCAGTGCACGGCAGATACACTTGCT	G
LacZ SK-WUStL-R	GCCACTGGTGTGGGCCATAATTCAATTC	G

BA-Neo-F	AGAGGCTATTCGGCTATGACTG	G
BA-Neo-R	CCTGATCGACAAGACCGGCTTC	G
Stra8CreF	GTGCAAGCTGAACAACAGGA	G
Stra8CreR	AGGGACACAGCATTGGAGTC	G
Xist 5LoxR_LW	ACC CTT GCC TTT TCC ATT TT	G
Xist3R_LW	CAC TGG CAA GGT GAA TAG CA	G
XpromL_LW	TTT CTG GTC TTT GAG GGC AC	G
XX-XY.F	CCGCTGCCAAATTCTTTGG	G
XX-XY.R	TGAAGCTTTTGGCTTTGAG	G
SRY-F	TTG TCT AGA GAG CAT GGA GGG CCA TGT CAA	G
SRY-R	CCA CTC CTC TGT GAC ACT TTA GCC CTC CGA	G
Zp3creF	CAG ATG AGG TTT GAG GCC ACA G	G
Zp3creR	CCC GGC AAA ACA GGT AGT TA	G

Acknowledgements

I would like to thank Alexander Tarakhovsky for gifting our lab *Ezh2*$^{fl/fl}$ mice and *Ezh1*$^{-/-}$ mice. I also thank the University of Michigan Transgenic Animal Core Facility for injecting our targeted *Eed* ES cell constructs into blastocysts and implanting these into pseudo-pregnant mice for generating germline transmission of our *Eed*$^{fl/fl}$ conditional mutation. I would also like to thank Emily Maclary for her extensive bioinformatic analysis of my *Eed*$^{-/-}$ TSCs lines. This work, although not included in my thesis in great detail, is presented and discussed in a manuscript (Maclary et al., 2016, in preparation). I would additionally like to thank Clair Harris for deriving the *Ezh2*$^{fl/fl}$ and the *Eed*$^{fl/fl}$ TSC line from which I was able to obtain mutant *Ezh2*$^{-/-}$ and *Eed*$^{-/-}$ lines, respectively.

Notice on Future Publication of This Work

This data chapter will be submitted for publication in a peer reviewed scientific journal. The following is the reference that will accompany the submission:

> Maclary, E., Hinten, M., Harris, C., Sethuraman, S., Kalantry, S. (2016). PRC2 prevents upregulation of genes with open chromatin architecture on the inactive X-chromosome. In preparation.

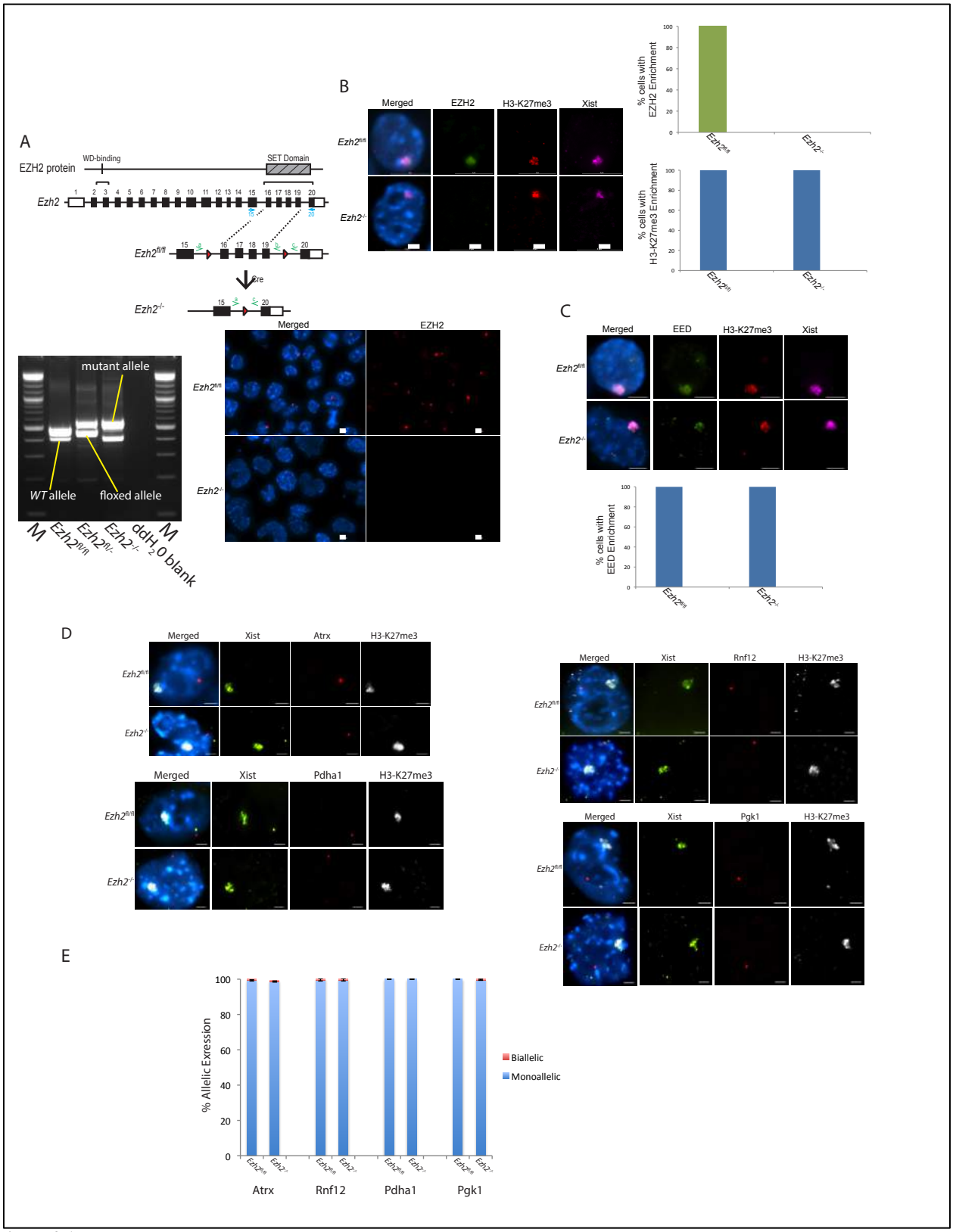
A
EZH2 protein
WD-binding
SET Domain
Ezh2
Ezh2fl/fl
Cre
Ezh2-/-
mutant allele
WT allele
floxed allele
M
Ezh2fl/fl
Ezh2fl/-
Ezh2-/-
ddH2O blank
M
B
Merged
EZH2
H3-K27me3
Xist
Ezh2fl/fl
Ezh2-/-
% cells with EZH2 Enrichment
% cells with H3-K27me3 Enrichment
C
Merged
EED
H3-K27me3
Xist
% cells with EED Enrichment
D
Merged
Xist
Atrx
H3-K27me3
Merged
Xist
Pdha1
H3-K27me3
Merged
Xist
Rnf12
H3-K27me3
Merged
Xist
Pgk1
H3-K27me3
E
% Allelic Exression
Biallelic
Monoallelic
Atrx
Rnf12
Pdha1
Pgk1

Figure 2.1

Figure 2.1. EZH2 is dispensable for propagating the inactive-X state in mouse trophoblast stem cells.

A. Schematic diagram of our *Ezh2* mutation. Our mutation removes the SET domain, which spans exons 16-20 of *Ezh2*. loxP sites (red triangles) were integrated after exon 15 and before exon 20. Primers (in green) a and b will pick up *WT* and floxed alleles for *Ezh2,* while primers a and c will pick up the mutant *Ezh2* allele. The WD-binding domain is also indicated at exons 2 and 3. This is the site of interaction between EZH2 and EED. Below diagram is a PCR validation of the deletion of the SET domain in *Ezh2*$^{-/-}$ TSCs. Lane 1 is the *Ezh2*$^{fl/fl}$ cell line, lane 2 is a heterozygous sample (fl/-), and lane 3 is the *Ezh2*$^{-/-}$ cell line. Floxed, mutant, and *WT* (i.e. not floxed) bands are indicated by yellow line segments. Our cell lines sometimes pick up the *WT* allele, as these cells were grown on *WT* male mouse embryonic fibroblast (MEF) feeder cells to prevent TSCs from differentiating. M=Marker. To the right of the PCR image is an immunofluorescence detection of EZH2 as an additional genotyping measure of our cells. *Ezh2*$^{fl/fl}$ cells have EZH2 inactive-X enrichment, where as *Ezh2*$^{-/-}$ TSCs do not.

B. Individual nuclei from representative immunofluorescence/RNA-FISH experiments on *Ezh2*$^{fl/fl}$ and *Ezh2*$^{-/-}$ TSCs. EZH2 is in green, H3-K27me3 is in red, and Xist is in purple marking the inactive X-chromosome. Nuclei stained with DAPI. Scale bar is 2 μm. Quantifications below images. Graphs represent percent nuclei with EZH2 or H3-K27me3 inactive-X enrichment normalized to Xist RNA. Three independent experiments (technical replicates) were performed. 100 nuclei per genotype per experimental replicate were counted.

C. Individual nuclei from representative immunofluorescence/RNA-FISH experiments on *Ezh2*$^{fl/fl}$ and *Ezh2*$^{-/-}$ TS cells. EED is in green, H3-K27me3 is in red, and Xist is in purple marking the inactive X-chromosome. Nuclei stained with DAPI. Scale bar is 2 μm. Quantifications below images. Graph represents percent nuclei with EED inactive-X enrichment normalized to Xist RNA. Three independent experiments (technical replicates) were performed. 100 nuclei per genotype per experimental replicate were counted.

D. Representative nuclei from immunofluorescence/RNA-FISH experiments on *Ezh2*$^{fl/fl}$ and *Ezh2*$^{-/-}$ TSCs for Atrx, Rnf12, Pdha1, and Pgk1. Scale bar is 2 μm. Xist is in green, X-linked gene in red, and H3-K27me3 in white. Nuclei stained with DAPI. Scale bar is 2 μm. Three independent experiments (technical replicates) were performed for each X-linked gene. 100 nuclei per genotype per experimental replicate were counted.

E. Quantifications for each gene below the images in D. Averages + or - SEM from three independent experiments (technical replicates) were performed. 100 nuclei per genotype per experimental replicate were counted. p-value: Atrx: 0.518518519, Rnf12: 1, Pdha1: N/A (no variation in data), Pgk1: 0.422649731; Welch's two sample t-test.

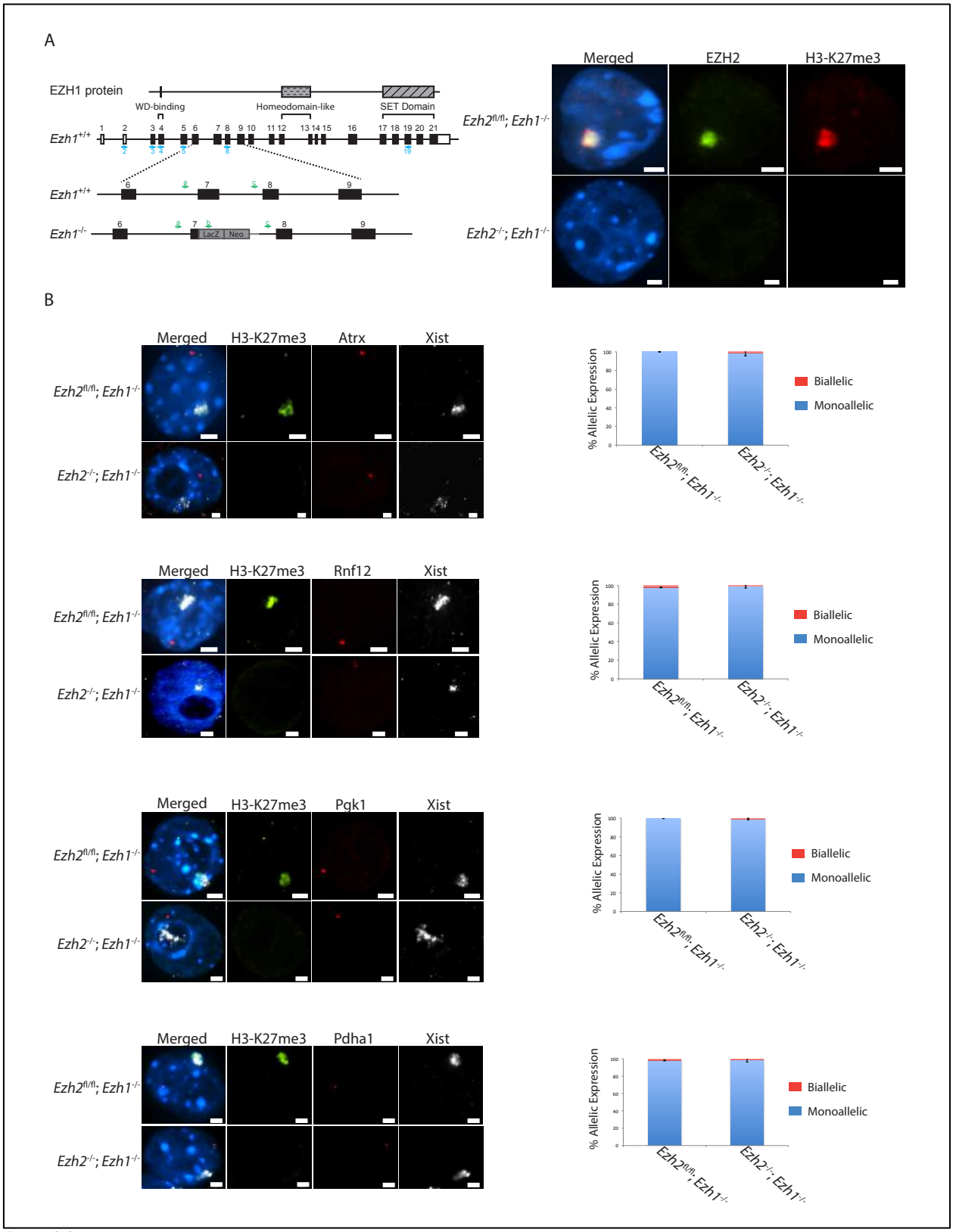
A
EZH1 protein
WD-binding
Homeodomain-like
SET Domain
Ezh1+/+
Ezh1+/+
Ezh1-/-
LacZ
Neo
Merged
EZH2
H3-K27me3
Ezh2fl/fl; Ezh1-/-
Ezh2-/-; Ezh1-/-
B
Merged
H3-K27me3
Atrx
Xist
Rnf12
Pgk1
Pdha1
% Allelic Expression
Biallelic
Monoallelic

Figure 2.2

Figure 2.2. EZH1 does not contribute to imprinted X-chromosome inactivation in mouse trophoblast stem cells.

A. Representative single nucleus images of *Ezh2*$^{fl/fl}$;*Ezh1*$^{-/-}$ and *Ezh2*$^{-/-}$;*Ezh1*$^{-/-}$ TSCs. *Ezh2*$^{-/-}$;*Ezh1*$^{-/-}$ TSCs are designated as such due to loss of EZH2 enrichment.
EZH2 is in green, H3-K27me3 in red. Nuclei stained with DAPI. Scale bar is 2 μm.
Schematic diagram of *Ezh1* mutation is to the left of image. Our mutation contains a LacZ/Neo cassette inserted into exon 7. This cassette renders the gene unable to be fully transcribed. It does not contain the SET domain. The SET domain for EZH1 is encoded by exons 17-21. Primers (in green) a and c will pick up *WT* alleles for *Ezh1,* while primers a and b will pick up the mutant *Ezh2* allele with the inserted LacZ/Neo cassette. The WD-binding domain is also indicated at exons 3 and 4. This is the site of interaction between EZH1 and EED.

B. Representative single nucleus images from immunofluorescence/RNA-FISH experiments on *Ezh2*$^{fl/fl}$;*Ezh1*$^{-/-}$ and *Ezh2*$^{-/-}$;*Ezh1*$^{-/-}$ TSCs (i.e. non-Cre and Cre-treated *Ezh2*$^{fl/fl}$;*Ezh1*$^{-/-}$ TSCs). H3-K27me3 is in green, X-linked gene in red, and Xist in white. Nuclei stained with DAPI. Scale bar is 2 μm. Quantifications of each gene for *Ezh2*$^{fl/fl}$;*Ezh1*$^{-/-}$ and *Ezh2*$^{-/-}$;*Ezh1*$^{-/-}$ TSCs are to the right of each image. Averages + or - SEM from three independent experiments (technical replicates) for each X-linked gene. 100 nuclei per genotype per experimental replicate were counted.

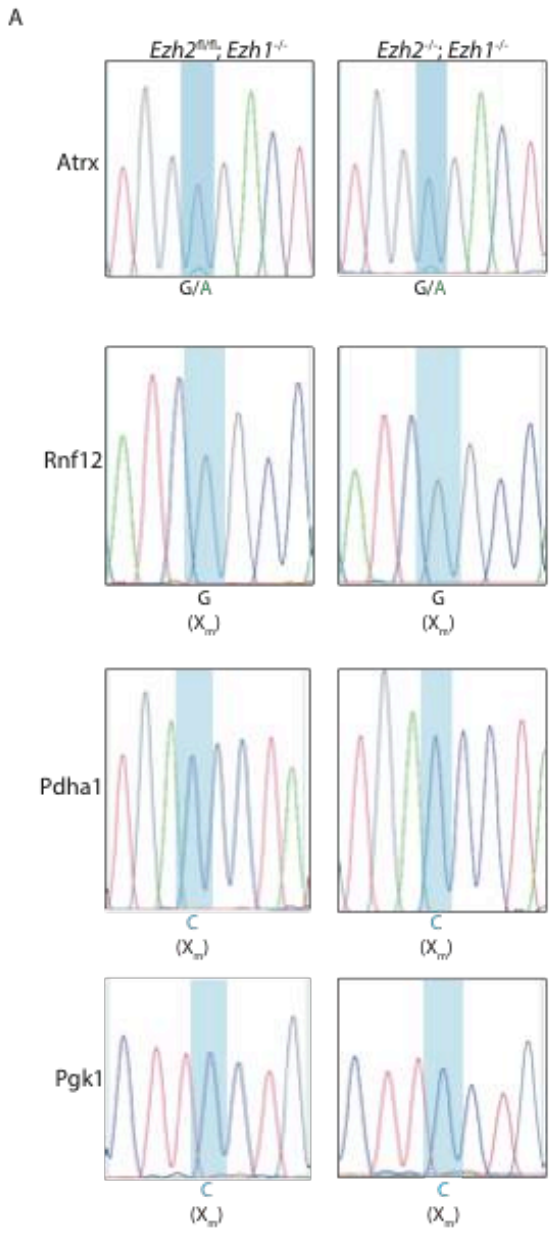
A
Ezh2fl/fl; Ezh1-/-
Ezh2-/-; Ezh1-/-
Atrx
G/A
G/A
Rnf12
G
(Xm)
G
(Xm)
Pdha1
C
(Xm)
C
(Xm)
Pgk1
C
(Xm)
C
(Xm)

Figure 2.3

Figure 2.3. EZH1 does not contribute to imprinted X-chromosome inactivation in mouse trophoblast stem cells.

A. Representative chromatograms from allele-specific experiments on *Ezh2*$^{fl/fl}$;*Ezh1*$^{-/-}$ and *Ezh2*$^{-/-}$;*Ezh1*$^{-/-}$ TSCs for Atrx, Rnf12, Pdha1, and Pgk1. Chromatograms represent cDNA from RT-PCR amplifications for each gene.

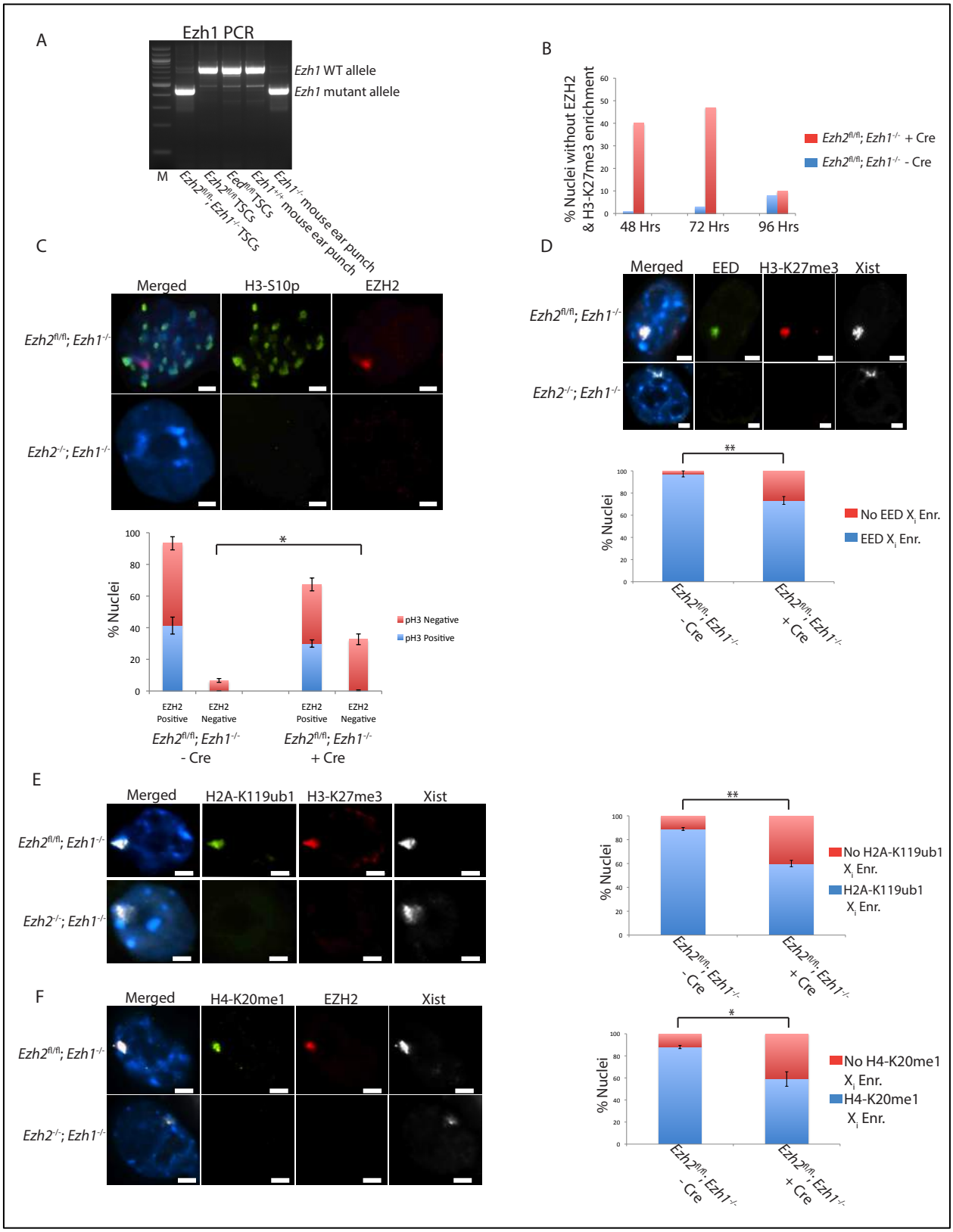
A
Ezh1 PCR
Ezh1 WT allele
Ezh1 mutant allele
M
Ezh2fl/fl; Ezh1-/- TSCs
Ezh2fl/fl TSCs
Eedfl/fl TSCs
Ezh1+/+ mouse ear punch
Ezh1-/- mouse ear punch
B
% Nuclei without EZH2 & H3-K27me3 enrichment
48 Hrs
72 Hrs
96 Hrs
Ezh2fl/fl; Ezh1-/- + Cre
Ezh2fl/fl; Ezh1-/- - Cre
C
Merged
H3-S10p
EZH2
Ezh2fl/fl; Ezh1-/-
Ezh2-/-; Ezh1-/-
% Nuclei
pH3 Negative
pH3 Positive
EZH2 Positive
EZH2 Negative
Ezh2fl/fl; Ezh1-/- - Cre
Ezh2fl/fl; Ezh1-/- + Cre
D
Merged
EED
H3-K27me3
Xist
Ezh2fl/fl; Ezh1-/-
Ezh2-/-; Ezh1-/-
% Nuclei
No EED Xi Enr.
EED Xi Enr.
Ezh2fl/fl; Ezh1-/- - Cre
Ezh2fl/fl; Ezh1-/- + Cre
E
Merged
H2A-K119ub1
H3-K27me3
Xist
Ezh2fl/fl; Ezh1-/-
Ezh2-/-; Ezh1-/-
% Nuclei
No H2A-K119ub1 Xi Enr.
H2A-K119ub1 Xi Enr.
F
Merged
H4-K20me1
EZH2
Xist
Ezh2fl/fl; Ezh1-/-
Ezh2-/-; Ezh1-/-
% Nuclei
No H4-K20me1 Xi Enr.
H4-K20me1 Xi Enr.

Figure 2.4

Figure 2.4. *Ezh2*$^{-/-}$;*Ezh1*$^{-/-}$ trophoblast stem cells do not proliferate and are devoid of other Polycomb factors/histone marks on the inactive-X.

A. *Ezh1* PCR denoting *Ezh1* genotyping of the *Ezh2*$^{fl/fl}$;*Ezh1*$^{-/-}$ TS cells used to derive *Ezh2*$^{-/-}$;*Ezh1*$^{-/-}$, genotypes and bands noted. M=Marker, 100 bp ladder.

B. Quantification of the deletion efficiency for EZH2 in transiently transduced *Ezh2*$^{fl/fl}$;*Ezh1*$^{-/-}$ TSCs. Mock *Ezh2*$^{fl/fl}$;*Ezh1*$^{-/-}$ versus Adeno-Cre transduced *Ezh2*$^{fl/fl}$;*Ezh1*$^{-/-}$ are shown. Transduction was carried out for 96 hours, with cells harvested at 48, 72, and 96 hours for analysis (immunofluorescence was performed for EZH2 and H3-K27me3 to assess efficiency of Cre-mediated deletion of *Ezh2* floxed alleles).

C. Representative single nucleus images of *Ezh2*$^{fl/fl}$;*Ezh1*$^{-/-}$ and *Ezh2*$^{-/-}$;*Ezh1*$^{-/-}$ TSCs from immunofluorescence detection of Histone H3-S10p, a marker of actively (mitotically) dividing cells. H3-S10p is in green and EZH2 in red. Nuclei stained with DAPI. Scale bar is 2 μm. Quantifications are below image. Averages + or - SEM from three independent experiments (technical replicates). 100 nuclei per genotype per experimental replicate were counted.*p-value: 0.013129833, Welch's two sample t-test (p-value is than 0.05).

D. Representative single nucleus images of *Ezh2*$^{fl/fl}$;*Ezh1*$^{-/-}$ and *Ezh2*$^{-/-}$;*Ezh1*$^{-/-}$ TSCs. EED is in green, H3-K27me3 in red, and Xist in white. Nuclei stained with DAPI. Scale bar is 2 μm. Quantifications are below image. Averages + or - SEM from three independent experiments (technical replicates). 100 nuclei per genotype per experimental replicate were counted. **p-value: 0.005967828, Welch's two sample t-test (p-value is less than 0.01).

E. Representative single nucleus images of *Ezh2*$^{fl/fl}$;*Ezh1*$^{-/-}$ and *Ezh2*$^{-/-}$;*Ezh1*$^{-/-}$ TSCs. H2A-K119ub1 is in green, H3-K27me3 in red, and Xist in white. Nuclei stained with DAPI. Scale bar is 2 μm. Quantifications are below image. Averages + or - SEM from three independent experiments (technical replicates). 100 nuclei per genotype per experimental replicate were counted. **p-value: 0.002867973, Welch's two sample t-test (p-value is less than 0.01).

F. Representative single nucleus images of *Ezh2*$^{fl/fl}$;*Ezh1*$^{-/-}$ and *Ezh2*$^{-/-}$;*Ezh1*$^{-/-}$ TSCs. H4-K20me1 is in green, EZH2 in red, and Xist in white. Nuclei stained with DAPI. Scale bar is 2 μm. Quantifications are below image. Averages + or - SEM from three independent experiments (technical replicates). 100 nuclei per genotype per experimental replicate were counted. *p-value: 0.028383675, Welch's two sample t-test (p-value is less than 0.05).

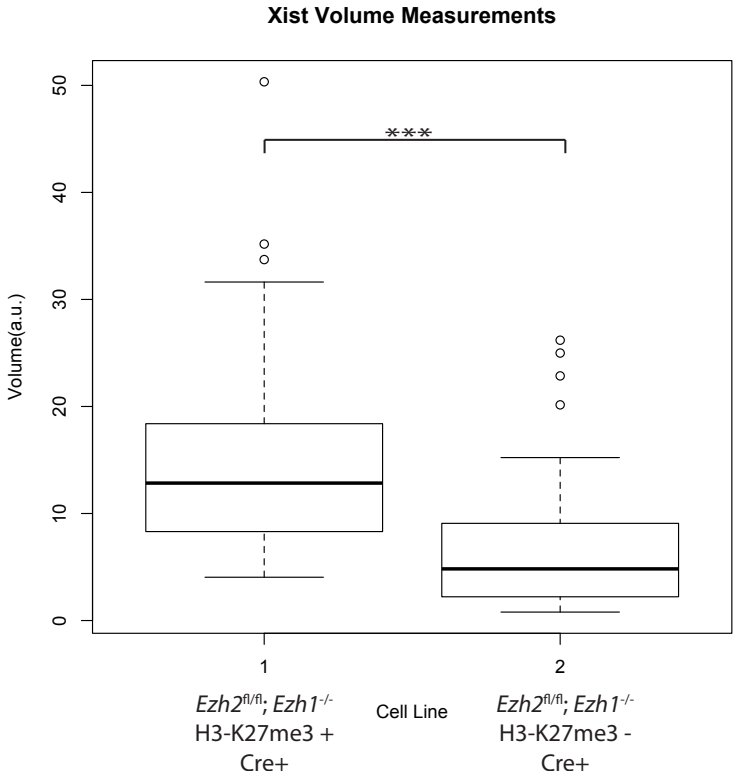
Xist Volume Measurements
Volume(a.u.)
0
10
20
30
40
50
***
1
2
Ezh2fl/fl; Ezh1-/-
H3-K27me3 +
Cre+
Cell Line
Ezh2fl/fl; Ezh1-/-
H3-K27me3 -
Cre+

Figure 2.5

Figure 2.5. Xist coats have a reduced volume in *Ezh2*$^{-/-}$;*Ezh1*$^{-/-}$ TSCs.

Boxplots of automated 3D measurements of volume of Xist RNA coats in *Ezh2*$^{fl/fl}$;*Ezh1*$^{-/-}$ TSCs and *Ezh2*$^{-/-}$;*Ezh1*$^{-/-}$ TSCs.

Left plot: *Ezh2*$^{fl/fl}$;*Ezh1*$^{-/-}$ TSCs that were H3-K27me3 positive from Adeno-Cre treated cells. Right plot: *Ezh2*$^{fl/fl}$;*Ezh1*$^{-/-}$ TSCs that were H3-K27me3 negative (i.e. *Ezh2*$^{-/-}$;*Ezh1*$^{-/-}$ TSCs) from Adeno-Cre treated cells.
***p-value: 7.01764E-07, Welch's two sample t-test; n=50 nuclei per genotype were analyzed (p-value less than 0.001).

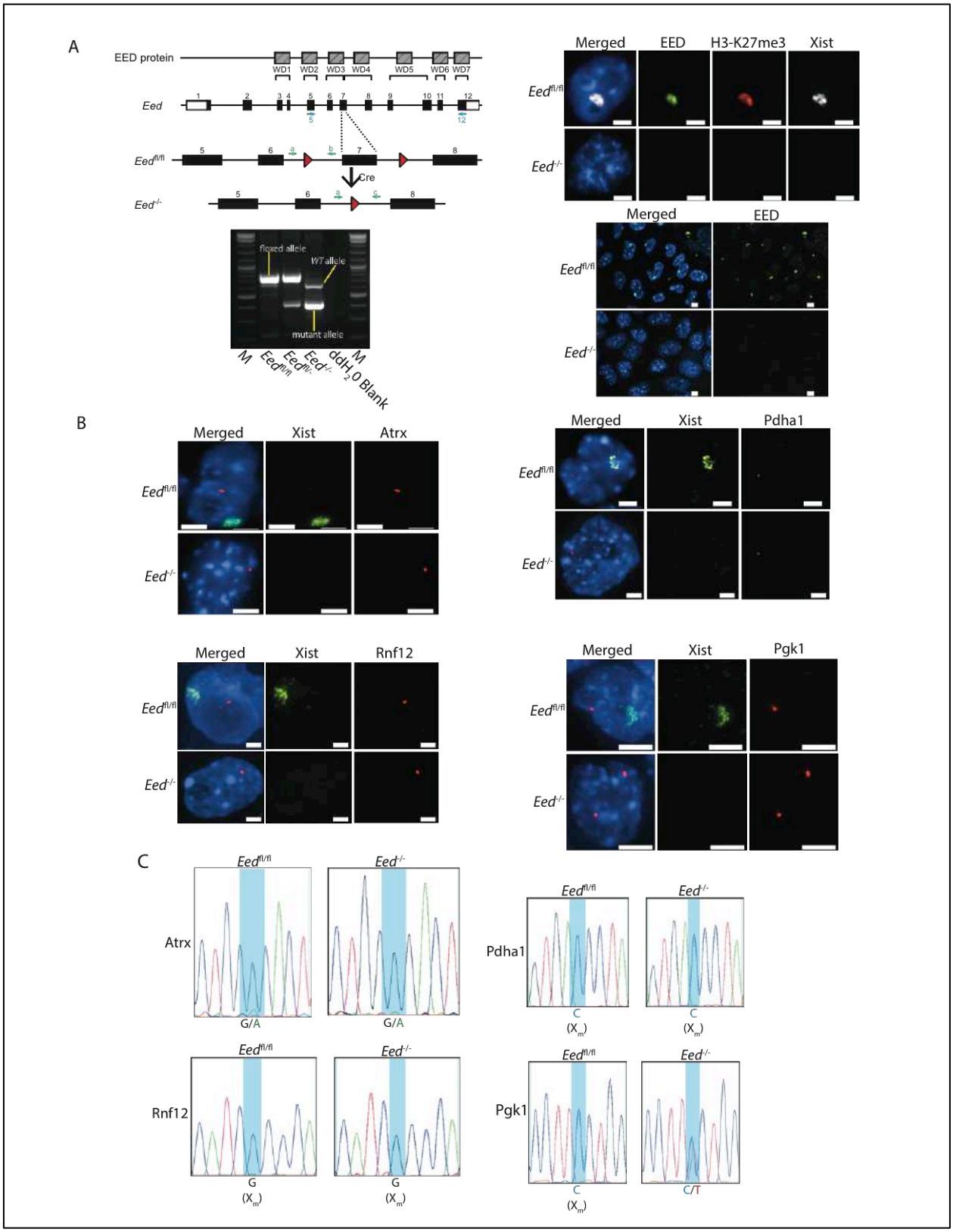
A
EED protein
WD1
WD2
WD3
WD4
WD5
WD6
WD7
Eed
Eed^fl/fl
Cre
Eed^-/-
floxed allele
WT allele
mutant allele
M
Eed^fl/fl
Eed^fl/fl
Eed^-/-
ddH2O
Blank
M
Merged
EED
H3-K27me3
Xist
Eed^fl/fl
Eed^-/-
Merged
EED
Eed^fl/fl
Eed^-/-
B
Merged
Xist
Atrx
Eed^fl/fl
Eed^-/-
Merged
Xist
Pdha1
Eed^fl/fl
Eed^-/-
Merged
Xist
Rnf12
Eed^fl/fl
Eed^-/-
Merged
Xist
Pgk1
Eed^fl/fl
Eed^-/-
C
Eed^fl/fl
Eed^-/-
Atrx
G/A
G/A
Eed^fl/fl
Eed^-/-
Pdha1
C
(Xm)
C
(Xm)
Eed^fl/fl
Eed^-/-
Rnf12
G
(Xm)
G
(Xm)
Eed^fl/fl
Eed^-/-
Pgk1
C
(Xm)
C/T

Figure 2.6

Figure 2.6. EED is only partially required for stable silencing of the inactive-X in mouse trophoblast stem cells.

A. Representative single nucleus immunofluorescence/RNA-FISH images of *Eed*$^{fl/fl}$ and *Eed*$^{-/-}$ TSCs. EED is in green, H3-K27m3 in red, and Xist in green. Nuclei stained with DAPI. Scale bar is 2 μm.
Schematic diagram of *Eed* mutation is to the left of image.
Our mutation removes exon 7, which encodes for WD40 domain #3. This domain is necessary for interaction between EZH2/1 and EED. loxP sites (red triangles) were integrated after exon 6 and before exon 8. Primers (in green) a and b will pick up *WT* and floxed alleles for *Eed,* while primers a and c will pick up the *Eed* allele with the excised exon 7 encoding for the WD40 domain #3 (mutant allele). The brackets also indicate other WD-binding domains.
Below diagram is PCR validation of deletion of exon 7 in *Eed* TSCs. Lane 1 is the *Eed*$^{fl/fl}$ cell line, lane 2 is a heterozygous sample (fl/-), and lane 3 is the *Eed*$^{-/-}$ cell line. Floxed, mutant, and *WT* (i.e. not floxed) bands are indicated by yellow line segments. Our cell lines sometimes pick up the *WT* allele, as these cells were grown on *WT* male MEF feeder cells to prevent TSCs from differentiating. M=Marker. To the right of the PCR image is an immunofluorescence detection of EED as an additional genotyping measure of our cells. *Eed*$^{fl/fl}$ cells have EED inactive-X enrichment, where as *Eed*$^{-/-}$ TSCs do not.

B. Representative single nucleus RNA-FISH images of *Eed*$^{fl/fl}$ and *Eed*$^{-/-}$ TSCs. X-linked gene is in red, and Xist in green. Nuclei stained with DAPI. Scale bar is 2 μm.

C. Representative chromatograms of *Eed*$^{fl/fl}$ and *Eed*$^{-/-}$ TSCs for Atrx, Rnf12, Pdha1, and Pgk1. Chromatograms represent cDNA from RT-PCR amplifications for each gene.

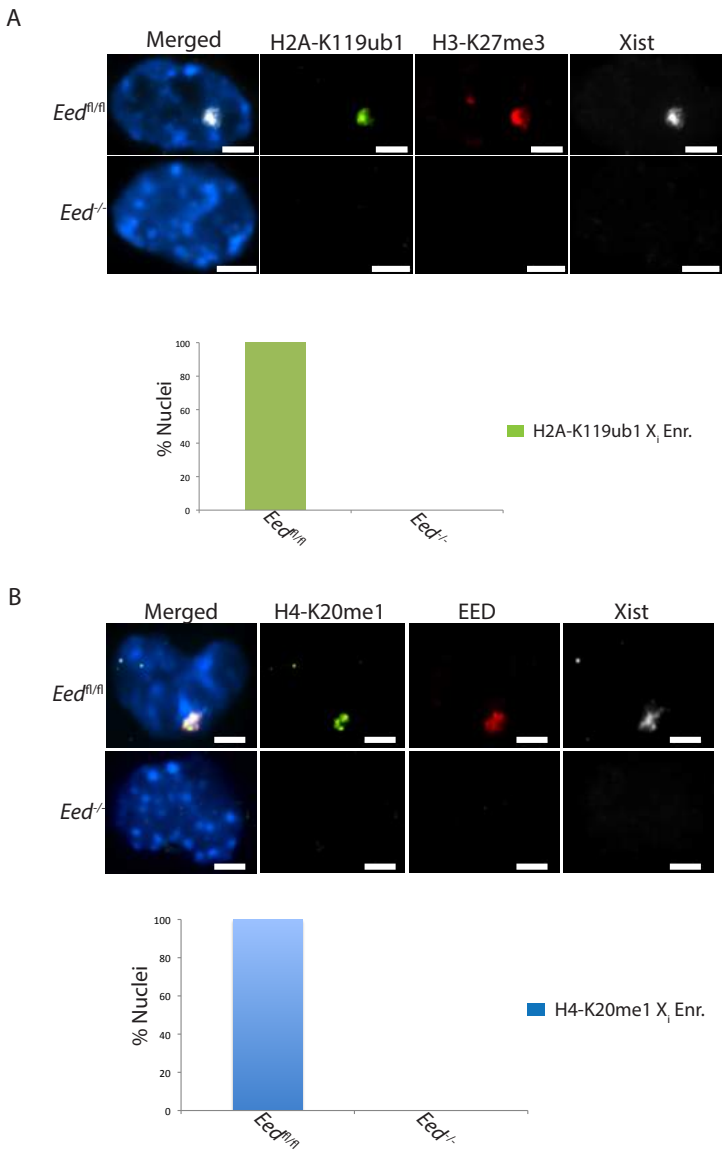
A
Merged
H2A-K119ub1
H3-K27me3
Xist
Eed fl/fl
Eed -/-
% Nuclei
100
80
60
40
20
0
H2A-K119ub1 Xi Enr.
Eed fl/fl
Eed -/-
B
Merged
H4-K20me1
EED
Xist
Eed fl/fl
Eed -/-
% Nuclei
100
80
60
40
20
0
H4-K20me1 Xi Enr.
Eed fl/fl
Eed -/-

Figure 2.7

Figure 2.7. *Eed*$^{-/-}$ trophoblast stem cells are devoid of other Polycomb proteins/histone marks on the inactive-X.

A. Representative single nucleus images of *Eed*$^{fl/fl}$ and *Eed*$^{-/-}$ TSCs. H2A-K119ub1 is in green, H3-K27me3 in red, and Xist in white. Nuclei stained with DAPI. Scale bar is 2 μm. Quantifications are below image. Three independent experiments (technical replicates) were performed. 100 nuclei per genotype per experimental replicate were counted.

B. Representative single nucleus images of *Eed*$^{fl/fl}$ and *Eed*$^{-/-}$ TSCs. H4-K20me1 is in green, EED in red, and Xist in white. Nuclei stained with DAPI. Scale bar is 2 μm. Quantifications are below image. Three independent experiments (technical replicates) were performed. 100 nuclei per genotype per experimental replicate were counted.

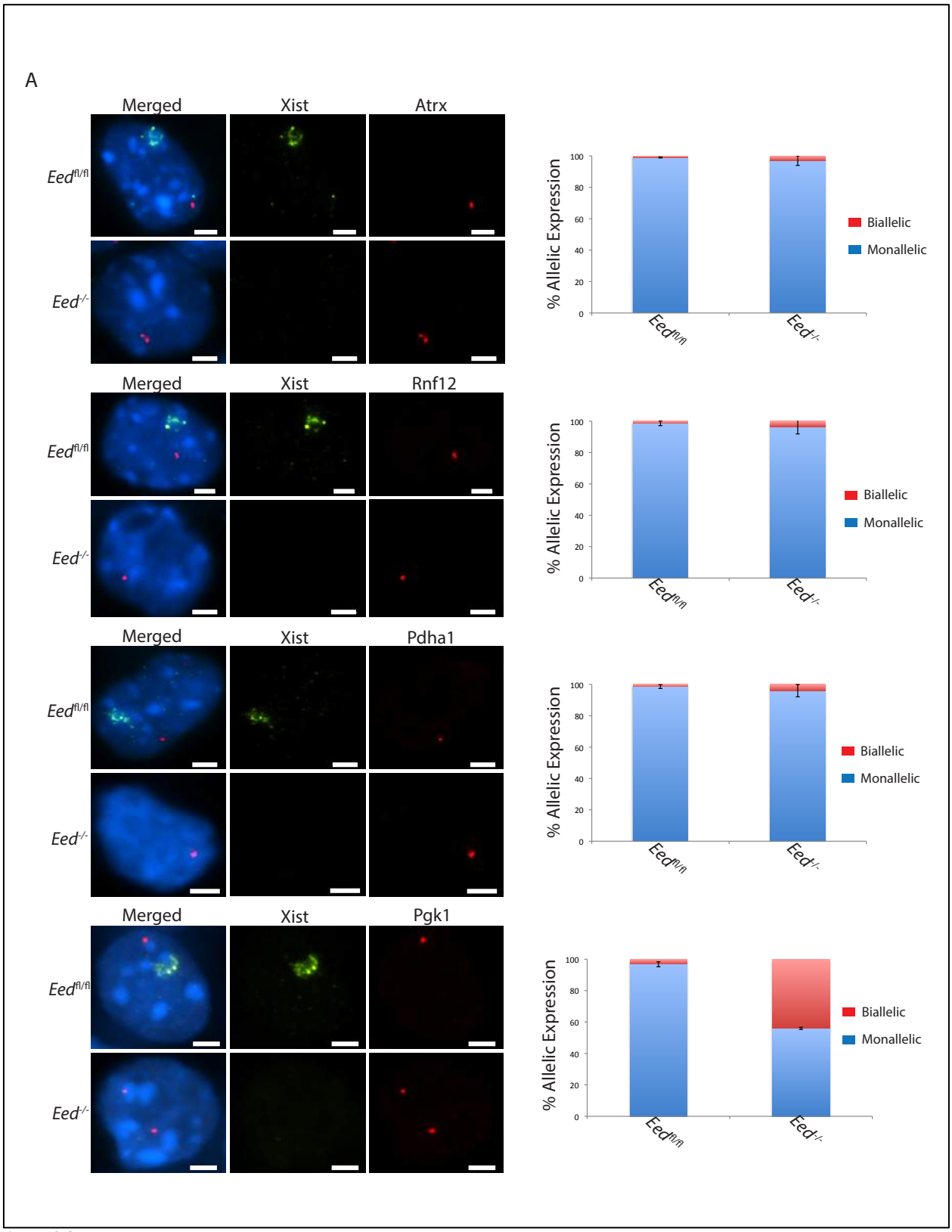
A
Merged
Xist
Atrx
Eed fl/fl
Eed -/-
Merged
Xist
Rnf12
Eed fl/fl
Eed -/-
Merged
Xist
Pdha1
Eed fl/fl
Eed -/-
Merged
Xist
Pgk1
Eed fl/fl
Eed -/-
% Allelic Expression
100
80
60
40
20
0
Eed fl/fl
Eed -/-
Biallelic
Monallelic

Figure 2.8

Figure 2.8. Transiently transduced *Eed*$^{fl/fl}$ TS cells show a similar pattern of derepressed genes compared to constitutively *Eed*$^{-/-}$ TSCs.

A. Representative single nucleus RNA-FISH images of *Eed*$^{fl/fl}$ and *Eed*$^{-/-}$ TSCs. X-linked gene is in red and Xist in green. Nuclei stained with DAPI. Scale bar is 2 μm. Quantifications to the right of each image is shown for each gene. Averages of percent monoallelic expression are plotted +/- SEM from three independent experiments (technical replicates) for each gene. 100 nuclei per genotype per experimental replicate were counted. Left bar for each graph represents the percent of nuclei that are monoallelic or biallelic for Xist positive nuclei in mock transduced *Eed*$^{fl/fl}$ TSCs, whereas the right bar for each graph represents the percent of nuclei that are monoallelic or biallelic for Xist negative nuclei in Cre transduced *Eed*$^{fl/fl}$ TSCs (Xist negative nuclei are effectively the *Eed*$^{-/-}$ TSCs). p-value for each gene: Atrx: 1; Rnf12: 1; Pdha1: 1; Pgk1: 0.075744447, Welch's two sample t-test, comparing the change in biallelic expression for each gene between mock and transiently Cre transduced *Eed*$^{fl/fl}$ TSCs.

References

Avner, P. and Heard, E. (2001). X-chromosome inactivation: counting, choice and initiation. Nature Rev. Genet. *2*, 59–67.

Bernstein, E., Duncan, E.M., Masui, O., Gil, J., Heard, E., and Allis, C.D. (2006). Mouse polycomb proteins bind differentially to methylated histone H3 and RNA and are enriched in facultative heterochromatin. Mol. Cell. Biol. *26*, 2560–2569.

Beutler, E., Yeh, M., and Fairbanks, V.F. (1962). The normal human female as a mosaic of X-chromosome activity: studies using the gene for C-6-PD-deficiency as a marker. Proc. Natl. Acad. Sci. U.S.A. *48*, 9–16.

Brown, C.J., Hendrich, B.D., Rupert, J.L., Lafrieniere, R.G., Xing, Y., Lawrence, J., and Willard, H.F. (1992). The Human XIST Gene: Analysis of a 17 kb Inactive X-Specific RNA that Contains Conserved Repeats and is Highly Localised within the Nucleus. Cell *71*, 527-542.

Cao, Q., Wang, X., Zhao, M., Yang, R., Malik, R., Qiao, Y., Poliakov, A., Yocum, A.K., Li, Y., Chen, W., Cao, X., Jiang, X., Dahiya, A., Harris, C., Feng, F.Y., Kalantry, S., Qin, Z.S., Dhanasekaran, S.M., and Chinnaiyan, A.M. (2014). The Central Role of EED in the Orchestration of Polycomb Group Complexes. Nat. Commun. *5*, 3127.

Cao, R., Wang, L., Wang, H., Xia, L., Erdjument-Bromage, H., Tempst, P., Jones, R.S., and Zhang, Y. (2002). Role of histone H3 lysine 27 methylation in Polycomb-group silencing. Science *298*, 1039–1043.

Chan, K.M., Zhang, H., Malureanu, L., van Deursen, J., and Zhang, Z. (2011). Diverse factors are involved in maintaining X chromosome inactivation. Proc. Natl. Acad. Sci. U.S.A. *108*, 16699–16704.

Chu, C., Zhang, Q.C., da Rocha, S.T., Flynn, R.A., Bharadwaj, M., Calabrese, J.M., Magnuson, T., Heard, E., and Chang, H.Y. (2015). Systematic discovery of Xist RNA binding proteins. Cell *161*, 404–416.

Clemson, C.M., Meneil, J.A., Willard, H.F., and Lawrence, J.B. (1996). XIST RNA paints the inactive X-chromosome at interphase evidence for a novel RNA involved in nuclear/chromosome structure. J. Cell Biol. *132*, 259-275

Corbel, C, Diabangouaya, P, Gendrel, AV, Chow, JC, and Heard, E. (2103). Unusual chromatin status and organization of the inactive X chromosome in murine trophoblast giant cells. Development. *140*, 861-872.

Czermin, B., Melfi, R., McCabe, D., Seitz, V., Imhof, A., and Pirrotta, V. (2002). Drosophila enhancer of Zeste/ESC complexes have a histone H3 methyltransferase activity that marks chromosomal Polycomb sites. Cell *111*, 185–196.

Denisenko, O., Shnyreva, M., Suzuki, H., and Bomsztyk, K. (1998). Point mutations in the WD40 domain of Eed block its interaction with Ezh2. Mol. Cell. Biol. *18*, 5634–5642.

Di Croce, L. and Helin, K. (2013). Transcriptional regulation by Polycomb group proteins. Nat. Struct. Mol. Biol. *20*, 1147–1155.

Eicher, E.M., Nesbitt, M.N., and Francke, U. (1972). Cytological identification of the chromosomes involved in Searle's translocation and the location of the centromere in the X chromosome of the mouse. Genetics *71*, 643–648

Erhardt, S., Su, I.-H., Schneider, R., Barton, S., Bannister, A.J., Perez-Burgos, L., Jenuwein, T., Kouzarides, T., Tarakhovsky, A., and Surani, M.A. (2003). Consequences of the depletion of zygotic and embryonic enhancer of zeste 2 during preimplantation mouse development. Development *130*, 4235–4248.

Han, Z., Xing, X., Hu, M., Zhang, Y., Liu, P., and Chai, J. (2007). Structural basis of EZH2 recognition by EED. Structure *15*, 1306–1315.

Hendzel, MJ, Wei, Y, Mancini, MA, Van Hooser, A, Ranalli, T, Brinkley, BR, Bazett-Jones, DP, Allis, CD. (1997). Mitosis-specific phosphorylation of histone H3 initiates primarily within pericentromeric heterochromatin during G2 and spreads in an ordered fashion coincident with mitotic chromosome condensation. Chromosoma. 106:348–360.

Jonkers, I., Monkhorst, K., Rentmeester, E., Grootegoed, JA., Grosveld, F., and Gribnau, J. (2008). Xist RNA is confined to the nuclear territory of the silenced X-chromosome throughout the cell cycle. Mol. Cell Biol. *28*, 5583-5594.

Kalakonda, N., Fischle, W., Boccuni, P., Gurvich, N., Hoya-Arias, R., Zhao, X., Miyata, Y., Macgrogan, D., Zhang, J., Sims, J.K., et al. (2008). Histone H4 lysine 20 monomethylation promotes transcriptional repression by L3MBTL1. Oncogene *27*, 4293–4304.

Kalantry, S., and Magnuson, T. (2006). The Polycomb group protein EED is dispensable for the initiation of random X-chromosome inactivation. PLoS Genet. *2*, e66.

Kalantry, S., Mills, K.C., Yee, D., Otte, A.P., Panning, B., and Magnuson, T. (2006). The Polycomb group protein Eed protects the inactive X-chromosome from differentiation-induced reactivation. Nat. Cell Biol. *8*, 195–202.

Kalantry, S., Purushothaman, S., Bowen, R.B., Starmer, J., and Magnuson, T. (2009). Evidence of Xist RNA-independent initiation of mouse imprinted X-chromosome inactivation. Nature *460*, 647–651.

Karachentsev, D., Sarma, K., Reinberg, D., and Steward, R. (2005). PR-Set7-dependent methylation of histone H4 Lys 20 functions in repression of gene expression and is essential for mitosis. Genes Dev. *19*, 431–435.

Kay, G.F., Barton, S.C., Surani, M. A., and Rastan, S. (1994). Imprinting and X-chromosome counting mechanisms determine Xist expression in early mouse development. Cell. 77, 639-650.

Keane, T.M., Goodstadt, L., Danecek, P., White, M.A., Wong, K., Yalcin, B., Heger, A., Agam, A., Slater, G., Goodson, M., et al. (2011). Mouse genomic variation and its effect on phenotypes

and gene regulation. Nature *477*, 289–294.

Kerppola, TK. (2009). Polycomb group complexes--many combinations, many functions. Trends Cell Biol. 19(12):692-704.

Kohlmaier, A., Savarese, F., Lachner, M., Martens, J., Jenuwein, T., and Wutz, A. (2004). A chromosomal memory triggered by Xist regulates histone methylation in X inactivation. PLoS Biol. *2*, E171.

Kuzmichev, A., Nishioka, K., Erdjument-Bromage, H., Tempst, P., and Reinberg, D. (2002). Histone methyltransferase activity associated with a human multiprotein complex containing the Enhancer of Zeste protein. Genes Dev. *16*, 2893–2905.

Lee, J. T. (2000). Disruption of imprinted X inactivation by parent-of-origin effects at Tsix. Cell 103, 17–27.

Lewis, E. B. (1978) A gene coplex controlling segmentation in *Drosophila*. Nature. *7*;*276(5688)*:565-70.

Lyon, M.F. (1961). Gene action in the X-chromosome of the mouse (Mus musculus L.). Nature *190*, 372–373.

Maclary, E., Hinten, M., Harris, C., Sethuraman, S., Kalantry, S. (2016). PRC2 prevents upregulation of genes with open chromatin architecture on the inactive X-chromosome. In preparation.

Mak W, Baxter J, Silva J, Newall AE, Otte AP, Brockdorff N. (2002). Mitotically stable association of polycomb group proteins eed and enx1 with the inactive x chromosome in trophoblast stem cells. Curr. Biol. 12(12), 1016-20.

Mak, W., Nesterova, T.B., de Napoles, M., Appanah, R., Yamanaka, S., Otte, A.P., and Brockdorff, N. (2004). Reactivation of the paternal X chromosome in early mouse embryos. Science *303*, 666–669.

Marahrens, Y., Panning, B., Dausman, J., Strauss, W., Jaenisch, R. (1997). Xist-deficient mice are defective in dosage compensation but not spermatogenesis. Genes Dev. *11(2)*, 156-66.

Margueron, R., Justin, N., Ohno, K., Sharpe, M.L., Son, J., Drury, W.J., Voigt, P., Martin, S.R., Taylor, W.R., De Marco, V., et al. (2009). Role of the polycomb protein EED in the propagation of repressive histone marks. Nature *461*, 762–767.

Margueron, R., Li, G., Sarma, K., Blais, A., Zavadil, J., Woodcock, C.L., Dynlacht, B.D., Reinberg**,** D. (2008). EZH2 and EZH1 maintain repressive chromatin through different mechanisms. Mol Cell. *32(4)*, 503-18.

Margueron, R., and Reinberg, D. (2011). The Polycomb complex PRC2 and its mark in life. Nature *469*, 343–349.

McHugh, C.A., Chen, C.-K., Chow, A., Surka, C.F., Tran, C., McDonel, P., Pandya-Jones, A., Blanco, M., Burghard, C., Moradian, A., et al. (2015). The Xist lncRNA interacts directly with SHARP to silence transcription through HDAC3. Nature *521*, 232–236.

McKeon, J., and Brock, H.W. (1991). Interactions of the Polycomb group of genes with homeotic loci of Drosophila. Roux's Arch. Dev. Biol. *199*, 387–396.

Minajigi, A., Froberg, J.E., Wei, C., Sunwoo, H., Kesner, B., Colognori, D., Lessing, D., Payer, B., Boukhali, M., Haas, W., et al. (2015). Chromosomes. A comprehensive Xist interactome reveals cohesin repulsion and an RNA-directed chromosome conformation. Science *349*.

Minkovsky, A., Sahakyan, A., Bonora, G., Damoiseaux, R., Dimitrova, E., Rubbi, L., Pellegrini, M., Radu, C.G., and Plath, K. (2015). A high-throughput screen of inactive X chromosome reactivation identifies the enhancement of DNA demethylation by 5-aza-2'-dC upon inhibition of ribonucleotide reductase. Epigenetics Chromatin *8*, 42.

Moindrot, B., Cerase, A., Coker, H., Masui, O., Grijzenhout, A., Pintacuda, G., Schermelleh, L., Nesterova, T.B., and Brockdorff, N. (2015). A Pooled shRNA Screen Identifies Rbm15, Spen, and Wtap as Factors Required for Xist RNA-Mediated Silencing. Cell Rep *12*, 562–572.

Monfort, A., Di Minin, G., Postlmayr, A., Freimann, R., Arieti, F., Thore, S., and Wutz, A. (2015). Identification of Spen as a Crucial Factor for Xist Function through Forward Genetic Screening in Haploid Embryonic Stem Cells. Cell Rep *12*, 554–561.

Montgomery, N.D., Yee, D., Chen, A., Kalantry, S., Chamberlain, S.J., Otte, A.P., and Magnuson, T. (2005). The murine polycomb group protein Eed is required for global histone H3 lysine-27 methylation. Curr. Biol. *15*, 942–947.

Müller, J., Hart, C.M., Francis, N.J., Vargas, M.L., Sengupta, A., Wild, B., Miller, E.L., O'Connor, M.B., Kingston, R.E., and Simon, J.A. (2002). Histone methyltransferase activity of a Drosophila Polycomb group repressor complex. Cell *111*, 197–208.

Ng, J., Hart, C.M., Morgan, K. and Simon, J.A. (2000). A Drosophila ESC-E(Z) protein complex is distinct from other polycomb group complexes and contains covalently modified ESC. Mol. Cell. Biol. *20*, 3069−3078.

Oda, M.1., Shiota, K., and Tanaka, S. (2006). Trophoblast stem cells. Methods Enzymol. *419*, 387-400.

Okamoto, I., Otte, A.P., Allis, C.D., Reinberg, D., and Heard, E. (2004). Epigenetic dynamics of imprinted X inactivation during early mouse development. Science *303*, 644–649.

Penny, G.D., Kay, G.F., Sheardown, S.A., Rastan, S., and Brockdorff, N. (1996). Requirement for Xist in X chromosome inactivation. Nature *379(6561)*, 131-7.

Pirrotta, V. (1997). PcG complexes and chromatin silencing. Curr. Opin. Genet. Dev. *7*, 249–258.

Pirrotta, V. (1998). Polycombing the genome: PcG, trxG, and chromatin silencing. Cell *93*,

333−336.

Plath, K., Fang, J., Mlynarczyk-Evans, S.K., Cao, R., Worringer, K.A., Wang, H., la Cruz, de, C.C., Otte, A.P., Panning, B., and Zhang, Y. (2003). Role of histone H3 lysine 27 methylation in X-inactivation. Science *300*, 131–135.

Rastan, S (1983). Non-random X-chromosome inactivation in mouse X-autosome translocation embryos–location of the inactivation centre. J Embryol Exp Morphol *78*, 1–22.

Rastan, S., and Brown, S.D. (1990). The search for the mouse Xchromosome inactivation centre. Genet Res *56*, 99–106

Sado, T., Wang, Z., Sasaki, H. and Li, E. (2001). Regulation of imprinted X-chromosome inactivation in mice by Tsix. Development 128, 1275–1286.

Schuettengruber, B., Chourrout, D., Vervoort, M., Leblanc, B., and Cavalli, G. (2007). Genome regulation by polycomb and trithorax proteins. Cell *128*, 735‑745.

Shao, Z. *et al.* Stabilization of chromatin structure by PRC1, a Polycomb complex. (1999). Cell *98*, 37−46.

Shen, X., Liu, Y., Hsu, Y.J., Fujiwara, Y., Kim, J., Mao, X., Yuan, G.C., and Orkin, SH. (2008). EZH1 mediates methylation on histone H3 lysine 27 and complements EZH2 in maintaining stem cell identity and executing pluripotency. Mol Cell. *32(4)*, 491-502.

Silva, J., Mak, W., Zvetkova, I., Appanah, R., Nesterova, T.B., Webster, Z., Peters, A.H.F.M., Jenuwein, T., Otte, A.P., and Brockdorff, N. (2003). Establishment of histone h3 methylation on the inactive X chromosome requires transient recruitment of Eed-Enx1 polycomb group complexes. Dev. Cell *4*, 481–495.

Simon, J., Chiang, A., Bender, W. (1992). Ten different Polycomb group genes are required for spatial control of the AbdA and AbdB homeotic products. Development 114, 493–505.

Simon, J.A. and Kingston, R.E. (2009). Mechanisms of polycomb gene silencing: knowns and unknowns. Nat. Rev. Mol. Cell Biol. *10*, 697-708.

Simon, J. (1995). Locking in stable states of gene expression: transcriptional control during Drosophila development. Curr. Opin. Cell Biol. *7*, 376–385.

Stavropoulos, N., Lu, N., and Lee, J.T. (2001). A functional role for Tsix transcription in blocking Xist RNA accumulation but not in X-chromosome choice. Proc Natl Acad Sci U.S.A. *28*; *98(18)*, 10232-7.

Struhl, G., and Akam, M. (1985). Altered distributions of Ultrabithorax transcripts in extra sex combs mutant embryos of Drosophila. EMBO J. *4*, 3259– 3264

Su, I.H., Basavaraj, A., Krutchinsky, A.N., Hobert, O., Ullrich, A., Chait, B.T., and Tarakhovsky, A. (2003). Ezh2 controls B cell development through histone H3 methylation and Igh rearrangement. Nat. Immunol. 2, 124-31.

Sun, B.K., Deaton, A.M., and Lee, J.T. (2006). A transient heterochromatic state in Xist preempts X inactivation choice without RNA stabilization. Mol Cell. *21(5)*, 617-28.

Takada, T., Ebata, T., Noguchi, H., Keane, T.M., Adams, D.J., Narita, T., Shin-I, T., Fujisawa, H., Toyoda, A., Abe, K., et al. (2013). The ancestor of extant Japanese fancy mice contributed to the mosaic genomes of classical inbred strains. Genome Res.

Takagi, N., and Sasaki, M. (1975). Preferential inactivation of the paternally derived X chromosome in the extraembryonic membranes of the mouse. Nature *256*, 640–642.

Takagi, N., Wake, N., and Sasaki, M. (1978). Cytologic evidence for preferential inactivation of the paternally derived X chromosome in XX mouse blastocysts. Cytogenet. Cell Genet. *20*, 240–248.

Takagi, N. (1980). Primary and secondary nonrandom X chromosome inactivation in early female mouse embryos carrying Searle's translocation T(X; 16)16H. Chromosoma *81*, 439–459

Tie, F., Furuyama, T. and Harte, P.J. (1998). The Drosophila Polycomb Group proteins ESC and E(Z) bind directly to each other and co-localize at multiple chromosomal sites. Development *125*, 3483−3496.

Tie, F., Furuyama, T., Prasad-Sinha, J., Jane, E., and Harte, P.J. (2001). The Drosophila Polycomb Group proteins ESC and E(Z) are present in a complex containing the histone-binding protein p55 and the histone deacetylase RPD3. Development *128*, 275–286.

van der Vlag, J. and Otte, A.P. (1999). Transcriptional repression mediated by the human polycomb-group protein EED involves histone deacetylation. Nature Genet. *23*, 474−478.

Wang, J.1., Mager, J., Chen, Y., Schneider, E., Cross, J.C., Nagy, A., Magnuson, T. (2001). Imprinted X inactivation maintained by a mouse Polycomb group gene. Nature Genet. *28*, 371–375.

Wang, H., Wang, L., Erdjument-Bromage, H., Vidal, M., Tempst, P., Jones, R.S., and Zhang, Y. (2004). Role of histone H2A ubiquitination in polycomb silencing. Nature *431*, 873–878.

West, J.D., Frels, W.I., Chapman, V.M., and Papaioannou, V.E. (1977). Preferential expression of the maternally derived X chromosome in the mouse yolk sac. Cell *12*, 873–882.

West, J.D., Papaioannou, V.E., Frels, W.I., and Chapman, V.M. (1978). Preferential expression of the maternally derived X chromosome in extraembryonic tissues of the mouse. Basic Life Sci. *12*, 361–377.

Williams, L. H., Kalantry, S., Starmer, J. & Magnuson, T. (2011). Transcription precedes loss of Xist coating and depletion of H3K27me3 during X-chromosome reprogramming in the mouse

inner cell mass. Development *138*, 2049–2057.

Yalcin, B., Wong, K., Agam, A., Goodson, M., Keane, T.M., Gan, X., Nellåker, C., Goodstadt, L., Nicod, J., Bhomra, A., et al. (2011). Sequence-based characterization of structural variation in the mouse genome. Nature *477*, 326–329.

Zhang, T., Cooper, S., and Brockdorff, N. (2015). The interplay of histone modifications - writers that read. EMBO Rep.

Zhao, J., Sun, B.K., Erwin, J.A., Song, J.J., and Lee, J.T. (2008). Polycomb proteins targeted by a short repeat RNA to the mouse X chromosome. Science *322(5902)*, 750-6.

Chapter 3

A Comparative Analysis of Polycomb Repressive Complex 2 Proteins In Imprinted X-chromosome Inactivation: Mouse Embryos

Abstract

A defect in X-linked gene silencing in undifferentiated trophoblast stem cells when EED, but not EZH2 or EZH1, is missing suggests that imprinted X-inactivation may operate in a similar manner in the early mouse embryo. During the pre-implantation stage of embryogenesis, all cells will preferentially silence the paternal X-chromosome, thus displaying the imprinted X-inactivation pattern found in TSCs. To assess if my findings from TSCs applied *in vivo*, I generated embryos lacking maternal and zygotic EZH2, EZH2 and EZH1, or EED. I discovered that maternal EED protein, but not maternal EZH2/1, is necessary to trigger imprinted X-inactivation in the embryo. This comparative analysis of PRC2 components suggests a PRC2-independent role for EED in triggering imprinted X-inactivation. Moreover, my results are the initial demonstration that a maternal factor controls the silencing of the X-chromosome in the embryo, an example of a transgenerational epigenetic regulation. The divergent requirements or EZH2/1 and EED in executing X-linked gene silencing thus highlight alternatives to H3-K27me3 in X-chromosome inactivation, and potentially epigenetic states more broadly.

Introduction

X-chromosome inactivation (X-inactivation) is a paradigm epigenetic phenomenon that

occurs in order to equalize the X-linked gene dosage between XX female and XY male mammals (Lyon, 1961; Beutler et al., 1962). Through classical genetic experiments in both mouse and human, a segment of the X-chromosome, denoted as the X-inactivation center (XIC), was found to be necessary and sufficient for X-inactivation (Eicher et al., 1972; Rastan et al., 1980 and 1983; Takagi, 1980). Within the XIC lie two critical long non coding (lnc)RNAs, Xist (X-inactive specific transcript), expressed from the inactive X-chromosome, and Tsix (Xist spelled backwards), expressed from the active X-chromosome. Xist RNA physically coats in *cis* the future inactive-X (Brown, et al. 1992; Clemson et al., 1996; Jonkers et al., 2008). Tsix, however, is expressed in the antisense orientation to Xist and is thought to repress Xist induction from the active X-chromosome. Both of these lncRNAs are widely believed to be necessary and sufficient for X-inactivation (Marahrens et al., 1997; Penny et al., 1996; Kalantry et al., 2009; Stavropoulos et al., 2001). The mutual exclusivity with which these two transcripts are expressed also suggests that they are active players in establishing and potentially maintaining the transcriptional fates of the X-chromosome from which they are transcribed (Marahrens et al., 1997; Penny et al., 1996; Kalantry et al., 2009; Stavropoulos et al., 2001; Avner and Heard, 2001). Thus, X-inactivation serves as a model system for understanding how epigenetic mechanisms occur broadly.

Two types of X-chromosome inactivation exist in the mouse, imprinted and random X-chromosome inactivation. Imprinted X-inactivation, exclusive silencing of the paternally inherited X-chromosome, occurs initially in all cells in the developing mouse embryo (Mak et al., 2004; Takagi et al., 1978; Kay 1994). This form of X-inactivation is subsequently maintained in the extra-embryonic tissues of the embryo, the trophectoderm and the primitive endoderm lineages (Takagi and Sasaki, 1975; West et al., 1977; 1978). At peri-implantation and post-

implantation, however, the cells in the epiblast will display a different pattern of X- chromosome inactivation (Mak et al., 2004). This form of X-inactivation, random X-inactivation, is unique to the epiblast precursors that will ultimately develop in to the embryo proper. At E4.5 the cells of the inner cell mass will reactivate the paternal X-chromosome (Mak et al., 2004; Williams et al., 2011). These cells will then randomly choose to inactivate either the maternal-X or the paternal-X (Mak et al., 2004). Importantly, once one X-chromosome in a given nucleoplasm is chosen for inactivation, descendant cells will maintain that same X-chromosome as the inactive-X through multiple mitotic divisions essentially for the lifetime of the organism. This stable and heritable transcriptional memory highlights one of the key facets of X-chromosome inactivation as a paradigm of epigenetic inheritance.

In the developing mouse embryo, a set of temporally specified events occurs as imprinted X-inactivation is initiated and established. At the two-cell stage Xist RNA is transcribed. It will then physically coat in *cis* the paternally inherited X-chromosome (the future inactive-X) at the four-cell stage; Xist RNA marks the inactive-X (Brown, et al. 1992; Clemson et al., 1996; Jonkers et al., 2008). By the eight-cell stage members of the Polycomb group (PcG) are found enriched coincident with Xist RNA on the inactive-X (Mak, 2002; Erhardt et al., 2003; Okamoto et al., 2004; Plath et al., 2003; Silva et al., 2003). As embryogenesis proceeds, these factors associate on the inactive-X while genes are being silenced along the future inactive (paternal) X-chromosome. Tsix expression from the active (maternal) X-chromosome occurs concomitant with Polycomb protein enrichment and silencing of genes on the future inactive (paternal) X-chromosome (Lee 2000; Sado et al., 2001). This pattern of X-inactivation, as well as the enrichment of the same epigenetic factors (Xist, H3-K27me3, etc.) along the inactive-X, is then maintained in the extra-embryonic tissue of the developing embryo. These epigenetic factors are

widely believed to be tightly associated with the initiation and maintenance of the appropriate pattern of X-inactivation in the developing embryo.

Polycomb proteins (PcGs) comprise a set of evolutionary conserved epigenetic factors first identified in *Drosophila melanogaster* (Pirrotta, 1997; Ng et al., 2000; Lewis, 1978). They were found to be necessary in maintaining the transcriptional repression of *Hox* loci once silencing of *Hox* loci was triggered by other epigenetic repressive factors during *Drosophila* embryogenesis (Ng et al., 2000; Simon, 1995; Pirrotta, 1997; Pirrotta et al., 1998; Shao et al., 1999; van der Vlag, et al., 1999; Tie et al., 1998; Lewis, 1978). This allowed for proper anterior-posterior (A-P) axial patterning (Ng et al., 2000; Simon, 1995; Pirrotta, 1997; Pirrotta et al., 1998; Shao et al., 1999; van der Vlag, et al., 1999; Tie et al., 1998; Lewis, 1978). In Polycomb mutants, flies showed misexpression of *Hox* genes outside of the normal A-P domains, thereby leading to phenotypic homeotic transformations (McKeon and Brock, 1991; Simon et al., 1992; Struhl and Akam, 1985). Polycomb proteins are catalogued into two major complexes, Polycomb repressive complex 2 (PRC2), and Polycomb repressive complex 1 (PRC1). Mammalian PRC2 comprises the core subunits Enhancer of Zeste Homologue 2 (EZH2), Suppressor of Zeste 12 (SU(Z)12) and Extra-embryonic Ectoderm Development (EED), derived from their *Drosophila* homologues Enhancer of Zeste (E(z)), Suppressor of Zeste (Su(z)), and Extra Sex Combs (Esc), respectively (Cao et al., 2002; Czermin et al., 2002; Kuzmichev et al., 2002; Müller et al., 2002; Tie et al., 2001). EZH2, the catalytic subunit of PRC2, serves to post-translationally modify Histone H3 by trimethylating lysine residue 27 (H3-K27me3) (Margueron and Reinberg, 2001; Di Croce and Helin, 2013; Zhang et al., 2015). CBX family members (which are integrated into PRC1) are then posited to read H3-K27me3 via their chromodomains and recruit PRC1 (Bernstein et al., 2006). PRC1 will monoubiquitinate Histone H2A at lysine residue 119 (H2A-

K119Ub1) (Wang et al., 2004). It is generally thought this will lead to facultative heterochromatin formation and transcriptional inactivation (Bernstein et al., 2006). Such histone modifications in chromatin are generally held to be a broad mechanism by which transcriptional states are propagated as epigenetic memories across multiple mitotic divisions (Margueron and Reinberg, 2011; Ragunathan et al., 2015; Zhang et al., 2015).

I, and others, have shown that Polycomb proteins (PcGs) are physically enriched on the inactive-X, both *in vitro* and *in vivo* (Plath et al., 2003; Silva et al., 2003; Kalantry et al., 2006). Given that these proteins coat the inactive-X during X-inactivation initiation in the mouse embryo supports my hypothesis that they are critical for proper X-linked gene silencing. Previous loss-of-function studies suggest that PRC2 is required to maintain imprinted X-inactivation (Wang et al., 2001). Furthermore, $Eed^{-/-}$ trophoblast stem cells (TSCs) are defective in maintaining silencing of paternal X-linked genes upon differentiation of extra-embryonic tissues (Kalantry et al., 2006). However, the explicit roles and the functional interdependence of Polycomb proteins in initiating imprinted X-inactivation remain elusive. Here, I have undertaken a systematic genetic approach to ascertain roles for PRC2 components in triggering imprinted X-chromosome inactivation. I hypothesized that these proteins are crucially required for X-linked gene silencing during early mouse embryogenesis. I show evidence of EZH2-independent initiation of imprinted X-inactivation. Furthermore, I found that EZH1, the only other known H3-K27me3 histone methyltransferase, does not contribute to X-inactivation. I identify, however, a strict requirement for EED in executing X-linked gene silencing in the early embryo. My findings suggest alternatives to canonical PRC2 and H3-K27me3 mediated mechanisms of gene silencing in X-inactivation initiation. Moreover, I have acquired evidence for the first time of a maternally deposited epigenetic factor necessary for triggering imprinted X-chromosome

inactivation. A crucial requirement for maternal EED in triggering X-linked gene silencing also sheds light on a meiotic influence of imprinted X-chromosome inactivation through a Polycomb protein. Until now, any indication of transgenerational control of X-chromosome inactivation is something that has remained indefinable.

Results

EZH2 is not required to initiate imprinted X-inactivation

I first set out to examine if EZH2 is necessary during the initiation phase of imprinted X-inactivation. I chose to interrogate EZH2 first because it is the primary catalytic subunit of canonical PRC2 (Margueron and Reinberg, 2001; Di Croce and Helin, 2013; Zhang et al., 2015). My conditional mutation for the *Ezh2* alleles harbors a SET domain flanked by loxP sites (Figure 3.1). Upon Cre expression, the SET domain, which spans exons 16-20 of *Ezh2*, is removed. loxP sites (red triangles), were integrated after exon 15 and before exon 20. The SET domain is a conserved domain of many chromatin modifying enzymes (Kerppola, 2009). Historically **SET** refers to **S**u(var)3-9, **E**nhancer of Zeste (E(z)), and **T**rithorax (Trx) proteins, enzymes discovered in *Drosophila* that contain this conserved enzymatic region (Kerppola, 2009; Herz et al., 2013). The WD binding domain is also indicated at exons 2 and 3 (Figure 3.1). This is the site of interaction between EZH2 and EED (Denisenko et al., 1998). Normally, EZH2, as well as its catalytic read-out H3-K27me3, are found co-enriched on the inactive-X along with the Xist RNA cloud during the early stages of mouse embryogenesis (Figure 3.1). Of note, other Polycomb proteins are also enriched on the inactive X-chromosome by this stage of development (Kalantry et al., 2006a). We previously showed that maternal EED deposited by the oocyte could enrich on the inactive-X at the early blastocyst stage in *Eed* zygotically null embryos (Kalantry et al.,

2006a). Interestingly, however, maternal EZH2 does not enrich on the inactive-X at the early blastocyst stage in *Ezh2* zygotically null embryos (Figure 3.2, Table 3.1). It is possible that the mere presence of maternal EZH2 suffices to function at this stage of embryogenesis. This would ultimately preclude our ascertaining a definitive role for EZH2 in triggering X-inactivation.

I therefore wanted to analyze blastocysts that were effectively maternally and zygotically null for EZH2 (Figure 3.3). Female *Ezh2*$^{fl/fl}$ mice harboring a *Zp3-Cre* transgene (to delete *Ezh2* in the oocytes early during oogenesis before completion of meiosis 1) (Lewandoski et al., 1997) were bred against *Ezh2*$^{fl/fl}$ males possessing a *Stra8-Cre* transgene (to delete *Ezh2* in premeiotic spermatogonia during spermatogenesis) (Sadate-Ngatchou et al., 2008). I found that all detectable H3-K27me3 inactive-X enrichment is lost in maternal and zygotic *Ezh2* (*Ezh2*$^{m-/-;z-/-}$) embryos (Figure 3.1, Figure 3.3). To assess the effect of EZH2 and H3-K27me3 loss on X-linked gene silencing initiation, I performed immunofluorescence (IF) for H3-K27me3 directly followed by RNA-FISH for Xist (to mark the inactive-X) and X-linked genes. To my surprise, *Ezh2*$^{m-/-;z-/-}$ embryos are able to initiate gene silencing along the inactive X-chromosome similar to *WT* embryos. *Rnf12* as well as other X-linked genes are still monoalellically expressed from the maternal (active) X-chromosome in a majority of nuclei in the *Ezh2*$^{m-/-;z-/-}$embryos, thus mimicking the *WT* (Figure 3.1, Figure 3.3). Furthermore, I noticed that Xist is able to enrich on the inactive-X in *Ezh2*$^{m-/-;z-/-}$ blastocysts comparably to *WT* (Figure 3.1, Figure 3.3). This is in direct contrast to reports that indicate drastically reduced Xist RNA levels when EZH2 is downregulated (Zhao et al., 2008). It should also be pointed out that even in *WT* embryos there are a small percentage of nuclei that exhibit a low degree of biallelic expression for each gene analyzed. As X-inactivation progresses through early embryogenesis there is a gradient of silencing; genes along the future inactive X-chromosome do not fully become transcriptionally

inert until the late blastocyst stage (Kalantry et al., 2009). The key observation here is that there is no significant difference between the degree of X-linked gene silencing between *WT* and *Ezh2*$^{m-/-;z-/-}$ embryos (Figure 3.1).

To validate my RNA-FSH data, I performed allele-specific RT-PCR coupled with pyrosequencing for a subset of the seven X-linked genes analyzed via RNA-FISH. Pyrosequencing offers a very strict method by which we can quantitate the relative ratio of allelic species for any given X-linked genes (i.e. inactive-X:active-X expression ratios). I derived F1 hybrid blastocysts from crossing *Ezh2*$^{fl/fl}$*;Zp3-Cre*-containing females possessing an X^{Lab} derived X-chromosome (*Ezh2* $^{fl/fl}$*;Zp3-Cre*;X^{Lab}/X^{Lab}) against *Ezh2*$^{fl/fl}$*;Stra8-Cre*-containing males possessing an X^{JF1} derived X-chromosome (*Ezh2* $^{fl/fl}$*,Stra8-Cre;*X^{JF1}*/Y)*. Female embryos derived from such a cross (*Ezh2*$^{m-/-;z-/-}$ X^{Lab}/X^{JF1}, heretofore referred to as *Ezh2*$^{m-/-;z-/-}$) will harbor multiple single nucleotide polymorphisms (SNPs) for genes across the X-chromosome. Having polymorphic embryos is quite advantageous; I can profile, in an allele-specific manner, the expression of X-linked genes by utilizing SNPs for any given gene. In my cross, the maternal-X is derived from the *Mus musculus* 129/S1 mouse strain and the paternal-X is from the *Mus molossinus* JF1/Ms strain. The genomes of the 129/S1 and JF1/Ms strains are highly divergent and contain many defined single nucleotide polymorphisms (SNPs) (Keane et al., 2011; Takada et al., 2013; Yalcin et al., 2011). After analyzing these embryos for allele-specific gene expression, I again find that there is not a significant difference in inactive-X specific gene silencing when comparing *WT* and *Ezh2*$^{m-/-;z-/-}$ embryos (Figure 3.1). Taken together, these data argue that EZH2 is not necessary during the initiation phase of X-inactivation. Furthermore, this suggests that loss of detectable, robust levels of H3-K27m3 is not sufficient to confer a defect in triggering X-linked gene silencing.

EZH2 is dispensable for the maintenance of imprinted X-inactivation

Because I did not observe a defect in imprinted X-inactivation initiation when maternal and zygotic EZH2 were lacking, I next hypothesized that EZH2 is critical for propagating an epigenetic memory once gene silencing is established along the inactive X-chromosome. This is logical, as Polycomb proteins are classically thought to control the maintenance of gene expression states (Ng et al., 2000; Pirrotta et al., 1998; Shao et al., 1999; van der Vlag et al., 1999; Tie et al., 1998; Lewis, 1978). To address this, I, and others in the lab, derived *Ezh2*$^{-/-}$ post-implantation (E6.5 and E7.5) stage embryos (Figure 3.4). I specifically investigated the extra-embryonic ectoderm (EE). It has been previously shown that the trophoblast lineage (destined to develop into the placenta) displays exclusive silencing of the paternally inherited X-chromosome, thus constituting maintenance of imprinted X-inactivation (Takagi and Sasaki, 1975; West et al., 1977; West et al., 1978). Our first test of EZH2 function in maintaining X-inactivation in EE tissue came from measuring a paternal X-linked GFP transgene (X^{GFP}) on the inactive X-chromosome. In *WT*, the EE is devoid of GFP fluorescence, due to exclusive silencing of the paternal X-chromosome. On the contrary, the epiblast cells display a mosaic pattern of GFP expression (due to random X-inactivation) (Kalantry et al., 2006a; Kalantry et al., 2006b) (Figure 3.5). To render the entire embryo devoid of any GFP fluorescence, we can introduce a *Tsix* mutation on the same X-chromosome bearing the GFP transgene ($XX^{\Delta Tsix; GFP}$). This effectively biases random X-inactivation such that cells in the entire embryo exclusively silence the mutant paternally inherited X-chromosome (Kalantry et al, 2006a, b). When we then introduce mutations in other PcGs genes, we can now use *Gfp* derepression (i.e. re-emergence of GFP fluorescence) as an indicator of faulty X-inactivation maintenance. In our E7.5 embryos we fail to pick up GFP expression in the *Ezh2*$^{-/-}$ EEs vis-à-vis our *WT* EE tissues (Figure 3.5). This

suggests that even at the maintenance phase of X-inactivation EZH2 is not required. This is contrary to an observed defect in maintaining silencing of the GFP transgene in E7.5 *Eed*$^{-/-}$ EE tissues (Kalantry et al., 2006a), thus suggesting that EZH2 and EED are differentially required in maintaining imprinted X-inactivation. To explore this further, I next assessed endogenous X-linked gene expression by performing allele-specific RT-PCR followed by Sanger sequencing in *Ezh2*$^{-/-}$ and *WT* X^{lab};X^{JF1} polymorphic embryos (heretofore referred to as *Ezh2*$^{-/-}$ and *WT*). Because *Ezh2*$^{-/-}$ post-implantation embryos die at E7.5 stage of embryogenesis, I generated E6.5 embryos instead to examine if EZH2 is necessary to maintain X-inactivation (Figure 3.4). Again I observed no difference in the ability of the inactive-X to remain silenced in the *Ezh2*$^{-/-}$ EEs. Both mutant and *WT* EEs display expression of the maternal allele indicating proper inactive-X (paternal-X)-specific gene silencing (Figure 3.5). I note that *Utx* cDNA from *WT* and *Ezh2*$^{-/-}$ contains both alleles. *Utx* normally escapes X-inactivation (Greenfield et al., 1998). I also want to point out the *Atrx* exhibits a slight peak for the paternal allele (A) in addition to the maternal allele (G), even in the *WT* EE tissue. It has been previously shown that *Atrx*, along with a subset of other X-linked genes, can relax its silencing from the inactive-X and consequently lead to leaky inactive-X expression as these tissues begin to differentiate (Corbel et al., 2013). As a control, I sequenced cDNA from *WT* and *Ezh2*$^{-/-}$ epiblasts to illustrate expression of both alleles (to verify polymorphisms in embryos for all genes analyzed) as a result of random X-inactivation in the embryo proper (Figure 3.5). Indeed, in my *WT* and *Ezh2*$^{-/-}$ epiblast tissues, I observed expression of both alleles for *Rnf12*, *Atrx*, *Pgk1*, and *Pdha1* due to a mosaic random X-inactivation pattern. These data strongly suggests that even loss of EZH2 in post-implantation embryos does not confer a defect in maintaining X-inactivation *in vivo*.

One possibility to explain why *Ezh2*$^{-/-}$ embryos do not show a defect in X-inactivation maintenance is because there might be H3-K27me3 catalysis and enrichment on the inactive-X, even in the absence of EZH2. To formally examine the H3-K27me3 profile in *Ezh2*$^{-/-}$ EEs, I carried out immunofluorescence for H3-K27me3 followed by Xist RNA-FISH to mark the inactive X-chromosome. Compared to the *Ezh2*$^{m-/-;z-/-}$ blastocysts, which do not display any detectable inactive-X-specific H3-K27me3 enrichment, a small percentage of cells from E6.5 *Ezh2*$^{-/-}$ EEs exhibit H3-K27me3 enrichment on the inactive-X, albeit to a lesser degree than cells from E6.5 *WT* EEs (Figure 3.5). This low level of H3-K27me3 might suffice to maintain gene silencing. Moreover, I still see Xist RNA coating of the inactive-X in *Ezh2*$^{-/-}$ post-implantation extra-embryonic tissues comparable to *WT*. Continued Xist RNA enrichment suggests that EZH2 is not required for robust Xist RNA induction and coating of the inactive-X (Figure 3.5). This observation again is in contrast to what has been previously reported (Zhao et al., 2008). All together, I conclude that not only is EZH2 not required for initiating imprinted X-inactivation, it is also dispensable for maintaining imprinted X-inactivation. All together, these data suggest other factors must operate to execute and propagate the X-inactive state *in vivo*.

<u>EZH1 does not contribute to X-inactivation initiation</u>

Enhancer of Zeste Homologue 1 (EZH1), a mammalian specific homologue of EZH2, can catalyze low-level H3-K27me3 in *Ezh2* null ES cells (Shen et al., 2008). Catalysis of H3-K27me3 despite EZH2 loss implies that EZH1 can compensate for loss of EZH2 function. Given that I found EZH2 to be dispensable for both the initiation and maintenance of imprinted X-inactivation, I next hypothesized that EZH1 may have a substantial contribution to triggering imprinted X-inactivation. To ascertain this, I generated polymorphic F1 (see discussion above for SNPs) *Ezh2*$^{m-/-;z-/-}$;*Ezh1*$^{-/-}$;X^{Lab}/X^{JF1} blastocysts (heretofore referred to as *Ezh2*$^{m-/-;z-/-}$;*Ezh1*$^{-/-}$)

(Figure 3.6). To generate such mice, I bred *Ezh2*$^{fl/fl}$;*Ezh1*$^{-/-}$;*Zp3-Cre*X^{Lab}/X^{Lab} females against *Ezh2*$^{fl/fl}$;*Ezh1*$^{-/-}$;*Prm-Cre*;X^{JF1}/*Y* males. *Prm-Cre* will delete floxed alleles in maturing round spermatids during spermiogenesis (Peschon et al., 1987). Of note, I could not effectively use *Ezh2*$^{fl/fl}$;*Ezh1*$^{-/-}$,*Stra8-Cre*;X^{JF1}/*Y* males, as loss of *Ezh2* combined with an already constitutive homozygous *Ezh1* deletion in premeiotic spermatogonia early led to infertility.

I first examined *Ezh2*$^{m-/-;\ z-/-}$;*Ezh1*$^{-/-}$ embryos (Figure 3.6). My *Ezh2* mutation is the same as described above, and my *Ezh1* mutation contains a LacZ/Neo cassette inserted into exon 7. This cassette prevents the gene from fully being transcribed; the Ezh1 transcript does not contain the SET domain. The SET domain for *Ezh1* is encoded by exons 17-21 (Figure 3.7). EED has also been shown to interact with EZH1 (Margueron et al., 2008). The WD-binding domain is thus indicated at exons 3 and 4. My mutation of *Ezh1* is a conventional null. I found that *Ezh2*$^{fl/fl}$;*Ezh1*$^{-/-}$ mice which are born in equal sex ratios (Table 3.2), are fertile, and live a normal life span. Furthermore, I note that E7.5 embryos generated from *Ezh1*$^{-/-}$ x *Ezh1*$^{-/-}$ intercrosses yield no observable sex distortion ratio at this stage of embryogenesis (data not shown). There is effectively no known observable phenotype for EZH1 homozygosity. Combined with my breeding these data imply that EZH1 is not required for X-inactivation, as any requirement for EZH1 in X-chromosome inactivation is expected to lead to a sex distortion ratio with an underrepresentation of females. I do not find this to be the case. After examining 16 litters (with an average litter size of around six) from a cross of *Ezh2*$^{fl/fl}$;*Ezh1*$^{-/-}$ females against *Ezh2*$^{fl/fl}$;*Ezh1*$^{-/-}$ males, I observed an equal female:male distribution (Table 3.2). The question then becomes, does EZH1 compensate for loss of EZH2 in triggering silencing of X-linked genes? If EZH1 compensates for EZH2 loss in X-inactivation, one would anticipate that absence of both EZH2 and EZH1 would lead to a significant difference in allele-specific inactive:active

(paternal:maternal) X-linked gene expression ratios compared to just EZH2 absence. I found that *Ezh2*$^{m-/-;\ z-/-}$;*Ezh1*$^{-/-}$ embryos display a slight delay in the kinetics of X-linked gene silencing for one gene (*Rnf12*), but not all of the genes (*Atrx*, *G6pdx*, and *Pdha1*) analyzed along the inactive-X vis-à-vis *WT* (*Ezh2*$^{fl/fl}$) and *Ezh2*$^{m-/-;z-/-}$ embryos (shown previously, compare Figure 3.7 back to Figure 3.1). For instance, *Atrx* displays no substantial biological difference in allelic-specific gene expression ratios among *WT*, *Ezh2*$^{m-/-;z-/-}$ and *Ezh2*$^{m-/-;z-/-}$;*Ezh1*$^{-/-}$ embryos, whereas *Rnf12* shows a slight difference (i.e. more inactive-X expression) in *Ezh2*$^{m-/-;z-/-}$;*Ezh1*$^{-/-}$ embryos compared to *WT* and *Ezh2*$^{m-/-;z-/-}$ embryos. This may imply that some genes are experiencing a delay in their silencing when EZH2 and EZH1 are missing. Importantly, the ratio of inactive-X:active-X (paternal-X:maternal-X) allele expression in *Ezh2*$^{m-/-;\ z-/-}$;*Ezh1*$^{-/-}$ blastocysts is essentially identical to *Ezh2*$^{fl/fl}$;*Ezh1*$^{-/-}$ blastocysts (Figure 3.7). So any effect in allelic ratios could be attributed to just EZH1 loss and not combined loss of EZH2 and EZH1. In the early mouse embryo, X-linked gene silencing has been shown to be highly variable, such that many genes undergo different kinetics of silencing as X-inactivation progresses during the early stages of embryogenesis (Kalantry et al., 2009). It is not completely illogical that what I am seeing is a kinetic difference in *Rnf12* silencing between *Ezh2*$^{m-/-;\ z-/-}$;*Ezh1*$^{-/-}$ or *Ezh2*$^{fl/fl}$;*Ezh1*$^{-/-}$ embryos and *Ezh2*$^{m-/-;z-/-}$ or *Ezh2*$^{fl/fl}$ embryos. Taken together, these data suggest that EZH1 is not required for triggering imprinted X-inactivation. I also conclude that EZH1 does not appear to compensate for loss of EZH2, and therefore EZH1, much like EZH2, does not contribute to initiating imprinted X-inactivation.

EED is critical for proper initiation of imprinted X-inactivation

EED has long been considered the glue of PRC2. When EED is missing, PRC2 as a complex fails to form appropriately, and the other core subunits are degraded (Montgomery et al.,

2005). When cells are lacking functional EED, it is also known that there is loss of H3-K27me3 deposition at PRC2 target genes (Montgomery et al., 2005). Moreover, defects in maintaining imprinted X-inactivation are noted in extra-embryonic compartments lacking EED (Kalantry et al., 2006a). Considering these prior findings and, furthermore, knowledge that EED is enriched on the inactive-X during the initiation phase of X-inactivation both *in vitro* and *in vivo* (Plath, et al. 2003; Silva et al., 2003; Kalantry et al., 2006a; 2006b), I hypothesized that EED is essential for triggering imprinted X-chromosome inactivation. To explore this, I generated polymorphic F1 (see rationale above for SNPs) $Eed^{m-/-;z-/-};X^{Lab}/X^{JF1}$ blastocysts (heretofore referred to as $Eed^{m-/-;z-/-}$) (Figure 3.8). To generate these embryos, I bred $Eed^{fl/fl}$;*Zp3-Cre*;X^{Lab}/X^{Lab} females against $Eed^{fl/fl}$,*Prm-Cre*;X^{JF1}/Y males (Figure 3.8). I was also unsuccessful in using $Eed^{fl/fl}$; *Stra8-Cre*;X^{JF1}/Y males, as these males were also infertile.

I aimed to use maternal and zygotic null *Eed* embryos because $Eed^{-/-}$ (zygotic nulls only) embryos display maternal EED enrichment on the inactive-X (Kalantry et al., 2006a and 2006b). My *Eed* mutation is a different mutation than the one in the Kalantry et al., 2006a study. I used a mutation that removes a core WD40 domain through deletion of exon 7 (Figure 3.9). This domain is necessary for EZH2 and EED to interact (Denisenko et al., 1998). loxP sites (red triangles) were integrated after exon 6 and before exon 8. The brackets also indicate other WD-binding domains (Figure 3.9). Deletion of WD40 domains of EED is known to adversely affect interaction with EZH2 (Denisenko et al., 1998; Han et al., 2007). The same logic also likely applies to the interaction for EED and EZH1 interaction (Margueron et al., 2008). I generated $Eed^{m-/-;z-/-}$ embryos (Figure 3.8) and assayed for X-linked gene expression via allele-specific RT-PCR followed by pyrosequencing. I discovered that there are significant defects in triggering X-linked gene silencing when comparing the allele-specific (inative-X:active-X) expression ratios

between *Eed*$^{m-/-;z-/-}$ blastocysts and *Eed*$^{fl/fl}$ blastocysts (Figure 3.9). This is in stark contrast to lack of a defect in triggering silencing when EZH2 is deleted with or without EZH1 (Figure 3.1 and Figure 3.7). My analysis suggests that EED is crucial for proper X-inactivation initiation, whereas EZH2 and EZH1 are dispensable. All together, such divergent requirements for EED versus EZH2/EZH1 in imprinted X-inactivation highlights for the first time a potential histone methylation (H3-K27me3 specific) independent function for PRC2 in executing imprinted X-chromosome inactivation. It is possible that EED is complexing with novel epigenetic factors to enact gene silencing in the early mouse embryo. Moreover, my data exemplify a requirement, for the first time, of a maternal factor in controlling a zygotic epigenetic process, lending intriguing insight into transgenerational control of X-chromosome inactivation.

Eed$^{m-/-;z-/-}$ blastocysts harbor Xist RNA enrichment at the inactive X-chromosome

I, and others, indicate that after EED loss Xist RNA coating is completely absent from the inactive-X in *Eed*$^{-/-}$ trophpblast stem cells. (Chapter 2; Kalantry et al., 2006a; Maclary et al, 2016, in preparation). I therefore wanted to investigate the Xist profile in our *Eed*$^{m-/-;z-/-}$ embryos. Upon assaying for Xist enrichment via RNA-FISH I surprisingly detect robust Xist coating of the inactive-X in *Eed*$^{m-/-;z-/-}$ blastocysts vis-à-vis *WT* embryos (Figure 3.10). This is in contrary to loss of Xist RNA coating of the inactive-X in *Eed* null trophoblast stem cells (TSCs), an *ex vivo* model of imprinted X-chromosome inactivation (Chapter 2; Kalantry et al., 2006a; Maclary et al., 2016, in preparation).

To explain a discrepancy in Xist RNA enrichment between *Eed*$^{m-/-;z-/-}$ and *Eed*$^{-/-}$ TSCs, it is important to consider the heterochromatic sate of the Xist promoter. In differentiating female embryonic stem cells (ESCs), which undergo random X-inactivation, prior reports revealed that the Xist promoter undergoes a transient heterochromatinization prior to X-inactivation and Xist

induction (Sun et al., 2006; Zhao et al., 2008). H4 hypoacetylation, reduced H3-K4 dimethylation, and increased PRC2-catalyzed H3-K27me3 characterize this heterochromatic state. The marking of the Xist chromatin in this manner may paradoxically be a prerequisite for Xist RNA expression, potentially explaining why EED and H3-K27me3 absence substantially hinders Xist RNA expression and ablates Xist coating in EED null TSCs (Chapter 2; Kalantry et al., 2006a; Maclary et al., 2016, in preparation). I firmly believe that perturbing PRC2 function in TSCs, through *Eed* mutation, negatively impacts this transient heterochromatic state.

Why then is there still Xist RNA enrichment in my $Eed^{m-/-;z-/-}$ blastocysts? One plausible explanation lies in the chromatin state of the paternally and maternally inherited genomes early during embryogenesis. I hypothesize that the chromatin architecture of the future inactive-X (paternally inherited X-chromosome) in the female mouse embryo is different from that in TSCs. Xist RNA is induced at the two cell stage of embryogenesis, right around the time of zygotic genome activation (Brown et al., 1992; Clemson et al., 1996; Jonkers et al., 2008). This early Xist expression may simply occur as a result of the ease with which the paternally inherited X-chromosome (and genome) is transcribed (Cho et al., 2002; Bouniol et al., 1995; Wiekowski et al., 1993). In other words, the paternal-X may be permissive to hypertranscription of Xist due to an open chromatin environment. To support the idea of open chromatin, histone to protamine exchange is known to occur during spermiogenesis, preceded by histone hyperacetylation events. Such an exchange results in a genome mostly devoid of histones and thus allows the haploid male genome to be properly packaged into the head of developing spermatozoa. The converse, protamine to histone exchange, occurs soon after fertilization concomitant with active paternal genome DNA demethylation and reprogramming (Mayer et al., 2000). The kinetics with which this occurs is not clearly understood, but there is likely

differential paternal and maternal genome reorganization/reprogramming occurring in the pronuclear phases of the zygote, the effects of which may sustain through early embryogenesis. This hypothesis is supported by data from Mayer et al. that maternal pronuclei have a higher level of 5-methylcytosine (5-MeC) compared to paternal pronuclei. Moreover, at the two-cell stage, Mayer et al. noted that the maternal vs. paternal compartments of the nuclei have differential levels of 5-MeC (with the maternal compartment bearing much higher levels of methylated cytosine). This disparity in parental specific demthylation between male and female genomes in the early cleavages of mouse embryogenesis may ultimately lead to a greater ease of transcription in the paternally inherited genome compared to the maternally inherited genome. The maternal genome does not noticeably begin to lose its 5-MeC levels until the four-cell embryonic stage (Mayer et al., 2000). Notably, the female genome does not undergo such protamine to histone replacement during fertilization. It is therefore possible that a transient heterochromatic state (through activities of EED and/or canonical PRC2) does not precede Xist RNA expression and coating of the inactive-X in the early embryo due to the paternal genome swapping out protamines for histones during the two-cell stage of embryogenesis. Alternatively, EED is dispensable for forming the transient heterochromatic state and subsequent Xist induction in the early mouse embryo. That Xist RNA enriches at all on the inactive X-chromosome in *Eed*$^{m-/-;z-/-}$ blastocysts importantly suggests that mere Xist RNA enrichment on the paternally inherited-X is not sufficient to silence X-linked genes. My pyrosequencing data strongly support a strict requirement for EED in X-inactivation, which indicate *Eed*$^{m-/-;\ z-/-}$ embryos fail to initiate X-linked gene silencing appropriately. Taken together, my data suggest that maternally deposited EED is essential for triggering X-inactivation.

Discussion

In this study, I evaluated the role of the Polycomb repressive complex 2 (PRC2) core components in triggering mouse imprinted X-chromosome inactivation. Furthermore, I showed for the first time a differential requirement for maternally deposited Polycomb proteins in initiating imprinted X-inactivation. Previous work clearly identified enrichment of PcGs on the inactive-X both *in vitro* and *in vivo* (Plath et al., 2003; Silva et al., 2003; Kalantry et al. 2006a). We also know that maternally derived protein, in the case of EED, coats the inactive-X in *Eed*$^{-/-}$ (only zygotic null) embryos (Kalantry et al., 2006a). Given that Polycomb proteins enrich on the inactive–X during the initiation phase of imprinted X-chromosome inactivation, both in *WT* and zygotically null embryos, led me to hypothesize that maternally derived proteins are essential for the X-inactivation process. However, this is the first study to take a systematic genetic approach to dissect the roles of the core PRC2 subunits in triggering X-inactivation. Indeed, I hypothesized that PRC2 is essential for proper X-inactivation. Here I elucidated the distinct function of PRC2 proteins in imprinted X-chromosome inactivation initiation.

First, I investigated the activity of EZH2, the major H3-K27me3 specific methyltransferase of PRC2 (Schuettengruber et al., 2007). Despite loss of detectable H3-K27me3 enrichment on the inactive-X in *Ezh2*$^{m-/-;z-/-}$ blastocysts, I surprisingly found that X-linked gene silencing is unaffected. These data are recapitulated in *Ezh2*$^{-/-}$ post-implantation embryos; I found that X-linked gene silencing still operates normally in *Ezh2*$^{-/-}$ E6.5 extra-embryonic (EE) tissue (which maintain imprinted X-inactivation). Such evidence of EZH2 independent initiation and maintenance of the inactive-X state suggests that other factors, perhaps a noncanonical PRC2, are more important for imprinted X-inactivation.

Absence of detectable levels of H3-K27me3 in *Ezh2*$^{m-/-;z-/-}$ embryos suggests that lack of robust levels of this histone mark is not sufficient to confer a defect in triggering X-linked gene silencing. Furthermore, because EZH2 itself is dispensable for X-linked gene silencing, I hypothesized that there must be factors that supplant the activities of EZH2 to properly carry out X-inactivation. EZH1, the only other known mammalian H3-K27me3 specific homologue of EZH2, is known to compensate for loss of EZH2 in mouse ESCs and execute H3-K27me3 catalytic activity, albeit to a lesser extent (Shen et al., 2008). To address the possibility that EZH1 contributes in executing imprinted X-chromosome inactivation in embryos, I generated *Ezh2*$^{m-/-;z-/-}$;*Ezh1*$^{-/-}$ blastocysts and assayed for X-linked gene silencing initiation. Loss of both EZH2 and EZH1 in early embryos appears to confer a slight delay in the kinetics of X-linked gene silencing for some, but not all, genes analyzed. Moreover, compared to loss of EZH1 alone (my *Ezh2*$^{fl/fl}$;*Ezh1*$^{-/-}$ embryos), *Ezh2*$^{m-/-;z-/-}$;*Ezh1*$^{-/-}$ embryos display a very similar degree of silencing for all genes analyzed. I observed extensively the normal capability of *Ezh2*$^{fl/fl}$;*Ezh1*$^{-/-}$ mice to interbreed and yield litters of equal sex ratios (Table 3.2). *Ezh2*$^{fl/fl}$;*Ezh1*$^{-/-}$ mice furthermore are fertile and appear to live a normal life span. These data would suggest EZH1 absence alone does not confer a defect in X-inactivation, thus implying that EZH1 is not required for X-inactivation. To reiterate, this idea is supported by my observation that relative allelic expression of X-linked genes is not significantly different among *Ezh2*$^{fl/fl}$;*Ezh1*$^{-/-}$ and *Ezh2*$^{m-/-;z-/-}$;*Ezh1*$^{-/-}$ blastocysts. That X-linked gene silencing is not substantially hindered in my *Ezh2*$^{m-/-;z-/-}$;*Ezh1*$^{-/-}$ embryos, my data further argue that EZH1 also does not compensate for EZH2 loss in triggering X-linked gene silencing. EZH1, much like EZH2, does not appear to be involved in triggering paternal-X silencing. My observations suggest that even additional epigenetic factors are appropriately necessary in triggering imprinted X-chromosome inactivation.

To my knowledge there is no known lasting phenotype for EZH1 Loss. However, an alternative interpretation of my *Ezh2*$^{m-/;\ z-/-}$;*Ezh1*$^{-/-}$ and *Ezh2*$^{fl/fl}$;*Ezh1*$^{-/-}$ data is that there is in fact a slight failure in X-linked gene silencing initiation when EZH1 is mutated. One could therefore hypothesize that EZH1 is required, albeit transiently, for imprinted X-inactivation. From this vantage point, one could explain, why I observe a difference in paternal X-linked gene silencing in my *Ezh2*$^{fl/fl}$;*Ezh1*$^{-/-}$or *Ezh2*$^{m-/-;z-/-}$;*Ezh1*$^{-/-}$ compared to my *Ezh2*$^{m-/-;z-/-}$ blastocysts, at least in the case of Rnf12 (Figures 3.1 and 3.7). If such a defect exists, it must inevitably resolve itself as *Ezh2*$^{fl/fl}$;*Ezh1*$^{-/-}$ mice are ultimately unaffected (Table 3.2). This might imply that if EZH1 is transiently involved in triggering X-inactivation, something else must eventually compensate for its loss. To address this idea, further experiments will need to be carried out on post-implantation extra-embryonic tissues of *Ezh2*$^{fl/fl}$;*Ezh1*$^{-/-}$ embryos. For example, allele-specific RT-PCR followed by Sanger sequencing for Rnf12 could be performed to see if the paternal allele is fully silent or not at a later stage of embryogenesis. Considering that *Ezh2*$^{fl/fl}$;*Ezh1*$^{-/-}$ and *Ezh2*$^{m-/-;z-/-}$;*Ezh1*$^{-/-}$ embryos have very similar allelic expression ratios (paternal-X:maternal-X), I still believe that EZH1 loss does not compensate for EZH2 loss in triggering imprinted X-inactivation. Presumably, the *Ezh2*$^{fl/fl}$;*Ezh1*$^{-/-}$ embryos are dying for the same reason that *Ezh2*$^{m-/-;z-/-}$ embryos are dying, i.e. a defect in development other than a lasting deficit in imprinted X-chromosome inactivation.

The third and final core PRC2 component I investigated was EED. EED is the "glue" of PRC2. Without EED, PRC2 does not form properly, other subunits are degraded, and H3-K27me3 catalysis is severely diminished at PRC2 target loci (Montgomery et al., 2005). Defects in X-inactivation both *in vivo and in vitro* when EED is missing have been previously documented (Mak et al., 2004; Kalantry et al., 2006a). I hypothesized that EED is critical for

triggering imprinted X-inactivation. Upon assaying X-linked gene silencing in *Eed*$^{m-/-;z-/-}$ blastocysts, I found that, compared to *Eed*$^{fl/fl}$, *Eed*$^{m-/-;z-/-}$ embryos display a significant defect in executing silencing of several genes along the future inactive-X. This is in stark contrast to the deletion of EZH2 together with, or separate from, EZH1, where comparison to the appropriate controls (*Ezh2*$^{fl/fl}$ or *Ezh2*$^{fl/fl}$;*Ezh1*$^{-/-}$ embryos) did not lead to significant differences in the allelic expression of X-linked genes. Altogether, my data strongly suggest that while EZH2 and EZH1 are dispensable during the initiation phase of imprinted X-chromosome inactivation, EED is essential in allowing proper transcriptional inactivation of genes to occur. A divergent result between EZH2/EZH1 and EED poses a potential histone methylation (H3-K27me3 specific) independent function of PRC2 in inducing an epigenetic silent sate on the future inactive X-chromosome (discussed below). Moreover, my data provides much insight into transgenerational control of an epigenetic silent state in the embryo through the activities of maternally deposited EED.

I also point out an interesting corollary in my data with respect to EED and EZH2. Maternal EED enriches on the inactive X in *Eed*$^{-/-}$ blastocysts, whereas maternal EZH2 does not enrich on the inactive-X in *Ezh2*$^{-/-}$ blastocysts (Kalantry et al., 2006a; Figure 3.2). Considering this dichotomy in maternal specific enrichment of maternal Polycomb proteins, I conclude that this is why maternal EED is required for triggering X-linked gene silencing (as it enriches on the inactive-X in *Eed*$^{-/-}$ embryos) whereas maternal EZH2 is dispensable (it does not enrich on the inactive-X in *Ezh2*$^{-/-}$ blastocysts).

The opposing requirement for EED versus EZH2 and EZH1 in triggering imprinted X-chromosome inactivation suggests that what I am observing is a histone H3-K27me3 independent function of PRC2 in X-chromosome inactivation. It is therefore possible that EED

complexes with other proteins to form a yet unidentified version of Polycomb repressive complex 2, a noncanonical PRC2 separate from the already known EZH1-containing noncanonical PRC2 complex (Margueron et al., 2008). Our lab participated in a study to show that EED in fact interacts with members of PRC1 (Cao et al., 2014). It is plausible that a requirement for EED in X-inactivation invokes a requirement for PRC1 itself in triggering X-inactivation. It remains to be fully known if PRC1 components, and PRC1 associated histone H2A-K119ub1 enrichment on the inactive-X are genetically required for proper X-inactivation initiation in the early mouse embryo. Future experiments will elucidate the activity of PRC1 and currently unidentified epigenetic factors in executing epigenetic gene silencing, including imprinted X-chromosome inactivation.

Conclusion

In conclusion, I elucidated the roles of PRC2 subunits in imprinted X-chromosome inactivation. Previously an enigmatic question in the epigenetic/X-chromosome inactivation field, here I have uncovered an answer with direct genetic evidence to support a divergent role for members of PRC2 in executing X-linked gene silencing *in vivo*. I report for the first time that a maternally deposited epigenetic factor is necessary for inducing an epigenetic transcriptionally inert state in the early mouse embryo, thus imparting keen insight towards transgenerational control of X-inactivation and potentially epigenetic mechanisms broadly. Whereas maternal EZH2 and/or EZH1 are not required for triggering imprinted X-inactivation, maternally deposited EED is vital for executing X-linked gene silencing. To make sense of these findings, I postulate that there is an H3-K27me3 independent function for PRC2 in X-linked gene silencing. Therefore, I believe that EED and EZH2/EZH1 are genetically distinct in terms of their requirement for X-inactivation *in vivo*. My results open up new routes of investigation to identify

the additional key factors at play in X-linked gene silencing. It is entirely possible that there are hordes of epigenetic factors, such as proteins, RNAs, or even other repressive complexes that contribute, in part, to imprinted X-inactivation. Moreover, PRC1, the sister complex of PRC2, may play an active role in imprinted X-chromosome inactivation. My work will hopefully engender future experiments towards understanding the X-inactivation process more clearly. In turn, better knowledge of the intricate molecular mechanism(s) underlying imprinted X-chromosome inactivation will shed light on the method(s) by which epigenetic phenomena are initiated broadly in normal development as well as in human disease.

Materials and Methods

Ethics Statement

This study was performed in strict accordance with the recommendations in the guide for the Care and Use of Laboratory Animals of the National Institutes of Health. All animals were handled according to protocols approved by the University Committee on Use and Care of Animals (UCUCA) at the University of Michigan (protocol #PRO00006455).

Mice

Mice harboring a conditional mutation in *Eed* were generated by the University of Michigan Transgenic Animal Model Core using $Eed^{tm1a(EUCOMM)Wtsi}$ targeted ES cells (EUCOMM). Briefly, ES cells were injected into blastocysts, and implanted into pseudo-pregnant females. Mice with high percentages of chimerism were bred and assessed for germline transmission. To generate homozygous *Eed* mutant mice harboring polymorphic X-chromosomes, first, male and female mice on a B6 *Mus musculus* background carrying the conditional mutant allele for *Eed* were intercrossed ($Eed^{fl/+}$ x $Eed^{fl/+}$) to achieve homozygosity. To obtain mice conditionally mutant for *Eed* and on the JF1 *Mus molossinus* divergent background, we bred $Eed^{fl/fl}$ males (B6 *Mus musculus* background) to *WT* JF1 *Mus molossinus* females. This gave us F1 hybrid $Eed^{fl/+}$ males that possessed an X-chromosome from the JF1 *Mus molossinus* background (X^{JF1}/Y). Such males were backcrossed to *WT* JF1 *Mus molossinus* females to derive $Eed^{fl/+}$ females that were a mix of B6 *Mus musculus* and JF1 *Mus molossinus* and also harbored two X-chromosomes from the JF1 *Mus molossinus* background (X^{JF1}/X^{JF1}). $Eed^{fl/+};X^{JF1}/X^{JF1}$ females were bred against $Eed^{fl/+};X^{JF1}/Y$ males to derive $Eed^{fl/fl};X^{JF1}/Y$ males. To obtain our female embryos used in experiments ($Eed^{m-/-;z-/-};X^{Lab}/X^{JF1}$ and $Eed^{fl/fl};X^{Lab}/X^{JF1}$), we crossed $Eed^{fl/fl}$ females with or without the *Zp3-Cre* transgene on the B6 *Mus musculus* background with an $Eed^{fl/fl}$ with or without the *Prm-Cre*

male that was a mix of B6 *Mus musculus* and JF1 *Mus molossinus* but possessed an X-chromosome from the JF1 *Mus molossinus* background (X^{JF1}/Y). The JF1/Ms strain has been described previously.

Ezh2 mice were gifted from Alexander Tarakhovsky, maintained on a 129 background. Mice were crossed in a similar manner as the *Eed* mice above for deriving the $Ezh2^{m-/-;z-/-};X^{Lab}/X^{JF1}$ and $Ezh2^{fl/fl};X^{Lab}/X^{JF1}$ blastocysts, using females with and without the *Zp3-Cre* transgene and males with and with out the *Stra8-Cre* transgene.

Ezh1 mice were gifted from Alexander Tarakhovsky, originally bred by Dønal O'Carroll in Thomas Jenuwein's laboratory, maintained on a BL/6 background.

$Ezh2^{fl/fl}$ and $Ezh1^{-/-}$ mice were intercrossed and bred to generate our $Ezh2^{fl/fl}$; $Ezh1^{-/-};X^{Lab/}X^{JF1}$ mice and our $Ezh^{m-/-;z-/-};Ezh1^{-/-};X^{Lab/}X^{JF1}$ $Ezh2^{fl/fl};Ezh1^{-/-};X^{Lab/}X^{JF1}$ blastocysts in a similar manner as described for the generation of our *Eed* and *Ezh2* mice/embryos. We used females with and without the *Zp3-Cre* transgene and males with and without the *Prm-Cre* transgene.

Embryo Dissections and Processing

Blastocyst stage embryos were flushed from the uterine limbs in 1X PBS (Invitrogen, #14200075) containing 6-mg/ml bovine serum albumin (BSA; Invitrogen, #15260037). Zona pellucidae surrounding E3.5 embryos were removed through incubation in cold Acidic Tyrode's Solution (ATS, Sigma, #T1788), followed by neutralization through several transfers of cold M2 medium (Sigma, #M7167). GFP fluorescence conferred by the paternal transmission of the X^{GFP} transgene was used to distinguish female from male embryos, since only females inherit the paternal X-chromosome. Embryos were either lysed for RNA isolation or plated onto gelatin-coated glass coverslips in 1X PBS with 6-mg/ml BSA for immunofluorescence (IF) or immunofluorescence combined with RNA fluorescence *in situ* hybridization (RNA-FISH)

staining. Excess solution was aspirated, and the plated embryos were air-dried for 15 min. After drying, embryos were permeabilized and fixed in 50 μL solution of 0.05% Tergitol (Sigma, #NP407) and 1% paraformaldehyde (Electron Microscopy Sciences, # 15710) in 1X PBS for five minutes. Excess solution was tapped off, and embryos were incubated at room temperature for an additional five minutes in 50 μL drops of just 1% paraformaldehyde (Electron Microscopy Sciences, # 15710) in 1X PBS. Excess solution was tapped off, and coverslips were rinsed three times with 70% ethanol and stored in 70% ethanol at -20^{o}C prior to IF or IF combined with RNA-FISH.

For isolation of post-implantation (E6.5 or E7.5) embryos, individual implantation sites were cut from the uterine limbs and decidua were removed with forceps in 1X PBS/6-mg/ml BSA. Embryos were dissected from the decidua, and the Reichert's membranes surrounding post-implantation embryos were removed using fine forceps. For separation of extra-embryonic and epiblast portions of E6.5 embryos, fine forceps were used to physically dissect the embryos at the junction of the epiblast and extra-embryonic ectoderm (at the amniotic cavity). The epiblast of female embryos was further distinguished by GFP fluorescence conferred by the paternally-transmitted X^{GFP} transgene; the transgene is mosaically expressed in the epiblast due to random X-inactivation but is silenced in the extra-embryonic tissues because of imprinted X-inactivation of the paternal-X. Extra-embryonic and embryonic epiblast cells were then separately plated in 0.25X PBS with 6-mg/mL BSA onto gelatinized coverslips. The samples were permeabilized and fixed at room temperature for 15 minutes in 0.1% Tergitol, 1% PFA in 1X PBS. Embryos pieces were then stored in 70% ethanol as described above for E3.5 embryos, prior to immunofluorescence or immunofluorescence combined with RNA-FISH.

Immunofluorescence

We began with fixed, permeabilized embryo samples that were plated on gelatinized glass coverslips and stored in 70% ethanol. Samples were then washed briefly with three changes of 1X PBS to remove ethanol, followed by three successive washes with 1X PBS for three minutes each on a rocker. Samples were blocked for 30 minutes at 37°C in 50 μl pre-warmed blocking buffer in a humid chamber. Samples were then incubated for one hour at 37°C in 50 μL diluted primary antibody (dilution depends on primary antibody used, 1:500 EED primary Ab, previously used in (Kalantry et al., 2006a; Plath et al., 2003; Silva et al., 2003); 1:5000 H3-K27me3 primary Ab; polyclonal Rabbit anti-mouse, Millipore, #ABE44; 1:100 EZH2 primary Ab, Cell Signaling) in a humid chamber. After incubation, samples were washed three times with 1X PBS/0.2% Tween-20 for three minutes each on a rocker. Coverslips were then placed back in 50 μL pre-warmed blocking buffer in a humid chamber for five minutes at 37°C. This was followed by an additional incubation for 30 minutes at 37°C in 50 μL diluted secondary antibody. Alexa Fluor conjugated secondary antibodies were used at a 1:300 dilution. Following secondary incubation, coverslips were washed two times with 1X PBS/0.2% Tween-20 for three minutes each on a rocker. Samples were then washed one time with 1X PBS/0.2% Tween-20 (containing 1:100,000-1:200,000 dilution of DAPI) for seven minutes on a rocker. This was followed by one more wash 1X PBS/0.2% Tween-20 (no DAPI for this final wash) for five minutes on a rocker. Sample coverslips were then mounted onto glass microscope slides with Vectashield. Coverslips were sealed to the glass slides with clear nail polish.

Immunofluorescence Combined with RNA-FISH

We began with fixed, permeabilized embryo samples that were plated on gelatinized glass coverslips and stored in 70% ethanol. Samples were then washed briefly with three changes of 1X PBS to remove ethanol, followed by three successive washes with 1X PBS for three minutes each on a rocker. Samples were blocked for 30 minutes at 37°C in 50 μl pre-warmed blocking buffer in a humid chamber. Samples were then incubated for one hour at 37°C in 50 μL diluted primary antibody (dilution depends on primary antibody used, 1:500 EED primary Ab, previously used in (Kalantry et al., 2006; Plath et al., 2003; Silva et al., 2003); 1:5000 H3-K27me3 primary Ab; polyclonal Rabbit anti-mouse, Millipore, #ABE44; 1:100 EZH2 primary Ab, Cell Signaling) in a humid chamber. After incubation, samples were washed three times with 1X PBS/0.2% Tween-20 for three minutes each on a rocker. Coverslips were then placed back in 50 μL pre-warmed blocking buffer in a humid chamber for five minutes at 37°C followed by an additional incubation for 30 minutes at 37°C in 50 μL diluted secondary antibody. Alexa Fluor conjugated secondary antibodies were used at a 1:300 dilution. Following secondary incubation, coverslips were washed three times with 1X PBS/0.2% Tween-20 for three minutes each on a rocker. Samples were incubated in 100 μl of 2% PFA on a glass plate wrapped in parafilm for ten minutes at room temperature. Following this, samples were dehydrated through room temperature ethanol series (five minutes each for 70%, 85%, 95%, and 100% ethanol). Coverslips were allowed to dry for 15 minutes after the 100% ethanol wash, followed by hybridizing the samples overnight with the appropriate RNA-FISH probe. After hybridization, samples were washed for seven minutes at 39°C, three times each in 2X SSC/50% formamide. This was followed by three-seven minute washes at 39°C, in 2X SSC (1:100,000-1:200,000 dilution of DAPI added at third wash of 2X SSC), followed by two-seven minute washes at 39°C,

in 1X SSC. Sample coverslips were then mounted onto glass microscope slides with Vectashield. Coverslips were sealed to the glass slides with clear nail polish.

RNA-FISH

Samples embryos were dehydrated through room temperature ethanol series (five minutes each for 70%, 85%, 95%, and 100% ethanol). Coverslips were allowed to dry for 15 minutes at room temperature after the 100% ethanol wash, followed by hybridizing the samples overnight with the appropriate RNA-FISH probe. After the hybridization, samples were washed for seven minutes at 39°C, three times each in 2X SSC/50% formamide. This was followed by three-seven minute washes at 39°C, in 2X SSC a dilution (1:100,000-1:200,000) of DAPI added at third wash of 2X SSC), followed by two-seven minute washes at 39°C, in 1X SSC. Sample coverslips were then mounted onto glass microscope slides with Vectashield. Coverslips were sealed to the glass slides with clear nail polish.

Allele-Specific Reverse Transcriptase/Polymerase Chain Reaction (RT-PCR)

mRNA was purified from whole blastocyst lysates according to manufacturers instructions (Life Technologies Dynabeads mRNA direct kit). SuperScript III One-Step RT-PCR Kit with Platinum *Taq* enzyme mixture (Invitrogen, #12574-035) was used to prepare and amplify the complimentary DNA (cDNA). Amplified cDNAs were run on agarose gels and purified using the Clontech NucleoSpin Kit (Clontech, #740609). The purified cDNAs were then sequenced and sequencing traces were examined for single nucleotide polymorphisms (SNPs) characteristic of the *M. molossinus*-derived X^{JF1} chromosome and the *M. musculus*-derived X^{Lab} chromosomes.

Isolation of Total RNA and mRNA from Embryos

Total RNA from E3.5 embryos was purified by lysis in 10 μL extraction buffer of the PicoPure® RNA Isolation Kit, followed by manufacturer's instructions (Life Technologies #KIT0204).

Purified total RNA was resuspended in 30 μL of elution buffer. mRNA from E3.5 embryos was purified by lysis in 100 μL lysis/binding buffer of the Dynabeads mRNA DIRECT Kit, followed by manufacturer's instructions. Purified mRNA was resuspended in 30-50 μL of elution buffer.

Pyrosequencing/Quantification of Allele-Specific Expression

Allele-specific expression in embryos was quantified using Qiagen PyroMark sequencing platform. *Rnf12*, *Atrx*, *G6pdx*, and *Pdha1* amplicons containing single nucleotide polymorphisms (SNPs) were designed using the PyroMark Assay Design software. cDNAs were synthesized using Invitrogen SuperScript III One-Step RT-PCR System (Invitrogen, #12574-026). Following the PCR reaction, five μL of a total of 25 μL was run on a 3% agarose gel to assess the efficacy of the reverse transcription and cDNA amplification. The samples were then prepared for pyrosequencing according to the standard recommendations for use with the PyroMark Q96 ID sequencer. All amplicons spanned at least one intron, thus excluding any amplified contaminating genomic DNA sequence due to size differences. Gene expression was compared between genotypes using Welch's two sample t-tests.

PCR

For DNA isolation, whole blastocysts or portions of E6.5 post-implantation embryos were lysed in buffer composed of 50mM KCl, 10mM Tris-Cl (pH 8.3), 2.5mM $MgCl_2$, 0.1mg/ml gelatin, 0.45%NP-40, and 0.45% Tween-20. Samples in lysis buffer were incubated at 50^0C overnight, and then stored at 4^0C until use. Genomic PCR reactions were carried out in ChromaTaq buffer (Denville Scientific) with 1.5mM Magnesium Chloride using RadiantTaq DNA polymerase (Alkali Scientific, #C109).

Microscopy

Stained samples were imaged using a Nikon Eclipse TiE inverted microscope with a Photometrics CCD camera. The images were deconvolved and uniformly processed using NIS-Elements software.

Statistical Analysis

For the RNA-FISH analyses, I utilized a Fischer's exact test with a 2 x 3 contingency table. For the allele-specific RT-PCR/pyrosequencing analyses, I utilized a Welch's two sample t-test. For the *Ezh2*$^{fl/-}$ x *Ezh2*$^{fl/fl}$;*Stra8-Cre* crosses and *Ezh2*$^{fl/fl}$;*Ezh1*$^{-/-}$ x *Ezh2*$^{fl/fl}$;*Ezh1*$^{-/-}$ breeding tabulations, I utilized a Chi-square test. Significance values (alpha) for all three statistical tests are as follows:

- Fischer's exact: 0.01
- Welch's t-test: 0.01
- Chi-square test: 0.05

Table of Primers II
Primers for PCR/RT-PCR
Sanger sequencing (S)/Genotyping (G)/Pyrosequencing (P)

Primer	Sequence	Use
XistF	CAAGAAGAAGGATTGCCTGGATTT	PCR (P)
XistR-biotin	GCGAGGACTTGAAGAGAAGTTCTG	RT, PCR (P)
Xist-seq	CAAACAATCCCTATGTGA	PCR (P)
Utx-F-biotin	CCAAAAGCATTATCTGCATACCA	PCR (P) (P)
Utx-R	CCAAACCAAGACCATATAAAAAGG	RT, PCR (P)
Utx-seq	TAGAACTTCCTTCAGGC	Pyroseq. (P)
Rnf12-F-biotin	TGCAGCCAACAAGTGAAATTCC	PCR (P)
Rnf12-R	TATCTGCTGTCTCAGGGTCACATG	RT, PCR (P)
Rnf12-seq	TAGAACTTCCTTCAGGC	Pyroseq. (P)
Atrx-F	ATAGCTTCAGATTCTGATGAAACC	PCR (P)
Atrx-R-biotin	ACATCGTTGTCACTGCCACTT	RT, PCR (P)
Atrx-seq	TAAGCTCAGATGAAAAGA	Pyroseq. (P)
Pdha1-F-biotin	AGCAATCTTGCAAGTGTTGAAGAA	PCR (P)
Pdha1-R	TTTTCAAGCCTTTTGTTGTCTGG	RT, PCR (P)
Atrx-F	GGGATTGCTGCTGTGAGTCT	PCR (S)

Atrx-R	CCACCATCTTCTTGCCATCT	RT, PCR (S)
Rnf12-F	GAGCCCCGATGAAAATAGAGC	PCR (S)
Rnf12-R	GGTCGGCACTTCTGTTACTGC	RT, PCR (S)
Pdha1-F	GGGACGTCTGTTGAGAGAGC	PCR (S)
Pdha1-R	GCACTTCAAAGGGAGGATCA	RT, PCR. (S)
Pgk1-F	GAAGGGAAGGGAAAAGATGC	PCR (S)
Pgk1-R	TGTGCCAATCTCCATGTTGT	RT, PCR (S)
Xist (XF)-9229	GACAACAATGGGAGCTGGTT	PCR (G)
Xist (XR)-9572	CCAGGCAATCCTTCTTCTTG	RT, PCR (G)
WUStL-Cre-F	GCATTACCGGTCGATGCAACGAGTGATGAG	G
WUStL-Cre-R	GAGTGAACGAACCTGGTCGAAATCAGTGCG	G
EED-F2	CCTGTCAGGCAGTCATTTCA	G
EED-R2	CCTACTGGTCGGTCTTGCAT	G
Eed-5’arm	GGACTCATCCTCTGGTAGAGCAGC	G
Eed-3’arm	TGCCTACTGCAAACTTTTAGTATGCC	G
WT-R2:	GCTCCTGTCCTCATAGCAAGA	G
SA-1:	GTACTCTTAACCACTGGACTG	G

LACZ-2:	AAGCGCCATTCGCCATTCAGG	G
Enx1-3-loxP:	CTGCTCTGAATGGCAACTCC	G
Ezh2-5-loxp-3	CTGGCTCTGTGGAACCAAAC	G
Ezh2-L5-loxp-1	ATGGGCCTCATAGTGACAGG	G
SK-Fabpi-S-F	TGGACAGAACTGGACCTCTGCTTTCCTA	G
SK-Fabpi-S-R	TAGAGCTTTGCCACATCACAGGTCATTC	G
Flp-F	GGT CCA ACT GCA GCC CAA GCT TCC	G
Flp-R	GTG GAT CGA TCC TAC CCC TTG CG	G
JR-eGFPf	CTG AAG TTC ATC TGC ACC ACC	G
JR-eGFPr	ATG CCG TTC TTC TGC TTG TCG	G
LacZ SK-WUStL-B-gal-F	GTTGCAGTGCACGGCAGATACACTTGCT	G
LacZ SK-WUStL-B-gal-R	GCCACTGGTGTGGGCCATAATTCAATTC	G
BA-Neo-F	AGAGGCTATTCGGCTATGACTG	G
BA-Neo-R	CCTGATCGACAAGACCGGCTTC	G
Stra8CreF	GTGCAAGCTGAACAACAGGA	G

Stra8CreR	AGGGACACAGCATTGGAGTC	G
Xist 5LoxR_LW	ACC CTT GCC TTT TCC ATT TT	G
Xist3R_LW	CAC TGG CAA GGT GAA TAG CA	G
XpromL_LW	TTT CTG GTC TTT GAG GGC AC	G
XX-XY.F	CCGCTGCCAAATTCTTTGG	G
XX-XY.R	TGAAGCTTTTGGCTTTGAG	G
SRY-F	TTG TCT AGA GAG CAT GGA GGG CCA TGT CAA	G
SRY-R	CCA CTC CTC TGT GAC ACT TTA GCC CTC CGA	G
Zp3creF	CAG ATG AGG TTT GAG GCC ACA G	G
Zp3creR	CCC GGC AAA ACA GGT AGT TA	G

Acknowledgements

I would like to thank Alexander Tarakhovsky for the *Ezh2*$^{fl/fl}$ mice and for the *Ezh1*$^{-/-}$ mice. I also thank the University of Michigan Transgenic Animal Core Facility for injecting our targeted *Eed* ES cell constructs into blastocysts and implanting these into pseudo-pregnant mice for generating a germline transmission of our *Eed*$^{fl/fl}$ conditional mutant construct. I wish to thank Clair Harris for breeding and maintaining the *Eed*$^{fl/fl}$ with and with out *Zp3-Cre* or *Prm-Cre* mice used for my embryo studies. I would also like to acknowledge Emily Maclary for her work on the *WT* and *Ezh2*$^{-/-}$ post-implantation embryos. She completed the confocal microscopy experiments assessing GFP fluorescence in both *WT* and *Ezh2*$^{-/-}$ E7.5 embryos. I also thank Peter Larson, who contributed to experiments, data collection, and analysis for the *WT* and *Ezh2*$^{m-/-;z-/-}$ blastocyst IF/RNA-FISH experiments.

Notice on Future Publication of This Work

This data chapter will be submitted for publication in a peer reviewed scientific journal. The following is the reference that will accompany the submission:

Hinten M, Maclary E, Harris C, Larson P, Kalantry S. Control of mouse imprinted X-chromosome inactivation by a maternal Polycomb protein (in preparation).

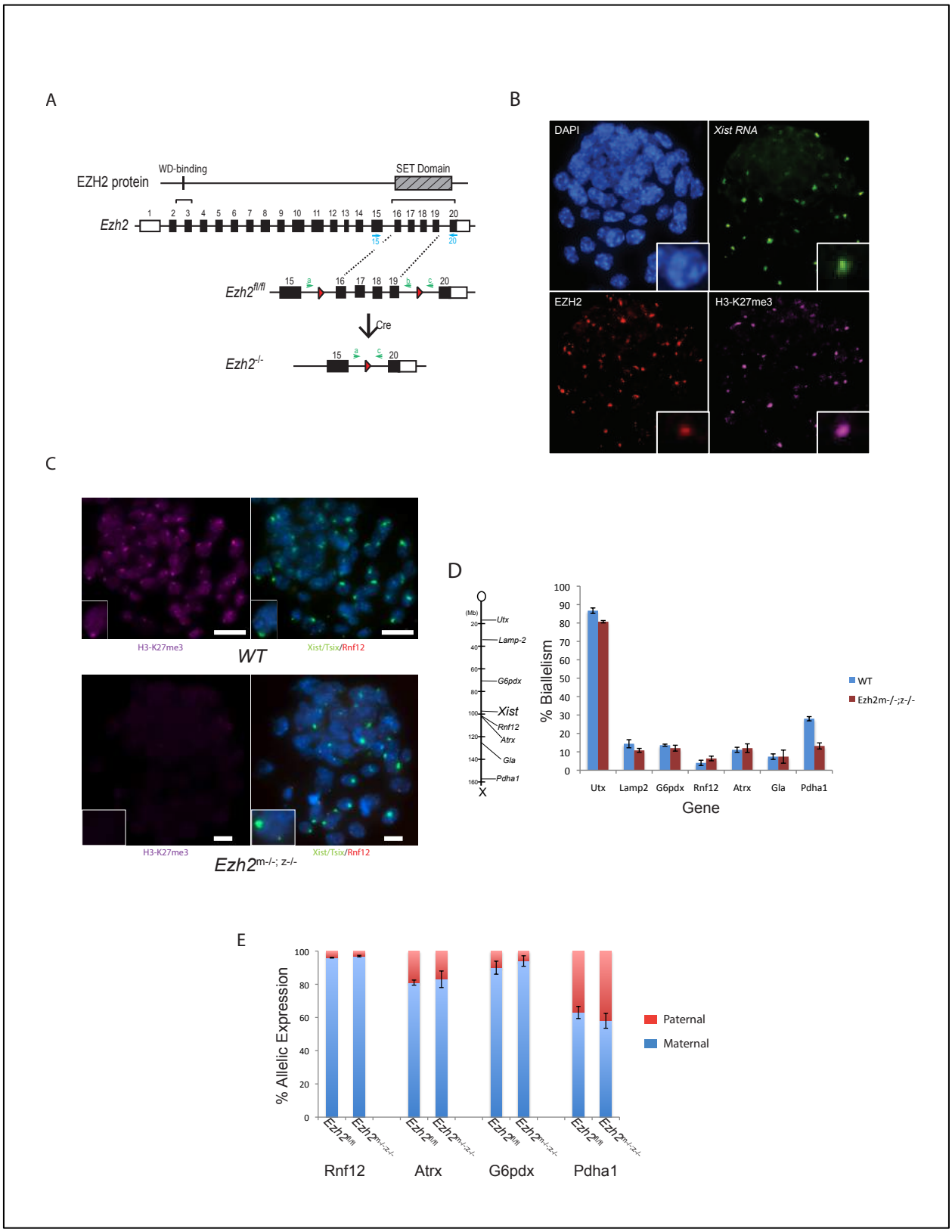
A
EZH2 protein
WD-binding
SET Domain
Ezh2
Ezh2fl/fl
Cre
Ezh2-/-
B
DAPI
Xist RNA
EZH2
H3-K27me3
C
H3-K27me3
Xist/Tsix/Rnf12
WT
Ezh2m-/-; z-/-
D
Utx
Lamp-2
G6pdx
Xist
Rnf12
Atrx
Gla
Pdha1
% Biallelism
Gene
WT
Ezh2m-/-;z-/-
E
% Allelic Expression
Paternal
Maternal
Rnf12
Atrx
G6pdx
Pdha1

Figure 3.1

Figure 3.1. EZH2 is dispensable during the initiation phase of imprinted X-chromosome inactivation.

A. Schematic of my *Ezh2* mutation (see chapter 2 for details).

B. Representative *WT* blastocyst is showing immunofluorescence detection of EZH2 and its catalytic read-out, H3-K27me3, as well as Xist enrichment (via RNA-FSH) on the inactive X-chromosome. EZH2 is in red, H3-K27me3 is in purple, and Xist in green marks the inactive X-chromosome. Representative inset nucleus at bottom right of each panel. Nuclei stained with DAPI. Scale bar is 10 μm.

C. Representative *WT* (top) and *Ezh2*$^{m-/-z;-/-}$ (maternal and zygotic null) (bottom) blastocysts are showing immunofluorescence detection of H3-K27me3 (in purple) and RNA-FISH detection of Xist RNA (in green) enrichment on the inactive-X chromosome. Nascent RNA detection of an X-linked gene, Rnf12 is a red pinpoint and Tsix, the Xist antisense RNA, is a green pinpoint, from the active X-chromosome. Representative inset nucleus at bottom of each panel. Nuclei stained with DAPI. Scale bar is 10 μm. Six or more biological replicates were performed for seven different genes for both *WT* and *Ezh2*$^{m-/-z;-/-}$.

D. RNA-FISH quantifications for seven X-linked genes along the X-chromosome. Quantifications represent immunofluorescence and RNA-FISH experiments on *WT* and *Ezh2*$^{m-/-z;-/-}$ blastocysts (see panel C above). Graph represents averages + or – SEM from six or more biological replicates for each of the seven X-linked genes for both *WT* and *Ezh2*$^{m-/-; z-/-}$ embryos. Cartoon of the X-chromosome and position of all genes (relative to *Xist*) analyzed are shown to the left of the graph.
p-values for each gene: *Utx*: 0.431, *Lamp-2*: 0.7275, *G6pdx*: 0.7805, *Rnf12*: 0.7702, *Atrx*: 0.8908, *Gla*: 0.05109, and *Pdha1*: 0.0303; Fischer's exact test, 2 x 3 contingency table.

E. Pyrosequencing quantifications of allele-specific RT-PCR for a subset of the seven genes analyzed by RNA-FISH for *Ezh2*$^{fl/fl}$ and *Ezh2*$^{m-/-z;-/-}$ blastocysts. Graphs represent averages + or – SEM from six or more biological replicates for each of the four X-linked genes for both *WT* and *Ezh2*$^{m-/-; z-/-}$. Maternal (active X-chromosome) allelic expression is in blue and paternal (inactive X-chromosome) allelic expression is in red.
p-values for each gene: *Rnf12*: 0.736798878, *Atrx*: 0.670339595, *G6pdx:* 0.426211803 and *Pdha1*: 0.471458586; Welch's two sample t-test.

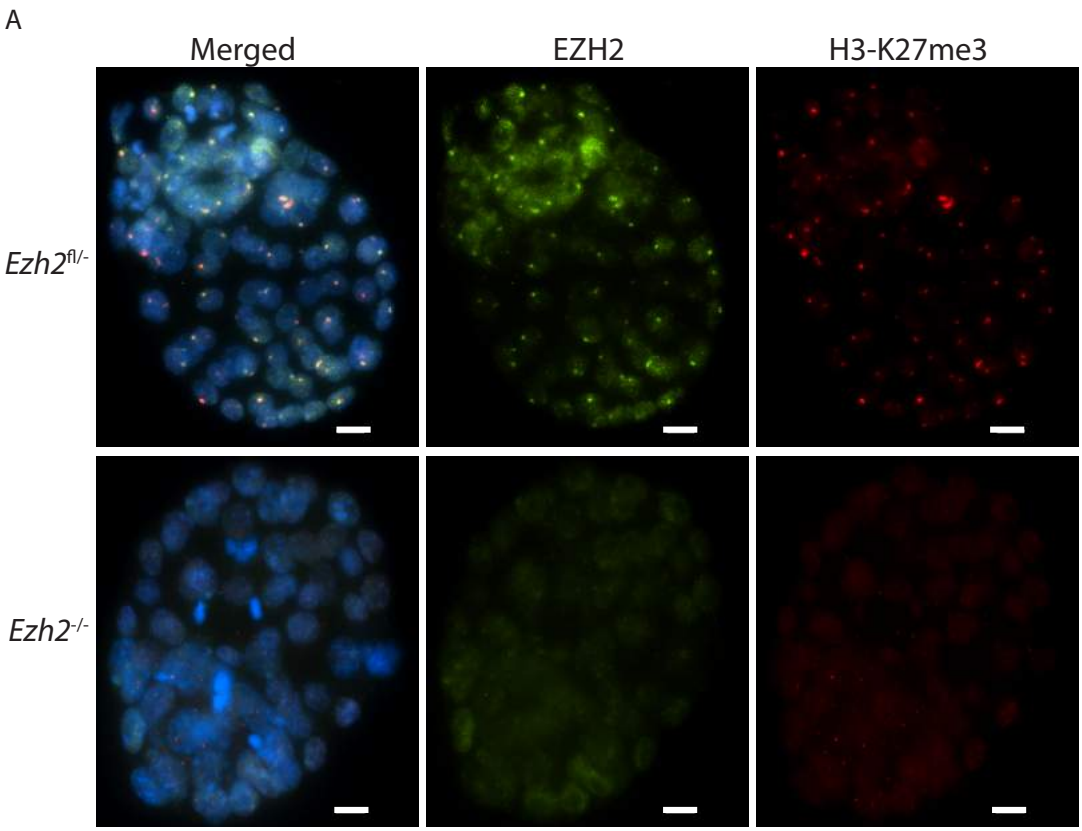

Figure 3.2

Figure 3.2. Maternal EZH2 does not enrich on the inactive-X in blastocysts.

A. Representative immunofluorescence detection of EZH2 and its catalytic read-out, H3-K27me3, on the inactive X-chromosome. Top row is an *Ezh2*$^{fl/-}$ embryo where maternal EZH2 and H3-K27me3 enrich on the inactive-X, while the bottom row represents an *Ezh2*$^{-/-}$ embryo where EZH2 and H3-K327me3 does not enrich on the inactive-X. EZH2 is in green and H3-K27me3 is in red. Nuclei stained with DAPI. Scale bar is 10 μm. 20 biological replicates were performed

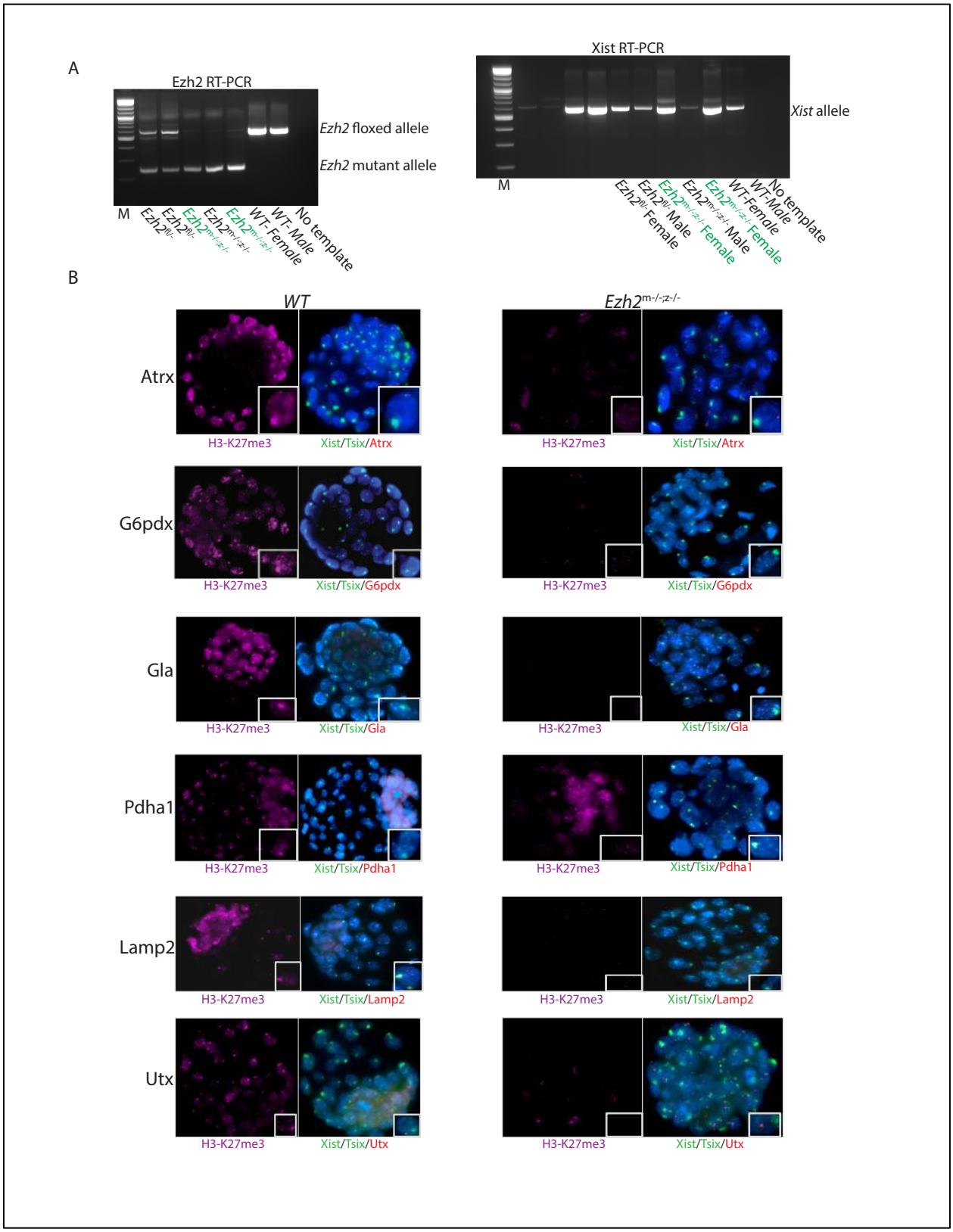
A
Ezh2 RT-PCR
Ezh2 floxed allele
Ezh2 mutant allele
M
Ezh2fl/-
Ezh2fl/-
Ezh2m-/-;z-/-
Ezh2m-/-;z-/-
Ezh2m-/-;z-/-
WT-Male
WT-Female
No template
Xist RT-PCR
Xist allele
M
Ezh2fl/- Female
Ezh2fl/- Male
Ezh2m-/-;z-/- Female
Ezh2m-/-;z-/- Male
Ezh2m-/-;z-/- Female
WT-Female
WT-Male
No template
B
WT
Ezh2m-/-;z-/-
Atrx
G6pdx
Gla
Pdha1
Lamp2
Utx
H3-K27me3
Xist/Tsix/Atrx
Xist/Tsix/G6pdx
Xist/Tsix/Gla
Xist/Tsix/Pdha1
Xist/Tsix/Lamp2
Xist/Tsix/Utx

Figure 3.3

Figure 3.3. EZH2 is dispensable during the initiation phase of imprinted X-chromosome inactivation.

A. Genotyping RT-PCR gel image for *WT* and *Ezh2*$^{m-/-;z-/-}$ blastocysts. Ezh2 RT-PCR is on the left, with genotypes and bands noted. Xist RT-PCR is on the right with genotypes, sex, and band noted. *Ezh2*$^{m-/-;z-/-}$ females are highlighted in green. M=Marker, 100 bp ladder.

B. Combined immunofluorescence and RNA-FISH for *WT* and *Ezh2*$^{m-/-;z-/-}$ blastocysts. H3-K27me3 is in purple, Xist (Tsix) is in green, and additional X-linked genes are in red. Nuclei stained with DAPI. Scale bar is 10 μm. Six or more biological replicates were performed for each gene for *WT* and *Ezh2*$^{m-/-;z-/-}$.

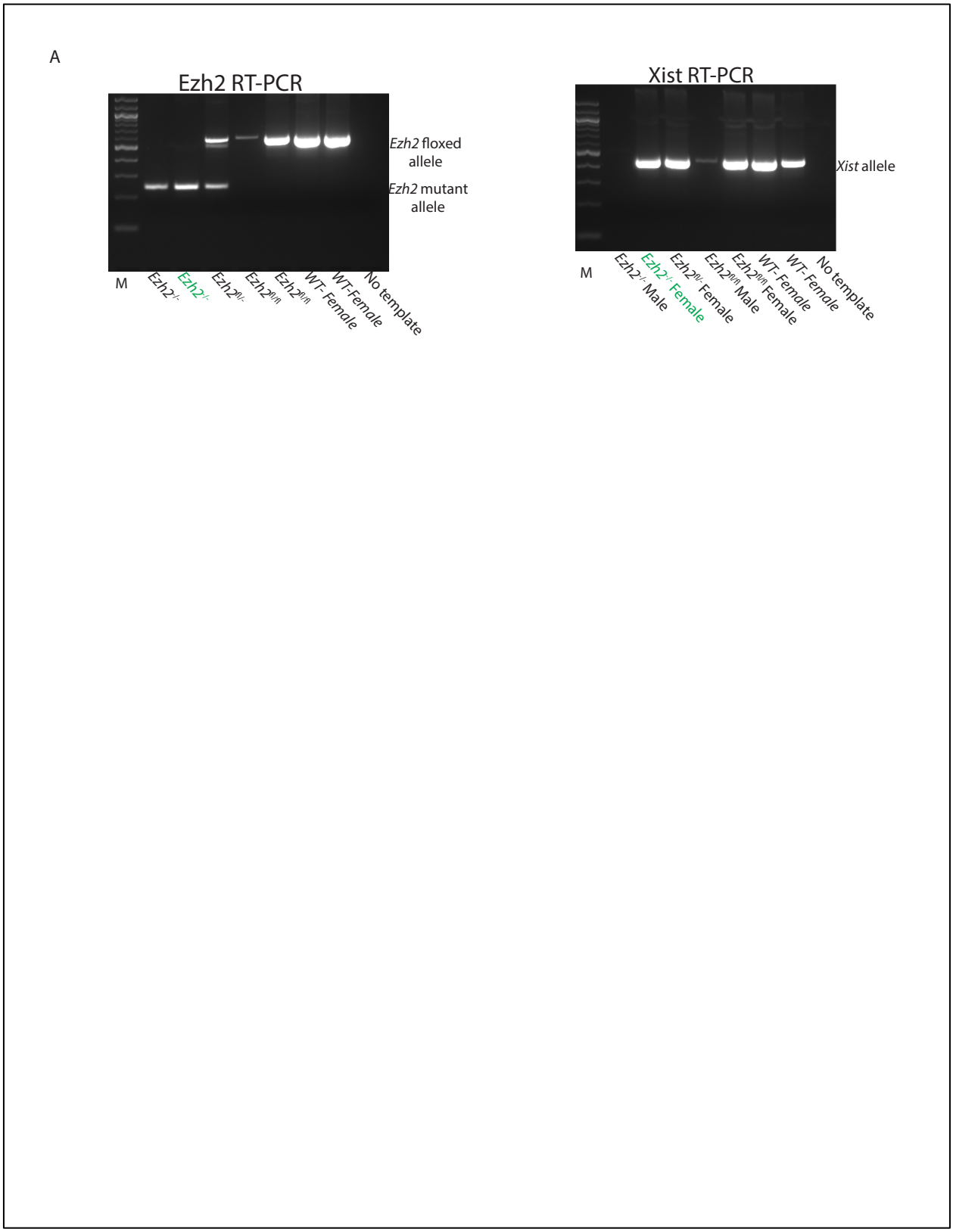
A
Ezh2 RT-PCR
Ezh2 floxed allele
Ezh2 mutant allele
M
Ezh2-/- Male
Ezh2-/- Female
Ezh2fl/- Female
Ezh2fl/fl Male
Ezh2fl/fl Female
WT-Female
WT-Female
No template
Xist RT-PCR
Xist allele
M
Ezh2-/- Male
Ezh2-/- Female
Ezh2fl/- Female
Ezh2fl/fl Male
Ezh2fl/fl Female
WT-Female
WT-Female
No template

Figure 3.4

Figure 3.4. EZH2 is not required to maintain imprinted X-chromosome inactivation.

A. Representative genotyping RT-PCR gel image for *WT* and *Ezh2*$^{-/-}$ E6.5 tissues. Ezh2 RT-PCR is on the left, with genotypes and bands noted. Xist RT-PCR is on the right with genotypes, sex, and band noted. *Ezh2* mutant females are highlighted in green. M=Marker, 100 bp ladder.

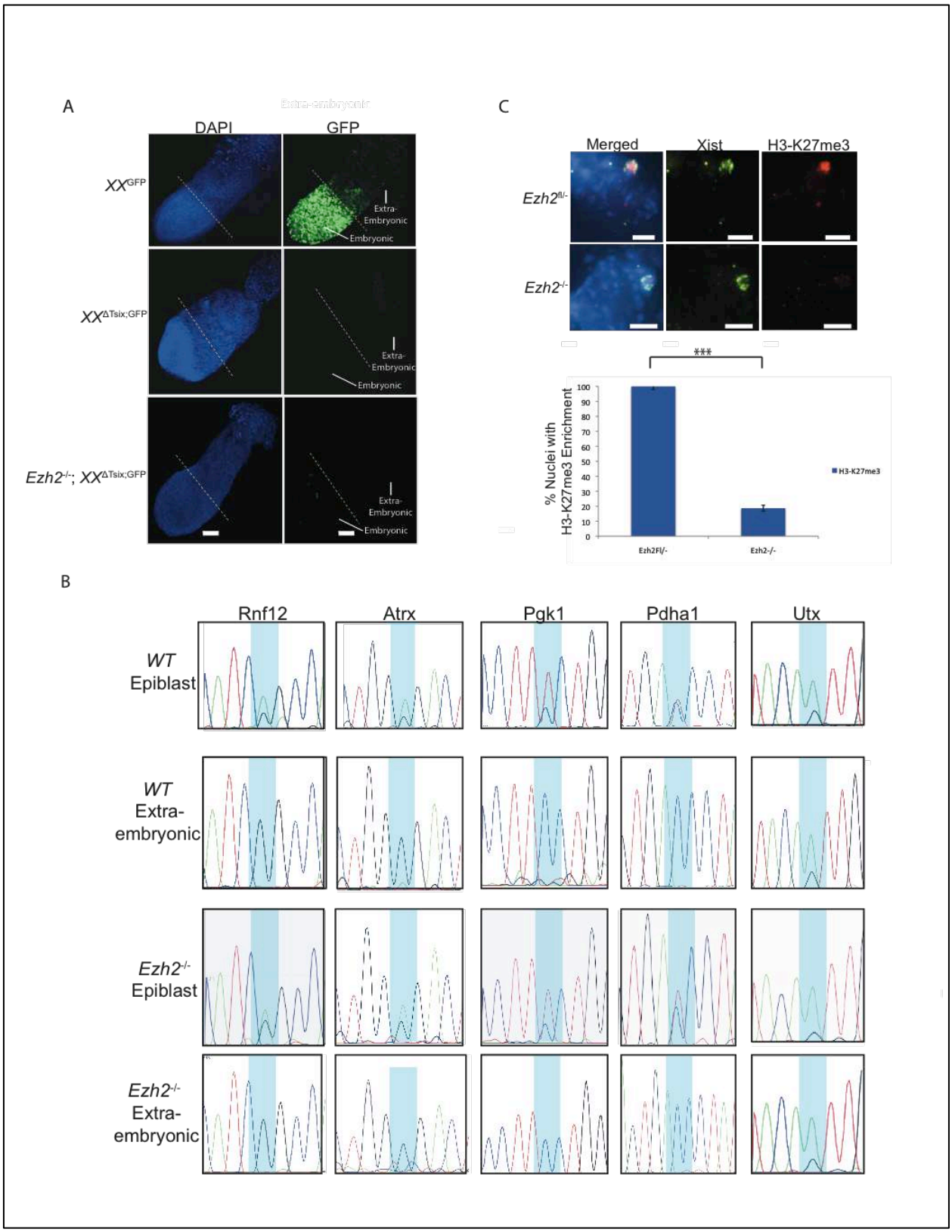
A
DAPI
GFP
XXGFP
XXΔTsix;GFP
Ezh2-/-; XXΔTsix;GFP
Extra-Embryonic
Embryonic
C
Merged
Xist
H3-K27me3
Ezh2fl/-
Ezh2-/-
***
% Nuclei with H3-K27me3 Enrichment
H3-K27me3
Ezh2Fl/-
Ezh2-/-
B
Rnf12
Atrx
Pgk1
Pdha1
Utx
WT Epiblast
WT Extra-embryonic
Ezh2-/- Epiblast
Ezh2-/- Extra-embryonic

Figure 3.5

Figure 3.5. EZH2 is not required to maintain imprinted X-chromosome inactivation

A. Representative confocal microscopy images of E7.5 *WT* and *Ezh2*$^{-/-}$ embryos. Line segments are pointing to the embryonic and extra-embryonic tissues (imprinted X-inactivation is maintained in the Trophoblast (TB) in these embryos). There is no defect in the silencing of an X-linked GFP transgene on the paternally inherited (inactive) X-chromosome in the mutants compared to the *WT*. Nuclei are stained with DAPI. Scale bar is 10 μm.

B. Representative chromatograms for Rnf12, Atrx, Pgk1, Pdha1, and Utx from allele-specific RT-PCR experiments on *WT* and *Ezh2*$^{-/-}$ extra-embryonic tissue (E6.5). *WT* epiblast is shown as a control to represent gene expression form both X-chromosomes as both alleles for these genes are expressed due to random X-chromosome inactivation. In the case of Rnf12 cDNA, for example, the G allele is the maternal (X^{Lab}) allele, and the A allele is the paternal (X^{JF1} allele). Three biological replicates were performed for each gene.

C. Individual nuclei from representative immunofluorescence/RNA-FISH experiments on post-implantation (E6.5) *WT* and *Ezh2*$^{-/-}$ extra-embryonic tissue. H3-K27me3 is in red and Xist in green to mark the inactive X-chromosome. Nuclei stained with DAPI. Scale bar is 2 μm. Quantifications below images represent percent nuclei with H3-K27me3 enrichment normalized to *Xist* for both *WT* and *Ezh2*$^{-/-}$ extra-embryonic tissue. Graph represents averages + or – SEM from three or more biological replicates.
***p-value: 3.23229E-05; Welch's two sample t-test (p-value less than 0.001).

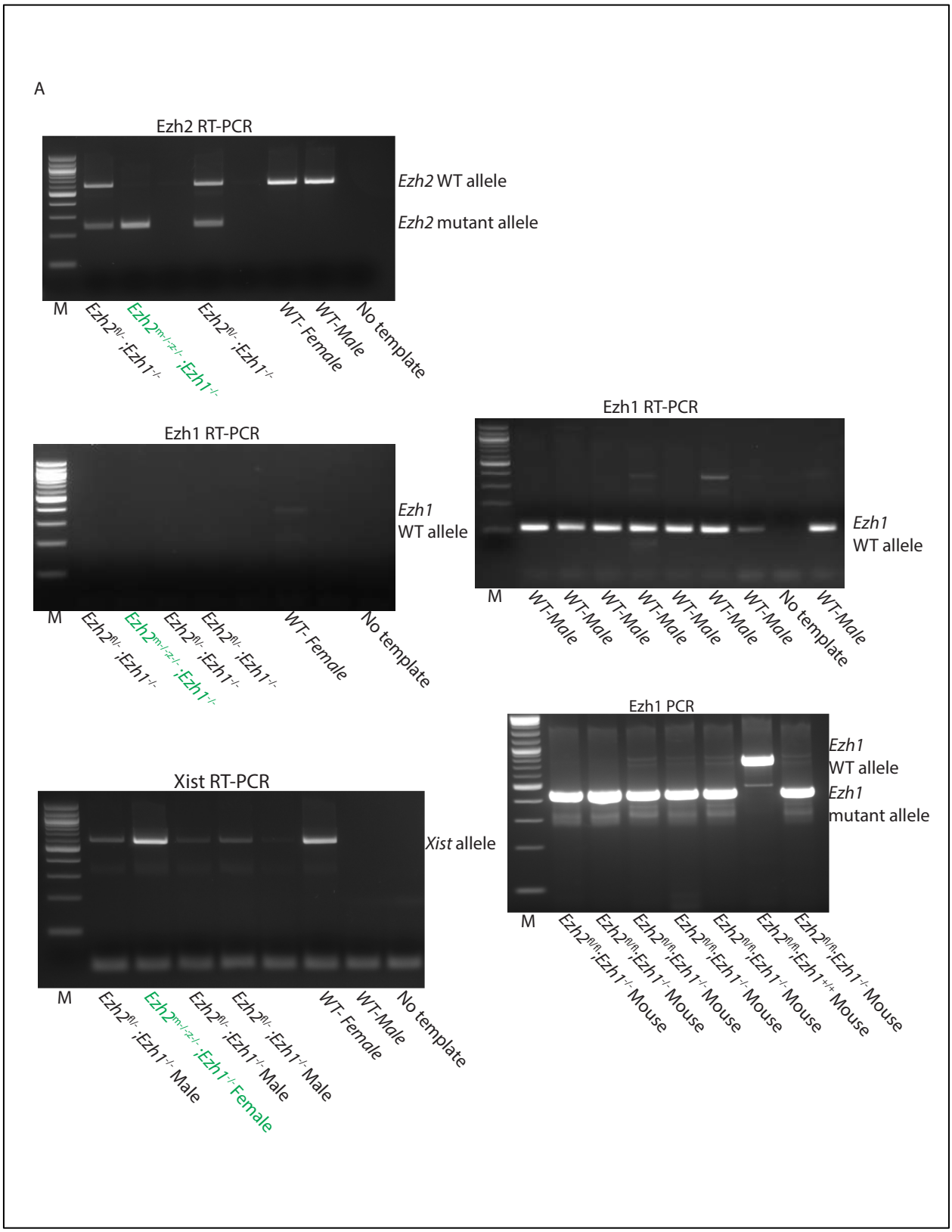
A
Ezh2 RT-PCR
Ezh2 WT allele
Ezh2 mutant allele
M
Ezh2fl/-;Ezh1-/-
Ezh2m-/-;Ezh1-/-
Ezh2fl/-;Ezh1+/-
WT-Female
WT-Male
No template
Ezh1 RT-PCR
Ezh1 WT allele
M
Ezh2fl/-;Ezh1-/-
Ezh2m-/-;Ezh1-/-
Ezh2fl/-;Ezh1+/-
WT-Female
No template
Ezh1 RT-PCR
Ezh1 WT allele
M
WT-Male
No template
Ezh1 PCR
Ezh1 WT allele
Ezh1 mutant allele
M
Ezh2fl/fl;Ezh1-/- Mouse
Ezh2fl/fl;Ezh1+/+ Mouse
Xist RT-PCR
Xist allele
M
Ezh2fl/-;Ezh1-/- Male
Ezh2m-/-;Ezh1-/- Female
Ezh2fl/-;Ezh1+/- Male
WT-Female
WT-Male
No template

Figure 3.6

Figure 3.6. EZH1 does not contribute to the initiation of imprinted X-chromosome inactivation.

A. Genotyping RT-PCR gel image for *Ezh2*$^{fl/-}$;*Ezh1*$^{-/-}$; and *Ezh2*$^{m-/-;z-/-}$;*Ezh1*$^{-/-}$ blastocysts. Ezh2 RT-PCR is on the top left, with genotypes and bands noted. Ezh1 RT-PCR is on the middle left with genotypes and band noted (note this primer pair anneals to a region downstream of the LacZ cassette, therefore it will not pick up a transcript from the mutant as there is no transcript past the inserted LacZ cassette). Ezh1 RT-PCR on the middle right with genotypes and band noted (note this primer pair will pick up a transcript from both WT and MT samples as it detects the transcript upstream of the inserted Lacz cassette). This Ezh1 RT-PCR also indicates that *Ezh1* is expressed at the blastocyst stage of development. Xist RT-PCR is on the bottom left with genotypes, sex, and band noted. *Ezh2*$^{m-/-;z-/-}$;*Ezh1*$^{-/-}$ females are highlighted in green. *Ezh1* PCR is on the bottom right denoting genotypes of *Ezh2*$^{fl/fl}$;*Ezh1*$^{-/-}$ (cross of *Ezh2*$^{fl/fl}$;*Ezh1*$^{-/-}$ mice) used to generate the *Ezh2*$^{m-/-;z-/-}$;*Ezh1*$^{-/-}$ embryos. This mutation is a conventional, constitutive mutant allele. Genotypes and bands noted. M=Marker, 100 bp ladder.

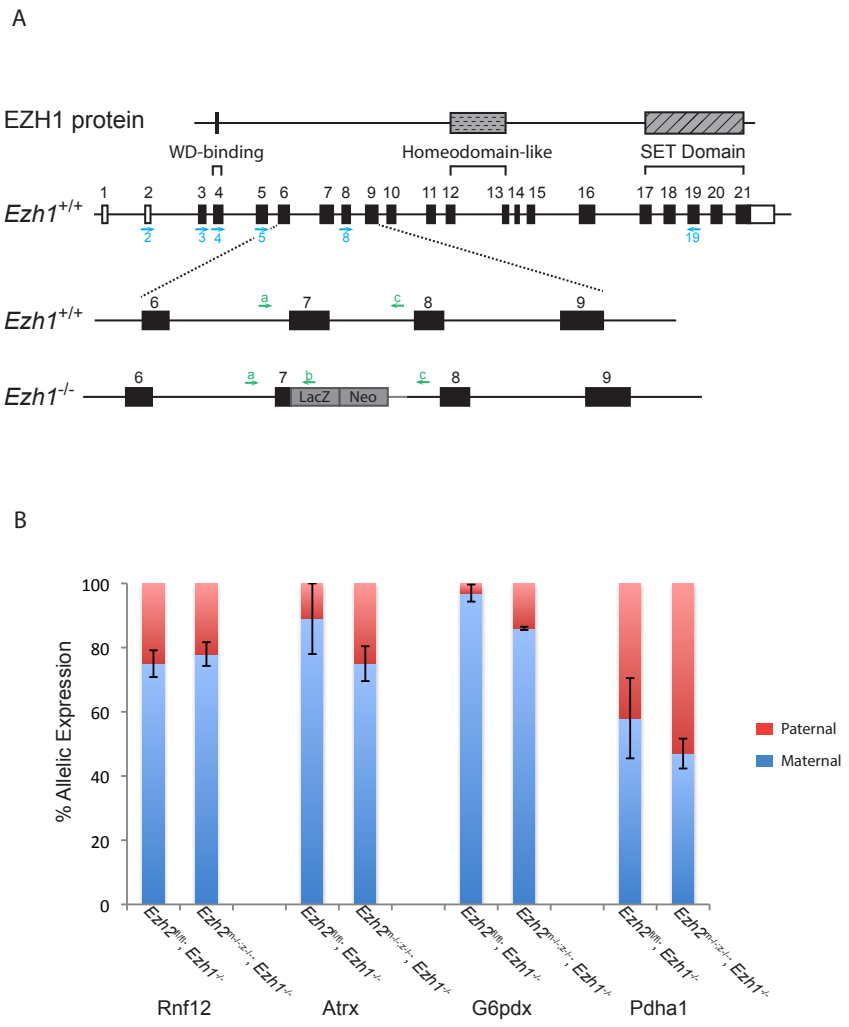
A
EZH1 protein
WD-binding
Homeodomain-like
SET Domain
Ezh1+/+
Ezh1+/+
Ezh1-/-
LacZ
Neo
B
% Allelic Expression
100
80
60
40
20
0
Paternal
Maternal
Rnf12
Atrx
G6pdx
Pdha1

Figure 3.7

Figure 3.7. EZH1 does not contribute to the initiation of imprinted X-chromosome inactivation.

A. Schematic of our *Ezh1* mutation (see chapter 2 for details).

B. Pyrosequencing quantifications of allele-specific RT-PCR for *Ezh2*$^{fl/fl}$*;Ezh1*$^{-/-}$ and *Ezh2*$^{m-/-z;-/-}$*;Ezh1*$^{-/-}$ blastocysts. Graphs represent averages + or – SEM from two or more biological replicates for each of the four X-linked genes *Atrx* (two *WT* and six Mutant), *Rnf12* (three *WT* and six Mutant), *G6pdx* (three *WT* and two Mutant) and *Pdha1* (two *WT* and six Mutant) for both *Ezh2*$^{fl/fl}$*;Ezh1*$^{-/-}$ and *Ezh2*$^{m-/-z;-/-}$;*Ezh1*$^{-/-}$. Maternal (active X-chromosome) allelic expression is in blue and paternal (inactive X-chromosome) allelic expression is in red.
p-values for each gene: *Rnf12*: 0.623585177 , *Atrx*: 0.405801495, *G6pdx*: 0.04318522 and *Pdha1*: 0.76748389; Welch's two sample t-test.

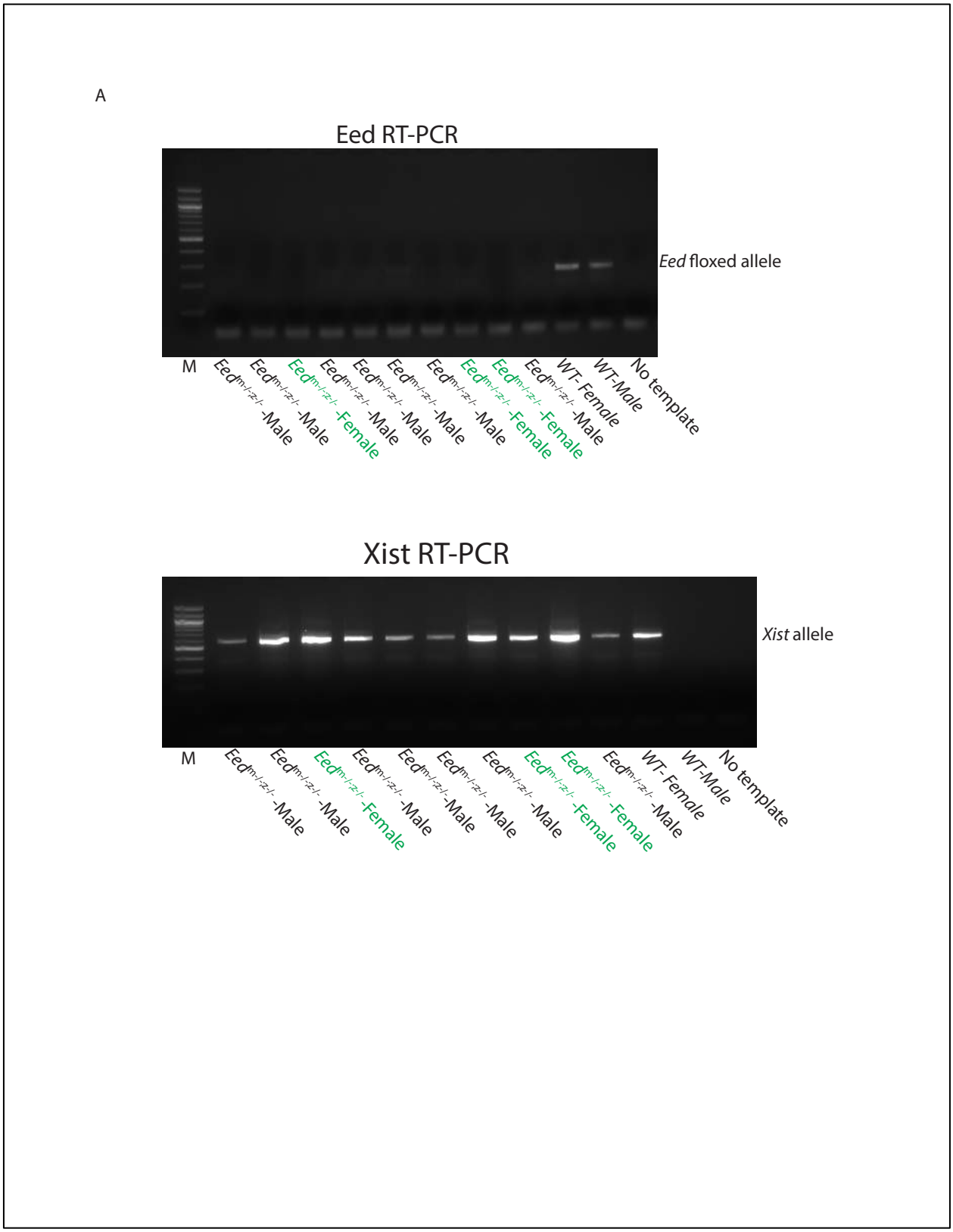
A
Eed RT-PCR
Eed floxed allele
M
Eed^fl-/-z-/- -Male
Eed^fl-/-z-/- -Male
Eed^fl-/-z-/- -Female
Eed^fl-/-z-/- -Male
Eed^fl-/-z-/- -Male
Eed^fl-/-z-/- -Male
Eed^fl-/-z-/- -Female
Eed^fl-/-z-/- -Female
Eed^fl-/-z-/- -Male
WT- Female
WT-Male
No template
Xist RT-PCR
Xist allele
M
Eed^fl-/-z-/- -Male
Eed^fl-/-z-/- -Male
Eed^fl-/-z-/- -Female
Eed^fl-/-z-/- -Male
Eed^fl-/-z-/- -Male
Eed^fl-/-z-/- -Male
Eed^fl-/-z-/- -Male
Eed^fl-/-z-/- -Female
Eed^fl-/-z-/- -Female
Eed^fl-/-z-/- -Male
WT- Female
WT-Male
No template

Figure 3.8

Figure 3.8. EED is critical for the proper initiation of imprinted X-chromosome inactivation.

A. Genotyping RT-PCR gel image for *WT* and *Eed*$^{m-/-;z-/-}$ blastocysts. Eed RT-PCR is on the left, with genotypes and band noted. Xist RT-PCR is on the right with genotypes, sex, and band noted. *Eed*$^{m-/-;z-/-}$ females are highlighted in green. M=Marker, 100 bp ladder.

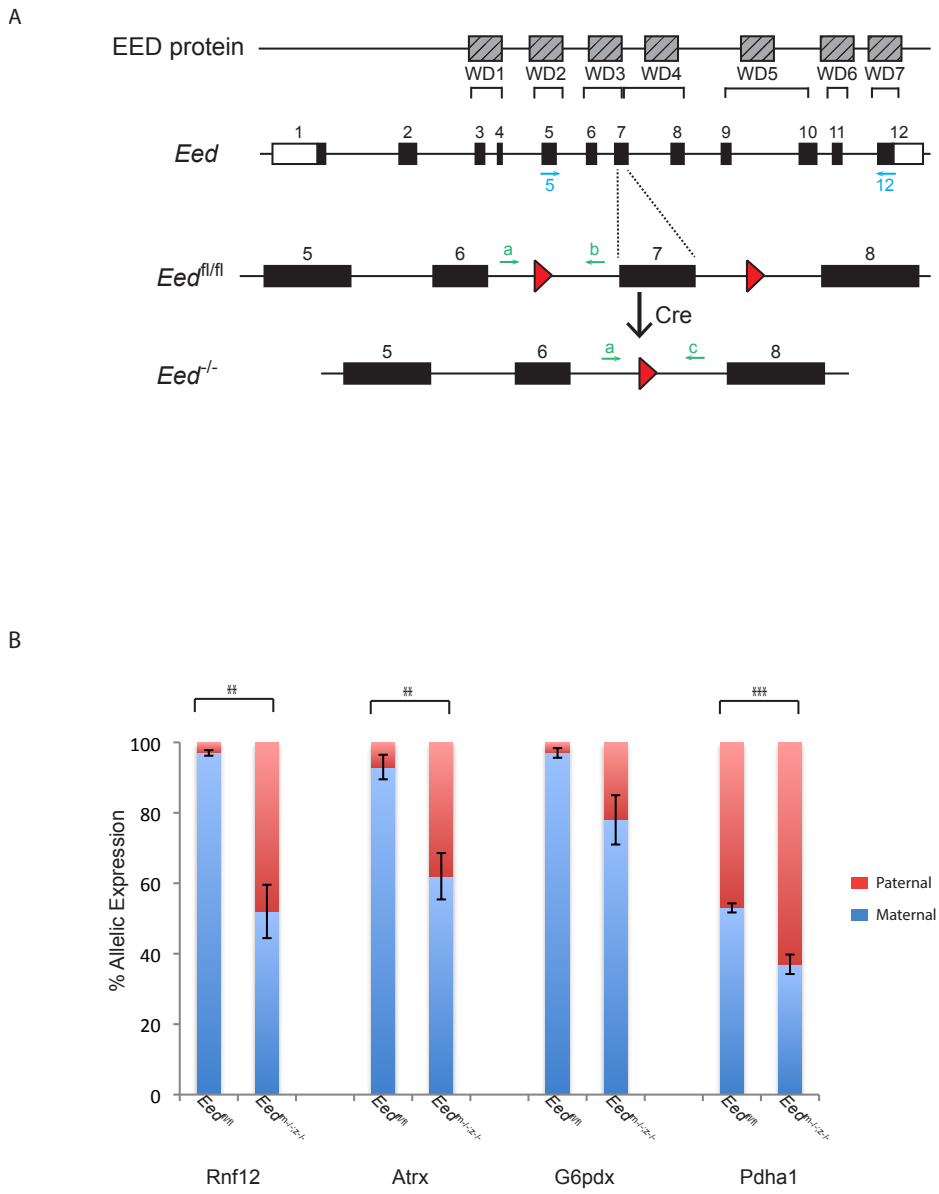
A
EED protein
WD1
WD2
WD3
WD4
WD5
WD6
WD7
Eed
1
2
3
4
5
6
7
8
9
10
11
12
5
12
Eed fl/fl
5
6
a
b
7
8
Cre
Eed -/-
5
6
a
c
8
B
##
##
###
100
80
60
40
20
0
% Allelic Expression
Paternal
Maternal
Eed fl/fl
Eed fl/+;Zp3-/-
Rnf12
Atrx
G6pdx
Pdha1

Figure 3.9

Figure 3.9. EED is critical for the proper initiation of imprinted X-chromosome inactivation.

A. Schematic of our *Eed* mutation (see chapter 2 for details).

B. Pyrosequencing quantifications of allele-specific RT-PCR for $Eed^{fl/fl}$ and $Eed^{m-/-;z-/-}$ blastocysts. Graphs represent averages + or – SEM from two or more biological replicates for each of the four X-linked genes *Atrx* (six *WT* and six Mutant), *Rnf12* (six *WT* and six Mutant), *G6pdx* (six *WT* and two Mutant), and *Pdha1* (six *WT* and six Mutant) for both $Eed^{fl/fl}$ and $Eed^{m-/-;z-/-}$. Maternal (active X-chromosome) allelic expression is in blue and paternal (inactive X-chromosome) allelic expression is in red.
p-values for each gene: ***Rnf12*: 0.00194847, ***Atrx:* 0.00385306, *G6pdx*: 0.21194848, and *Pdha1*: ***0.00010971; Welch's two sample t-test (**p-value less than 0.01, ***p-value less than 0.001).

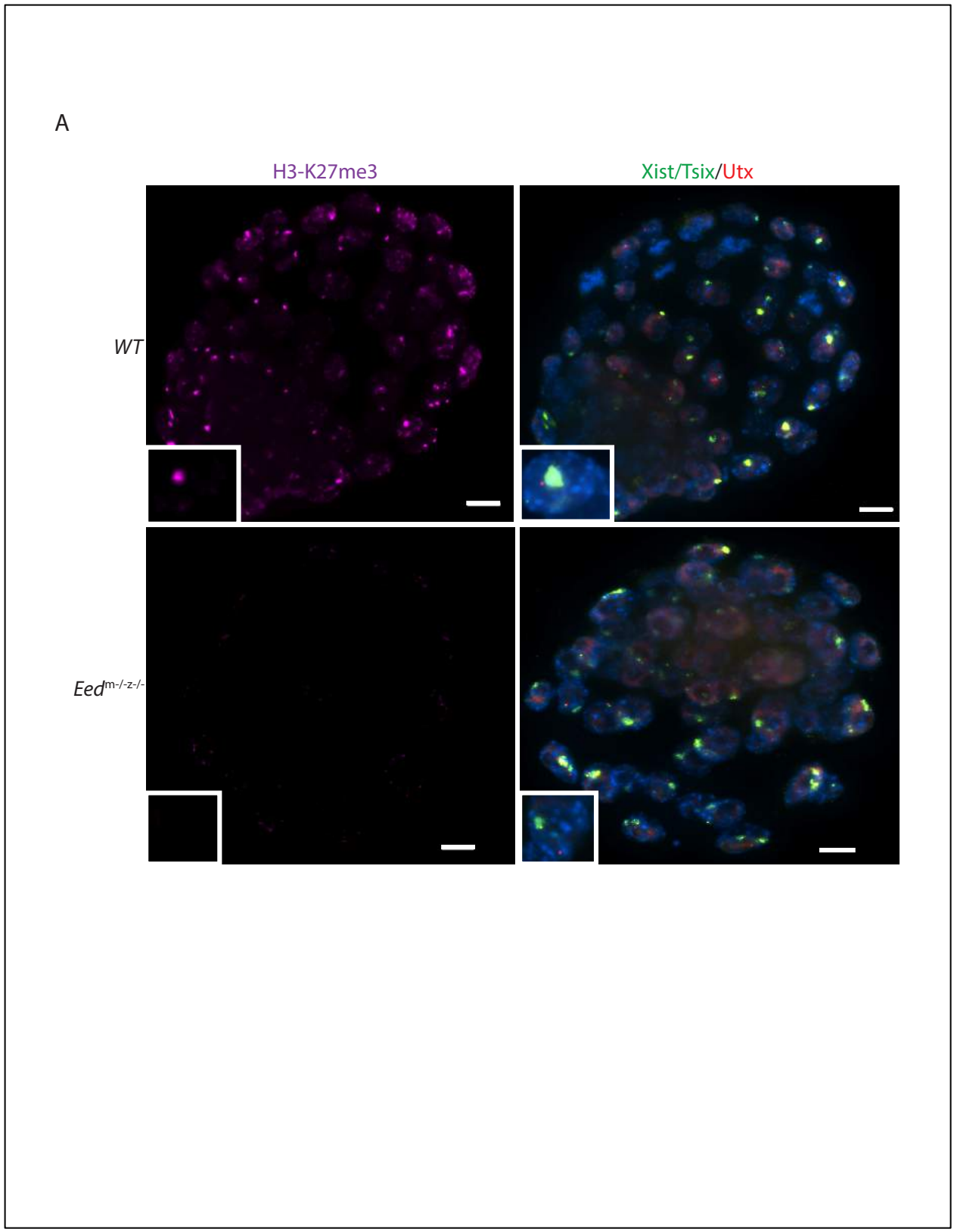

Figure 3.10

Figure 3.10. Xist RNA enriches on the inactive-X in *Eed*$^{m-/-;z-/-}$ blastocysts.

A. Representative immunofluorescence detection of H3-K27me3 followed by RNA-FISH detection of Xist RNA on the inactive X-chromosome and nascent expression of an X-linked gene, *Utx*, in *WT* and *Eed*$^{m-/-;z-/-}$ embryos. Top row is a *WT* embryo where H3-K27me3 and Xist RNA enriches on the inactive-X, while the bottom row represents an *Eed*$^{m-/-;z-/-}$ embryo where H3-K27me3 does not enrich but Xist RNA does enrich on the inactive-X. H3-K27me3 is in purple, Xist RNA is in green, and Utx RNA is in red. Representative inset nucleus at bottom right of each panel. Two biological replicates were performed. Nuclei stained with DAPI. Scale bar is 10 μm.

Table 3.1

Ezh2$^{fl/-}$ x *Ezh2*$^{fl/fl}$;*Stra8-Cre* Crosses

	With EZH2 and H3-K27me3 Enrichment	Without EZH2 and H3-K27me3 Enrichment	Total
Observed	8	12	20
Expected	10	10	20

Chi-square value: 0.404, at alpha=0.05, p-value: 0.525

20 E3.5 blastocysts were dissected out of *Ezh2*$^{fl/-}$ x *Ezh2*$^{fl/fl}$;*Stra8-Cre* crosses. If maternal EZH2 suffices to enrich on the inactive-X in *Ezh2*$^{-/-}$ (just zygotically null) embryos, then all embryos are expected to have EZH2 (and H3-K27me3) enrichment regardless of *Ezh2* zygotic genotypic status. However, I observed that roughly 50% of embryos do not have EZH2 and H3-K27me3 enrichment. This means that the enrichment of EZH2 and H3-K27me3 on the inactive-X I am observing must result from zygotic expression of EZH2 in the blastocyst, as 50% of embryos from this cross are expected to be *Ezh2*$^{fl/-}$. No statistically significant difference was observed between genotypes, Chi-square test, p-value: 0.525.

Table 3.2

Ezh2$^{fl/fl}$;*Ezh1*$^{-/-}$ x *Ezh2*$^{fl/fl}$;*Ezh1*$^{-/-}$ Breeding Tabulation

	Male	Female	Total
Observed	50	48	98
Expected	49	49	98

Chi-square value: 0.0204, at alpha=0.05, p-value: 0.8864

Liveborns were tabulated and sex ratios were assessed for any sex distortion ratios in *Ezh2*$^{fl/fl}$;*Ezh1*$^{-/-}$ x *Ezh2*$^{fl/fl}$;*Ezh1*$^{-/-}$ crosses. 16 litters were tabulated. Average litter size was 6.125 mice per litter. No statistically significant difference was observed, Chi-square test, p-value: 0.8864

References

Avner, P., and Heard, E. (2001). X-chromosome inactivation: counting, choice and initiation. Nature Rev. Genet. *2*, 59–67.

Bernstein, E., Duncan, E.M., Masui, O., Gil, J., Heard, E., and Allis, C.D. (2006). Mouse polycomb proteins bind differentially to methylated histone H3 and RNA and are enriched in facultative heterochromatin. Mol. Cell. Biol. 26, 2560–2569.

Beutler E., Yeh, M., and Fairbanks, V.F. (1962). The normal human female as a mosaic of X-chromosome activity: studies using the gene for C-6-PD-deficiency as a marker. Proc Natl Acad Sci U S A *48*, 9–16.

Bouniol, C., Nguyen, E., and Debey, P. (1995). Endogenous transcription occurs at the 1-cell stage in the mouse embryo. Exp Cell Res. *218(1)*, 57-62.

Brown, C.J., Hendrich, B.D., Rupert, J.L., Lafrieniere, R.G., Xing, Y., Lawrence, J., and Willard, H.F. (1992). The Human XIST Gene: Analysis of a 17 kb Inactive X-Specific RNA that Contains Conserved Repeats and is Highly Localised within the Nucleus. Cell *71*, 527-542.

Cao, R., Wang, L., Wang, H., Xia, L., Erdjument-Bromage, H., Tempst, P., Jones, R.S., and Zhang, Y. (2002). Role of histone H3 lysine 27 methylation in Polycomb-group silencing. Science *298*, 1039–1043.

Cao, Q., Wang, X., Zhao, M., Yang, R., Malik, R., Qiao, Y., Poliakov, A., Yocum, A.K., Li, Y., Chen, W., Cao, X., Jiang, X., Dahiya, A., Harris, C., Feng, F.Y., Kalantry, S., Qin, Z.S., Dhanasekaran, S.M., and Chinnaiyan, A.M. (2014). The Central Role of EED in the Orchestration of Polycomb Group Complexes. Nat. Commun. *5*, 3127.

Chan, K.M., Zhang, H., Malureanu, L., van Deursen, J., and Zhang, Z. (2011). Diverse factors are involved in maintaining X chromosome inactivation. Proc. Natl. Acad. Sci. U.S.A. *108*, 16699–16704.

Cho T, et al. (2002). Involvement of chromatin structure in the regulation of mouse zygotic gene activation.Animal Science Journal. *73(2)*, 113–122.

Clemson, C.M., Meneil, J.A., Willard, H.F., and Lawrence, J.B. (1996). XIST RNA paints the inactive X-chromosome at interphase evidence for a novel RNA involved in nuclear/chromosome structure. J. Cell Biol. *132*, 259-275

Corbel, C, Diabangouaya, P, Gendrel, AV, Chow, JC, and Heard, E. (2103). Unusual chromatin status and organization of the inactive X chromosome in murine trophoblast giant cells. Development. *140*, 861-872.

Czermin, B., Melfi, R., McCabe, D., Seitz, V., Imhof, A., and Pirrotta, V. (2002). Drosophila enhancer of Zeste/ESC complexes have a histone H3 methyltransferase activity that marks chromosomal Polycomb sites. Cell *111*, 185–196.

Denisenko, O., Shnyreva, M., Suzuki, H., and Bomsztyk, K. (1998). Point mutations in the WD40 domain of Eed block its interaction with Ezh2. Mol. Cell. Biol. *18*, 5634–5642.

Di Croce, L., and Helin, K. (2013) Transcriptional regulation by Polycomb group proteins. Nat. Struct. Mol. Biol. *20*, 1147–1155.

Dobin, A., Davis, C.A., Schlesinger, F., Drenkow, J., Zaleski, C., Jha, S., Batut, P., Chaisson, M., and Gingeras, T.R. (2013). STAR: ultrafast universal RNA-seq aligner. Bioinformatics *29*, 15–21.

Eicher, E.M., Nesbitt, M.N., and Francke, U. (1972). Cytological identification of the chromosomes involved in Searle's translocation and the location of the centromere in the X chromosome of the mouse. Genetics *71*, 643–648.

Erhardt, S., Su, I.-H., Schneider, R., Barton, S., Bannister, A.J., Perez-Burgos, L., Jenuwein, T., Greenfield, A., Carrel, L., Pennisi, D., Philippe, C., Quaderi, N., Siggers, P., Steiner, K., Tam, P.P., Monaco, A.P., Willard, H.F., and Koopman, P. (1998). The Utx gene escapes X-inactivation in mice and humans. Hum. Mol. Genet. *7(4)*, 737-42.

Greenfield, A., Carrel, L., Pennisi, D., Philippe, C., Quaderi, N., Siggers, P., Steiner, K., Tam, P.P., Monaco, A.P., Willard, H.F., and Koopman, P. (1998). The UTX gene escapes X inactivation in mice and humans. Hum. Mol. Genet. *7(4)*, 737-42.

Han, Z., Xing, X., Hu, M., Zhang, Y., Liu, P., and Chai, J. (2007). Structural basis of EZH2 recognition by EED. Structure *15*, 1306–1315.

Herz, H.M., Garruss, A., and Shalatifard, A. (2013). SET for life: biochemical activities and biological functions of SET domain-containing proteins. Trends Biochem Sci. *8(12)*, 621-39.

Jonkers, I., Monkhorst, K., Rentmeester, E., Grootegoed, JA., Grosveld, F., and Gribnau, J. (2008). Xist RNA is confined to the nuclear territory of the silenced X-chromosome throughout the cell cycle. Mol. Cell Biol. *28*, 5583-5594.

Kalantry, S., Mills, K.C., Yee, D., Otte, A.P., Panning, B., and Magnuson, T. (2006a). The Polycomb group protein Eed protects the inactive X-chromosome from differentiation-induced reactivation. Nat. Cell Biol. *8*, 195–202.

Kalantry, S. and Maguson, T. (2006b). The Polycomb protein EED is dispensable for the initation of random X-chromosome inactivation. PLoS Genet. *2(5)*, e66.

Kalantry, S., Purushothaman, S., Bowen, R.B., Starmer, J., and Magnuson, T. (2009). Evidence of Xist RNA-independent initiation of mouse imprinted X-chromosome inactivation. Nature *460*, 647–651.

Karachentsev, D., Sarma, K., Reinberg, D., and Steward, R. (2005). PR-Set7-dependent methylation of histone H4 Lys 20 functions in repression of gene expression and is essential for mitosis. Genes Dev. *19*, 431–435.

Kay, G.F., Barton, S.C., Surani, M. A., and Rastan, S. (1994). Imprinting and X-chromosome counting mechanisms determine Xist expression in early mouse development. Cell. *77*, 639-650.

Keane, T.M., Goodstadt, L., Danecek, P., White, M.A., Wong, K., Yalcin, B., Heger, A., Agam, A., Slater, G., Goodson, M., et al. (2011). Mouse genomic variation and its effect on phenotypes and gene regulation. Nature *477*, 289–294.

Kerppola, TK. (2009). Polycomb group complexes--many combinations, many functions. Trends Cell Biol. 19(12):692-704.

Kuzmichev, A., Nishioka, K., Erdjument-Bromage, H., Tempst, P., and Reinberg, D. (2002). Histone methyltransferase activity associated with a human multiprotein complex containing the Enhancer of Zeste protein. Genes Dev. *16*, 2893–2905.

Lee, J. T. (2000). Disruption of imprinted X inactivation by parent-of-origin effects at Tsix. Cell *103*, 17–27.

Lewandoski, M., Wassarman, K.M., and Martin , G.R. (1997). Zp3-cre, a transgenic mouse line for the activation or inactivation of loxP-flanked target genes specifically in the female germ line. Curr Biol. *7(2)*, 148-51.

Lewis, E. B. (1978) A gene coplex controlling segmentation in *Drosophila*. Nature. *7*;*276(5688)*, 565-70.

Love, M.I., Huber, W., and Anders, S. (2014). Moderated estimation of fold change and dispersion for RNA-seq data with DESeq2. Genome Biol. *15*, 550.

Lyon, M.F. (1961). Gene action in the X-chromosome of the mouse (Mus musculus L.). Nature *190*, 372–373.

Mak, W., Baxter, J., Silva, J., Newall, A.E., Otte, A.P., and Brockdorff, N. (2002). Mitotically stable association of polycomb group proteins eed and enx1 with the inactive x chromosome in trophoblast stem cells. Curr. Biol. *12(12)*, 1016-20.

Mak, W., Nesterova, T.B., de Napoles, M., Appanah, R., Yamanaka, S., Otte, A.P., and Brockdorff, N. (2004). Reactivation of the paternal X chromosome in early mouse embryos. Science *303*, 666–669.

Marahrens, Y., Panning, B., Dausman, J., Strauss, W., and Jaenisch, R. (1997). Xist-deficient mice are defective in dosage compensation but not spermatogenesis. Genes Dev. *11(2),* 156-66.

Margueron, R., Li, G., Sarma, K., Blais, A., Zavadil, J., Woodcock, C.L., Dynlacht, B.D., and Reinberg**,** D. (2008). EZH2 and EZH1 maintain repressive chromatin through different mechanisms. Mol Cell. *32(4)*, 503-18.

Margueron, R., Justin, N., Ohno, K., Sharpe, M.L., Son, J., Drury, W.J., Voigt, P., Martin, S.R., Taylor, W.R., De Marco, V., et al. (2009). Role of the polycomb protein EED in the propagation of repressive histone marks. Nature *461*, 762–767.

Margueron, R., and Reinberg, D. (2011). The Polycomb complex PRC2 and its mark in life. Nature *469*, 343–349.

Mayer, W., Niveleau, A., Walter, J., Fundele, R., and Haaf, T. (2000). Embryogenesis: Demethylation of the zygotic paternal genome. Nature *403*, 501-502.

McKeon, J., and Brock, H.W. (1991). Interactions of the Polycomb group of genes with homeotic loci of Drosophila. Roux's Arch. Dev. Biol. *199*, 387–396.

Montgomery, N.D., Yee, D., Chen, A., Kalantry, S., Chamberlain, S.J., Otte, A.P., and Magnuson, T. (2005). The murine polycomb group protein Eed is required for global histone H3 lysine-27 methylation. Curr. Biol. *15*, 942–947.

Müller, J., Hart, C.M., Francis, N.J., Vargas, M.L., Sengupta, A., Wild, B., Miller, E.L.,

Ng, J., Hart, C.M., Morgan, K. and Simon, J.A. (2000). A Drosophila ESC-E(Z) protein complex is distinct from other polycomb group complexes and contains covalently modified ESC. Mol. Cell. Biol. *20*, 3069−3078.

Okamoto, I., Otte, A.P., Allis, C.D., Reinberg, D., and Heard, E. (2004). Epigenetic dynamics of imprinted X inactivation during early mouse development. Science *303*, 644–649.

Penny, G.D., Kay, G.F., Sheardown, S.A., Rastan, S., and Brockdorff, N. (1996). Requirement for Xist in X chromosome inactivation. Nature *379(6561)*, 131-7.

Peschon, J.J., Behringer, R.R., Brinster, R.L., Palmiter, R.D. (1987). Spermatid-specific expression of protamine 1 in transgenic mice. Proc Natl Acad Sci U.S.A. *84*, 5316–5319.

Pirrotta, V. (1997). PcG complexes and chromatin silencing. Curr. Opin. Genet. Dev. *7*, 249–258.

Pirrotta, V. (1998). Polycombing the genome: PcG, trxG, and chromatin silencing. Cell *93*, 333−336.

Plath, K., Fang, J., Mlynarczyk-Evans, S.K., Cao, R., Worringer, K.A., Wang, H., la Cruz, de, C.C., Otte, A.P., Panning, B., and Zhang, Y. (2003). Role of histone H3 lysine 27 methylation in X inactivation. Science *300*, 131–135.

Ragunathan, K., Jih, G., and Moazed, D. (2015). Epigenetics. Epigenetic inheritance uncoupled from sequence-specific recruitment. Science *348*, 1258699.

Rastan, S (1983). Non-random X-chromosome inactivation in mouse X-autosome translocation embryos–location of the inactivation centre. J Embryol. Exp. Morphol. *78*, 1–22.

Rastan, S., Brown, S.D. (1990) The search for the mouse Xchromosome inactivation centre. Genet Res *56*, 99–106.

Sadate-Ngatchou, P.I., Payne, C.J., Dearth, A.T., and Braun, R.E. (2008). Cre recombinase activity specific to postnatal, premeiotic male germ cells in transgenic mice. Genesis. *46(12)*, 738-42.

Sado, T., Wang, Z., Sasaki, H. and Li, E. (2001). Regulation of imprinted X-chromosome inactivation in mice by Tsix. Development 128, 1275–1286.

Schuettengruber, B., Chourrout, D., Vervoort, M., Leblanc, B., and Cavalli, G. (2007). Genome regulation by polycomb and trithorax proteins. Cell *128*, 735‑745.

Shao, Z. et al. (1999). Stabilization of chromatin structure by PRC1, a Polycomb complex. Cell *98*, 37−46.

Shen, X., Liu, Y., Hsu, Y.J., Fujiwara, Y., Kim, J., Mao, X., Yuan, G.C., and Orkin, S.H. (2008). EZH1 mediates methylation on histone H3 lysine 27 and complements EZH2 in maintaining stem cell identity and executing pluripotency. Mol. Cell. *32(4)*, 491-502.

Silva, J., Mak, W., Zvetkova, I., Appanah, R., Nesterova, T.B., Webster, Z., Peters, A.H.F.M., Jenuwein, T., Otte, A.P., and Brockdorff, N. (2003). Establishment of histone h3 methylation on the inactive X chromosome requires transient recruitment of Eed-Enx1 polycomb group complexes. Dev. Cell *4*, 481–495.

Simon, J., Chiang, A., and Bender, W. (1992). Ten different Polycomb group genes are required for spatial control of the AbdA and AbdB homeotic products. Development *114*, 493–505.

Simon, J. (1995). Locking in stable states of gene expression: transcriptional control during Drosophila development. Curr. Opin. Cell Biol. *7*, 376–385.

Stavropoulos, N., Lu, N., and Lee, J.T. (2001). A functional role for Tsix transcription in blocking Xist RNA accumulation but not in X-chromosome choice. Proc Natl Acad Sci U.S.A. *289*8*(18)*, 10232-7.

Struhl, G. and Akam, M. (1985). Altered distributions of Ultrabithorax transcripts in extra sex combs mutant embryos of Drosophila. EMBO J. *4*, 3259– 3264

Sun, B.K., Deaton, A.M., and Lee, J.T. (2006). A transient heterochromatic state in Xist preempts X inactivation choice without RNA stabilization. Mol Cell. *21(5)*, 617-28.

Takada, T., Ebata, T., Noguchi, H., Keane, T.M., Adams, D.J., Narita, T., Shin-I, T., Fujisawa, H., Toyoda, A., Abe, K., et al. (2013). The ancestor of extant Japanese fancy mice contributed to the mosaic genomes of classical inbred strains. Genome Res.

Takagi, N., and Sasaki, M. (1975). Preferential inactivation of the paternally derived X chromosome in the extraembryonic membranes of the mouse. Nature *256*, 640–642.

Takagi, N., Wake, N., and Sasaki, M. (1978). Cytologic evidence for preferential inactivation of the paternally derived X chromosome in XX mouse blastocysts. Cytogenet. Cell Genet. *20*, 240–248.

Takagi, N. (1980). Primary and secondary nonrandom X chromosome inactivation in early female mouse embryos carrying Searle's translocation T(X; 16)16H. Chromosoma *81*, 439–459.

Tie, F., Furuyama, T. and Harte, P.J. The Drosophila Polycomb Group proteins ESC and E(Z) bind directly to each other and co-localize at multiple chromosomal sites. Development *125*, 3483−3496.

Tie, F., Furuyama, T., Prasad-Sinha, J., Jane, E., and Harte, P.J. (2001). The Drosophila Polycomb Group proteins ESC and E(Z) are present in a complex containing the histone-binding protein p55 and the histone deacetylase RPD3. Development *128*, 275–286.

van der Vlag, J. and Otte, A.P. Transcriptional repression mediated by the human polycomb-group protein EED involves histone deacetylation. Nature Genet. *23*, 474−478 (1999).

Wang, H, Wang, L, Erdjument-Bromage, H, Vidal, M, Tempst, P, Jones, RS, Zhang, Y. (2004) Role of histone H2A ubiquitination in polycomb silencing. Nature *431*, 873–878.

Wang, J.1., Mager, J., Chen, Y., Schneider, E., Cross, J.C., Nagy, A., and Magnuson, T. (2001). Imprinted X inactivation maintained by a mouse Polycomb group gene. Nature Genet. 28, 371–375.

West, J.D., Frels, W.I., Chapman, V.M., and Papaioannou, V.E. (1977). Preferential expression of the maternally derived X chromosome in the mouse yolk sac. Cell *12*, 873–882.

West, J.D., Papaioannou, V.E., Frels, W.I., and Chapman, V.M. (1978). Preferential expression of the maternally derived X chromosome in extraembryonic tissues of the mouse. Basic Life Sci. *12*, 361–377.

Wiekowski, M., Miranda, M., and DePamphilis, M.L. (1993). Requirements for promoter activity in mouse oocytes and embryos distinguish paternal pronuclei from maternal and zygotic nuclei. Dev Biol. *159(1)*, 366-78.

Williams, L. H., Kalantry, S., Starmer, J. and Magnuson, T. (2011). Transcription precedes loss of Xist coating and depletion of H3K27me3 during X-chromosome reprogramming in the mouse inner cell mass. Development 138, 2049–2057.

Yalcin, B., Wong, K., Agam, A., Goodson, M., Keane, T.M., Gan, X., Nellåker, C., Goodstadt, L., Nicod, J., Bhomra, A., et al. (2011). Sequence-based characterization of structural variation in the mouse genome. Nature *477*, 326–329.

Zhang, T., Cooper, S., and Brockdorff, N. (2015). The interplay of histone modifications - writers that read. EMBO Rep.

Zhao, J., Sun, B.K., Erwin, J.A., Song, J.J., and Lee, J.T. (2008). Polycomb proteins targeted by a short repeat RNA to the mouse X chromosome. Science *322*(*5902*), 750-6.

Chapter 4

Unveiling a Differential Requirement for the Xist RNA and the *Xist* DNA In Imprinted Mouse X-Chromosome Inactivation

Abstract

Trophoblast stem cells (TSCs) are often used in X-chromosome inactivation research as an *ex vivo* model of imprinted X-inactivation. TSCs faithfully maintain exclusive silencing of the paternal X-chromosome. I showed in chapter 2 that *Eed*$^{-/-}$ TSCs, which are functionally null for EED due to deletion of exon 7, lose H3-K27me3 enrichment on the inactive-X. Moreover, EED and H3-K27me3 absence surprisingly abrogated Xist RNA coating on the inactive-X, despite an intact *Xist* locus. Such loss of epigenetic markers from the inactive-X strikingly did not lead to a broad defect in stable silencing of X-linked genes. Rather, I found that only a fraction of genes is upregulated in *Eed*$^{-/-}$ TSCs. Absence of a large-scale defect in X-linked gene silencing when Xist RNA is missing calls into question our understanding of the role of this lncRNA in X-inactivation. Xist RNA has long been believed to be necessary and sufficient for X-inactivation. I therefore generated and analyzed TSCs missing DNA corresponding to exons 1-3 of *Xist*, segments that when transcribed to RNA have been previously shown to be critical for silencing of X-linked genes. I found that every gene analyzed in *Xist*$^{+/-}$TSCs displayed defective silencing from the inactive-X vis-à-vis *Eed*$^{-/-}$ TSCs, where only a subset of these genes is affected. I have thus disentangled a differential role for the Xist RNA from that of the Xist DNA in X-chromosome inactivation. My data argue that the Xist RNA is not necessary to maintain broad

scale chromosome wide silencing of X-linked genes. Indeed, loss of the DNA leads to a more pronounced malfunction in transcriptional silencing of genes along the inactive X-chromosome. My discovery strongly suggests that the *Xist* DNA itself plays a more fundamental role in X-linked gene silencing. The *Xist* locus apparently functions in X-inactivation separately from producing Xist RNA.

Introduction

X-chromosome inactivation (X-inactivation) is a paradigmatic dosage compensation mechanism that occurs in order to equalize the X-linked gene dosage between XX female and XY male mammals (Lyon, 1961; Beutler et al., 1962). Through classical genetic experiments in both mouse and human, a segment of the X-chromosome, denoted the X-inactivation center (XIC), was found to be necessary and sufficient for X-inactivation (Eicher et al., 1972; Rastan et al., 1980 and1983; Takagi, 1980). Within the XIC lie two lncRNAs, Xist (X-inactive specific transcript) that is expressed from the inactive X-chromosome, and Tsix that is expressed from the active X-chromosome. Xist RNA physically coats in *cis,* the future inactive-X (Brown et al., 1992; Clemson et al., 1996; Jonkers et al., 2008). Tsix, however, is expressed in the antisense orientation to Xist and is thought to repress Xist induction from the active X-chromosome (Stavropoulos et al., 2001). Both of these long non-coding (lnc)RNAs are widely believed to be necessary and sufficient for X-inactivation (Marahrens et al., 1997; Penny et al., 1996; Stavropoulos et al., 2001). The mutual exclusivity with which these two transcripts are expressed also suggests that they are important players in establishing and perhaps maintaining the transcriptional fates of the X-chromosome from which they are transcribed (Marahrens et al., 1997; Penny et al., 1996; Kalantry et al., 2009; Stavropoulos et al., 2001; Avner and Heard,

2001). Thus, X-inactivation serves as a model system for understanding how epigenetic mechanisms occur broadly.

Two types of X-chromosome inactivation exist in the mouse, imprinted and random X-chromosome inactivation. Imprinted X-inactivation, exclusive silencing of the paternally inherited X-chromosome, occurs initially in all cells in the developing mouse embryo (Mak et al., 2004; Takagi et al., 1978; Kay, 1994). This form of X-inactivation is subsequently maintained in the extra-embryonic tissues of the embryo, the trophectoderm and the primitive endoderm lineages (Takagi and Sasaki, 1975; West et al., 1977; West et al., 1978). At peri-implantation, and subsequently post-implantation, cells within the inner cell mass will display a different pattern of X- chromosome inactivation (Mak et al., 2004). Random X-inactivation is unique to the epiblast precursors that ultimately become the embryo proper. At E4.5 these precursor cells will reactivate the paternal X-chromosome (Mak et al., 2004; Williams et al., 2011). These cells will then randomly choose to inactivate either the maternal-X or the paternal-X (Mak et al., 2004). Importantly, once one X-chromosome in a given nucleoplasm is chosen for inactivation, descendant cells will maintain that same X-chromosome as inactive through multiple mitotic divisions essentially for the lifetime of the organism. This stable and heritable transcriptional memory highlights a major facet of X-chromosome inactivation as a paradigm of epigenetic inheritance.

In the developing mouse embryo, a set of temporally distinct events occurs as imprinted X-inactivation is initiated and established. At the two-cell stage Xist RNA is transcribed. It will then physically coat in *cis,* the paternally inherited X-chromosome (the future inactive-X), at the four-cell stage; Xist RNA marks the inactive-X (Brown et al., 1992; Clemson et al., 1996; Jonkers et al., 2008). By the eight-cell stage, members of the Polycomb group of proteins (PcGs)

are found enriched coincident with Xist RNA on the inactive-X (Mak, 2002; Erhardt et al., 2003; Okamoto et al., 2004; Plath et al., 2003; Silva et al., 2003). As embryogenesis proceeds, these factors associate on the inactive-X while genes are being silenced along the inactive (paternal) X-chromosome. Tsix expression from the active (maternal) X-chromosome occurs concomitant with Polycomb protein enrichment and silencing of paternal X-linked genes on the future inactive X-chromosome (Lee, 2000; Sado et al., 2001). This pattern of X-inactivation, as well as the associated enrichment of the same epigenetic factors (Xist, H3-K27me3, etc.) along the inactive-X, is then maintained in the extra-embryonic tissue of the developing embryo. These embryogenic events are widely believed to be tightly linked to the initiation and maintenance of the appropriate pattern of X-inactivation in the developing embryo.

Functional studies of the Xist lncRNA have provided essential insight into the inner workings of X-chromosome inactivation. The observation that Xist RNA is induced and coats the X-chromosome from which it is transcribed strongly suggest that Xist RNA is a key player in X-linked gene silencing (Okamoto et al., 2004; Kalantry et al., 2009; Namekawa et al., 2010; Patrat et al., 2009; Mak et al., 2004; Rastan et al., 1982; MacMahon et al., 1983). To support this idea, embryos inheriting a paternal X-chromosome bearing an *Xist* mutation on the paternal-X die around post-implantation due to extra-embryonic developmental defects, including X-inactivation defects (Marahrens et al., 1997; Kalantry et al., 2009). The epiblast tissues in $Xist^{+/-}$ embryos were found to have biased random X-inactivation such that all embryonic derived cells possessed a WT inactive X-chromosome (Marahrens et al., 1997; Kalantry et al., 2009). Similar results were also obtained *in vitro* with mouse embryonic stem cells (mESCs) (Penny et al., 1996). Furthermore, we know that multicopy transgenes present on autosomes are sufficient to ectopically induce Xist expression (Wutz et al., 2002). Silencing, albeit to a variable degree, has

been additionally observed for genes in a spatial or proximity specific manner resulting from Xist induction from multicopy Xist transgenes (Lee et al., 1996). Based on these data, it is largely believed that Xist RNA is the epicenter of X-inactivation.

Although Xist RNA is thought to be necessary and sufficient for X-inactivation substantial evidence conversely suggests that Xist RNA is not the major focal point of X-inactivation. Mouse embryos inheriting a deletion for Xist on the paternal X-chromosome were found to still trigger silencing of X-linked genes during the pre-implantation phase of embryogenesis; although, these embryos do manifest a defect during the maintenance phase of imprinted X-inactivation after implantation (Kalantry et al., 2009). Furthermore, our lab has shown that loss of Xist RNA enrichment in an *Eed*$^{-/-}$ trophoblast stem cells (TSC) leads to a very modest paternal-X derepression phenotype, even when the cells are in an undifferentiated state (chapter 2). This is in contrast to a separate TSC line harboring a point mutation in the Polycomb protein EED (Kalantry et al., 2006). In this particular line, Xist RNA enrichment is still lost along the inactive-X, but the Kalantry et al. study showed that there is only a failure to maintain inactive-X silencing in *Eed*$^{-/-}$ extra-embryonic tissues upon trophoblast tissue differentiation. These differentiation-induced effects were recapitulated *in vivo*, utilizing *Gfp* transgene reporter expression as a readout for defective X-inactivation (Kalantry et al., 2006). Considering that only a subset of genes are derepressed upon Xist RNA loss in my *Eed*$^{-/-}$ TSCs prompted me to conclude that the Xist RNA is not strictly necessary for stable maintenance of the X-inactive state. There are likely other factors at work that are integral to the X-inactivation process.

Absence of a large-scale defect in X-linked gene silencing when Xist RNA is missing calls into question our understanding of the role of this lncRNA in X-inactivation. Xist RNA has long been believed to be necessary and sufficient for X-inactivation (Marahrens et al., 1997;

Penny et al., 1996). In light of the data from my *Eed*$^{-/-}$ TSCs (see chapter 2 above), the Xist RNA is not necessary for broadly propagating gene silencing along the inactive-X. I therefore tested the hypothesis that *Xist* DNA, separate from transcription of the Xist RNA, serves a greater role in X-inactivation. I generated and analyzed TSCs missing DNA corresponding to exons 1-3 of *Xist*, segments, when transcribed to RNA, have been previously shown to be crucial for silencing of X-linked genes (Marahrens et al., 1997; Penny et al., 1996). I found that every gene analyzed in *Xist*$^{+/-}$ TSCs displayed defective silencing (i.e. derepression) on the inactive-X vis-à-vis *Eed*$^{-/-}$ TSCs, where only a subset of these genes is affected. This is a strong paradigm shift; it changes how we perceive the role of the Xist RNA in X-inactivation. These data argue that the Xist RNA is not necessary to maintain broad scale chromosome-wide silencing of X-linked genes. Indeed, mutation of the DNA leads to a more pronounced loss of transcriptional inactivation of genes along the inactive X-chromosome. My discovery strongly suggests that the *Xist* DNA itself plays a more essential role in X-linked gene silencing, separate from its role in generating the Xist RNA.

Results

Strategy for functionally distinguishing Xist RNA from *Xist* DNA in imprinted X-inactivation

To gain insight into a potential disparity between the Xist RNA and the *Xist* DNA in imprinted X-chromosome inactivation, I derived a TSC line, one where the paternally inherited Xist allele possesses loxP sites flanking exons 1 and 3 of *Xist* (*Xist*$^{+/fl}$) (Figure 4.1). I already know that loss of Xist RNA enrichment (despite any genomic lesion at the Xist locus) in my *Eed*$^{-/-}$ TSCs (see chapter 2 above) does not affect every X-linked gene (Figure 4.1, see chapter 2 above). *Atrx*, one X-linked gene, is among the genes that are not subject to a derepressive

phenotype when Xist RNA enrichment is gone in *Eed*$^{-/-}$ TSCs (Figure 4.1). If the DNA is more critical, I hypothesized that *Xist*$^{+/-}$ TSCs will display derepression of *Atrx*. Much, if not all, of what is previously concluded about Xist function in X-inactivation is exclusively attributed to the Xist RNA, even if loss of function of the RNA results from an *Xist* DNA mutation. To test my hypothesis that the *Xist* DNA itself is more crucial to the X-inactivation process, I infected my *Xist*$^{+/fl}$ cells with an Adeno-Cre viral construct (to convert *Xist*$^{+/fl}$ to *Xist*$^{+/-}$) and asked whether loss of Xist RNA through *Xist* DNA mutation phenocopies loss of Xist RNA through *Eed* mutation (Figure 4.1).

Atrx is derepressed in *Xist*$^{+/-}$ TSCs

Upon attempting to obtain a pure population of *Xist*$^{+/-}$ TS cells, after much effort, I was unsuccessful in establishing a constitutive line. Over several rounds of simultaneous Adeno-Cre (or Lenti-Cre) transduction and subsequent subcloning the *Xist*$^{-}$ allele eventually disappeared among the *Xist*$^{+}$ and *Xist*^{fl} alleles. This indicates that *Xist*$^{+/-}$ cells that are effectively mutated for the paternally inherited *Xist* allele are ultimately lost. I resorted to a transient method by which I could hopefully capture enough *Xist*$^{+/-}$ cells and ascertain a role for *Xist* DNA in X-inactivation. To optimize this, I developed and optimized a time course experimental strategy to pinpoint the range during which Cre delivery through Adeno-Cre transduction yielded a substantial proportion of *Xist*$^{+/-}$ TSCs among *Xist*$^{+/fl}$ TSCs. This is outlined in Figure 4.2. At roughly 30-48 hours post transduction, I achieved a fairly high rate of Cre mediated excision of the *Xist* floxed allele (*Xist*$^{+/fl}$ conversion to *Xist*$^{+/-}$). I quantified this deletion efficiency on a single nucleus level by exploiting RNA-FISH detection of Xist RNA enrichment, or lack thereof, on the inactive-X. To gauge the effect on X-linked gene silencing at these time points, I carried out simultaneous Xist RNA-FISH (to pick out mutant from WT cells due to loss of Xist RNA) in tandem with

RNA-FISH detection of Atrx. I found that there were a substantially higher proportion of cells biallelic for Atrx when exposed to Cre compared to cells not transduced with Cre (Figure 4.2). Furthermore, I noticed that there were two broad categories of cells in my samples, cells that were biallelic for Atrx and absent for Xist RNA coating of the inactive-X, as well as cells that were biallelic for Atrx but continued to harbor Xist RNA enrichment. The former category of cells (Figure 4.2A) were vastly lower in relative population number compared to the latter (Figure 4.2B); however, both categories of cells (biallelic for Atrx) were significantly higher in absolute population number in the samples transduced with Adeno-Cre compared to cells that were not transduced (Figure 4.2). These data suggest that cells effectively deleted for *Xist* exons 1-3 are unable to maintain silencing of Atrx, a divergent result from cells that lose just Xist RNA (i.e. no derepression of Atrx in $Eed^{-/-}$ TSCs). That Xist RNA continues to enrich on the inactive-X in cells biallelic for Atrx is indicative of the insufficiency with which Xist RNA coating actively contributes to gene silencing. My data therefore strongly suggest that the Xist RNA is neither broadly necessary nor is it sufficient to stably maintain silencing of X-linked genes. Continued presence of the Xist RNA coat in cells biallelic for Atrx may simply signify that Xist RNA molecules have a long half-life, an idea that has been entertained previously (Yamada et al., 2015).

$\underline{Xist^{+/-}}$ <u>TSCs exhibit a broader derepressive phenotype compared to $Eed^{-/-}$ TSCs</u>

To gauge the effect of my Xist mutation on X-linked gene silencing more broadly, I carried out additional RNA-FISH experiments to detect Xist and nascent transcription of 3 other X-linked genes, *Rnf12*, *Pdha1*, and *Pgk1*. Compared to mock transduced TSCs, cells infected with Adeno-Cre for 48 hours displayed a significantly higher proportion of cells that lacked Xist RNA enrichment and were biallelic for each of the four genes analyzed (Figure 4.3). Importantly,

the genes *Atrx*, *Rnf12*, *Pdha1*, and *Pgk1,* all exhibited a much higher degree of derepression from the inactive X-chromosome in Cre treated versus mock treated $Xist^{+/fl}$ TS cells. This is in stark contrast to my $Eed^{-/-}$ TSCs that only display derepression of *Pgk1*, while *Atrx*, *Rnf12*, and *Pdha1* remain tightly silenced vis-à-vis $Eed^{fl/fl}$ TSCs (chapter 2). Of note, I still observed substantial number of nuclei biallelic for Atrx, Rnf12, Pdha1, and Pgk1, which still possessed Xist RNA accumulation on the inactive-X (data not shown). Nevertheless, continued Xist RNA at the inactive-X in these cells was not sufficient to maintain silencing of X-linked genes (data not shown). These data argue that Xist RNA loss simply is not equivalent to an *Xist* DNA lesion. Previously thought to be necessary and sufficient for X-chromosome inactivation, the Xist RNA is suggestively not as critical for silencing as is the *Xist* DNA itself. And until now, prior studies investigating Xist have attributed X-inactivation defects (or lack thereof) to functional loss of only the RNA, even if exons 1-3 of the *Xist* DNA are mutated (Marahrens et al., 1997; Penny et al., 1996). I have unequivocally shown that loss of RNA through *Xist* DNA mutation is considerably more detrimental to X-inactivation compared to just loss of RNA through *Eed* mutation. My data highlight the true importance of the *Xist* DNA in X-inactivation and further exemplify *Xist* exons 1-3 as a key source of genomic material that is crucial for proper X-linked gene silencing. Further investigation will uncover any additional element(s) that may lie within exons 1-3 of *Xist* as well as the involvement of these DNA segments in X-chromosome inactivation.

Discussion

Here I showed that the Xist RNA is not functionally equivalent to that of the *Xist* DNA in imprinted mouse X-chromosome inactivation. In chapter 2, my $Eed^{-/-}$ TSCs tell me that Xist RNA loss is not strictly necessary to maintain an X-inactive state. Only a fraction of genes are

upregulated when Xist RNA is missing. Furthermore this implies that *Eed*$^{-/-}$ TSCs can tolerate a higher dose of X-linked genes resulting from inactive-X upregulation, as these cells are fully competent in their replication abilities. However, the above data from my *Xist*$^{+/fl}$ transiently transduced TSCs illustrate that if the *Xist* DNA (exons 1-3) is deleted, the previously inactivated X-chromosome suffers a more dire fate. That 4 times as many genes are affected in *Xist*$^{+/-}$ TSCs compared to *Eed*$^{-/-}$ TSCs is indicative of an essential role for *Xist* DNA itself in X-linked gene silencing, one which readily supersedes the role of the Xist RNA. The exons that are deleted in our conditional mutation (exons 1-3) likely play vital roles in X-inactivation. Perhaps these genomic regions serve as docking sites for chromatin remodeling factors or other lncRNAs, which in turn positively influence the X-inactivation process. Or perhaps exons 1-3 house independent functional transcriptional units that act separately from Xist RNA to bring about stable silencing of X-linked genes. Along those lines, our lab identified such a different lncRNA. Xist-AR (Xist Activating RNA) is transcribed from *Xist* exon 1 in the antisense orientation to Xist exclusively from the inactive X-chromosome (Sarkar et al., 2015). Xist-AR has been shown to positively regulate Xist RNA levels both *in vivo* and *in vitro* (Sarkar et al., 2015). Furthermore, Sarkar et al. show evidence that loss of function of Xist-AR is sufficient to lead to defective X-linked gene silencing *in vivo*. These data highlight that there are important factors intimately entangled within *Xist* DNA that act upstream of *Xist* to positively influence Xist RNA expression and ultimately X-inactivation. Further experiments will indicate the true extent to which Xist-AR is encompassed in the regulation of Xist and its associated transient heterochromatic state (Sun et al., 2006). For example, if Xist-AR is deleted (as performed by Sarkar et al., 2015), to what extent is the enrichment of repressive chromatin marks, such as H3-K27me3 and H2AK119ub1,

affected on the inactive-X? My data implicate additional features of the *Xist* locus, yet to be discovered, which contribute to X-inactivation independently of Xist RNA.

Conclusion

In this study, I conclude that *Xist* DNA is more integral to the X-inactivation process whereas the Xist RNA is largely dispensable. Taken together, my data strongly suggest that loss of Xist RNA through *Eed* mutation does not greatly affect the X-inactive state, whereas loss of Xist RNA through functional deletion of *Xist* DNA more broadly abrogates X-linked gene silencing. This RNA-DNA dichotomy highlights the fundamental difference of these two molecules in X-chromosome inactivation, something of which has remained enigmatic until my work. Future molecular biology and bioinformatics experiments with my *Xist* mutation will uncover the extent to which my observed derepressive phenotype applies to the entire paternal X-chromosome. Moreover, future work will reveal additional key players in the X-inactivation process that are intimately intertwined within *Xist* exons 1-3.

Materials and Methods

Ethics Statement

This study was performed in strict accordance with the recommendations in the guide for the Care and Use of Laboratory Animals of the National Institutes of Health. All animals were handled according to protocols approved by the University Committee on Use and Care of Animals (UCUCA) at the University of Michigan (protocol #PRO00006455).

Mice

Mice harboring a conditional mutation in *Eed* were generated by the University of Michigan Transgenic Animal Model Core using $Eed^{tm1a(EUCOMM)Wtsi}$ targeted ES cells (EUCOMM). Briefly, ES cells were injected into blastocysts, and implanted into pseudo-pregnant females. Mice with high percentages of chimerism were bred and assessed for germline transmission. To generate homozygous *Eed* mutant mice harboring polymorphic X-chromosomes, first, male and female mice on a B6 *Mus musculus* background carrying the conditional mutant allele for *Eed* were intercrossed ($Eed^{fl/+}$ x $Eed^{fl/+}$) to achieve homozygosity. To obtain mice conditionally mutant for *Eed* and on the JF1 *Mus molossinus* divergent background, we bred $Eed^{fl/fl}$ males (B6 *Mus musculus* background) to *WT* JF1 *Mus molossinus* females. This gave us F1 hybrid $Eed^{fl/+}$ males that possessed an X-chromosome from the JF1 *Mus molossinus* background (X^{JF1}/Y). Such males were backcrossed to *WT* JF1 *Mus molossinus* females to derive $Eed^{fl/+}$ females that were a mix of B6 *Mus musculus* and JF1 *Mus molossinus* and also harbored two X-chromosomes from the JF1 *Mus molossinus* background (X^{JF1}/X^{JF1}). $Eed^{fl/+};X^{JF1}/X^{JF1}$ females were bred against $Eed^{fl/+};X^{JF1}/Y$ males to derive $Eed^{fl/fl};X^{JF1}/Y$ males. To obtain our female embryos used for TS cell

derivation, we crossed an *Eed*$^{fl/fl}$ female on the B6 *Mus musculus* background with an *Eed*$^{fl/fl}$ male that was a mix of B6 *Mus musculus* and JF1 *Mus molossinus* but possessed an X-chromosome from the JF1 *Mus molossinus* background (X^{JF1}/Y). The JF1/Ms strain has been described previously.

Xist$^{+/fl}$;X^{GFP}/Y *M. musculus* males (maintained on a 129 background) and JF1 *M. molossinus* females were bred in house and maintained by Clair Harris in the Kalantry lab.

TS Cell Derivation and Culture

Blastocysts were dissected out of pregnant mice 3.5 dpc and plated in four well dishes pre-seeded with mouse embryonic fibroblasts (MEFs). Hatched embryos were cultured in standard TS medium supplemented with 1.5x FGF4 and Heparin for 4-5 days until blastocyst outgrowths were of ideal size. Blastocysts were then trypsinized in 0.05% Trypsin-EDTA, neutralized with TS media supplemented with 1.5x FGF4 and Heparin, and cultured in 96 well dishes. Once lines were well established, XX/XY PCRs confirmed female lines and PCRs for *Eed* and *Xist* confirmed *Eed*$^{fl/fl}$;X^{Lab}/X^{JF1} and *Xist*$^{+/fl}$;X^{JF1}/X^{Lab} lines, respectively. Cell lines were then cultured in standard TS media supplemented with FGF4 and Heparin. RNA was harvested from TS cells using TRIzol (Invitrogen, #15596-018) and RT-PCR was performed as described below. For RNA-FISH, TS cells were split onto gelatin-coated glass coverslips and allowed to grow for 2-3 days. The cells were then permeabilized through sequential treatment with ice-cold cytoskeletal extraction buffer (CSK; 100 mM NaCl, 300 mM sucrose, 3 mM MgCl2, and 10 mM PIPES buffer, pH 6. 8) for 30 seconds, ice-cold CSK buffer containing 0.4% Triton X-100 (Fisher Scientific, #EP151) for 30 seconds, followed twice with ice-cold CSK for 30 seconds. After permeabilization, cells were fixed by incubation in 4% paraformaldehyde at room temperature

for 10 minutes. Cells were then rinsed three times each in 70% ethanol and stored in 70% ethanol at -20°C prior to RNA-FISH.

Generating Stable *Eed*$^{-/-}$ TSCs

Eed$^{fl/fl}$ TSCs were plated at a 1:24-1:48 dilution into six well dishes pre-seeded with MEFs and allowed to adhere until the next day. Cells were then transduced with Ad5-CMV-Cre (Adenovirus serotype type 5, University of Michigan Viral Vector Core adenoviral construct, 4 x 10^{12} particles/mL) at multiplicity of infection (MOI) of 1000. Once cell colonies were large enough following the initial transduction, they were subcloned into 96 well dishes pre-seeded with MEFs and re-transduced 24 hours later with Adeno-Cre at a MOI of 1000. Following this, expanded 96 well samples were split to six well dishes pre-seeded MEFs and again transduced 24 hours later. A portion of each 96 well samples was lysed for DNA genotyping to assess the efficiency of Cre-mediated deletion of the *Eed* floxed alleles. Subcloning, transduction, and genotyping procedures were repeated until a pure population of *Eed*$^{-/-}$ TSCs was achieved. *Eed*$^{-/-}$ TSCs were maintained in culture as described above.

Generating Transient *Xist*$^{+/-}$ TSCs

Xist$^{+/fl}$ TS cells were plated at a 1:24 dilution on gelatinized coverslips in six well dishes. Cells were transduced with Ad5-CMV-Cre viral vector at an MOI of 1000 for 12, 24, 30, and 48 hours. Cells adherent on the coverslips were then CSK-treated and fixed with 4% PFA and stored for immunofluorescence and/or RNA-FISH. The remaining adherent cells on the edges of each well of the six well dishes were washed once with 1 mL cold 1X PBS, followed by aspiration of PBS. Cells were then incubated in 1mL TRIzol at 4°C for 5 minutes. Lysates were stored in TRIzol at -80°C until RNA extraction.

RNA-FISH

Samples were dehydrated through room temperature ethanol series (five minutes each for 70%, 85%, 95%, and 100% ethanol). Coverslips were allowed to dry for 15 minutes at room temperature after the 100% ethanol wash, followed by hybridizing the samples overnight with the appropriate RNA-FISH probe. After the hybridization, samples were washed for seven minutes at 39°C, three times each in 2X SSC/50% formamide. This was followed by three-seven minute washes at 39°C in 2X SSC (1:100,000-1:200,000 dilution of DAPI added at third wash of 2X SSC), followed by two-seven minute washes at 39°C, in 1X SSC. Sample coverslips were then mounted onto glass microscope slides with Vectashield. Coverslips were sealed to the glass slides with clear nail polish.

PCR

For DNA isolation, cell pellets from TSCs were lysed in buffer composed of 50mM KCl, 10mM Tris-Cl (pH 8.3), 2.5mM $MgCl_2$, 0.1mg/ml gelatin, 0.45%NP-40, and 0.45% Tween-20. Cells in lysis buffer were incubated at 50^0C overnight, and then stored at 4^0C until use. Genomic PCR reactions were carried out in ChromaTaq buffer (Denville Scientific) with 1.5mM Magnesium Chloride using RadiantTaq DNA polymerase (Alkali Scientific, #C109).

Microscopy

Images of all stained samples were captured using a Nikon Eclipse TiE inverted microscope build with a Photometrics CCD camera. The images were analyzed after deconvolution using NIS-Elements software. All images were processed uniformly.

Statistical Analysis

All analyses utilized Welch's two sample t-tests. Significance level was set at α=0.05.

Table of Primers III
for Genotyping (G)

Xist 5LoxR_LW	ACC CTT GCC TTT TCC ATT TT	G
Xist3R_LW	CAC TGG CAA GGT GAA TAG CA	G
XpromL_LW	TTT CTG GTC TTT GAG GGC AC	G

Acknowledgements

I would like to thank Arushi Varshney for her assistance in the RNA-FISH experiments. I acknowledge her for her help in quantifying some of the coverslips for the four X-linked genes analyzed for their X-inactivation status in *Xist*$^{+/fl}$ mock and Adeno-Cre transduced TSCs.

I also wish to acknowledge the University of Michigan Animal Transgenics Core for injecting our targeted *Eed* ES cell constructs for generation of our *Eed*$^{fl/fl}$ mice. I also thank Clair Harris for breeding and maintaining the Eed$^{fl/fl}$, *Xist*$^{+/fl}$;*X*^{GFP}/*Y*, and JF1 mouse colonies.

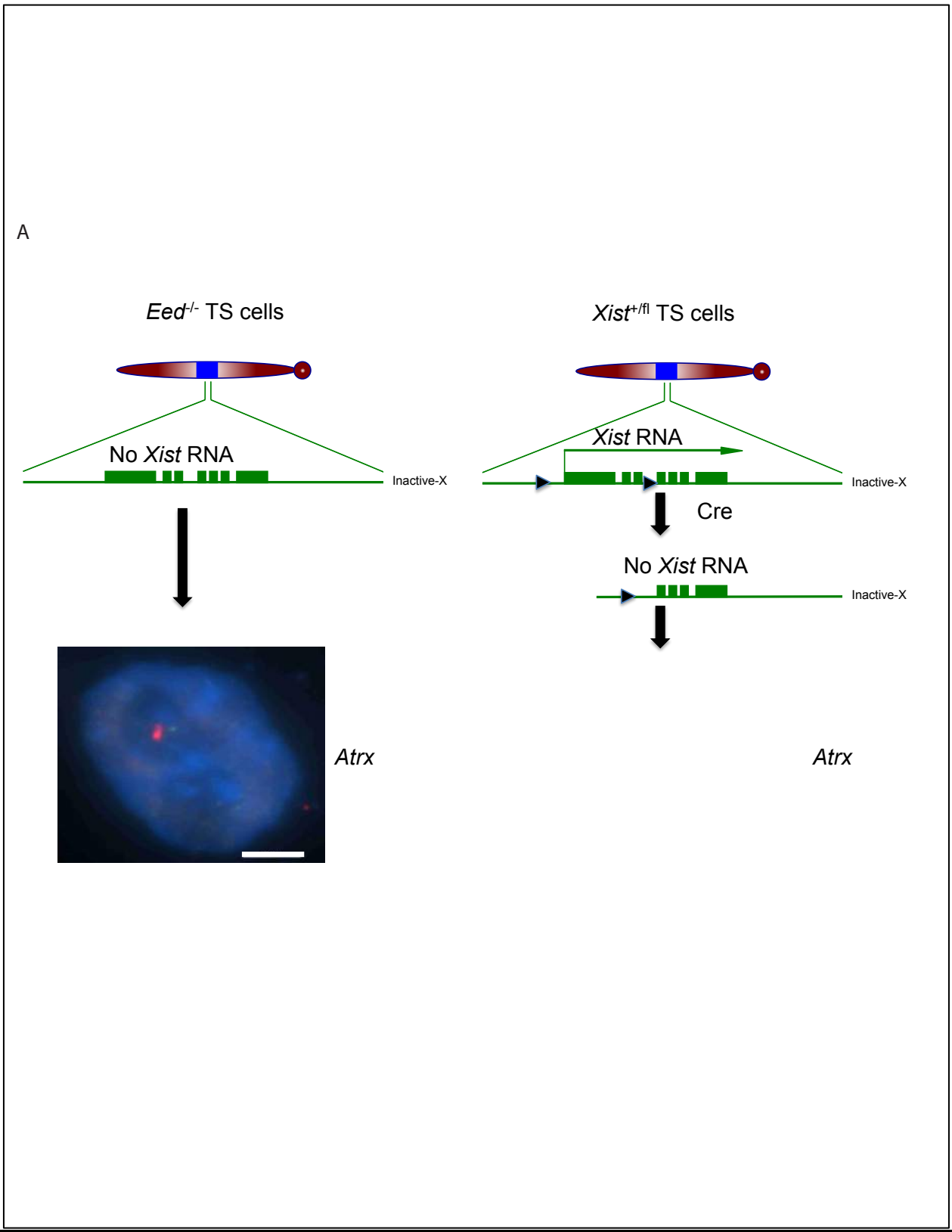
A
Eed-/- TS cells
No Xist RNA
Inactive-X
Atrx
Xist+/fl TS cells
Xist RNA
Inactive-X
Cre
No Xist RNA
Inactive-X
Atrx

Figure 4.1

Figure 4.1. Outline of rational for studying *Xist*$^{+/-}$ TSCs vis-à-vis *Eed*$^{-/-}$ TSCs

A. Left: *Xist* DNA, with exons 1 through 7 (left to right) illustrated. In *Eed*$^{-/-}$ TSCs, Xist transcription is severely diminished and the RNA does not coat in *cis* the inactive X-chromosome. However, only roughly 25% of genes are derepressed in *Eed* null TSCs, despite complete loss of Xist RNA enrichment. Shown here, *Atrx*, is one of the genes that is not affected. Right: To differentiate a role between the Xist RNA and the *Xist* DNA in X-chromosome inactivation, *Xist*$^{+/fl}$ TSCs were derived. Upon transduction with an Adeno-Cre construct, *Xist* exons 1-3 (flanked by loxP sites) are deleted. This results in loss of Xist RNA transcription and ultimately loss of Xist RNA coating of the inactive-X. The objective was to ascertain if loss of Xist RNA through *Xist* DNA mutation phenocopies loss of Xist RNA through *Eed* mutation.

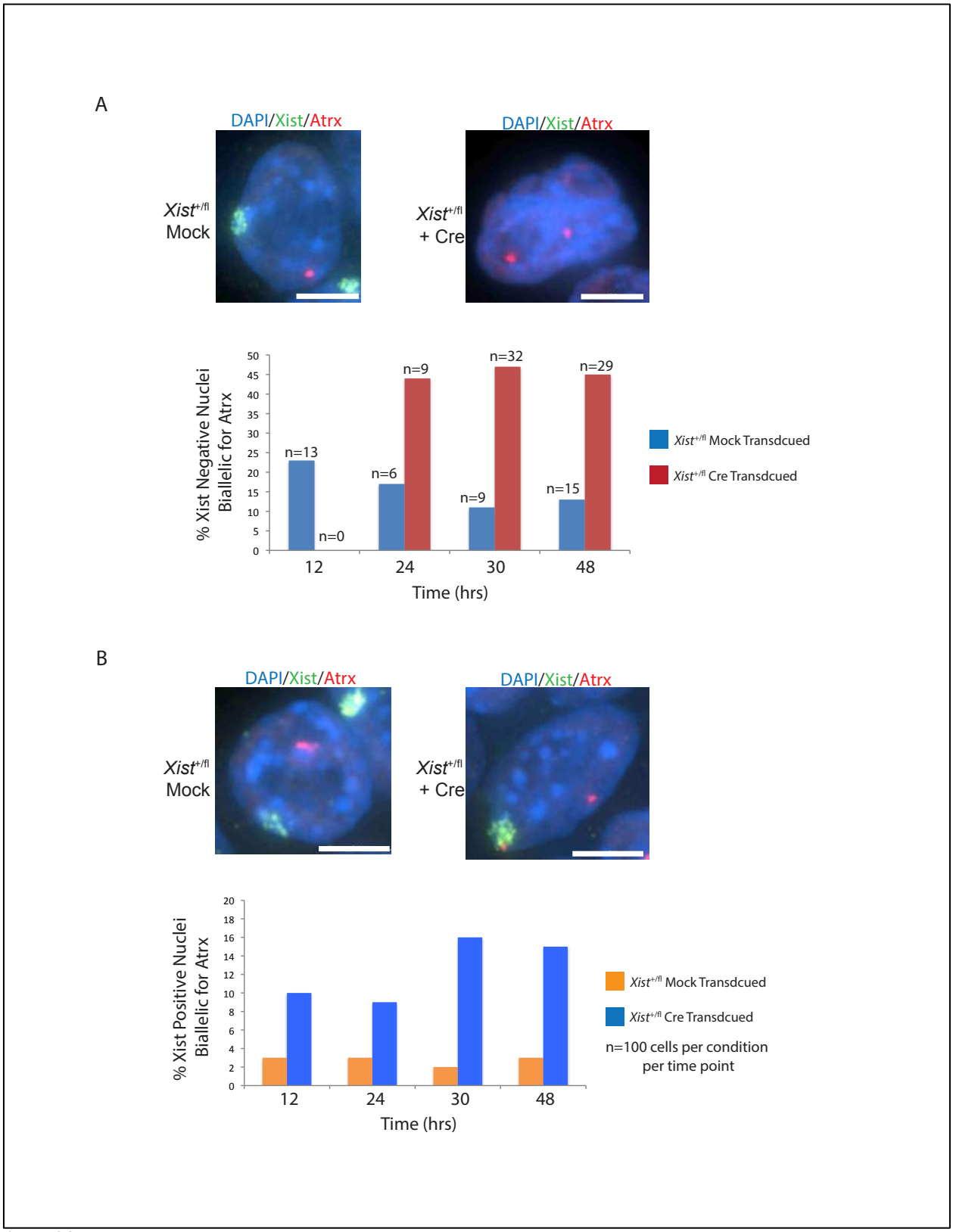
A
DAPI/Xist/Atrx
Xist+/fl
Mock
DAPI/Xist/Atrx
Xist+/fl
+ Cre
% Xist Negative Nuclei
Biallelic for Atrx
50
45
40
35
30
25
20
15
10
5
0
n=13
n=0
n=6
n=9
n=9
n=32
n=15
n=29
12
24
30
48
Time (hrs)
Xist+/fl Mock Transdcued
Xist+/fl Cre Transdcued
B
DAPI/Xist/Atrx
Xist+/fl
Mock
DAPI/Xist/Atrx
Xist+/fl
+ Cre
% Xist Positive Nuclei
Biallelic for Atrx
20
18
16
14
12
10
8
6
4
2
0
12
24
30
48
Time (hrs)
Xist+/fl Mock Transdcued
Xist+/fl Cre Transdcued
n=100 cells per condition
per time point

Figure 4.2

Figure 4.2. Transient transduction of *Xist*$^{+/fl}$ with Cre reveals derepression of *Atrx* and two classes of nuclei with respect to Xist RNA enrichment.

A. Top: Representative single nucleus panels of Mock and Cre transduced *Xist*$^{+/fl}$ TSCs. RNA-FISH for Xist is in green (but absence of Xist detection in mutant nuclei because such nuclei are Xist negative) and nascent transcription detection of Atrx in red. Nuclei stained blue with DAPI. Scale bar is 2μm.
Below: Quantifications of nuclei over a transient transduction time course. The % Xist negative nuclei with biallelic (derepressed) Atrx expression are plotted for Mock and Cre transduced cells for each of four time points, 12, 24, 30, and 48 hrs. Note n=total number Xist negative and biallelic Atrx nuclei observed on each coverslip for each time point.

B. Top: Representative single nucleus panels of Mock and Cre transduced *Xist*$^{+/fl}$ TSCs. RNA-FISH for Xist is in green and nascent transcription detection of Atrx in red. Nuclei stained blue with DAPI. Scale bar is 2μm.
Below: Quantifications of nuclei over a transient transduction time course. The % Xist positive nuclei with biallelic (de-repressed) Atrx expression are plotted for Mock and Cre transduced cells for each of four time points, 12, 24, 30, and 48 hrs. Note n=100 nuclei counted for Mock and Cre transduced cells for each of the four time points.

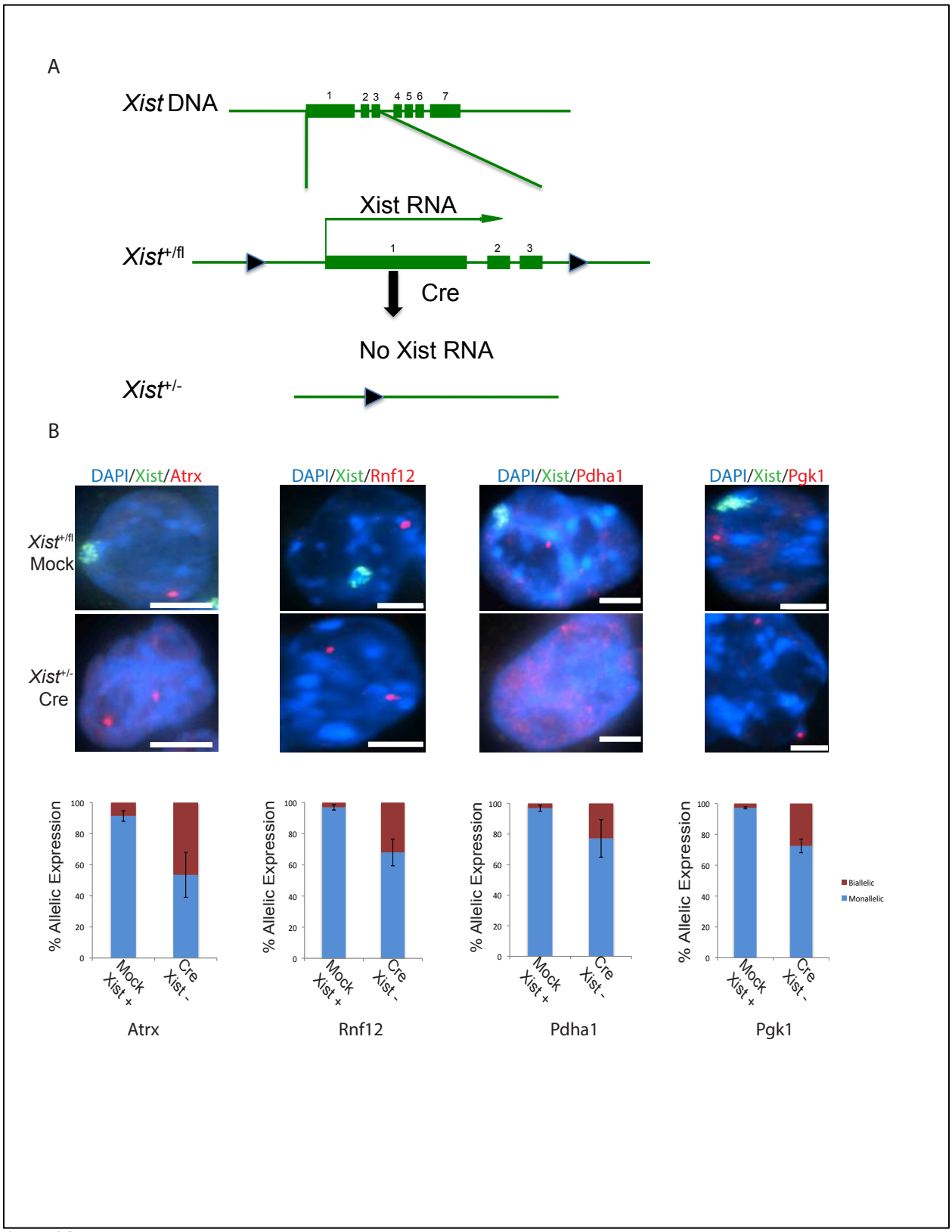
A
Xist DNA
1
2 3
4 5 6
7
Xist RNA
Xist+/fl
1
2
3
Cre
No Xist RNA
Xist+/-
B
DAPI/Xist/Atrx
DAPI/Xist/Rnf12
DAPI/Xist/Pdha1
DAPI/Xist/Pgk1
Xist+/fl Mock
Xist+/- Cre
% Allelic Expression
100
80
60
40
20
0
Mock Xist +
Cre Xist -
Atrx
Rnf12
Pdha1
Pgk1
Biallelic
Monallelic

Figure 4.3

Figure 4.3. Deletion of *Xist* exons 1-3 in $Xist^{+/fl}$ TSCs leads to derepression of genes that are not derepresssed in $Eed^{-/-}$ TSCs.

A. Outline of the Xist mutation as illustrated in Figure 4.1.

B. Representative single nuclei images of $Xist^{+/fl}$ TSCs with or without Cre transduction ($Xist^{+/fl}$ Mock, no Cre transduction; $Xist^{+/-}$ Cre, transduction with Adeno-Cre). RNA-FISH for Xist is in green and nascent transcription detection of X-linked genes in red. Nuclei stained blue with DAPI. Scale bar is 2µm. Four X-linked genes were assayed: *Atrx*, *Rnf12*, *Pdha1*, and *Pgk1*. Quantifications for each gene are below respective images.
For each gene: Mock represents the average percentage of nuclei out of an absolute total of 300 nuclei that were Xist positive; Cre represents the average percentage of nuclei out of a total of 300 nuclei that are Xist negative; relative allelic expressions are indicated as monoallelic in blue and biallelic in red. RNA-FISH experiments were performed after 48 hours of transient transduction. Averages + or – SD from three independent experiments (technical replicates) for each gene are plotted. 100 nuclei per transduction condition per replicate were counted.
p-value: *Atrx: 0.038934873, *Rnf12: 0.027040686, Pdha1: 0.12497886, *Pgk1: 0.010956774, Welch's two-sample t-test *(p-value less then 0.05).

References

Avner, P., and Heard, E. (2001). X-chromosome inactivation: counting, choice and initiation. Nature Rev. Genet. *2*, 59–67.

Beutler, E., Yeh, M., and Fairbanks, V.F. (1962). The normal human female as a mosaic of X-chromosome activity: studies using the gene for C-6-PD-deficiency as a marker. Proc. Natl. Acad. Sci. U.S.A. *48*, 9–16.

Brown, C.J., Hendrich, B.D., Rupert, J.L., Lafrieniere, R.G., Xing, Y., Lawrence, J., and Willard, H.F. (1992). The Human XIST Gene: Analysis of a 17 kb Inactive X-Specific RNA that Contains Conserved Repeats and is Highly Localised within the Nucleus. Cell *71*, 527-542.

Clemson, C.M., Meneil, J.A., Willard, H.F., and Lawrence, J.B. (1996). XIST RNA paints the inactive X-chromosome at interphase evidence for a novel RNA involved in nuclear/chromosome structure. J. Cell Biol. *132*, 259-275

Eicher, E.M., Nesbitt, M.N., and Francke, U. (1972). Cytological identification of the chromosomes involved in Searle's translocation and the location of the centromere in the X chromosome of the mouse. Genetics *71*, 643–648

Erhardt, S., Su, I.-H., Schneider, R., Barton, S., Bannister, A.J., Perez-Burgos, L., Jenuwein, T.,

Jonkers, I., Monkhorst, K., Rentmeester, E., Grootegoed, JA., Grosveld, F., and Gribnau, J. (2008). Xist RNA is confined to the nuclear territory of the silenced X-chromosome throughout the cell cycle. Mol. Cell Biol. *28*, 5583-5594.

Kalantry, S., Mills, K.C., Yee, D., Otte, A.P., Panning, B., and Magnuson, T. (2006). The Polycomb group protein Eed protects the inactive X-chromosome from differentiation-induced reactivation. Nat. Cell Biol. *8*, 195–202.

Kalantry, S., Purushothaman, S., Bowen, R.B., Starmer, J., and Magnuson, T. (2009). Evidence of Xist RNA-independent initiation of mouse imprinted X-chromosome inactivation. Nature *460*, 647–651.

Kay, G.F., Barton, S.C., Surani, M. A., and Rastan, S. (1994). Imprinting and X-chromosome counting mechanisms determine Xist expression in early mouse development. Cell 77, 639-650.

Lee, J. T. (2000). Disruption of imprinted X inactivation by parent-of-origin effects at Tsix. Cell 103, 17–27.

Lyon, M.F. (1961). Gene action in the X-chromosome of the mouse (Mus musculus L.). Nature *190*, 372–373.

Maclary, E., Hinten, M., Harris, C., Sethuraman, S., Kalantry, S. (2016). PRC2 prevents upregulation of genes with open chromatin architecture on the inactive X-chromosome. In preparation.

Mak, W., Baxter, J., Silva, J., Newall, A.E., Otte, A.P., Brockdorff, N. (2002). Mitotically stable association of polycomb group proteins eed and enx1 with the inactive x chromosome in trophoblast stem cells. Curr. Biol. *12(12)*, 1016-20.

Mak, W., Nesterova, T.B., de Napoles, M., Appanah, R., Yamanaka, S., Otte, A.P., and Brockdorff, N. (2004). Reactivation of the paternal X chromosome in early mouse embryos. Science *303*, 666–669.

Marahrens Y, Panning B, Dausman J, Strauss W, Jaenisch R. (1997). Xist-deficient mice are defective in dosage compensation but not spermatogenesis. Genes Dev. 11(2), 156-66.

Namekawa, S.H., Payer, B., Huynh, K.D., Jaenisch, R., and Lee, J.T. (2010). Two-step imprinted X inactivation: repeat versus genic silencing in the mouse. Mol. Cell Biol. *30*, 3187–205.

Okamoto, I., Otte, A.P., Allis, C.D., Reinberg, D., and Heard, E. (2004). Epigenetic dynamics of imprinted X inactivation during early mouse development. Science *303*, 644–649.

Patrat, C., Okamoto, I., Diabangouaya, P., Vialon, V., Le Baccon, P., Chow, J., and Heard, E. (2009). Dynamic changes in paternal X-chromosome activity during imprinted X-chromosome inactivation in mice. Proc. Natl. Acad. Sci. U.S.A. *106*, 5198–203.

Penny, G.D., Kay, G.F., Sheardown, S.A., Rastan, S., and Brockdorff, N. (1996). Requirement for Xist in X chromosome inactivation. Nature *379(6561)*, 131-7.

Plath, K., Fang, J., Mlynarczyk-Evans, S.K., Cao, R., Worringer, K.A., Wang, H., la Cruz, de, C.C., Otte, A.P., Panning, B., and Zhang, Y. (2003). Role of histone H3 lysine 27 methylation in X inactivation. Science *300*, 131–135.

Rastan, S (1983). Non-random X-chromosome inactivation in mouse X-autosome translocation embryos–location of the inactivation centre. J. Embryol. Exp. Morphol. *78*, 1–22

Rastan, S., and Brown, S.D. (1990). The search for the mouse Xchromosome inactivation centre. Genet. Res. *56*, 99–106.

Sado, T., Wang, Z., Sasaki, H. and Li, E. (2001). Regulation of imprinted X-chromosome inactivation in mice by Tsix. Development 128, 1275–1286.

Sarkar, M.K., Gayen, S., Kumar, S., Maclary, E., Buttigieg, E., Hinten, M., Kumari, A., Harris, C., Sado, T., and Kalantry, S. (2015). An Xist-activating antisense RNA required for X-chromosome inactivation. Nat. Commun. 6:8564. doi ,10.1038/ncomms9564.

Silva, J., Mak, W., Zvetkova, I., Appanah, R., Nesterova, T.B., Webster, Z., Peters, A.H.F.M., Jenuwein, T., Otte, A.P., and Brockdorff, N. (2003). Establishment of histone h3 methylation on the inactive X chromosome requires transient recruitment of Eed-Enx1 polycomb group complexes. Dev. Cell *4*, 481–495.

Stavropoulos, N., Lu, N., and Lee, J.T. (2001). A functional role for Tsix transcription in blocking Xist RNA accumulation but not in X-chromosome choice. Proc Natl Acad Sci U S A.

98(18), 10232-7.

Sun, B.K., Deaton, A.M., and Lee, J.T. (2006). A transient heterochromatic state in Xist preempts X inactivation choice without RNA stabilization. Mol Cell. *21(5)*, 617-28.

Takagi, N., and Sasaki, M. (1975). Preferential inactivation of the paternally derived X chromosome in the extraembryonic membranes of the mouse. Nature *256*, 640–642.

Takagi, N., Wake, N., and Sasaki, M. (1978). Cytologic evidence for preferential inactivation of the paternally derived X chromosome in XX mouse blastocysts. Cytogenet. Cell Genet. *20*, 240–248.

Takagi, N. (1980). Primary and secondary nonrandom X chromosome inactivation in early female mouse embryos carrying Searle's translocation T(X; 16)16H. Chromosoma *81*, 439–459.

West, J.D., Frels, W.I., Chapman, V.M., and Papaioannou, V.E. (1977). Preferential expression of the maternally derived X chromosome in the mouse yolk sac. Cell *12*, 873–882.

West, J.D., Papaioannou, V.E., Frels, W.I., and Chapman, V.M. (1978). Preferential expression of the maternally derived X chromosome in extraembryonic tissues of the mouse. Basic Life Sci. *12*, 361–377.

Williams, L. H., Kalantry, S., Starmer, J. and Magnuson, T. (2011). Transcription precedes loss of Xist coating and depletion of H3K27me3 during X-chromosome reprogramming in the mouse inner cell mass. Development 138, 2049–2057.

Wutz, A., Rasmussen, T.P., and Jaenisch, R. (2002). Chromosomal silencing and localization are mediated by different domains of Xist RNA. Nat. Genet. *30*, 167–74.

Yamada, N., Hasegawa, Y., Yue, M., Hamada, T., Nakagawa, S., and Ogawa, Y. (2015). *Xist* Exon 7 Contributes to the Stable Localization of Xist RNA on the Inactive X-Chromosome. PLoS Genet. *11(8)*.

Chapter 5

Discussion, Reflections, Future Directions, and Concluding Remarks

I have systematically compared the core components of Polycomb repressive complex 2 (PRC2) in imprinted mouse X-chromosome inactivation. By genetically dissecting the major subunits of PRC2, I gained insight into the true function of these proteins in propagating the X-inactive state. Furthermore, I illuminated a differential requirement for PRC2 proteins in triggering X-linked gene silencing in the early stage mouse embryo, something that has remained elusive until my work. Prior to my studies, a requirement for PRC2 in contributing to imprinted X-chromosome inactivation was ascribed to a simple observation that PRC2 components are found co-enriched on the inactive-X both in mouse trophoblast stem cells and cells of the early blastocyst stage mouse embryo (Plath et al., 2003; Silva et al., 2003). Many groups, including ours, therefore hypothesized that PRC2 proteins are necessary to execute and maintain imprinted X-linked gene silencing *in vitro* and *in vivo* (Plath et al., 2003; Silva et al., 2003; Kalantry et al., 2006). Through a systematic genetic approach, I elucidated the functions of PRC2 proteins with respect to imprinted X-chromosome inactivation. I found that there is not a genetic equivalency among the PRC2 proteins in propagating the X-inactive state. Based on my current data, I believe EZH2 and EZH1 are dispensable for maintaining X-inactivation, but EED is required to dampen expression of a fraction of genes along the inactive X-chromosome. These conclusions are similar to those drawn from my *in vivo* experiments. I find, based on my data and interpretations to date, that maternal EZH2 and EZH1 are not required for triggering silencing of X-linked genes

in the early mouse embryo. However, I note that maternally deposited EED is essential for inducing silencing of genes along the future inactive (paternal) X-chromosome. A requirement for maternal EED during the initiation phase of imprinted X-inactivation highlights a previously unidentified requisite for any maternally deposited epigenetic factor in triggering X-linked gene silencing, or more broadly any epigenetic state. Furthermore, a requirement for maternal EED protein sheds light on a transgenerational meiotic control of zygotic imprinted X-chromosome inactivation through an epigenetic factor, something that, as far as I know, has not been observed before. In the ensuing discussion, I describe my conclusions and interpretations of my data, I postulate alternative ways of understanding my observations, and I put forth future experiments and new research directions to gain further insight into Polycomb group protein control of imprinted X-chromosome inactivation.

A Comparative Analysis of Polycomb Repressive Complex 2 Proteins in Imprinted X-chromosome Inactivation: Mouse Trophoblast Stem Cells

In my first study, I evaluated the role of the Polycomb repressive complex 2 in mouse imprinted X-chromosome inactivation by utilizing an *ex vivo* model of imprinted X-chromosome inactivation, trophoblast stem cells (TSCs) (Oda et al., 2006). Furthermore, by dissecting apart PRC2 and individually investigating its core subunits, I ascertained a more complete understanding of the differential requirement for PRC2 proteins in X-inactivation. Previous work identified enrichment of Polycomb group proteins (PcGs) on the inactive-X *in vitro* (Plath et al., 2003; Silva et al., 2003; Kalantry et al., 2006). Given that PcGs enrich on the inactive–X during imprinted X-chromosome inactivation, I hypothesized that PcGs are required for proper X-linked gene silencing in TSCs.

First, I investigated the activity of EZH2, the major H3-K27me3 methyltransferase of PRC2 (Schuettengruber et al., 2007; Di Croce and Helin, 2013; Margueron and Reinberg, 2011; Zhang et al., 2015). In *Ezh2*$^{-/-}$ TSCs, I found that H3-K27me3 is still enriched on the inactive-X similar to *Ezh2*$^{fl/fl}$ TSCs. Moreover, X-linked gene silencing is unaffected in *Ezh2*$^{-/-}$ TSCs. In other words, *Ezh2*$^{-/-}$ TSCs displayed maintained silencing of their X-linked genes compared to *Ezh2*$^{fl/fl}$ TSCs. Such evidence of EZH2 independent maintenance of the inactive-X state suggests that other epigenetic factors are more important for the execution of X-inactivation. I hypothesized that continued catalysis of H3-K27me3 is occurring by a non-canonical PRC2 complex. To support this idea, I observed persistent EED enrichment, along with H3-K27me3, along the inactive-X in *Ezh2*$^{-/-}$ TSCs. EED is known to bind H3-K27me3 allosterically and further propagate H3-K27me3 catalysis (through EZH2) and enrichment on the inactive-X (Margueron and Reinberg, 2011). By all accounts, I believe that EZH2 is dispensable for imprinted X-chromosome inactivation in TSCs.

I next hypothesized that because EZH2 is dispensable for X-linked gene silencing, there must be factors that supplant the activities of EZH2 to properly carry out H3-K27me3 catalysis and X-inactivation. EZH1, the only other known H3-K27me3 mammalian homologue of EZH2, has previously been shown to compensate for loss of EZH2 in mouse embryonic stem cells and execute H3-K27me3 catalytic activity, although to a lesser extent (Shen et al., 2008). Importantly, I, and others, note that there is essentially no known phenotype for EZH1 loss. I observed extensively the normal capability of *Ezh1*$^{-/-}$ mice (and *Ezh2*$^{fl/fl}$;*Ezh1*$^{-/-}$ mice) to interbreed and yield litters of equal sex ratios (see chapter 3 Table 3.2). These mice furthermore can live a normal life span and are themselves fertile. These data would suggest that absence of EZH1 alone does not confer a defect in X-inactivation, further implying that EZH1 is not

necessary for X-inactivation. To assess a role for EZH1 in compensating for EZH2 loss in X-inactivation in TSCs, I generated *Ezh2*$^{-/-}$;*Ezh1*$^{-/-}$ TSCs and compared them to my parental *Ezh2*$^{fl/fl}$;*Ezh1*$^{-/-}$ cell line (and my *Ezh2*$^{-/-}$ TSCs). I found that absence of both EZH2 and EZH1, but not loss of EZH1 alone, led to H3-K27me3 enrichment depletion from the inactive-X. Surprisingly, in my *Ezh2*$^{-/-}$;*Ezh1*$^{-/-}$ TSCs, H3-K27me3 loss did not confer a defect in X-inactivation, as my RNA-FISH and allele-specific RT-PCR results indicated no derepression of X-linked genes from the inactive-X in *Ezh2*$^{-/-}$;*Ezh1*$^{-/-}$ TSCs vis-à-vis my parental *Ezh2*$^{fl/fl}$;*Ezh1*$^{-/-}$ TSCs (and my *Ezh2*$^{-/-}$ TSCs). To rule out sustained activity of PRC2 in X-inactivation, I further profiled these cells for EED enrichment. *Ezh2*$^{-/-}$;*Ezh1*$^{-/-}$ TSCs lose enrichment of EED at the inactive-X. These data argue that EED, and any conventional PRC2 complex, do not operate to silence genes on the inactive-X. This does not, however, exclude the possibility of EED participating with other repressive factors, which may transiently associate with the inactive-X to maintain X-linked gene silencing. Further experimentation will shed light on this alternate hypothesis.

To gauge whether Polycomb repressive complex 1 (PRC1) may be participating in gene silencing, I profiled my *Ezh2*$^{-/-}$;*Ezh1*$^{-/-}$ TSCs for inactive-X enrichment of H2A-K119ub1, the catalytic readout of PRC1 (Wang et al., 2004). *Ezh2*$^{-/-}$;*Ezh1*$^{-/-}$ TSCs do not display H2A-K119ub1 enrichment on the inactive-X, whereas *Ezh2*$^{fl/fl}$;*Ezh1*$^{-/-}$ TSCs do show H2A-K119ub1 enrichment. This suggests that PRC1 may not be an active player in X-inactivation, although this hypothesis requires systematic genetic evaluation of individual PRC1 proteins. Lack of H2A-K119ub1 enrichment in the absence of H3-K27me3 does however suggest that PRC1 works in tandem with PRC2 to lay down their respective histone marks at target loci, at least in the case of the inactive X-chromosome in mouse TSCs. The conventional model is that PRC2 deposits H3-

K7me3 via EZH2, which is then read by the CBX subunit of PRC1 (Margueron and Reinberg, 2011). In turn PRC1 catalyzes H2A-K119ub1 through Ring1B/A activity (Wang et al., 2004). Taking all of these data together, I conclude that gene silencing is occurring at the inactive-X in *Ezh2*$^{-/-}$;*Ezh1*$^{-/-}$ TSCs by a mechanism other than canonical PRC2 function and also potentially independent of PRC1 activity. To shed light on this hypothesis, I profiled my *Ezh2*$^{-/-}$;*Ezh1*$^{-/-}$ TSCs for H4K20me1 enrichment, a mark that is observed to coat the inactive-X in *WT* TSCs and one that has been associated with gene silencing (Kalakonda et al., 2008; Karachentsev et al., 2005; Kohlmaier et al., 2004). *Ezh2*$^{-/-}$;*Ezh1*$^{-/-}$ TSCs also do not harbor H4-K20me1 enrichment (compared to *Ezh2*$^{fl/fl}$;*Ezh1*$^{-/-}$ cells that do have H4-K20me1 foci on the inactive-X), indicating that this mark is not responsible for X-inactivation. More work will need to be performed, however, to address a true role for PRSET7, the enzyme that catalyzes H4-K20me1, in imprinted X-inactivation in mouse TSCs.

I also found that *Ezh2*$^{-/-}$*;Ezh1*$^{-/-}$ TSCs do not proliferate. Upon assaying the mitotic index of my cells with immunofluorescence detection of H3-S10p, I failed to observe any *Ezh2*$^{-/-}$;*Ezh1*$^{-/-}$ TSCs cells that were positive for phosphorylated H3-S10 foci, compared to roughly 30% of *Ezh2*$^{fl/fl}$;*Ezh1*$^{-/-}$ TSCs that do possess H3-S10p foci. This histone mark is well established as a marker of entry into G2 phase of the cell cycle (Hendzel et al., 1997). I conclude that *Ezh2*$^{-/-}$;*Ezh1*$^{-/-}$ TSCs are mitotically arrested, whereas *Ezh2*$^{fl/fl}$;*Ezh1*$^{-/-}$ TSCs can freely divide. Further investigation, including apoptosis assays, will uncover a potential combinatorial mechanistic role for EZH2 and EZH1 in trophoblast stem cell proliferation and survival.

Ezh2$^{-/-}$;*Ezh1*$^{-/-}$ TSCs also appear to a possess a more diffuse Xist staining pattern and have a smaller volume for their Xist domain at the inactive-X compared to *Ezh2*$^{fl/fl}$;*Ezh1*$^{-/-}$ TSCs. This implies that Xist RNA may in due course be completely lost from the inactive X-

chromosome in *Ezh2*$^{-/-}$;*Ezh*1$^{-/-}$ TSCs. I alternatively hypothesize that, although I did not observe a defect in X-linked gene silencing in my transient *Ezh2*$^{-/-}$;*Ezh1*$^{-/-}$ TSCs, eventual Xist RNA loss may inevitably result in an X-inactivation defect. However, as described above, I found that *Ezh2*$^{-/-}$;*Ezh1*$^{-/-}$ TSCs do not divide. Further experimentation and optimization (with a tamoxifen inducible system, for example) will need to be carried out to potentially derive a constitutive *Ezh2*$^{-/-}$;*Ezh1*$^{-/-}$ TS cell line to probe *Ezh2*$^{-/-}$;*Ezh1*$^{-/-}$ cells for defects in X-inactivation. Towards that end, I propose that if these cells were actually able to proliferate, a constitutive null cell line for *Ezh2* and *Ezh1* might display defects in X-inactivation. Such a defect would be in synchrony with what I observed with my *Eed*$^{-/-}$ TSCs (discussed below and previously reported, Kalantry et al., 2006; Maclary et al., 2016, in preparation). Instead, my observation that Xist RNA coat is smaller in *Ezh2*$^{-/-}$;*Ezh1*$^{-/-}$ TSCs may simply indicate that combined loss of EZH2 and EZH1 has a negative effect on the extent to which Xist RNA is tightly sequestered to the inactive-X. This relaxed association of Xist RNA need not ultimately result in complete Xist RNA removal from the inactive-X, nor must it result in loss of transcriptional silencing of X-linked genes. As my studies were done with a heterogeneous population of *Ezh2*$^{-/-}$;*Ezh1*$^{-/-}$ and *Ezh2*$^{fl/fl}$;*Ezh1*$^{-/-}$ cells, perhaps single cell qRT-PCR experiments would elucidate any negative effect, or lack thereof, on Xist expression when both EZH2/EZH1 are lost.

The third and final core PRC2 component I investigated was EED. EED is the "glue" of PRC2. Without EED, PRC2 does not form properly and core subunits are degraded (Montgomery et al., 2005). Defects in X-inactivation both *in vivo* and *in vitro* when EED is missing have been previously documented (Mak et al., 2004; Kalantry et al., 2006; Maclary et al., 2016, in preparation; discussed below). To more thoroughly investigate the role of EED in propagating the X-inactive state, I derived an *Eed*$^{-/-}$ from an *Eed*$^{fl/fl}$ line. My line is conditionally

deficient for exon 7, which encodes for a WD40 domain (#3) necessary for proper interaction with EZH2 (Denisenko et al., 1998; Han et al., 2007). Whereas the Kalantry et al. 2006 study concluded (using a point mutant for *Eed*) EED loss was only detrimental to cells upon differentiation of trophoblast tissues, I observed in my study a defect in X-inactivation in undifferentiated cells. It is possible that my mutant (deletion of exon 7) is more detrimental compared to an *Eed* point mutant. Our lab observed a non-differentiated induced loss of transcriptional repression of only a fraction of genes in $Eed^{-/-}$ TSCs (RNA-FISH and allele-specific RT-PCR in chapter 2; Maclary et al., 2016, in preparation). Together, these data are in contrast to a lack of an observed defect in X-linked gene silencing when *Ezh2* and/or *Ezh1* are deleted. It is therefore possible that EED complexes with other proteins to form a yet unidentified noncanonical PRC2 separate from the already known EZH1-containing noncanonical PRC2 complex (Margueron et al., 2008). Alternatively, EED interacts with other epigenetic factors outside of PRC2. Towards that end, our lab has participated in studies showing that EED binds with members of PRC1 (Cao et al., 2014). One hypothesis is that PRC1 is involved in X-inactivation through interaction with EED. However, my data suggest that PRC1 may perhaps not be involved in X-inactivation, as loss of H2A-K119ub1 is observed in both $Ezh2^{-/-};Ezh1^{-/-}$ and $Eed^{-/-}$ TSCs. It remains to be fully known, though, if PRC1 components themselves are genetically required for proper X-inactivation in TSCs. Further genetic experiments will elucidate a more complete role for PRC1 components in X-linked gene silencing. To interrogate additional histone marks that enrich on the inactive-X, I profiled H4-K20me1 in my $Eed^{-/-}$ TSCs vis-à-vis my $Eed^{fl/fl}$ TSCs. I found that my $Eed^{-/-}$ TSCs also lack H4-K20me1 inactive-X enrichment, further discounting a potential role for PRSET7 in imprinted X-chromosome inactivation. Loss of multiple PRC2/PRC1 associated components, PRC2 as well as

PRC1 catalyzed histone modifications, and other inactive-X-associated repressive histone marks do indeed imply that the majority of X-linked genes are continually and tightly silenced by some other epigenetic factor(s). Future work will unravel the key players in X-inactivation and, in turn, disclose novel mechanisms of X-chromosome inactivation.

Based on my current data, I propose that EZH2/EZH1 and EED are genetically distinct in terms of their requirement for X-chromosome condensation and X-linked gene silencing in mouse TSCs. Absence of a defect in *Ezh2*$^{-/-}$ and *Ezh2*$^{-/-}$;*Ezh1*$^{-/-}$ TSCs but an observed upregulation of a fraction of genes in *Eed*$^{-/-}$ TSCs also highlights a mechanism independent of H3-K27me3/canonical PRC2 activity in X-linked gene silencing. I believe that EED loss leads to loss of the transiently induced heterochromatinization of the inactive-X, which is paradoxically thought to be important in Xist transcriptional activation and subsequent inactivation of the paternal X-chromosome (Sun et al., 2006; Zhao et al., 2008). Indeed, I lose associated repressive chromatin marks as well as Xist RNA enrichment concomitant with severely diminished Xist RNA induction in *Eed*$^{-/-}$ TSCs. In turn, EED and Xist RNA absence led to upregulation of a select set of genes along the inactive-X. This is in stark contrast to *Ezh2*$^{-/-}$ or *Ezh2*$^{-/-}$;*Ezh1*$^{-/-}$ TSCs, which, according to my data, both display continued Xist RNA coating and harbor an inactive X-chromosome (based on the genes analyzed to date). However, due to the transient nature of our *Ezh2*$^{-/-}$;*Ezh1*$^{-/-}$ double mutant cells, Xist RNA may eventually be lost from the inactive-X, as I note that the Xist RNA coats in *Ezh2*$^{-/-}$;*Ezh1*$^{-/-}$ TSCs appear more diffuse and less voluminous versus the robust and compact coating of the Xist domain in *Ezh2*$^{fl/fl}$;*Ezh1*$^{-/-}$ TSCs. Leisured RNA loss may signify unavoidable derepression in *Ezh2*$^{-/-}$;*Ezh1*$^{-/-}$ TSCs; although, this may never be fully observed, as my current *Ezh2*$^{-/-}$;*Ezh1*$^{-/-}$ cell line does not divide indefinitely. If in the future we are somehow able to achieve a constitutively *Ezh2*$^{-/-}$;*Ezh1*$^{-/-}$ TSC line, derepression may be

observed once Xist has had sufficient time to vacate the inactive-X in *Ezh2*$^{-/-}$;*Ezh1*$^{-/-}$ cells. Alternatively, then, combined EZH2 and EZH1 loss is similar to EED loss. To understand why there is a defect in X-linked gene silencing when ultimately Xist RNA is absent, I speculate that loss of Xist RNA in *Eed*$^{-/-}$ TSCs perturbs interaction among several major players implicated in X-inactivation. Thus, silencing may be maintained in part by the multitude of epigenetic factors recently found to interact with Xist RNA (Chan et al., 2011; Chu et al., 2015; McHugh et al., 2015; Minajigi et al., 2015; Minkovsky et al., 2015; Moindrot et al., 2015; Monfort et al., 2015). Future studies will disentangle the extent to which other epigenetic factors are involved in stable silencing of X-linked genes in mouse trophoblast stem cells. Such further experimentation will in turn elucidate the potential additional mechanism(s) that must operate to silence the majority of X-linked genes.

Future Directions

I report that EZH2 and EZH1 are observably dispensable for imprinted X-chromosome inactivation, whereas EED is necessary to maintain silencing of a subset of genes along the inactive-X *in vitro*. To further understand the differential requirement for Polycomb proteins in X-linked gene silencing, it is important to consider epigenetic factors outside of canonical PRC2 and their potentials roles in faithfully maintaining silencing of the inactive-X chromosome.

PRC1 components along with its catalytic readout, H2A-K119ub1, are found co-enriched on the inactive X-chromosome (Simon and Kingston, 2009). Hypothesizing and invoking a requirement for PRC1 in propagating the X-inactive state in mouse TSCs must be met with substantial experimental evidence. I propose a systematic evaluation of individual core PRC1 components, those that are commonly enriched along the inactive-X, to include

RING1A/RING1B (the catalytic subunits of the PRC1) and CBX2, an H3-K27me3 reader. In the future we would need to derive polymorphic TSC lines, which are conditionally mutant for *Ring1A/B* and/or *Cbx2*. Mutating *Ring1A/B* and/or *Cbx2* would formally address a functional requirement for PRC1 in imprinted X-chromosome inactivation. In such cell lines we could employ immunofluorescence experiments to gauge Polycomb and histone modification enrichment on the inactive-X. We can further use RNA-FISH/allele-specific RT-PCR analyses to assess the Xist expression/enrichment profile and the inactive-X: active-X gene expression ratios, respectively. Moreover, allele-specific RNA-sequencing will reveal the extent to which PRC1 proteins are involved in X-linked gene silencing X-chromosome wide. With these future studies we can begin to understand a requirement, or lack thereof, for PRC1 in X-inactivation in mouse TSCs.

Continued silencing of a majority of genes on the inactive-X in my *Eed*$^{-/-}$ TSCs also implies that there is at least one additional mechanism that maintains silencing of most of the X-linked genes on the paternal X-chromosome. Likely there are multiple combinatorial mechanisms that might function cooperatively to keep the inactive-X tightly silenced. Other epigenetic factors other than those found in canonical PRC2, and potentially PRC1, must silence the vast majority of genes along the inactive-X. To identify additional factors involved in X-inactivation, we could utilize, in particular, the data set previously generated by Chu et al. to interrogate known protein binding partners of Xist. By performing a comprehensive identification of RNA-binding proteins by mass spectrometry (ChIRP-MS), Chu et al. uncovered a multitude of proteins that interact with Xist RNA. It is therefore possible that many of these factors contribute to maintaining silencing of the inactive-X. Many of these hits were intriguingly found in TSCs (Chu et a., 2015). It would be important to systematically and

genetically evaluate the top hits uncovered from ChIRP-MS in mouse TSCs. This could be done by generating independent conditionally mutant TSC lines for these epigenetic factors followed by assaying for maintenance of X-inactivation via RNA-FISH and/or allele-specific RT-PCR/RNA-sequencing. Unveiling a novel requirement for additional epigenetic factors in X-linked gene silencing may then open up new avenues of investigation towards understanding the additional mechanism(s) by which X-inactivation operates.

It will also be important to carry out biochemistry experiments to find out the novel proteins with which EED may be interacting. Such an approach would elucidate the factors at play together with EED that serve to maintain repression of those genes that are upregulated in *Eed*$^{-/-}$ TSCs. Using EED as the bait, we could pull down EED and perform mass spectrometry. In turn, identifying novel binding partners of EED in mouse TSCs may shed light on the potential means by which a portion of X-inactivation is occurring. Novel protein interactions with EED would also indicate that EED itself is functioning outside of its normal occupation in PRC2 to control repression of a fraction of X-linked genes. It will therefore be pertinent to understand the expression profile of EED in *Ezh2*$^{-/-}$;*Ezh1*$^{-/-}$ TSCs, as EED enrichment is lost from the inactive-X in *Ezh2*$^{-/-}$;*Ezh1*$^{-/-}$ TSCs. We hypothesize that, because X-inactivation is not currently observed to be defective in my *Ezh2*$^{-/-}$;*Ezh1*$^{-/-}$ cells, EED is expressed at the protein level in *Ezh2*$^{-/-}$;*Ezh1*$^{-/-}$ cells and therefore functions outside of a canonical PRC2 complex to ensure repression of a select set of genes.

A Comparative Analysis of Polycomb Repressive Complex 2 Proteins in Imprinted X-chromosome Inactivation: Mouse Embryos

In my next study, I evaluated the role of PRC2 core proteins in inducing paternal X-linked gene silencing during mouse embryogenesis. Furthermore, I showed for the first time a

differential requirement for maternally deposited Polycomb proteins in initiating an epigenetic silent state on the paternal X-chromosome. Prior work clearly identified enrichment of Polycomb group proteins (PcGs) on the inactive-X both *in vivo* and *in vitro* (Plath et al., 2003; Silva et al., 2003; Kalantry et al., 2006). As a field, we also know that maternally deposited EED coats the inactive-X in *Eed*$^{-/-}$ (only zygotic null) embryos (Kalantry et al., 2006). Given that maternal PcGs enrich on the inactive–X during the initiation phase of imprinted X-chromosome inactivation, both in *WT* and homozygous zygotically null embryos, led me to the hypothesis that maternally derived PcGs are critically required to execute X-linked gene silencing during embryogenesis. However, until this study, no one took the systematic genetic approach to dissect PRC2 components and evaluate their role in triggering X-linked gene silencing. Indeed, I hypothesized that maternal PRC2 proteins are essential for triggering X-inactivation. Here I elucidated the distinct function of PRC2 components in imprinted X-chromosome inactivation initiation.

First, I investigated the activity of maternal EZH2. Despite loss of detectable H3-K27me3 enrichment on the inactive-X in *Ezh2*$^{m-/-;z-/-}$ blastocysts, I unexpectedly found that X-linked gene silencing was unaffected. Both RNA-FISH and allele-specific RT-PCR coupled with pyrosequencing revealed the same result. Absence of detectable levels of H3-K27me3 in *Ezh2*$^{m-/-;z-/-}$ embryos suggests that lack of robust levels of this histone mark is not sufficient to confer a defect in triggering X-linked gene silencing. Furthermore, analysis of *Ezh2*$^{-/-}$ E6.5 extra-embryonic (EE) tissue (which maintain imprinted X-inactivation) demonstrated that X-linked gene silencing still operates normally in *Ezh2*$^{-/-}$ post-implantation embryos. Alternatively, it is possible that my observed H3-K27me3 enrichment on the inactive-X, albeit to a lesser extent in a minority of cells, may suffice to maintain gene silencing in *Ezh2*$^{-/-}$ extra-embryonic compartments of the post-implantation embryo (see chapter 3). Nonetheless, such evidence of

EZH2 independent initiation and maintenance of X-inactivation *in vivo* suggests that other factors, perhaps a noncanonical PRC2, are necessary for triggering X-linked gene silencing.

I therefore hypothesized that there must be factors aside from EZH2 that execute X-inactivation. EZH1, the only other known mammalian H3-K27me3 specific homologue of EZH2, is known to compensate for loss of EZH2 in mouse ESCs and perform H3-K27me3 catalytic activity, notwithstanding to a lesser degree (Shen et al., 2008). To address this possibility with respect to imprinted X-chromosome inactivation in embryos, I generated *Ezh2*$^{m-/-;z-/-}$;*Ezh1*$^{-/-}$ blastocysts and assayed for X-linked gene silencing initiation. Loss of both EZH2 and EZH1 in early embryos appeared to confer a delay in the kinetics of X-linked gene silencing for one (*Rnf12*), but not all (*Atrx*, *G6pdx*, and *Pdha1*), genes analyzed via pyrosequencing when compared to *Ezh2*$^{m-/-;z-/-}$ embryos. Moreover, compared to loss of EZH1 alone (my *Ezh2*$^{fl/fl}$;*Ezh1*$^{-/-}$ embryos), *Ezh2*$^{m-/-;z-/-}$;*Ezh1*$^{-/-}$ embryos display a very similar (no significant difference) degree of silencing for all genes analyzed (*Rnf12*, *Atrx*, *G6pdx*, and *Pdha1*). I observed extensively the normal capability of *Ezh2*$^{fl/fl}$;*Ezh1*$^{-/-}$ mice to interbreed and yield litters of equal sex ratios (See Table 3.2). These mice furthermore can live a normal life span and are themselves fertile. These data would suggest EZH1 absence alone does not confer a defect in X-inactivation, thus implying that EZH1 is not necessary for X-inactivation. To reiterate, this idea is supported by my observation that relative allelic expression ratio (inactive-X:active-X) of X-linked genes is not significantly different between *Ezh2*$^{fl/fl}$;*Ezh1*$^{-/-}$ and *Ezh2*$^{m-/-;z-/-}$;*Ezh1*$^{-/-}$ blastocysts. That silencing of a majority of X-linked genes assayed is not significantly different in my *Ezh2*$^{m-/-;z-/-}$;*Ezh1*$^{-/-}$ embryos compared to *Ezh2*$^{m-/-;z-/-}$ embryos, my data further argue that EZH1 also does not compensate for EZH2 loss in triggering X-linked gene silencing. The observed delay (i.e. difference) in the inactive-X:active-X allelic expression ratios for *Rnf12* between *Ezh2*$^{m-/-;z-/-}$ and

Ezh2$^{m-/;z-/-}$;*Ezh1*$^{-/-}$ (or *Ezh2*$^{fl/fl}$;*Ezh1*$^{-/-}$) embryos (compare figures 3.1 and 3.7) imply that there may be a subtle loss of function phenotype for EZH1, the effects of which are short lasting. *Ezh2*$^{fl/fl}$;*Ezh1*$^{-/-}$ and *Ezh2*$^{m-/-;\ z-/-}$;*Ezh1*$^{-/-}$ have very similar allelic expression ratios for Rnf12, and *Ezh2*$^{fl/fl}$;*Ezh1*$^{-/-}$ breeding schemes do not yield a sex distortion ratio. Hence I conclude that EZH1, much like EZH2, is not necessary in initiating imprinted X-inactivation. This suggests that even additional epigenetic factors are required for initiating X-linked gene silencing in the early mouse embryo, potentially through an H3-K27me3 independent pathway.

The third PRC2 component I wished to investigate was EED. EED is the "glue" of PRC2. To reiterate, without EED, PRC2 does not form properly, other subunits are degraded, and H3-K27me3 catalysis is severely diminished at PRC2 target loci (Montgomery et al., 2005). Defects in X-inactivation both *in vivo and in vitro*, when EED is missing, have been previously documented (Mak et al., 2004; Kalantry et al., 2006). I hypothesized that EED is therefore critical for the initiation of imprinted X-inactivation. Upon assaying X-linked gene silencing in *Eed*$^{m-/-;z-/-}$ blastocysts, compared to *WT* (*Eed*$^{fl/fl}$), *Eed*$^{-/-}$ embryos display a significant defect in executing silencing of multiple genes along the future inactive-X (paternally inherited X-chromosome). This phenotype is manifested in significantly and biologically different allelic expression ratios between *Eed*$^{fl/fl}$ and *Eed*$^{m-/-;z-/-}$ embryos for genes (*Atrx*, *Rnf12*, *G6pdx*, and *Pdha1*) that are supposed to undergo silencing by the blastocysts stage of embryogenesis. This is in stark contrast to EZH2 deletion together with or separate from EZH1 loss, where comparison to the appropriate controls (*Ezh2*$^{fl/fl}$ or *Ezh2*$^{fl/fl}$;*Ezh1*$^{-/-}$ embryos) did not lead to significant differences in the allelic expression ratios (inactive-X:active-X) for X-linked genes. Altogether, my data strongly suggest that while maternal EZH2 and/or EZH1 are dispensable during the initiation phase of imprinted X-chromosome inactivation, maternal EED is necessary for

properly inactivating genes along the future inactive-X. My observations also pose a PRC2 independent activity of EED in inducing a transcriptionally inert sate on the future inactive X-chromosome. Moreover, my data has importantly engendered much needed insight into meiotic transgenerational control of an epigenetic silent inactive-X state through the activities of a maternally deposited Polycomb protein (EED).

I also point out an interesting corollary in my data regarding EED and EZH2. Maternal EED enriches on the inactive X in *Eed*$^{z-/-}$ blastocysts, whereas maternal EZH2 (and H3-K27me3) does not enrich on the inactive-X in *Ezh2*$^{z-/-}$ blastocysts (Kalantry et al., 2006; Figure 3.2). This establishes a dichotomy in maternal-specific enrichment of maternal PcGs. I propose that this is in part why maternal EED is required for triggering X-linked gene silencing (in an H3-K27me3 independent manner, see below) and maternal EZH2 is not.

The divergent requirement for EED versus EZH2/EZH1 in triggering imprinted X-chromosome inactivation suggests that what I am observing is a potential histone H3-K27me3 specific independent function of PRC2, or altogether a PRC2 independent role for EED, in X-chromosome inactivation. It is therefore possible that EED complexes with other proteins to form a novel complex, one that is critical for triggering X-linked gene silencing. EED has been shown to interact with PRC1 components (Cao et al., 2014). It is plausible that a requirement for EED in X-inactivation invokes a requirement for PRC1 itself in triggering X-linked gene silencing in the early mouse embryo. It remains to be fully understood if PRC1 components, and the PRC1 associated histone H2A-K119ub1 enrichment on the inactive-X, are genetically required for proper X-inactivation initiation *in vivo*. Future genetic experiments will elucidate the activity of PRC1 and currently unidentified epigenetic factors in executing epigenetic gene silencing along the paternal X-chromosome.

Future Directions

To more comprehensively gauge the effect of my PRC2 mutations on triggering imprinted X-chromosome inactivation, I propose whole, single blastocyst RNA-sequencing to profile the entire X-chromosome. Embryos from the following genotypes will need to be collected and analyzed: 1. *Ezh2*$^{fl/fl}$, 2. *Ezh2*$^{m-/-;z-/-}$, 3. *Ezh2*$^{fl./fl}$;*Ezh1*$^{-/-}$, 4. *Ezh2*$^{m-/-;z-/-}$;*Ezh1*$^{-/-}$, 5. *Eed*$^{fl/fl}$, and 6. *Eed*$^{m-/-;z-/-}$. As a control for a failure to trigger silencing of paternally inherited X-linked genes, we should sequence *Xist*$^{+/-}$ blastocysts (paternal-X is mutant for *Xist*). We must ultimately compare differential paternal-X:maternal-X (inactive-X:active-X) X-linked gene expression ratios systematically for each genotype. To validate what we will analyze in our RNA-sequencing results, we could also subjected left over mRNA from these blastocysts to RT-PCR coupled with pyrosequencing.

To address a requirement for PRC1 in triggering imprinted X-chromosome inactivation, it will be important in the future to genetically evaluate individual PRC1 core proteins for their contributions to X-linked gene silencing *in vivo*. To accomplish this, we could breed to homozygosity mice conditionally mutant for *Ring1A*, *Ring1B*, and *Cbx2*. RING1A and RING1B are the two known mammalian enzymes which catalyze H2A-K119ub1, a repressive histone mark found enriched on the inactive X-chromosome and one which is associated with physical compaction of the surrounding chromatin/gene silencing (Simon and Kingston, 2009). Functionally addressing the role of RING1A and RING1B will shed light on additional enzymatic PcGs (in addition to EZH2 and EZH1) and their histone marks (in addition to H3-K27me3) that may function in triggering an epigenetic silenced state on the paternal X-chromosome. CBX2 (chromobox homologue) is one among several *Drosophila* homologues of Pc (Polycomb) (Kaustov, et al., 2011). CBX2 is found enriched on the inactive-X in mouse TSCs

(Kalantry et al., 2006). CBX2 is also abundantly upregulated in differentiating pluripotent cells; it is not until differentiation of pluripotent cells (i.e. mouse embryonic stem cells (ESCs)), to induce random X-inactivation, that we begin to see downregulation of *Cbx7* through PRC1 complexes that contain CBX2, CBX4, and CBX8 (O'Loghlen et al., 2012). This is a model proposed for the molecular switch of pluripotency to differentiation mediated though control of *Cbx7* expression levels, thereby providing insight into the control of X-inactivation in differentiating mouse ESCs (O'Loghlen et al., 2012). Investigating the activities of CBX2 in the early mouse embryo may thus provide additional insight into the control of mouse imprinted X-inactivation by additional Polycomb proteins. To conditionally delete *Ring1A*, *Ring1B*, or *Cbx2* we must be true to my second study and utilize females that are *Ring1A*$^{fl/fl}$, *Ring1B*$^{fl/fl}$, or *Cbx2*$^{fl/fl}$ and bear the *Zp3-Cre* transgene. Cre expression driven by the *Zp3* (Zona pellucida 3) promoter will conditionally delete floxed alleles in oocytes early during oogenesis before completion of meiosis 1 (Lewandoski et al., 1997). Likewise, we would use males that are *Ring1A*$^{fl/fl}$, *Ring1B*$^{fl/fl}$, or *Cbx2*$^{fl/fl}$ and bear either the *Stra8-Cre* or *Prm-Cre* transgene. Cre expression driven either by the *Stra8* (stimulated by retinoic acid 8) promoter or by the *Prm* (protamine) promoter will conditionally delete floxed alleles in pre-meiotic spermatogonia early on during spermatogenesis or in maturing round spermatids during spermiogenesis, respectively (Sadate-Ngatchou et al., 2008; Peschon et al., 1987). Caution must be admonished and the appropriate experiments need to be undertaken to ascertain if *Ring1A*, *Ring1B*, or *Cbx2* deletion leads to male-specific infertility through either *Stra8-Cre* or *Prm-Cre* activity. We previously faced male infertility in our *in vivo* imprinted X-inactivation experiments with PRC2 mutants. Mutation of *Ezh2* with *Stra8-Cre* combined with an already constitutive homozygous *Ezh1* deletion leads to overt male infertility. The same held true when we utilized *Eed*$^{fl/fl}$;*Stra8-Cre* males. I resorted to

using *Ezh2*$^{fl/fl}$;*Ezh1*$^{-/-}$ and *Eed*$^{fl/fl}$ males, which also possessed the *Prm-Cre* transgene. RNA-FISH experiments as well as allele-specific RT-PCR analyses coupled with pyrosequencing will reveal the extent to which X-linked gene silencing is affected in *Ring1A*, *Ring1B*, or *Cbx2* maternal and zygotic deficient embryos. Furthermore, allele-specific RNA-sequencing on whole individual blastocysts will shed light on the degree to which PRC1 components are required to trigger silencing of X-linked genes X-chromosome wide. These above experiments will provide much needed insight into a role for maternally deposited PRC1 components in controlling imprinted X-chromosome inactivation.

An alternate future direction to assess the functional requirement for PRC1 in triggering X-linked gene silencing in the early mouse embryo is as follows. We could profile *Ezh2*$^{m-/-;z-/-}$ and *Ezh2*$^{m-/-;z-/-}$;*Ezh1*$^{-/-}$ blastocysts for their RING1A or RING1B (and the associated H2A-K119Ub1 histone mark) inactive-X enrichment profile. This experiment would address the functional dependency, or lack thereof, for in tandem PRC2 and PRC1 activity in triggering target loci silencing. One prevailing model is that PRC2 recruitment to target loci (the inactive-X included) begets PRC1 recruitment to those same loci (Simon and Kingston, 2009). Epigenetic transcriptional silencing of target genes is then believed to occur either though repressive histone modifications and/or physical compaction of the surrounding chromatin (Simon and Kingston, 2009). Based on my current data in my second study where imprinted X-inactivation appears to initiate just fine in *Ezh2*$^{m-/-;z-/-}$ and *Ezh2*$^{m-/-;z-/-}$;*Ezh1*$^{-/-}$ embryos, it would be important to know if RING1A, RING1B, or H2A-K119ub1 enriches on the inactive-X in *Ezh2*$^{m-/-;z-/-}$ and *Ezh2*$^{m-/-;z-/-}$;*Ezh1*$^{-/-}$ blastocysts vis-à-vis *WT* blastocysts. If these epigenetic factors were in fact enriched on the inactive-X in *Ezh2*$^{m-/-;z-/-}$ and/or *Ezh1*$^{-/-}$ embryos, such data would suggest that PRC2 and PRC1 are functionally distinct, and PRC1 targeting to the inactive-X does not require

PRC2 and its associated H3-K27me3 catalytic readout. Furthermore, presence of RING1A/B and/or H2A-K119ub1 inactive-X enrichment in *Ezh2*$^{m-/-;z-/-}$ and/or *Ezh1*$^{-/-}$ embryos would necessitate the appropriate genetic experiments to evaluate the contribution of maternal PRC1 components to X-linked gene silencing initiation, as my data suggest that *Ezh2*$^{m-/-;z-/-}$ and/or *Ezh1*$^{-/-}$ embryos do not to display a failure in triggering X-linked gene silencing. Furthermore, formally investigating if maternally deposited PRC1 components function in initiating imprinted X-inactivation may shed light on any genetic equivalency between PRC1 core proteins and EED in triggering X-linked gene silencing; EED is known to associate with PRC1 components (Cao et al., 2014). Moreover, maternal EED is necessary to trigger silencing of paternal X-linked genes (see chapter 3). So perhaps if the phenotype with maternal PRC1 mutants is similar to my observed *Eed*$^{m-/-;z-/-}$ embryos, then we might conclude that EED is in fact participating as a component of PRC1 to enact X-linked gene silencing. Perhaps a better, more direct experiment would be to look in *Eed*$^{m-/-;z-/-}$ blastocysts. If EED is a central component and orchestrator of PRC1 (let alone PRC2, Montgomery et al., 2005), its core subunits and associated H2A-K119ub1 histone modification should not be enriched on the inactive-X when maternal EED is absent. If however RING1A, RING1B, and H2-AK119ub1 are not enriched on the inactive-X in *Ezh2*$^{m-/-;z-/-}$ and/or *Ezh1*$^{-/-}$ embryos this might suggest that PRC1 recruitment to the inactive-X requires PRC2 activity thereby indicating that these two complexes potentially cooperate at the inactive X-chromosome.

To further understand if EED is participating with novel epigenetic factors outside of PRC2 and potentially PRC1, it will be important to investigate with what EED may be interacting. To approach this we could easily turn to our cell models, TSCs. If EED is indeed acting outside canonical PRC2 and PRC1, we should detect EED protein expression in

Ezh2$^{-/-}$;*Ezh1*$^{-/-}$ TSCs. If this ends up being true, then we must execute a series of biochemical experiments to ascertain the other factors with which EED is interacting. Immunoprecipitation (IP) pulldown of EED and subsequent mass spectrometry (MS) should elucidate this. Knowledge of novel interactors of EED will in turn provide insight into novel epigenetic factors responsible for imprinted X-inactivation both *in vitro* and *in vivo*. Further experimentation on newly identified proteins implicated in X-inked gene silencing will then shed light on the additional mechanisms critical to the X-inactivation process, both *in vitro* and *in vivo*.

Unveiling a Differential Requirement for the Xist RNA and the *Xist* DNA in Imprinted Mouse X-chromosome Inactivation

In my third and final study, I discovered a differential requirement between the Xist RNA and the *Xist* DNA in imprinted mouse X-chromosome inactivation. Here I showed that the Xist RNA is not functionally equivalent to that of the *Xist* DNA in mouse imprinted X-chromosome inactivation. My *Eed*$^{-/-}$ TSCs (chapter 2) tell me that Xist RNA loss is not completely necessary for the X-inactive state. Only a small fraction of genes are upregulated when Xist RNA is missing (25% RNA-FSIH/allele-specific RT-PCR, chapter 2; 18% RNA-seq, Maclary et al., 2016, in preparation). These cells can therefore tolerate a higher dose of X-linked genes resulting from increased inactive-X expression, as these cells can still divide normally. However, results from chapter 4 illustrate that if a portion of the *Xist* DNA (exons 1-3) is deleted, the inactivated X-chromosome suffers a more serious fate (all genes assayed show derepression from the mutant X-chromosome in *Xist*$^{+/-}$ TSCs). That many more genes are affected in *Xist*$^{+/-}$ TSCs compared to *Eed*$^{-/-}$ TSCs is indicative of a crucial role for the *Xist* DNA in X-linked gene silencing. My data importantly suggests that the Xist locus functions independently of generating Xist RNA in stable X-linked gene silencing. What is it about the *Xist* locus then that is more important than

Xist RNA? The exons that are deleted in our conditional mutation (exons 1-3) likely play critical roles in X-inactivation. Perhaps these genomic regions serve as docking sites for chromatin remodeling factors or other lncRNAs, which in turn recruit a host of protein complexes that positively influence the X-inactivation process. Or maybe exons 1-3 house independent functional transcriptional units that act separately from the Xist RNA to bring about stable silencing of X-linked genes. In agreement with this idea, our lab has identified a novel lncRNA, Xist-AR (Xist-Activating RNA), which is transcribed from *Xist* exon 1 in the antisense orientation to Xist exclusively from the inactive-X (Sarkar et al., 2015). Xist-AR has previously been shown to positively regulate Xist RNA levels both *in vivo* and *in vitro* (Sarkar et al., 2015). Furthermore, Sarkar et al. showed evidence that loss of function of Xist-AR is sufficient to confer dysfunctional X-linked gene silencing *in vivo*. These data highlight that there are important factors intimately entangled with *Xist* DNA that act upstream of *Xist* to positively influence Xist RNA expression and ultimately X-inactivation. Further experiments will indicate the true extent to which Xist-AR is encompassed in the regulation of Xist and its associated transient heterochromatic state. For example, if Xist-AR is deleted (as performed by Sarkar et al., 2015), to what extent is enrichment of repressive chromatin marks, such as H3-K27me3 and H2A-K119ub1, along the inactive-X affected? Future experiments will also likely uncover additional independent transcripts housed within the *Xist* locus. That there is a host of parental X-chromosome-specific sense and antisense transcription occurring at the Xist locus underscores the functional complexity of this genomic region, one which is undoubtedly replete with several independently functioning units that must be finely tuned to bring about proper X-chromosome inactivation. Nevertheless, we as a field cannot look at the Xist RNA and the *Xist* DNA as one in the same any longer. We must therefore be cautious in our future conclusions when dealing with

an experimental system that renders the Xist RNA dysfunctional through mutagenesis of the genomic locus. Is it really RNA loss that is responsible for any potentially observed phenotype or is it rather a direct consequence of a DNA lesion itself?

Future Directions

I note that I was unsuccessful in acquiring a pure population of *Xist*$^{+/-}$ TSCs. Instead I resorted to a mutagenic strategy whereby I transiently transduced cells with an Adeno-Cre viral vector construct to achieve a heterogeneous population of mutant cells among non-mutated cells. Towards that end, at 48 hours post-Cre delivery to our *Xist*$^{+/fl}$ TSCs, I observed a significantly higher proportion of cells that were negative for Xist RNA enrichment at the inactive-X and biallelic for all X-linked genes analyzed (*Atrx*, *Rnf12*, *Pdha1*, and *Pgk1*) compared to my mock transduced cells. This is in contrast to my *Eed*$^{-/-}$ TSCs, which lose Xist RNA inactive-X enrichment but display only 25% derepression for the genes assayed (RNA-FISH and allele-specific RT-PCR). This therefore suggests that *Xist* DNA is more important than Xist RNA in X-linked gene silencing. What would make this study more complete is to assess on an X-chromosome wide level, what happens to X-linked gene silencing when Xist exons 1-3 are deleted. To accomplish this, we must have an *Xist*$^{+/fl}$ polymorphic TS cell line (X^{JF1}/X^{Lab}, see SNP discussion in chapters 2 and 3) that is able to be converted to more of a pure population (higher deletion efficiency of the *Xist* paternal floxed allele) of mutant cells. This would allow us to subject such cells to RNA-sequencing and compare results to what we already know from my polymorphic *Eed*$^{-/-}$ and *Eed*$^{fl/fl}$ TSCs.

To attempt a constitutive *Xist*$^{+/-}$ TS cell line, we could utilize a system with an inducible deletion of Xist, since our previous efforts at obtaining a pure mutant line with viral constructs

(both Adeno-Cre and Lenti-Cre) were not successful. Many inducible systems exist; I propose an Estrogen Receptor (ER)-Cre/Tamoxifen inducible system. For example, deriving a line that is $Xist^{+/fl}$;*Ert2-Cre*;X/X^{GFP};X^{JF1}/X^{Lab} from crossing a JF1 (*M. moll sinus*) female with an $Xist^{fl}/Y$;*Ert2-Cre*;$X^{GFP(Lab)}/Y$ male (*M. musculus*) may adequately allow us to accomplish this endeavor. It may be important to use an *Ert2-Cre* that is under the control of a TSC specific lineage promoter, such as *Cdx2*, to ensure high expression of the ER-Cre fusion construct. Exposure of these cells to tamoxifen (a selective estrogen-receptor modulator) will stimulate the ERT2-Cre fusion protein to unrequested itself from the cell membrane and translocate to the nucleus, whereby the Cre will then act to delete the floxed *Xist* allele (convert $Xist^{+/fl}$ cells to $Xist^{+/-}$ cells). Having a paternal X-linked *Gfp* transgene in this cell line would be advantageous; we could potentially utilize GFP re-expression form the inactive (paternal) X-chromosome to isolate the mutant from the non-mutant cells by flow automated cell sorting (FACS). Ultimately, we could then extract the RNA from our mutant cells and differentially compare the inactive-X transcription between $Xist^{+/-}$ and $Xist^{+/fl}$ TSCs via allele-specific RNA-sequencing. Such an experiment would address the extent to which mutation of *Xist* exons 1-3 affects X-inactivation in an X-chromosome wide manner.

To understand the functional contribution of *Xist* exons 1-3 in stable silencing of the inactive X-chromosome, I hypothesize that additional transcripts are housed within the deleted region of Xist exons 1-3, which may contribute to X-inactivation. Alternatively, the chromatin environment of the Xist DNA is potentially the instructive element in the deleted segment.

Concluding Remarks

In summary, the above thesis chapters describe my work on three projects to address the role of Polycomb group proteins and the *Xist* locus in imprinted mouse X-chromosome inactivation. By critically examining the intricate role of PRC2 and *Xist* in imprinted X-inactivation, I gained insight into how these epigenetic factors function broadly, including roles in initiating and maintaining epigenetic transcriptional states both in normal embryonic development and potentially in human disease.

Notice on Converting Chapters 2 and 3 into Publishable Manuscripts

The content in chapters 2 and 3 will ultimately be turned into separate scientific manuscripts, which will be submitted to peer reviewed journals. For chapter 2, the major focus is that EED, and not EZH2 and EZH1, is required for X-inactivation, albeit for a fraction of X-linked genes. RNA-seq. analysis of the paternal (inactive-X) in my $Eed^{-/-}$ TSCs indicates that approximately 18-20% of paternal X-linked genes are derepressed in $Eed^{-/-}$ TSCs. Furthermore, those genes which are upregulated share common features: they possess bivalent chromatin domains and are expressed at low levels even in $Eed^{fl/fl}$ TSCs (Maclary et al., 2016, in preparation). EED is therefore required for dampening the expression levels of a subset of genes on the paternal X-chromosome. These results have been formulated into a manuscript awaiting submission:

> Maclary, E., Hinten, M., Harris, C., Sethuraman, S., Kalantry, S. (2016). PRC2 prevents upregulation of genes with open chromatin architecture on the inactive X-chromosome. In preparation.

For chapter 3, the major focus is that maternal deposited EED from the oocyte is necessary for triggering X-linked gene silencing along the paternally inherited X-chromosome, while maternal EZH2 and/or EZH1 are dispensable for initiating imprinted X-inactivation in the early mouse embryo. My results suggest that EED executes a function other than assisting EZH2 and/or EZH1 catalyze H3-K27me3 to trigger X-linked gene silencing *in vivo*. My data also suggest a PRC2 independent role for EED in imprinted X-inactivation. Moreover, my findings highlight the first demonstration of a maternal factor responsible for inducing silencing of the X-chromosome in the embryo, an example of transgenerational epigenetic regulation. We have extended our analysis to a future direction, which takes advantage of an allele-specific RNA-sequencing method to understand how loss of PRC2 components affects X-linked gene silencing chromosome wide. This will be the last data set we will incorporate into the material from chapter 3. We will then prepare chapter 3 into a manuscript for submission:

Hinten M, Maclary E, Harris C, Larson P, Kalantry S. Control of mouse imprinted X-chromosome inactivation by a maternal Polycomb protein (in preparation).

Future Investigations for Chapter 4 and Additional Data Requirements for Publication

Since I was unsuccessful in acquiring a pure population of *Xist*$^{+/-}$ TSCs, I instead resorted to a mutagenic strategy whereby I transiently transduced cells with an Aden-Cre viral vector construct to achieve a heterogeneous population of mutant cells among non-mutated cells. Towards that end, at 48 hours post-Cre delivery to our *Xist*$^{+/fl}$ TSCs, I observed a significantly higher proportion of cells that were negative for Xist RNA enrichment at the inactive-X and biallelic for all X-linked genes analyzed (*Atrx*, *Rnf12*, *Pdha1*, and *Pgk1*) compared to my mock transduced cells. This is in contrast to my *Eed*$^{-/-}$ TSCs, which lose Xist RNA inactive-X enrichment but display only 25% derepression for the genes assayed (RNA-FISH and allele-

specific RT-PCR). This therefore suggests that *Xist* DNA is more important than Xist RNA in X-linked gene silencing. What would make this study more complete is to assess on an X-chromosome wide level, what happens to X-linked gene silencing when *Xist* exons 1-3 are deleted. To accomplish this, we must have an $Xist^{+/fl}$ polymorphic TS cell line (X^{JF1}/X^{Lab}, see SNP discussion in chapters 2 and 3) that is able to be converted to more of a pure population (higher deletion efficiency of the *Xist* paternal floxed allele) of mutant cells. This would allow us to subject such cells to allele-specific RNA-sequencing and compare results to what we already know from my polymorphic $Eed^{-/-}$ and $Eed^{fl/fl}$ TSCs.

To attempt a constitutive $Xist^{+/-}$ TS cell line, we could utilize a system with an inducible deletion of Xist, since my previous efforts at obtaining a pure mutant line with viral constructs (both Adeno-Cre and Lenti-Cre) were not successful. Many inducible systems exist; I propose an Estrogen Receptor (ER)-Cre/Tamoxifen inducible system. For example, deriving a line that is $Xist^{+/fl}$;*Ert2-Cre*;X/X^{GFP};X^{JF1}/X^{Lab} from crossing a JF1 (*M. mollosinus*) female with an $Xist^{fl}/Y$;*Ert2-Cre*;$X^{GFP(Lab)}/Y$ male (*M. musculus*) may adequately allow us to accomplish this endeavor. It may be important to use an *Ert2-Cre* that is under the control of a TSC specific lineage promoter, such as *Cdx2*, to ensure high expression of the ER-Cre fusion construct. Ultimately, we could then extract the RNA from our mutant cells and differentially compare the inactive-X transcription between $Xist^{+/-}$ and $Xist^{+/fl}$ TSCs via allele-specific RNA-sequencing. Such an experiment would address the extent to which mutation of *Xist* exons 1-3 affects X-inactivation in an X-chromosome wide manner.

To understand the functional contribution of *Xist* exons 1-3 in stable silencing of the inactive X-chromosome, I hypothesize that additional transcripts are housed within the deleted region of *Xist* exons 1-3, which may contribute to X-inactivation. To address this, we would

ultimately need to identify independent transcripts contained within exons 1-3 of *Xist* and systematically characterize them. Upon perturbing their expression, we would then need to assess how loss of one or more of these transcripts impacts X-linked gene silencing. To do this, we could employ RNA-FISH, RT-PCR, and allele-specific RNA-seq. methods. $Eed^{fl/fl}$, $Eed^{-/-}$, $Xist^{+/fl}$, and $Xist^{+/-}$ TSCs should be used as controls in comparison to cells that are deficient for novel transcript activity from the inactive-X. Alternatively, the chromatin environment of the *Xist* DNA is potentially the instructive element in the deleted segment. To ascertain this, I propose a systematic analysis of the long-range interactions of the inactive X-chromosome through HI-C approaches. We would need to do this in $Xist^{+/fl}$, $Xist^{+/-}$, and $Eed^{-/-}$ TSCs. Acquiring such data will allow us to compare the chromatin changes between mutation scenarios, ultimately lending insight into whether the chromatin configuration/chromosome interactions impacts X-inactivation. We will then put these data together with what I acquired from chapter 4 into a manuscript.

References

Cao Q., Wang X., Zhao, M., Yang R., Malik R., Qiao Y., Poliakov A., Yocum A.K., Li Y., Chen W., Cao X., Jiang X., Dahiya A., Harris, C., Feng, F.Y., Kalantry, S., Qin Z.S., Dhanasekaran, S.M., Chinnaiyan, A.M. (2014). The Central Role of EED in the Orchestration of Polycomb Group Complexes. Nat. Commun. *5*, 3127.

Chan, K.M., Zhang, H., Malureanu, L., van Deursen, J., and Zhang, Z. (2011). Diverse factors are involved in maintaining X chromosome inactivation. Proc. Natl. Acad. Sci. U.S.A. *108*, 16699–16704.

Chu, C., Zhang, Q.C., da Rocha, S.T., Flynn, R.A., Bharadwaj, M., Calabrese, J.M., Magnuson, T., Heard, E., and Chang, H.Y. (2015). Systematic discovery of Xist RNA binding proteins. Cell *161*, 404–416.

Denisenko, O., Shnyreva, M., Suzuki, H., and Bomsztyk, K. (1998). Point mutations in the WD40 domain of Eed block its interaction with Ezh2. Mol. Cell *Biol*. 18*,* 5634–5642.

Di Croce, L., and Helin, K. (2013) Transcriptional regulation by Polycomb group proteins. Nat. Struct. Mol. Biol*,* 20, 1147–1155.

Han, Z., Xing, X., Hu, M., Zhang, Y., Liu, P., and Chai, J. (2007). Structural basis of EZH2 recognition by EED. Structure *15*, 1306–1315.

Hendzel, M.J., Wei, Y., Mancini, M.A., Van Hooser, A., Ranalli, T., Brinkley, B.R., Bazett-Jones, D.P., and Allis, C.D. (1997). Mitosis-specific phosphorylation of histone H3 initiates primarily within pericentromeric heterochromatin during G2 and spreads in an ordered fashion coincident with mitotic chromosome condensation. Chromosoma *106*, 348–360.

Kalakonda, N., Fischle, W., Boccuni, P., Gurvich, N., Hoya-Arias, R., Zhao, X., Miyata, Y., Macgrogan, D., Zhang, J., Sims, J.K., et al. (2008). Histone H4 lysine 20 monomethylation promotes transcriptional repression by L3MBTL1. Oncogene *27*, 4293–4304.

Kalantry, S., and Magnuson, T. (2006). The Polycomb group protein EED is dispensable for the initiation of random X-chromosome inactivation. PLoS Genet. *2*, e66.

Kalantry, S., Mills, K.C., Yee, D., Otte, A.P., Panning, B., and Magnuson, T. (2006). The Polycomb group protein Eed protects the inactive X-chromosome from differentiation-induced reactivation. Nat. Cell Biol. *8*, 195–202.

Karachentsev, D., Sarma, K., Reinberg, D., and Steward, R. (2005). PR-Set7-dependent methylation of histone H4 Lys 20 functions in repression of gene expression and is essential for mitosis. Genes Dev. *19*, 431–435.

Kaustov, L., Ouyang, H., Amaya, M,, et al. (2011). Recognition and specificity determinants of the human cbx chromodomains. J Biol Chem. *286*, 521–9

Kohlmaier, A., Savarese, F., Lachner, M., Martens, J., Jenuwein, T., and Wutz, A. (2004). A chromosomal memory triggered by Xist regulates histone methylation in X inactivation. PLoS Biol. *2*, E171.

Lewandoski, M., Wassarman, K.M., and Martin , G.R. (1997). Zp3-cre, a transgenic mouse line for the activation or inactivation of loxP-flanked target genes specifically in the female germ line. Curr Biol. *7(2)*, 148-51.

Maclary, E., Hinten, M. Harris, C., Sethuraman, S., and Kalantry, S. (2016). PRC2 prevents upregulation of genes with open chromatin architecture on the inactive X-chromosome. In preparation.

Margueron, R., and Reinberg, D. (2011). The Polycomb complex PRC2 and its mark in life. Nature *469*, 343–349

McHugh, C.A., Chen, C.-K., Chow, A., Surka, C.F., Tran, C., McDonel, P., Pandya-Jones, A., Blanco, M., Burghard, C., Moradian, A., et al. (2015). The Xist lncRNA interacts directly with SHARP to silence transcription through HDAC3. Nature *521*, 232–236.

Minajigi, A., Froberg, J.E., Wei, C., Sunwoo, H., Kesner, B., Colognori, D., Lessing, D., Payer, B., Boukhali, M., Haas, W., et al. (2015). Chromosomes. A comprehensive Xist interactome reveals cohesin repulsion and an RNA-directed chromosome conformation. Science *349*.

Minkovsky, A., Sahakyan, A., Bonora, G., Damoiseaux, R., Dimitrova, E., Rubbi, L., Pellegrini, M., Radu, C.G., and Plath, K. (2015). A high-throughput screen of inactive X chromosome reactivation identifies the enhancement of DNA demethylation by 5-aza-2'-dC upon inhibition of ribonucleotide reductase. Epigenetics Chromatin *8*, 42.

Moindrot, B., Cerase, A., Coker, H., Masui, O., Grijzenhout, A., Pintacuda, G., Schermelleh, L., Nesterova, T.B., and Brockdorff, N. (2015). A Pooled shRNA Screen Identifies Rbm15, Spen, and Wtap as Factors Required for Xist RNA-Mediated Silencing. Cell Rep. *12*, 562–572.

Monfort, A., Di Minin, G., Postlmayr, A., Freimann, R., Arieti, F., Thore, S., and Wutz, A. (2015). Identification of Spen as a Crucial Factor for Xist Function through Forward Genetic Screening in Haploid Embryonic Stem Cells. Cell Rep. *12*, 554–561.

Montgomery, N.D., Yee, D., Chen, A., Kalantry, S., Chamberlain, S.J., Otte, A.P., and Magnuson, T. (2005). The murine polycomb group protein Eed is required for global histone H3 lysine-27 methylation. Curr. Biol. *15*, 942–947.

Oda, M.1., Shiota, K., and Tanaka, S. (2006). Trophoblast stem cells. Methods Enzymol. *419*, 387-400.

O'Loghlen, A., Muñoz-Cabello, A.M., Gaspar-Maia, A., Wu, H.A., Banito, A., Kunowska, N., Racek, T., Pemberton, H.N., Beolchi, P., Lavial, F., Masui, O., Vermeulen, M., Carroll, T., Graumann, J., Heard, E., Dillon, N., Azuara, V., Snijders, A.P., Peters, G., Bernstein, E., and Gil,

J.(2012).MicroRNA regulation of Cbx7 mediates a switch of Polycomb orthologs during ESC dif ferentiation. Cell Stem Cell. *10(1)*, 33-46.

Peschon, J.J., Behringer, R.R., Brinster, R.L., Palmiter, R.D. (1987). Spermatid-specific expression of protamine 1 in transgenic mice. Proc Natl Acad Sci U.S.A. *84*, 5316–5319.

Plath, K., Fang, J., Mlynarczyk-Evans, S.K., Cao, R., Worringer, K.A., Wang, H., la Cruz, de, C.C., Otte, A.P., Panning, B., and Zhang, Y. (2003). Role of histone H3 lysine 27 methylation in X inactivation. Science *300*, 131–135.

Sadate-Ngatchou, P.I., Payne, C.J., Dearth, A.T., and Braun, R.E. (2008). Cre recombinase activity specific to postnatal, premeiotic male germ cells in transgenic mice. Genesis. *46(12)*, 738-42.

Sarkar, M.K., Gayen, S., Kumar, S., Maclary, E., Buttigieg, E., Hinten, M., Kumari, A., Harris, C., Sado, T., and Kalantry, S. (2015). An Xist-activating antisense RNA required for X-chromosome inactivation. Nat. Commun. 6:8564. doi ,10.1038/ncomms9564.

Schuettengruber, B., Chourrout, D., Vervoort, M., Leblanc, B., and Cavalli, G. (2007), Genome regulation by polycomb and trithorax proteins. Cell *128* ,735‑745.

Shen, X., Liu, Y., Hsu, Y.J., Fujiwara, Y., Kim, J., Mao, X., Yuan, G.C., and Orkin, S.H. (2008). EZH1 mediates methylation on histone H3 lysine 27 and complements EZH2 in maintaining stem cell identity and executing pluripotency. Mol Cell. *32(4)*, 491-502.

Silva, J., Mak, W., Zvetkova, I., Appanah, R., Nesterova, T.B., Webster, Z., Peters, A.H.F.M., Jenuwein, T., Otte, A.P., and Brockdorff, N. (2003). Establishment of histone h3 methylation on the inactive X chromosome requires transient recruitment of Eed-Enx1 polycomb group complexes. Dev. Cell *4*, 481–495.

Simon, J.A. and Kingston, R.E. (2009). Mechanisms of polycomb gene silencing: knowns and unknowns. Nat. Rev. Mol. Cell Biol. *10*, 697-708.

Wang, H., Wang, L., Erdjument-Bromage, H., Vidal, M., Tempst, P., Jones, R.S., and Zhang, Y. (2004). Role of histone H2A ubiquitination in polycomb silencing. Nature 431, 873–878.

Zhang, T., Cooper, S., and Brockdorff, N. (2015). The interplay of histone modifications – writers that read. EMBO Rep.

Zhao, J., Sun, B.K., Erwin, J.A., Song, J.-J., and Lee, J.T. (2008). Polycomb proteins targeted by a short repeat RNA to the mouse X chromosome. Science *322*, 750–756.

Appendix A

Towards Understanding a Role for Novel Antisense lncRNAs within the Xist Locus in X-chromosome Inactivation

Based on my data from chapter 2 and 4, I believe that Xist RNA is not as critical as the *Xist* DNA for stable silencing of the inactive X-chromosome. One reason for this is that there are likely separate transcriptional entities housed within the *Xist* locus that function as lncRNAs to stably silence X-linked genes. This is plausibly why we see massive derepression of X-linked genes in TSCs missing *Xist* exons 1-3; excising this region of *Xist* will consequently obliterate any independent genetic elements contained inside of this genomic region. Along those lines, our lab has identified a second antisense transcript (separate from Xist-AR (Sarkar et al., 2015)) mapping to exon 1 of *Xist*. For now this transcript is designated as Novel antisense transcript II (Novel-II). Novel-II, like Xist-AR, is only transcribed from the inactive-X. Novel-II is also found to interact in *cis* with the inactive X-chromosome in WT female TSCs (Figure A.1). Its notable size and adjacent localization to the Xist RNA domain suggests that it may participate in silencing genes along the inactive X-chromosome, perhaps separately from Xist RNA.

It is therefore conceivable that a reason for why we observe a majority of genes to maintain their silencing in *Eed*$^{-/-}$ TSCs, despite EED, H3-K27me3, and Xist RNA loss, is because Novel-II is acting separate from Xist to silence X-linked genes. The mechanism by which this silencing may occur remains to be discovered and substantiated with sufficient

experimental evidence, however. Loss of canonical repressive markers (i.e. H3-K27me3, H2A-K119ub1, and H4-K20me1) as well as canonical PRC2 and PRC1 protein components on the inactive-X in *Eed*$^{-/-}$ TSCs suggests that if Novel-II functions in recruiting chromatin modifiers that it does so by employing yet unidentified proteins to the inactive X-chromosome. To address a role for Novel-II in X-linked gene silencing, I initially wanted to gauge the expression profile of Novel-II in my *Eed*$^{-/-}$ TSCs vis-à-vis my *Eed*$^{fl/fl}$ TSCs. After subjecting my cells to RNA-FISH experiments, I indeed find that Novel-II is expressed in both *Eed*$^{fl/fl}$ and *Eed*$^{-/-}$ TSCs. I observed two signals for Novel-II in *Eed*$^{fl/fl}$ and *Eed*$^{-/-}$ TSCs (one is adjacent/within the Xist RNA domain in *WT* (i.e. *Eed*$^{fl/fl}$) cells) (Figure A.1). In my *Eed*$^{-/-}$ TS cells, one of these signals is presumably emanating from the inactive X-chromosomes, whereas the other is produced from the active X-chromosome. Although my probe is a single stranded probe (to differentiate among sense versus antisense transcripts) I found that our probe generated against Novel-II cDNA will pick up Tsix, the antisense counterpart to Xist. Only with a single-stranded allele-specific RNA-FISH probe could I then detect just Novel-II expression from the inactive-X. Such an experiment could in theory be performed.

Since Novel-II is expressed in both *Eed*$^{fl/fl}$ and *Eed*$^{-/-}$ TSCs, it will be important in the future to functionally test its contribution to imprinted X-chromosome inactivation. To do so, we could subtly arrest the transcription (in an orientation-specific manner) by utilizing a CRISPR-sgRNA-dCAS9 approach. A catalytically dead CAS9 enzyme will be recruited to the Novel-II genomic location and block its expression. We cold then assay these TSCs for allele-specific gene expression via RNA-FISH, allele-specific RT-PCR/pyrosequencing, and allele-specific RNA-sequencing. Understanding the effect on gene silencing when we prevent Novel-II transcription will give insight into this particular transcriptional unit in X-inactivation. Absent a

defect in stable X-linked gene silencing in cells lacking functional Novel-II transcripts may suggest that other potentially yet undiscovered independent entities within exons 1-3 of *Xist* are positively regulating X-linked gene silencing. I cannot formally exclude that a serious defect in X-inactivation in my transient $Xist^{+/-}$ TSCs results simply from a change in the chromatin architecture by deleting such a large portion of the *Xist* DNA. Future experiments will uncover important motifs that impact the chromatin configuration surrounding the 5' exons of *Xist* and which, in turn, substantially affect the stable X-inactive state.

Materials and Methods

Ethics Statement

This study was performed in strict accordance with the recommendations in the guide for the Care and Use of Laboratory Animals of the National Institutes of Health. All animals were handled according to protocols approved by the University Committee on Use and Care of Animals (UCUCA) at the University of Michigan (protocol #PRO00006455).

Mice

Mice harboring a conditional mutation in *Eed* were generated by the University of Michigan Transgenic Animal Model Core using $Eed^{tm1a(EUCOMM)Wtsi}$ targeted ES cells (EUCOMM). Briefly, ES cells were injected into blastocysts, and implanted into pseudopregnant females. Mice with high percentages of chimerism were bred and assessed for germline transmission. To generate homozygous *Eed* mutant mice harboring polymorphic X-chromosomes, first male and female mice on a B6 *Mus musculus* background carrying the conditional mutant allele for *Eed* were intercrossed ($Eed^{fl/+}$ x $Eed^{fl/+}$) to achieve homozygosity. To obtain mice conditionally mutant for *Eed* and on the divergent JF1 *Mus molossinus* background, we bred $Eed^{fl/fl}$ males (B6 *Mus musculus* background) to *WT* JF1 *Mus molossinus* females. This gave us F1 hybrid $Eed^{fl/+}$ males that possessed an X-chromosome from the JF1 *Mus molossinus* background (X^{JF1}/Y). Such males were backcrossed to *WT* JF1 *Mus molossinus* females to derive $Eed^{fl/+}$ females that were a mix of B6 *Mus musculus* and JF1 *Mus molossinus* and also harbored two X-chromosomes from the JF1 *Mus molossinus* background (X^{JF1}/X^{JF1}). $Eed^{fl/+};X^{JF1}/X^{JF1}$ females were bred against $Eed^{fl/+};X^{JF1}/Y$ males to derive $Eed^{fl/fl};X^{JF1}/Y$ males. To obtain our female embryos used for TS cell derivation, we crossed an $Eed^{fl/fl}$ female on the B6 *Mus musculus* background with an $Eed^{fl/fl}$ male that was a mix of B6 *Mus musculus* and JF1 *Mus molossinus* but possessed an X-chromosome from the JF1 *Mus molossinus* background (X^{JF1}/Y). The JF1/Ms strain has been

described previously (See Keane et al., 2011; Takada et al., 2013; Yalcin et al., 2011; references from chapter 2 and 3).

TS Cell Derivation and Culture

Blastocysts were dissected out of pregnant mice 3.5 dpc and plated in four well dishes pre-seeded with MEFs. Hatched embryos were cultured in standard TS medium supplemented with 1.5x FGF4 and Heparin for 4-5 days until blastocyst outgrowths were of ideal size. Blastocysts were then trypsinized in 0.05% Trypsin-EDTA, neutralized with TS media supplemented with 1.5x FGF4 and Heparin, and cultured in 96 well dishes. Once lines were well established, XX/XY PCRs confirmed female lines and genotype PCRs for $Eed^{fl/fl}$;X^{Lab}/X^{JF1} lines. Cell lines were then cultured in standard TS media supplemented with FGF4 and Heparin. RNA was harvested from TS cells using TRIzol (Invitrogen, #15596-018) and RT-PCR was performed as described below. For Immunofluorescence combined with or without RNA-FISH, TS cells were split onto gelatin-coated glass coverslips and allowed to grow for 2-3 days. The cells were then permeabilized through sequential treatment with ice-cold cytoskeletal extraction buffer (CSK; 100 mM NaCl, 300 mM sucrose, 3 mM MgCl2, and 10 mM PIPES buffer, pH 6. 8) for 30 seconds, ice-cold CSK buffer containing 0.4% Triton X-100 (Fisher Scientific, #EP151) for 30 seconds, followed twice with ice-cold CSK for 30 seconds. After permeabilization, cells were fixed by incubation in 4% paraformaldehyde at room temperature for 10 minutes. Cells were then rinsed three times each in 70% ethanol and stored in 70% ethanol at -20°C prior to immunofluorescence with or without RNA-FISH.

Generating Stable *Eed*$^{-/-}$ TSCs

$Eed^{fl/fl}$ TSCs were plated at a 1:24-1:48 dilution into six well dishes pre-seeded with MEFs and allowed to adhere until the next day. Cells were then transduced with Ad5-CMV-Cre

(Adenovirus serotype 5, University of Michigan Viral Vector Core adenoviral construct, 4 x 10^{12} particles/mL) at a multiplicity of infection (MOI) of 1000. Once cell colonies were large enough following the initial transduction, they were subcloned into 96 well dishes pre-seeded with MEFs and re-transduced 24 hours later with Adeno-Cre again at an MOI of 1000. Following this expanded 96 well samples were split to six well dishes pre-seeded MEFs and again transduced 24 hours later. A portion of each 96 well samples was lysed for DNA genotyping to assess the efficiency of Cre-mediated deletion of the *Eed* floxed alleles. Subcloning, transduction, and genotyping procedures were repeated until a pure population of $Eed^{-/-}$ TSCs was achieved. $Eed^{-/-}$ TSCs were maintained in culture as described above.

Immunofluorescence

Sample coverslips containing CSK-treated and 4% PFA-fixed cells were placed in a six well dish that contained 2ml of 1X PBS in each well. Samples were then washed briefly with three changes of 1X PBS to remove ethanol followed by three successive washes with 1X PBS for three minutes each on a rocker. Samples were blocked for 30 minutes at 37°C in 50 μl pre-warmed blocking buffer in a humid chamber. Samples were then incubated for one hour at 37°C in 50 μL diluted primary antibody (dilution depends on primary antibody used, i.e. 1:500 EED primary Ab, previously used in (Kalantry et al., 2006; Plath et al., 2003; Silva et al., 2003); 1:5000 H3-K27me3 primary Ab: polyclonal Rabbit anti-mouse, Millipore, #ABE44) in a humid chamber. After incubation, samples were washed 3 times with 1X PBS/0.2% Tween-20 for three minutes each on a rocker. Coverslips were then placed back in 50 μL pre-warmed blocking buffer in a humid chamber for five minutes at 37°C followed by an additional incubation for 30 minutes at 37°C in 50 μL diluted secondary antibody. Alexa Fluor conjugated secondary antibodies were used at a 1:300 dilution. Following secondary incubation, coverslips were

washed three times with 1X PBS/0.2% Tween-20 for three minutes each on a rocker. Samples were incubated in 100 μl of 2% PFA on a glass plate wrapped in parafilm for 10 minutes at room temperature. Following this, samples were dehydrated through room temperature ethanol series (five minutes each for 70%, 85%, 95%, and 100% ethanol). Coverslips were allowed to dry for 15 minutes after the 100% ethanol wash, followed by hybridizing the samples overnight with the appropriate RNA-FISH probe. After hybridization, samples were washed for seven minutes at 39°C, three times each in 2X SSC/50% formamide. This was followed by three-seven minute washes at 39°C in 2X SSC (1:100,000-1:200,000 dilution of DAPI added at third wash of 2X SSC), followed by two-seven minute washes at 39°C in 1X SSC. Sample coverslips were then mounted onto glass microscope slides with Vectashield. Coverslips were sealed to the glass slides with clear nail polish.

RNA-FISH

Samples were dehydrated through room temperature ethanol series (five minutes each for 70%, 85%, 95%, and 100% ethanol). Coverslips were allowed to dry for 15 minutes at room temperature after the 100% ethanol wash, followed by hybridizing the samples overnight with the appropriate RNA-FISH probe. After the hybridization, samples were washed for seven minutes at 39°C, three times each in 2X SSC/50% formamide. This was followed by three-seven minute washes at 39°C in 2X SSC (1:100,000-1:200,000 dilution of DAPI added at third wash of 2X SSC), followed by two-seven minute washes at 39°C in 1X SSC. Sample coverslips were then mounted onto glass microscope slides with Vectashield. Coverslips were sealed to the glass slides with clear nail polish.

PCR

For DNA isolation, cell pellets from TSCs were lysed in buffer composed of 50mM KCl, 10mM Tris-Cl (pH 8.3), 2.5mM $MgCl_2$, 0.1mg/ml gelatin, 0.45%NP-40, and 0.45% Tween-20. Cells in lysis buffer were incubated at 50^0C overnight, then stored at 4^0C until use. Genomic PCR reactions were carried out in ChromaTaq buffer (Denville Scientific) with 1.5mM Magnesium Chloride using RadiantTaq DNA polymerase (Alkali Scientific, #C109).

Microscopy

Images of all stained samples were captured using a Nikon Eclipse TiE inverted microscope build with a Photometrics CCD camera. The images were analyzed after deconvolution using NIS-Elements software. All images were processed uniformly.

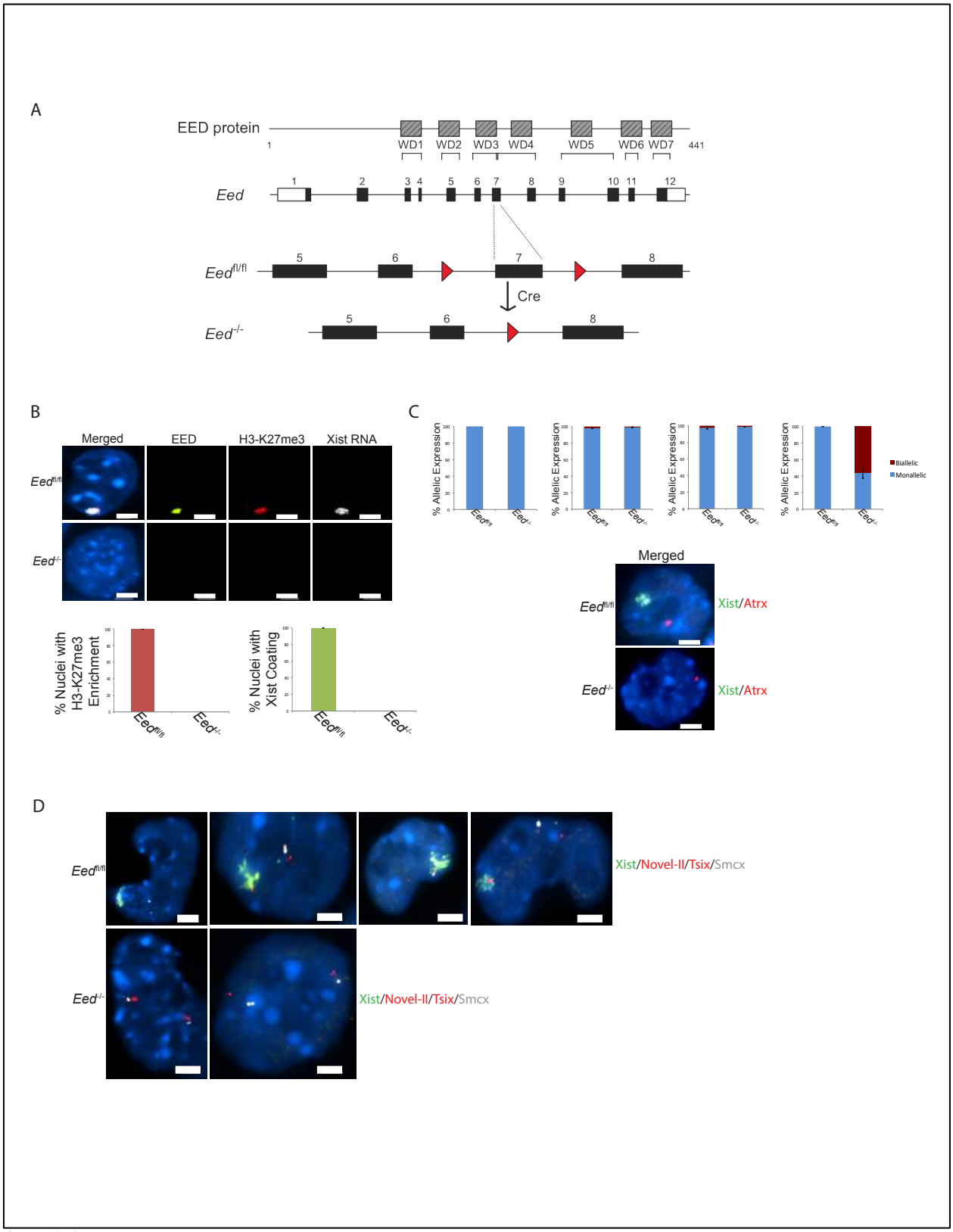
A
EED protein
1
WD1
WD2
WD3
WD4
WD5
WD6
WD7
441
Eed
Eed^fl/fl
Cre
Eed^-/-
B
Merged
EED
H3-K27me3
Xist RNA
Eed^fl/fl
Eed^-/-
% Nuclei with H3-K27me3 Enrichment
% Nuclei with Xist Coating
C
% Allelic Expression
Biallelic
Monallelic
Merged
Xist/Atrx
D
Xist/Novel-II/Tsix/Smcx

Figure A.1

Figure A.1. Novel-II, an RNA transcript expressed antisense to Xist, is expressed from the inactive X-chromosome in *Eed*$^{-/-}$ TSCs.

A. Schematic of our *Eed* mutation (See detailed description for this mutation in chapter 2)

B. Representative single nucleus images from combined immunofluorescence/RNA-FISH experiments on *Eed*$^{fl/fl}$ and *Eed*$^{-/-}$ TSCs. EED is in green, H3-K27me3 is in red, and Xist (to mark the inactive-X) is in white. Nuclei stained blue with DAPI. Scale bar is 2 μm. Graphs representing quantifications for H3-K27me3 and Xist RNA inactive-X enrichment in *Eed*$^{fl/fl}$ and *Eed*$^{-/-}$ TSCs are below images. Three independent experiments (technical replicates) were performed. 100 nuclei per genotype per replicate were counted.

C. Quantifications of RNA-FISH experiments for X-linked genes *Atrx*, *Rnf12*, *Pdha1*, and *Pgk1* (in that order left to right) on *Eed*$^{fl/fl}$ and *Eed*$^{-/-}$ TSCs. Monoallelic expression is in blue and biallelic expression is in red. Three independent experiments (technical replicates) were performed for each gene for *Eed*$^{fl/fl}$ and *Eed*$^{-/-}$ TSCs. 100 nuclei per genotype per replicate were counted. Representative image from RNA-FISH experiments on *Eed*$^{fl/fl}$ and *Eed*$^{-/-}$TSCs. Xist (to mark the inactive-X) is in green and nascent transcript detection of the X-lined gene Atrx is in red. Nuclei stained blue with DAPI. Scale bar is 2 μm.

D. Representative single nucleus images from RNA-FISH experiments on *Eed*$^{fl/fl}$ and *Eed*$^{-/-}$ TSCs. Xist (to mark the inactive-X) is in green, nascent transcript detection of Novel-II/Tsix is in red, and nascent transcript detection of *Smcx* (a known escaper of X-inactivation, to mark both X-chromosomes) is in white. Nuclei are stained blue with DAPI. Scale bar is 2 μm.

References

Sarkar, M.K., Gayen, S., Kumar, S., Maclary, E., Buttigieg, E., Hinten, M., Kumari, A., Harris, C., Sado, T., and Kalantry, S. (2015). An Xist-activating antisense RNA required for X-chromosome inactivation. Nat. Commun. *6*, 8564.

Appendix B

Understanding the Contribution of the Polycomb Protein EZH2

to the Pluripotency Network During Mouse Embryogenesis

Previous published work has identified a requirement for the histone mark H3-K27me3 in forming pluripotent stem cells (Lee et al., 2006; Boyer et al., 2006; Surface et al., 2010; Pietersen et al., 2008). On the contrary, H3-K27me3 deficient embryos can yield embryonic stem cells (ESCs) (Kalantry et al., 2006; Shen et al., 2008). It is plausible that maternal catalyzed H3-K27me3 suffices to establish a ground state pluripotency early during embryogenesis, thereby allowing H3-K27me3 deficient embryos to form ESCs after the fact. Maternally deposited H3-K27me3 results from maternal EZH2, the catalytic subunit of Polycomb repressive complex 2 (PRC2) (see chapter 1, chapter 2, and chapter 3 for references and a more complete discussion of Polycomb repressive complexes).

To understand a role for PRC2 in setting up the pluripotency state in embryonic precursors, I took advantage of my maternal and zygotic null *Ezh2 (Ezh2*$^{m-/-;z-/-}$) mutagenic strategy (used in chapter 3 to study a role for EZH2 in triggering mouse imprinted X-inactivation). My working hypothesis was that maternal EZH2 (and H3-K27me3) absence will negatively impact the number of *Nanog*- and *Oct4*-expressing cells of the inner cell mass. NANOG and OCT4 are two pluripotent lineage markers of epiblast precursors (cells that will be come the embryo proper). I anticipated observing, at the expense *Nanog*- and *Oct4*-

expressing pluripotent cells, a rise in the *Cdx2*- and *Gata6*-expressing cells of the embryo, which mark the presumptive primitive endoderm and trophectoderm lineages, respectively. To test this hypothesis, I subjected *WT* and *Ezh2*$^{m-/-;z-/-}$ blastocysts to immunofluorescence detection of NANOG, GATA6, and CDX2. I independently measured NANOG, GATA6, and H3-K27me3 in *WT* embryos vis-à-vis *Ezh2*$^{m-/-;z-/-}$ embryos. To reiterate, NANOG marks the embryonic precursors, GATA6 marks the presumptive primitive endoderm, and CDX2 marks the trophectoderm. I found that, compared to WT, mutant embryos (both male and female) display an apparent decrease in the number of NANOG positive cells in the inner cell mass. However, NANOG positive cells are not completely ablated (Figure B.1), suggesting that maternal EZH2 (and perhaps maternal H3-K27me3) positively regulates NANOG expressing cells to an extent. I also preliminarily observed some cells in the inner cell mass compartment to be positive for CDX2, suggesting that there is an increase in trophectoderm cells at the expense of the pluripotent embryonic precursors. I did not observe the same effect on presumptive primitive endoderm cells; both *WT* and *Ezh2*$^{m-/-;z-/-}$ embryos seemingly possess similar staining patterns for GATA6 (Figure B.1). If anything, some mutant embryos appear to have slightly less GATA6 positive cells. One important point is that the mutant embryo that appears to have less GATA6 positive cells and more CDX2 positive cells is a male (Figure B.1A). Our mutant female has similar numbers of GATA6 positive cells compared to the WT female (Figure B.1B). It will therefore be critical in the future to profile more *Ezh2*$^{m-/-;z-/-}$ males and females and compare any sex specific differences in the NANOG, GATA6, and CDX2 profiles. This will provide additional insight into control of the pluripotency network in the early embryo by Polycomb proteins. It will also be essential to assess the pluripotency establishment in mouse embryos devoid of both maternal and zygotic EZH2 and/or EZH1 to examine any role for EZH1 in this

process. EZH1 has been postulated to subsume EZH2 function upon EZH2 mutation (Shen et al., 2008).

To further address a requirement for the Polycomb proteins (i.e. EZH2 and/or EZH1) in forming pluripotent states in the early mouse embryo, we could derive ESCs from *WT* and *Ezh2*$^{m-/-;z-/-}$ and/or *Ezh1*$^{-/-}$ embryos. If there is a true requirement for EZH2/EZH1 in establishing pluripotency, I hypothesize that *Ezh2*$^{-/-}$;*Ezh1*$^{-/-}$ ESCs will not be able to be derived. This could result from one of two outcomes, either *Ezh2*$^{-/-}$ and/ or *Ezh1*$^{-/-}$ embryos cannot form ESCs due to a defect in establishing pluripotency, or EZH2 and/or EZH1 absence leads to a proliferative defect in embryonic precursors. Future experiments will uncover any contribution among the Polycomb group proteins in establishing a ground state pluripotency and lineage specification in the early mouse embryo.

Materials and Methods

Embryo Dissections and Processing

Embryos (E3.5 blastocysts) were flushed from the uterine limbs in 1X PBS (Invitrogen, #14200075) containing 6-mg/ml bovine serum albumin (BSA; Invitrogen, #15260037). Zona pellucidae surrounding E3.5 embryos were removed through incubation in cold Acidic Tyrode's Solution (ATS, Sigma, #T1788), followed by neutralization through several transfers of cold M2 medium (Sigma, #M7167). GFP fluorescence conferred by the paternal transmission of the X^{GFP} transgene was used to distinguish female from male embryos, since only females inherit the paternal X-chromosome. Embryos plated onto gelatin-coated glass coverslips in 1X PBS with 6 mg/ml BSA for immunofluorescence (IF). Excess solution was aspirated, and the plated embryos were air-dried for 15 min. After drying, embryos were permeabilized and fixed in 50 μL solution of 0.05% Tergitol (Sigma, #NP407) and 1% paraformaldehyde (PFA) (Electron Microscopy Sciences, # 15710) in 1X PBS for five minutes. Excess solution was tapped off, and embryos were incubated at room temperature for an additional five minutes in 50 μL drops of just 1% paraformaldehyde (Electron Microscopy Sciences, # 15710) in 1X PBS. Excess solution was tapped off, and coverslips were rinsed three times with 70% ethanol and stored in 70% ethanol at -20^{o}C prior to downstream applications.

Immunofluorescence

Sample coverslips containing 0.05% tergitol-treated and 1% PFA-fixed embryos were placed in a six well dish that contained 2ml of 1X PBS in each well. Samples were then washed briefly with three changes of 1X PBS to remove ethanol followed by three successive washes with 1X PBS for three minutes each on a rocker. Samples were blocked for 30 minutes at 37°C in 50 μl pre-warmed blocking buffer in a humid chamber. Samples were then incubated for one hour at

37°C in 50 μL diluted primary antibody (dilution depends on primary antibody used, 1:1000 H3-K27me3, 1:200 NANOG, 1:500 GATA6, 1:75 CDX2) in a humid chamber. After incubation, samples were washed three times with 1X PBS/0.2% Tween-20 for three minutes each on a rocker. Coverslips were then placed back in 50 μL pre-warmed blocking buffer in a humid chamber for five minutes at 37°C followed by an additional incubation for 30 minutes at 37°C in 50 μL diluted secondary antibody. Alexa Fluor conjugated secondary antibodies were used at a 1:300 dilution. Following secondary incubation, coverslips were washed three times with 1X PBS/0.2% Tween-20 for three minutes each on a rocker at room temp. Samples were then washed once for seven minutes at room temperature in 1X PBS/0.2% Tween-20 (1:100,000-1:200,000 dilution of DAPI added during this wash), followed by two-five minute washes at room temperature in 1X PBS/0.2% Tween-20. Sample coverslips were then mounted onto glass microscope slides with Vectashield. Coverslips were sealed to the glass slides with clear nail polish.

Microscopy

Images of all stained samples were captured using a Nikon Eclipse TiE inverted microscope build with a Photometrics CCD camera. The images were analyzed after deconvolution using NIS-Elements software. All images were processed uniformly.

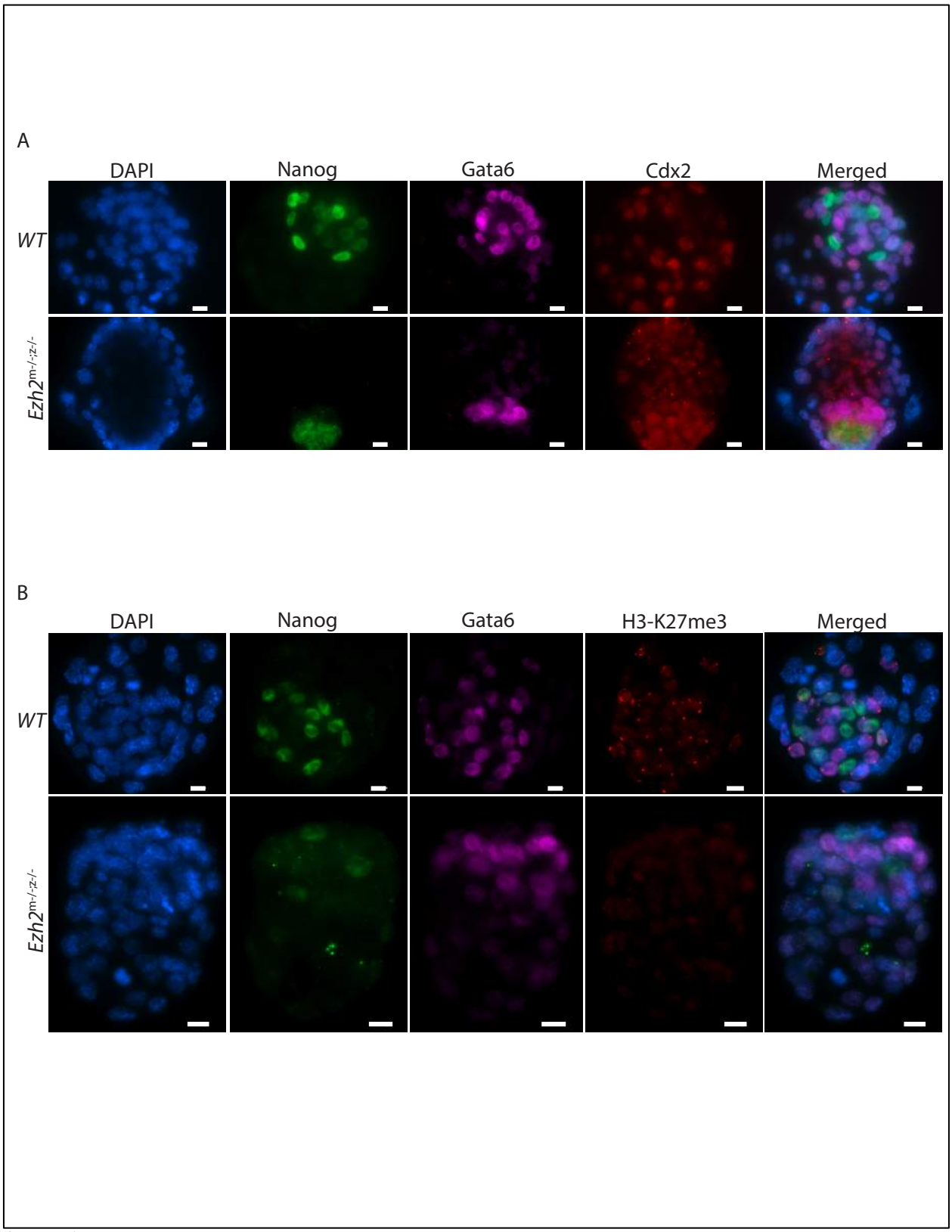
A
DAPI
Nanog
Gata6
Cdx2
Merged
WT
Ezh2m-/-zf-/-
B
DAPI
Nanog
Gata6
H3-K27me3
Merged
WT
Ezh2m-/-zf-/-

Figure B.1

Figure B.1. Assessing the pluripotency network in *Ezh2*$^{m-/-;z-/-}$ blastocysts.

A. *WT* and *Ezh2*$^{m-/-;z-/-}$ male embryos. Shown is immunofluorescence detection of NANOG in green (marks the epiblast precursors), GATA6 in purple (marks the presumptive primitive endoderm), and CDX2 in red (marks the trophectoderm). Nuclei are stained blue with DAPI. Scale bar 10 μm.

B. *WT* and *Ezh2*$^{m-/-;z-/-}$ female embryos. Shown is immunofluorescence detection of NANOG in green (marks the epiblast precursors), GATA6 in purple (marks the presumptive primitive endoderm), and H3-K27me3 in red (marks the inactive X-chromosome). Nuclei are stained blue with DAPI. Scale bar 10 μm.

References

Boyer, L.A. et al. (2006). Polycomb complexes repress developmental regulators in murine embryonic stem cells. Nature *441*, 349-353.

Kalantry, S., and Magnuson, T. (2006). The Polycomb group protein EED is dispensable for the initiation of random X-chromosome inactivation. PLoS Genet. *2*, e66.

Lee, T. I. et al. (2006). Control of developmental regulators by Polycomb in human embryonic stem cells. Cell *125*, 301-313.

Pietersen, A.M. and van Lohuizen, M. (2008). Stem cell regulation by polycomb repressors: postponing commitment. Curr Opin Cell Biol. *20*, 201-207.

Shen, X., Liu, Y., Hsu, Y.J., Fujiwara, Y., Kim, J., Mao, X., Yuan, G.C., and Orkin, S.H. (2008). EZH1 mediates methylation on histone H3 lysine 27 and complements EZH2 in maintaining stem cell identity and executing pluripotency. Mol Cell. *32(4)*, 491-502.

Surface, L.E., Thornton, S.R., and Boyer, L.A. (2010). Polycomb group proteins set the stage for early lineage commitment. Cell Stem Cell *7*, 288-298.